DOCTOR OF PHILOSOPHY

Dissecting the molecular mechanisms of the TGF-ß/BMP signal transduction pathways mapping new players and critically assessing established tools

Vogt, Janis

Award date:
2013

Awarding institution:
University of Dundee

DOCTOR OF PHILOSOPHY

Dissecting the molecular mechanisms of the TGF-ß/BMP signal transduction pathways :

mapping new players and critically assessing established tools

Janis Vogt

2013

University of Dundee

Dissecting the molecular mechanisms of the TGF-ß/BMP signal transduction pathways: Mapping new players and critically assessing established tools

By

Janis Vogt

A thesis submitted for the degree of Doctor of Philosophy,

University of Dundee

June 2013

Table of Contents

List of Figures

List of Tables

Abbreviations:

°C	degree celsius
µ	micro
ABL	abelsonmurine leukemiaviral oncogenehomolog
ACN	acetonitrile
ActR-II	activin receptor type-2
ADT	androgen-deprivation therapy
AI	amelogenesis imperfecta
ALK	activin-receptor-like-kinase
AMH	anti-Müllerian hormone
AMHR-II	anti-Müllerian hormone receptor type II
AMP	Ampicillin
AMPK	AMP-activated protein kinase
APC	anaphase promoting complex
AR	androgen receptor
ARHGAP44	Rho GTPase activating protein 44
ASK	apoptosis signal regulating kinase
ASNS	asparagine synthetase
ATP	adenosine 5'-triphosphate
BAMBI	BMP and Activin receptor membrane bound inhibitor
BEX1	brain expressed, X-linked 1
BMP	bone morphogenic protein
BMPR-II	bone morphogenic protein receptor type II
BRE	BMP responsive element
BRK	breast tumor kinase
BRSK	brain-specific kinase
BSA	Bovine serum albumin
BTB	Brachydactyly Type B
BTK	Brutonagammaglobulinemia tyrosine kinase
CaMK	calmodulin-dependent kinase
CaMKK	CaMK kinase
CCNA1	cyclin A1
CD2AP	CD2-associated protein
Cdc42	cell division control protein 42 homolog
CDK	cyclin-dependent kinases
cDNA	complementary DNA
CHIP	carboxy terminus of Hsc70-interacting protein
CHK	checkpoint kinase
CIN85	Cbl-interacting protein of 85 kDa
CK	casein kinase
CKAP2	Cytoskeleton-associated protein 2
CLK	CDC-like Kinase
c-Raf	Raf proto-oncogene serine/threonine-protein kinase
CSK	C-terminal Src kinase
C-terminal	carboxy-terminal
CUL3	CULLIN3

Da	dalton
DAPI	4',6-diamidino-2-phenylindole
DAPK	death-associated protein kinase
DKK	dickkopf
DMEM	Dulbecco's modified Eagle medium
DMSO	dimethyl sulphoxide
DNA	deoxyribonucleic acid
Dpp	decapentaplegic
DSP	dithiobis (succunimidyl propionate)
DSTT	Division of Signal Transduction Therapy
DTT	dithiothreitol
DUB	deubiquitylases
DYRK	dual-specificity tyrosine-phosphorylated and regulated
E.coli	*Escherichia coli*
ECL	enhanced chemiluminescence
ECM	extra cellular matrix
EDTA	ethylenediaminetetraacetate
EF2K	elongation-factor-2-kinase
EGFR	epidermal growth factor receptor
EGTA	ethyleneglycol bis (2-aminoethylether)-N'N'tetraacetic
eIF	eukaryotic translation initiation factor
EMT	epithelial-mesenchymal transition
EPH	ephrin
EPSM	ERK-targetedserines mutated to aspartates
ERK	extracellular signal-regulated kinase
FAK	focal adhesion kinase
FAM83	family with sequence similarity member 83
FBN1	FIBRILLIN1
FBS	foetal bovine serum
FGF-R	fibroblast-growth-factor receptor
FoxH1	forkhead homology H1
FoxO	forkhead-box-protein O
FRT	FLP recombination target
FST	follistatin
g	gram
G418	geneticin
GAPDH	glycerinaldehyd-3-phosphat-dehydrogenase
GAPs	GTPase-activating proteins
GCK	germinal centre kinase
GDF	growth and differentiation factor
GDP	guanosindiphosphat
GEF	guanine-nucleotide-exchange factor
GFP	green fluorescent protein
GID	guanine nucleotide-dissociation inhibitor
GRB2	growth factor receptor-bound protein 2
GRK2	G protein-coupled receptor kinase 2
GSK	glycogen synthase kinase
GSK3	glycogen synthase kinase-3
GST	glutathione-S-transferase
GTF2F2	general transcription factor IIF subunit 2
GTP	guanosintriphosphat

h	h
HA	haemagglutinin
HATs	histone acetyltransferases
HDAC	Histone deacetylases
HECT	homologous to E6-AP C-terminus
HEK	human embryonic kidney
HEPES	N-[2-hydroxyethyl]piperazine-N'-[2-ethanesulphonic
HER4	V-erb a erythroblastic leukemia viral oncogene
HHT	hereditary haemorrhagic telangiectasia
HIPK	homeodomain-interacting protein kinase
HPLC	high-pressure liquid chromatography
HPRTI	hypoxanthin-phosphoribosyl-transferase I
HRP	horseradish peroxidase
IC_{50}	half maximal inhibitory concentration
ID1	inhibitor of differentiation
IGF	insulin-like growth factor
IgG	immunoglobulin G
IKK	inhibitory κB kinase
IP	immunoprecipitation
IR	insulin receptor
IRAK	Interleukin-1Receptor-Associated Kinase
IRR	insulin related receptor
I-SMAD	Inhibitory SMAD
JAK	Janus Kinase
JNK	c-Jun-N-terminal kinase
JPS	Juvenile polyposis syndrome
K	kilo
L	linker
l	litre
LB	Luria Bertani broth
Lck	lymphocyte cell-specific protein tyrosine kinase
LC-MS/MS	liquid chromatography coupled to high-resolution
LDS	Loeys-Dietz syndrome
LKB1	liver kinase B1
LRP4	low-density lipoprotein receptor-related protein 4
m	milli
M	molar
MAD	mothers against decapentaplegic
MAPK	mitogen-activated protein kinases
MAPKAP-K	MAPK-activated protein kinase
MARK	microtubule-affinity-regulating kinase
MEKK	mitogen-activated protein kinase kinase kinase
MELK	maternal embryonic leucine-zipper kinase
meso-DAP	D-glutamyl-meso-diaminopimelic acid
MH1	Mad homology domain 1
MH2	Mad homology domain 2
min	minute
MINK	misshapen-like kinase
MLCK	smooth-muscle myosin light-chain kinase
MLK	mixed lineage kinase
MLLT11	myeloid/lymphoid or mixed-lineage leukemia

MMP	Matrix metalloproteinase
MNK	MAPK-integrating protein kinase
MO25	armadillo repeat scaffolding-like protein
mol	mole V
MOPS	3-(N-morpholino) propanesulfonic acid
MRC-PPU	Medical Research Council Protein Phosphorylation
MS	mass spectrometry
MSK	mitogen- and stress-activated protein kinase
MSPK	myristoylated and palmitoylated serine/threonine
MSSE	multiple self-healing squamous epithelioma
MST	mammalian homologue Ste20-like kinase
mTORC	mammalian target of rapamycin complex
MW	molecular weight
NCI	national cancer institute
NEDD4L	neural precursor cell expressed, developmentally
NEDD8	neural precursor cell expressed, developmentally
NEDD9	neural precursor cell expressed, developmentally
NEK	NIMA (never in mitosis in Aspergillus nidulans)-related
NFκB	nuclear factor κ light-chain-enhancer of activated B
NOG	NOGGIN
NPY1R	Neuropeptide Y receptor Y 1
N-terminal	amino-terminus
NUAK	SnF1-like Kinase
OD	optical density
OSR	Oxidative Stress Responsive
p	pico
PAGE	polyacrylamide gel electrophoresis
PAI1	plasminogen activator inhibitor1
PAK	p21-activated protein kinase
PAR6	partitioning defective 6
PAWS1	protein associated with SMAD1
PBS	phosphate buffered saline
PCR	polymerase chain reaction
PDGF	platelet-derived growth factor
PDGFRA	platelet-derived growth factor receptor, alpha
PDK	3-phosphoinositide-dependent protein kinase
PDP	pyruvate dehydrogenase
PDZRN3	PDZ domain containing ring finger 3
PEI	polyethylenimine
PHK	phosphorylase kinase
PI3K	phosphatidylinositide 3 kinase
PIM	provirus integration site for Moloney murine leukaemia
PKA	cAMP-dependent protein kinase
PKB	protein kinase B/AKT
PKC	protein kinase C
PKD	protein kinase D
PLDc	phospholipase D active site motif
PLK	polo-like kinase
PMDS	Persistent Müllerian duct syndrome
PMSF	phenylmethylsulfonyl fluoride
PPM1A	protein phosphatase, Mg2+/Mn2+-dependent 1A

PRAK	p38-regulated activated kinase
PRK	protein kinase C-related kinase
PTM	post-translational modification
PVDF	Polyvinylidene fluoride
qRT-PCR	quantitative reverse transcriptase PCR
Rac	RAS-related C3 botulinum toxin substrate
RBX1	RING-box protein 1
RhoA	ras homolog family member A
RING	really interesting new gene
RIPK	receptor interacting protein kinase
RNA	ribonucleic acid
RNAi	RNA-interference
RNF12	RING finger protein, LIM domain interacting
ROCK	Rho-dependent protein kinase
rpm	revolutions per minute
RSK	p90 ribosomal S6kinase
R-SMAD	receptor regulated SMAD
RT	room temperature
Runx	runt-related transcription factor
s	seconds
S6K	S6kinase
SAR	structure–activity relationship
SBE	SMAD binding element
SCAR/WAV	Wiskott–Aldrich syndrome protein
SCP	small C-terminal domain phosphatase
SDS	sodium dodecyl sulphate
SGK	serum- and glucocorticoid-induced kinase
siRNA	small interfering RNA
SMAD	mothers against DPP homolog
SMURF	SMAD ubiquitylation regulatory factor1
SnoN	V-ski sarcoma viral oncogene homolog
SOS	son of sevenless
SPC	subtilisin-like proprotein convertase
Src	sarcoma kinase
SRPK	serine-arginine protein kinase
STK	serine-threonine Kinase
SYK	spleen tyrosine kinase
TAB	TGFß-associated kinase 1 binding protein
TAE	Tris-acetate-EDTA
TAK1	TGFß-activated kinase 1
TAO	thousand and one amino acid protein kinase
TBK	TANK-binding kinase
TBS-T	Tris-buffered saline-Tween
TEMED	tetramethylethylenediamine
TFA	trifluoroacetic acid
TGFBI	TGF-ß-inducted
TGF-ß	transforming growth factor-ß
TGFßR-II	transforming growth factor-ß receptor type II
TIE	Tunica Internal Endothelial cell kinase
TKI	tyrosine kinase inhibitor
TLK	tousled-like kinase

TPX2	targeting protein for Xklp2
TRAF6	tumour necrosis factor receptor associated protein 6
TRIM33	tripartite motif-containing member 33
Triton	t-octylphenoxypolyethoxyethanol
TrkA	Neurotrophic tyrosine kinase, receptor, type 1
tRNA	transfer RNA
TSC22D1	TSC22 domain family, member 1
TTK	Phosphotyrosine picked threonine kinase
Tween	polyethylene glycol sorbitan monolaurate
V	volts
v/v	volume to volume
VBIM	validation-based insertional mutagenesis
VEGFR	vascular endothelial growth factor receptor
w/v	weight to volume
WASF3	Wiskott-Aldrich syndrome protein family member 3
WCL	whole cell lysate
wly	wooly
Wnt	wingless-related integration site
WT	wild type
WWP	WW domain-containing E3 ubiquitin protein ligase
X.laevis	*Xenopus laevis*
YAP	yes-associated protein
YES	Yamaguchi sarcoma viral oncogene homologue
ZAP	zeta chain associated protein kinase

Amino acid code:

Amino acid	Thee letter code	One letter symbol
Alanine	Ala	A
Arginine	Arg	R
Asparagine	Asn	N
Aspartic acid	Asp	D
Cysteine	Cys	C
Glutamic acid	Glu	E
Glutamine	Gln	Q
Glycine	Gly	G
Histidine	His	H
Isoleucine	Ile	I
Leucine	Leu	L
Lysine	Lys	K
Methionine	Met	M
Phenylalanine	Phe	F
Proline	Pro	P
Serine	Ser	S
Theonine	Th	T
Tryptophan	Trp	W
Tyrosine	Tyr	Y
Valine	Val	V
any amino acid	Xaa	X

Declarations:

I declare that the following thesis is based on the results of investigations conducted by myself, and that this thesis is of my own composition. Work other than my own is clearly indicated in the text by reference to the relevant researchers or to their publications. This dissertation has not been previously submitted for a higher degree.

Janis Vogt

I certify that Janis Vogt has spent the equivalent of at least nine terms in research work at the School of Life Sciences, University of Dundee, and that he has fulfilled the conditions of the Ordinance General No. 14 of the University of Dundee and is qualified to submit the accompanying thesis in application for the degree of Doctor of Philosophy.

Dr Gopal P. Sapkota

Acknowledgements:

First, I would like to thank my supervisor Gopal Sapkota for giving me the opportunity to undertake a PhD in his laboratory. His guidance and support during the last 4 years enabled me to always believe in the project, my PhD and my abilities as a scientist.

I also would like to thank everyone in the Sapkota group, past and present members, especially Lina and David, who made my time in the lab really enjoyable. I want to thank David in particular, because he supported me from day one and now became a friend. I would like to thank all the staff, students and post-docs that shared their knowledge with me and made me having a good time over the last 4 years.

I would like to thank Allison and Judith for their support and the numerous great conversations we had! I would also like to thank the DSTT and DNA sequencing staff for providing me with all their reagents, in particular Tom for all the constructs he generated for me. I would like to thank Bob for all his help with the mass spec and HPLC.

I would like to acknowledge and thank Kevin Dingwell and Jim Smith for the collaboration during my studies. Their knowledge and expertise was vital for the project. I would also like to thank everyone in the MRC-PPU as well as the CLS.

I want to thank my parents for all their support. A very special thanks goes to my grandparents for their lifelong support and help, therefore I dedicate this thesis to them. Finally I would like to thank all my friends and especially my girlfriend Hannah. Without her patience, support and love I would not have been able to do this.

Summary:

Signalling pathways downstream of the transforming growth factor ß (TGF-ß) family of cytokines, including the bone morphogenetic protein (BMP), play crucial roles during development and in adult tissue homeostasis in vertebrates. Aberrant TGF-ß and BMP signalling is associated with many human disorders including cancer. TGF-ß and BMP cytokines signal through the activation of type I receptor kinases, which then phosphorylate SMAD transcription factors (1/5/8 in the BMP pathway and 2/3 in the TGF-ß pathway). In the canonical pathway, this triggers the association of these SMADs with SMAD4 and their translocationto the nucleus, where they regulate the expression of target genes. TGF-ß and BMP can also control cellular responses independently of SMAD4, although how these are achieved is poorly understood. Although the fundamental steps in the TGF-ß pathway are established, gaps remain in our understanding of the context-specific regulation of the pathway.

In the first part of my thesis, I report the discovery and characterisation of FAM83G/PAWS1 as a novel interactor of SMAD1. I demonstrate that FAM83G/PAWS1 forms a complex with SMAD1 in a SMAD4-independent manner. Furthermore, BMP induces the phosphorylation of FAM83G/PAWS1 through BMPR1A, which is essential for the BMP dependent expression of SMAD4-independent BMP-target genes NEDD9 and ASNS. This uncovers FAM83G/PAWS1 as the first non-SMAD substrate for BMPR1A and a novel player in the BMP pathway. Furthermore, FAM83G/PAWS1 expression in *Xenopus laevis* embryos induces a complete duplication of axis phenotype,

suggesting putative regulatory roles in the BMP and Wnt signalling. I also demonstrate that FAM83G/PAWS1 regulates the expression of over 800 genes independent of BMP-stimulation suggesting wider roles for FAM83G/PAWS1 beyond the BMP pathway.

In the second part of my thesis, I analyse the specificities and potencies of the most frequently used small molecule inhibitors of the TGF-ß and BMP pathways. Small molecule inhibitors of type 1 receptor kinases have been extensively used to assess the physiological roles of TGF-ß and BMP signalling in cells and organisms. While all of these inhibitors have been reported as selective inhibitors of specific ALKs, extensive specificity tests against a wide array of protein kinases have not been performed. In this thesis, I report on the specificities and potencies of the small molecule inhibitors of the TGF-ß (SB-431542, SB-505124, LY-364947 and A-83-01) and BMP (Dorsomorphin and LDN-193189) signalling pathways against a panel of kinases covering approximately one fourth of the human kinome. On the whole, the inhibitors of the TGF-ß pathway appeared to be more selective to their targets than the inhibitors of the BMP pathway. Based on the derived specificity and potency profiles, I recommend SB-505124 as the most suitable molecule for use as an inhibitor of the TGF-ß pathway. Dorsomorphin is not suitable for use as an inhibitor of the BMP pathway. LDN-193189 is a very potent inhibitor of the BMP pathway but at concentrations used to inhibit ALKs 2&3, it also potently inhibits a number of other protein kinases. Hence, its use as a selective BMP-pathway inhibitor has to be considered with caution. These results highlight the need for

caution when using any small molecule inhibitors as tools for assessing the physiological roles for BMP and TGF-ß signalling.

Publications:

Vogt, J., Dingwell, K., Herhaus, L., Macartney, T., Smith, J. & Sapkota, G. 2013. Protein Associated With SMAD1 (PAWS1/FAM83G) is a substrate for type I BMP receptors and modulates BMP signalling. *In preparation*

Vogt, J., Traynor, R. & Sapkota, G. 2011. The specificities of small molecule inhibitors of the TGFß and BMP pathways. *Cell Signal,* 23**,** 1831-42.

1 Introduction

1.1 TGF-ß Ligands

In humans, the transforming growth factor-ß (TGF-ß) family of cytokines consists of at least 33 different ligands. These play crucial roles in a large range of cellular processes, including cell proliferation, differentiation, apoptosis, immune response, and extracellular matrix organisation as well as development (Derynck and Miyazono, 2007, Shi and Massague, 2003, Massague, 2008, Akhurst and Hata, 2012). The TGF-ß family of cytokines can be divided into two sub-families: the TGF-ß sub-family comprising TGFß1, 2, and 3, Activin and Nodal on one hand and the bone morphogenic protein (BMP) sub-family comprising BMPs, growth and differentiation factors (GDFs) and anti-Müllerian hormone (AMH) on the other. The subdivision of the ligands is based on the difference displayed by the ligands in receptor binding and specific SMAD protein activation (Shi and Massague, 2003). The expression pattern of the different ligands is often tissue and context dependent. While most TGF-ß and BMP ligands are expressed in and impact many cells and tissues, others such as AMH is only expressed during development for a relatively short period of time (Massague, 2008).

TGF-ß and BMP cytokines are expressed as precursor proteins in cells. These pro-cytokines are subsequently cleaved by specific proprotein convertases belonging to the subtilisin-like proprotein convertase (SPC) family in order to generate active cytokines (Dubois et al., 1995, Nachtigal and Ingraham, 1996, Constam and Robertson, 1999). Endopeptidase

cleavage results in the production of active C-terminal mature protein. These active TGF-ß/BMP molecules subsequently form either homo or hetero dimers with other members of their cytokine subfamily. The processed ligands are then secreted to the extra cellular matrix (ECM) (Cui et al., 1998, Annes et al., 2003). These ligand dimers are stabilised by hydrophobic interactions and disulphide bonds between conserved cysteine residues (Griffith et al., 1996, Scheufler et al., 1999, Sun and Davies, 1995). Initiation of the intracellular signalling pathway starts with the binding of the excreted ligand dimers to the extracellular domains of their cognate transmembrane cell receptor pairs.

1.2 TGF-ß membrane receptors and pathway initiation

TGF-ß cell membrane receptors are transmembrane proteins that are divided into three different groups: Type I, type II and type III receptors (Shi and Massague, 2003). Type I and II receptors are serine/threonine protein kinases. Type III receptors function as co-receptors by enhancing the binding of the TGF-ß ligands to the type I and type II receptors but do not possess serine/threonine protein kinase activity (Shi and Massague, 2003).

There are five type II receptors (ActR-IIA, ActR-IIB, BMPR-II, AMHR-II and TGFßR-II) and seven type I receptors (also known as Activin-receptor-Like-Kinases: ALKs 1–7) in humans (Manning et al., 2002). These are classified according to their affinity for selective TGF-ß ligands. As the TGF-ß ligand dimers bind to two type I and II receptors; the activated receptor complex comprises two type I and two type II receptors bound to a specific ligand dimer (Shi and Massague, 2003). Ligand binding induces a

conformational change in the complex that enables type II receptor kinases to phosphorylate type I receptor kinases at the cytoplasmic GS domain. This activates the type I receptor kinases. The phosphorylation and activation of the type I receptor kinase enables the binding of receptor regulated (R)-SMAD proteins (SMADs 1,2,3,5 and 8) and subsequently leads to the phosphorylation of R-SMADs at their C-terminal SXS motif by the type I receptor kinase (Kim et al., 2008, Wright et al., 2009, Shi and Massague, 2003, Wrana et al., 1994).

The BMP signalling pathway can be inhibited at the ligand-receptor-binding initiation step by proteins that bind to the secreted ligands. These ligand traps, such as CHORDIN and NOGGIN, bind to their corresponding BMP ligands and thereby inhibit the BMP ligand from binding to the receptors (McMahon et al., 1998, Piccolo et al., 1996). CHORDIN has been reported to predominantly bind BMP-2 and BMP-4, whereas NOGGIN, has been reported to bind BMP-4 and BMP-7, thus demonstrating that ligand traps can selectively bind and regulate the activity of specific BMP cytokines at the extracellular level (Groppe et al., 2002, Larrain et al., 2000). CHORDIN and NOGGIN are prominent inhibitiors of BMP signalling during embryogenesis (De Robertis and Kuroda, 2004). Furthermore, BMP signalling can also be inhibited by the pseudo-receptor BAMBI (Onichtchouk et al., 1999). BAMBI displays a homology to the BMP type I receptor kinase extracellular domain, which allows binding to BMP cytokines but no SMAD protein activation occurs (Onichtchouk et al., 1999). Activin ligand traps, such as FOLLISTATIN, also function in a similar manner and regulate the activity of these ligands (Massague and Chen, 2000).

1.3 SMAD proteins

SMAD proteins are the intracellular mediators of the BMP and TGF-ß signalling pathways. The SMAD proteins are the human homologs of SMA (*Caenorhabditis elegans*) and MAD (*Drosophila melanogaster*) (Raftery et al., 1995, Sekelsky et al., 1995, Savage et al., 1996). In humans there are eight different SMAD proteins, some of which also express splice variants. These are classified in three distinct groups according to their functions in cells: R-SMADs (SMADs 1, 2, 3, 5 and 8), co-SMAD4 and inhibitory SMADs (I-SMADs 6 and 7). Subsequent to the receptor complex activation, the R-SMADs are phosphorylated at the two Serines at the extreme C-terminal SXS motif (also known as tail-phosphorylation) as described above. Unless stated otherwise, phosphorylation of SMAD proteins in this thesis refers to tail-phosphorylation of R-SMADs. R-SMAD proteins can be further sub-divided into two groups based on the specific ligands that induce their phosphorylation: BMP ligands induce the phosphorylation of SMADs 1, 5 and 8 (BMP R-SMADs), whereas TGF-ß ligands induce the phosphorylation of SMADs 2 and 3 (TGF-ß R-SMADs) (Shi and Massague, 2003, Hinck, 2012). However, it has also been reported that in certain cell types TGF-ß ligands can induce the phosphorylation of BMP R-SMADs (Goumans et al., 2003, Daly et al., 2008).

Once phosphorylated, R-SMADs bind and build a heterotrimeric complex with the co-SMAD4, comprising SMAD4 and two R-SMADs. This complex formation is a key feature for both BMP and TGF-ß activated signalling and occurs with all R-SMADs (Wang et al., 2013, ten Dijke and Hill, 2004). The phosphorylation of R-SMADs induces their translocation to the

nucleus (Chen and Xu, 2011). Although R-SMADs have been reported to shuttle back and forth from the nucleus through their nuclear import and export domains in the presence or absence of ligands (Hill, 2009), their ligand-induced nuclear localisation and association with SMAD4 is essential for regulation of transcription of hundreds of canonical target genes (Shi and Massague, 2003, Ross and Hill, 2008, Wang et al., 2013). When SMAD4 expression is absent or it is mutated, TGF-ß and BMP ligands no longer induce the expression of canonical target genes but can still induce the transcription of some genes (Levy and Hill, 2005, Deng et al., 2009). In this case, the signalling pathways are usually referred to as non-canonical (or SMAD4-independent) TGF-ß or BMP signalling (see below section 1.5).

1.3.1 Structure of SMAD proteins

R-SMAD proteins consist of two highly conserved domains: MAD homology domain 1 (MH1) at the N-terminus and MAD homology domain 2 (MH2) at the C-terminus. The main feature of the MH1 domain in SMADs 1, 3, 4, 5 and 8 is its ability to bind DNA. While SMAD2 just lacks a critical short sequence for DNA binding (Dennler et al., 1999), the I-SMADs 6 and 7 have much shorter and truncated MH1 domains and therefore do not possess DNA binding ability in that manner. The MH2 domain, present in all SMAD proteins, although the SXS activation motif is only found in R-SMADs, has been reported to serve as a scaffold to facilitate interaction with several regulatory proteins and other transcription factors (Massague et al., 2005).

The MH1 and MH2 domains of SMAD proteins are connected by a Linker region. This region is rather diverse compared to the MH1 and MH2

domains and has been reported to integrate cross-talk regulatory inputs from other signalling pathways (see section 1.3.2.2)

1.3.2 Regulation of SMADs by post-translational modifications

As the intracellular TGF-ß and BMP signalling pathway transducers, the activity and function of SMAD proteins are tightly regulated at all stages of the pathway by post-translational modifications (PTMs) and inputs from other signalling networks. These PTMs have been studied extensively in the past and define our current knowledge of the regulation of TGF-ß and BMP signalling pathways (Xu et al., 2012). However, gaps remain on the precise molecular mechanisms by which the TGF-ß and BMP pathways are regulated. As key mediators of the TGF-ß and BMP signals, SMAD proteins have been the subject of focus over the years at understanding their regulation by PTMs including reversible phosphorylation and reversible ubiquitylation (Al-Salihi et al., 2012, Bruce and Sapkota, 2012, Xu et al., 2012).

1.3.2.1 Regulation of R-SMADs by reversible phosphorylation

Although the phosphorylation motif of BMP and TGF-ß activated R-SMADs is very similar, distinct protein phosphatases have been reported for each sub-groups. Pyruvate dehydrogenase (PDP) was reported to dephosphorylate the SMAD1-tail (Chen et al., 2006a). The nuclear small C-terminal domain phosphatase OS4/SCP2 was identified in *Xenopus* as an inhibitor of BMP pathway. OS4/SCP2, as well as their human homologs

SCP1, 2 and 3, were subsequently shown to dephosphorylate BMP-activated SMAD tail-phosphorylation (Knockaert et al., 2006). PPM1A was reported to dephosphorylate both TGF-ß and BMP R-SMAD tail-phosphorylation (Bruce and Sapkota, 2012, Chen et al., 2006b). Despite these reports, the precise nature of regulation of R-SMADs by phosphatases remains undefined (Bruce and Sapkota, 2012).

1.3.2.2 Reversible phosphorylation of SMADs at the linker region

Another well-established regulatory input of R-SMADs is the phosphorylation of the divergent linker region. This phosphorylation occurs not only as a direct consequence of BMP or TGF-ß stimulation but has also been reported to be mediated by other signalling pathways (Xu et al., 2012). Cyclin-dependent kinases 8 and 9 have been shown to phosphorylate SMAD1 subsequent to BMP stimulation (Alarcon et al., 2009). This phosphorylation leads on one hand to the interaction of SMAD1 with YAP and results in enhanced transcription activity but on the other hand it also primes SMAD1 for association with the SMAD E3 ubiquitin ligase SMURF1, which in turn causes SMAD1 to be ubiquitylated and subsequently degraded (Alarcon et al., 2009). Other kinases such as MAPK and GSK3 have also been reported to regulate SMAD1 and SMAD3 turn-over by phosphorylating conserved residues within the SMAD linker regions. The phosphorylation by MAPK and GSK3 leads to the recognition of the E3 ubiquitin ligases SMURF1 and NEDD4L by SMADs resulting in their ubiquitylation and degradation (Aragon et al., 2011, Sapkota et al., 2007). The G protein-coupled receptor kinase 2 (GRK2) has been reported to phosphorylate

SMAD2 and 3 linker region and prevent SMADs from tail-phosphorylation and nuclear shuttling, thus inhibiting TGF-ß signalling (Ho et al., 2005).

The only reported R-SMAD linker region protein phosphatases are the SCPs 1, 2 and 3. In contrast to their ability to dephosphorylate the tail-phosphorylation of only BMP activated SMADs, they have been shown to dephosphorylate BMP and TGF-ß activated SMADs at the linker regions (Knockaert et al., 2006, Sapkota et al., 2006, Wrighton et al., 2006).

1.3.2.3 Regulation of R-SMADs by reversible ubiquitylation

Attachment of ubiquitin molecules or chains on target proteins by E3 ubiquitin ligases marks the proteins for fates that include degradation or ubiquitin related signalling (Al-Salihi et al., 2012). SMAD proteins, as well as, type I receptor kinases, have been reported to be modified by ubiquitylation. Polyubiquitylation of R-SMADs has been reported to target SMADs for proteasomal degradation (Sapkota et al., 2007, Ebisawa et al., 2001, Al-Salihi et al., 2012). In contrast to this, K-48 polyubiquitylation of SMADs has been shown to enhance its activity (Bai et al., 2004).

SMURF1, SMURF2, NEDD4L, ITCH, WWP1 and WWP2, all members of the C2-WW domain containing HECT E3 ligase family, have been reported to regulate BMP and TGF-ß signalling (Soond and Chantry, 2011, Seo et al., 2004, Bai et al., 2004, Kavsak et al., 2000, Zhu et al., 1999). Critical for the ubiquitylation of their substrates in these proteins is the WW domain, as it mediates the interaction to SMADs via the SMAD “PPXY” motif (Al-Salihi et

al., 2012). The PPXY motif is located at the linker region of R-SMAD proteins, with the exception of SMAD8 which lacks the PPXY motif. The binding of the E3 ubiquitin ligases to the linker region of R-SMADs is regulated by the conserved phosphorylation sites surrounding the PPXY motif within R-SMADs (Aragon et al., 2011). SMURF1 and SMURF2 have been shown to catalyse the ubiquitylation of SMAD1 and 5, as well as the ubiquitylation of TGF-ß type I and II receptor kinases, which leads to their degradation via the proteasome (Sapkota et al., 2007, Ebisawa et al., 2001, Zhu et al., 1999, Zhang et al., 2001, Kavsak et al., 2000). In addition, SMURF2 has also been linked to the ubiquitylation mediated degradation of SMAD2 (Lin et al., 2000) and monoubiquitylation of SMAD3, which does not lead to proteasomal degradation (Tang et al., 2011). NEDD4L and WWP1 have been reported to ubiquitylate SMAD2 and 3 leading to their degradation (Gao et al., 2009, Seo et al., 2004). WWP2 was recently shown to ubiquitylate SMAD2 and 3 as well as SMAD7 (Soond and Chantry, 2011). Despite the lack of a PPXY motif, SMAD4 has been reported to be ubiquitylated by SMURF1/2, NEDD4L and WWP1 (Al-Salihi et al., 2012).

The other class of E3 ubiquitin ligases involved in the regulation of BMP and TGF-ß signalling are RING domain E3 ubiquitin ligases. The RING E3 ubiquitin ligase CHIP has been reported to ubiquitylate SMAD1, 2, 3 and 4 , which results in the proteasomal degradation of SMADs and the inhibition of the BMP or TGF-ß signalling pathways (Li et al., 2004). Another RING E3 ubiquitin ligase, ARKADIA, has been reported to enhance TGF-ß signalling by binding to SMAD2 and 3 and thereby ubiquitylating other SMAD2 and 3 signal-inhibiting binding partners, such as SnoN and SMAD7 (Levy et al.,

2007, Koinuma et al., 2003). A recent study in *Zebrafish* and RNF12-/- mouse embryonic stem cells, revealed that the E3 ubiqutin ligase RNF12 impacts TGF-ß and BMP signalling by ubiquitylating SMAD7 (Zhang et al., 2012).

The RING E3 ligase TRIM33 has been shown to ubiquitylate SMAD4 in *Xenopus* (Dupont et al., 2005). The ubiquitylated SMAD4 was further shown to be unable to bind activated SMAD2 and 3, thus TRIM33 inhibits TGF-ß signalling (Dupont et al., 2005). Furthermore, the recruitment of TRIM33 to chromatin has been reported to activate TRIM33 and in turn leads to the ubiquitylation of SMAD4 (Agricola et al., 2011). On the other hand, TRIM33 has been reported to, independently of SMAD4, bind activated SMAD2 and 3 (He et al., 2006).

1.4 Transcriptional Targets of TGF-ß signalling

Once activated, R-SMAD/SMAD4 complexes in the nucleus, together with other transcriptional cofactors, assemble at the promoters of many target genes and regulate their transcription. TGF-ß ligands are reported to regulate the expression of hundreds of genes (Massague et al., 2005, Shi and Massague, 2003). To regulate the expression of these genes, SMADs bind the DNA, albeit with a much lower affinity than most other transcription factors (Chai et al., 2003). The DNA binding sites for SMADs are well-established and are known as SMAD binding elements (SBE) for TGF-ß activated SMAD2/3 and 4 complexes (Zawel et al., 1998). BMP activated SMAD1/5/8 and 4 complexes have been shown to preferentially bind to GC-rich promoter regions, also known as BMP responsive element (BRE)

(Katagiri et al., 2002, Zawel et al., 1998). Ligand induced SMADs have been reported to associate with many different transcription factors, which enhance their transcriptional activity by enhancing the DNA binding ability. These DNA binding co-factors include members of the E2F4, Mixer, FoxH1, FoxO and Runx families (Massague et al., 2005). The association of specific co-factors to SMAD proteins is cell type and context dependent and therefore helps to fine tune the BMP and TGF-ß signalling pathways (Ross and Hill, 2008).

Two of the transcriptional targets regulated by both BMP and TGF-ß signalling pathways are I-SMAD6 and 7. The expression of I-SMADs downstream of BMP and TGF-ß signalling acts as a negative feedback loop (Figure 1-1). I-SMADs have been reported to regulate the BMP and TGF-ß signalling pathways by facilitating ubiquitin E3 ligases and deubiquitylases (DUBs) to target the BMP and TGF-ß type I kinase receptor proteins as well as competing with R-SMADs for access to receptors (Al-Salihi et al., 2012)

SMAD proteins have also been reported to act on transcription by remodelling of histones and chromatin structures (Ross et al., 2006). Acetylation of histones at conserved lysine residues weakens their interaction with DNA thereby allowing transcription factors to bind to the DNA more efficiently. The binding of SMADs to histone acetylation modifiers like histone acetyltransferases (HATs) has been associated with transcriptional activation and many co-activation transcription factors display HAT activity. SMAD1, 2, 3 and 4 have been shown to interact with p300, which in turn acetylates histones in order to facilitate transcription (Ross et al., 2006).

Histone deacetylases (HDACs) inhibit transcription by reversing the acetylation of histones. Transcriptional repressors often display HDAC activity. Binding of these repressors to activated SMAD complexes as co-factors demonstrates a neat mechanism by which BMP and TGF-ß signalling pathways can inhibit transcription (Ross and Hill, 2008).

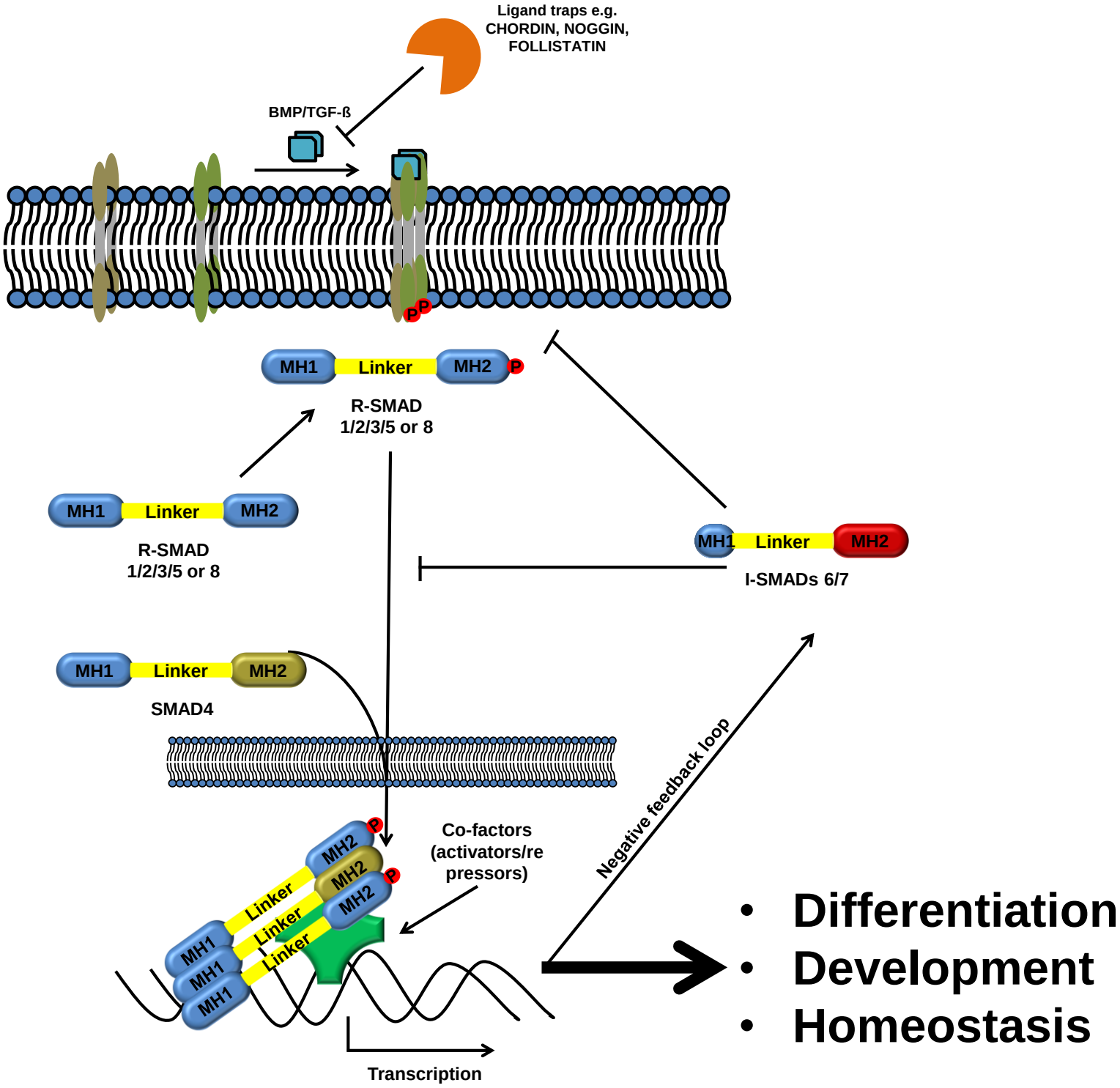

Figure 1-1 Schematic overview of the TGF-ß/BMP signalling pathway

BMP or TGF-ß ligands bind to their corresponding type I (light green) and type II (light brown) receptor kinases. This triggers the phosphorylation and activation of type I receptor kinase by type II receptor kinase. Subsequently the type I receptor kinase phosphorylates its corresponding R-SMAD. The phosphorylated R-SMADs translocate to the nucleus, where together with SMAD4 and other co-factors they regulate the transcription of hundreds of target genes that impact context-dependent cell differentiation, development and homeostasis. The expression of negative feedback genes I-SMADs 6 and 7 is also controlled by BMP/TGF-ß. The signalling pathway can also be inhibited by the ligand traps.

1.5 Non-canonical TGF-ß and BMP signalling

Activated R-SMADs binding to SMAD4 to regulate the expression of general target genes such as *ID1, SnoN* and *PAI1* is often referred to as the canonical BMP and TGF-ß signalling. However, TGF-ß and BMP ligands can exert effects on other signalling pathways and gene expression independent of R-SMAD activation or R-SMAD/SMAD4 complex formation. These are commonly referred to as non-canonical effects of BMP and TGF-ß signalling. Non-canonical BMP and TGF-ß signalling pathways are linked to the modulation of mitogen-activated protein kinases (MAPKs: ERK, JNK and p38 MAPK), PI3 kinase/AKT and protein kinase C (PKC) signalling pathways as well as Rho-GTPases (Moustakas and Heldin, 2005, Zhang, 2009). Non-canonical signalling has also been reported to be involved in processes like EMT, apoptosis and cytoskeleton rearrangement (Zhang, 2009). Some of the non-canonical signalling downstream of TGF-ß and BMP ligand could rely on non-SMAD substrates of type I/type II receptor kinases. This possibility has been poorly investigated and to date there are few or no reports of non-SMAD substrates of TGF-ß and BMP receptor kinases.

1.5.1 MAPK mediated non-canonical signalling

Most studies on non-canonical BMP and TGF-ß signalling have focussed on the activation of MAPKs. MAPKs are a large family of protein kinases that can be further divided into three subgroups: extracellular signal-regulated kinases (ERKs), c-Jun-N-terminal kinases (JNKs) and p38 MAP kinases (Yue and Mulder, 2000).

ERK1/2 are activated by TGF-ß and BMP cytokines (Zhou et al., 2007, Moustakas and Heldin, 2005). TGF-ß ligands have been shown to activate ERK1/2 via a signalling cascade from the activated receptor complex, involving the phosphorylation of ShcA, which then associates with the adapter proteins GRB2 and SOS. This leads to activation of RAS, which in turn triggers the sequential activation of c-Raf, MEK and finally ERK1/2 (Lee et al., 2007). It has been reported that GRB2 dependent ERK1/2 activation by TGF-ß ligands is essential for the TGF-ß mediated EMT (Davies et al., 2005, Galliher-Beckley and Schiemann, 2008). Interestingly, ERK1/2 also phosphorylate SMAD1, 2 and 3 at the linker region as discussed before (see section 1.3.2.2).

While BMP ligands can also induce ERK1/2 activity, reported by several research groups, in different cellular contexts, the underlying cellular process of BMP ligand induced ERK1/2 activation remains largely elusive (Finelli et al., 2013, Wiley et al., 2011, Jun et al., 2010, Zhou et al., 2007, Beck and Carethers, 2007). Nonetheless BMP-induced ERK1/2 signalling has been shown to be involved in angiogenesis (Wiley et al., 2011, Zhou et al., 2007), axon development (Finelli et al., 2013) and SMAD4 independent cell proliferation (Beck and Carethers, 2007). It is clear that understanding of the biochemical mechanisms of BMP-induced ERK1/2 activation would be essential.

Activation of JNK and p38 MAPK by TGF-ß ligands has been extensively studied (Zhang, 2009). The general activation of JNK and p38 MAPK are reported to be mediated by TRAF6, which binds to the activated

TGF-ß cell membrane receptor complexes. It has been reported that this interaction subsequently leads to the association and activation of TAK1 (Sorrentino et al., 2008, Yamashita et al., 2008). TAK1 in turn has been reported to phosphorylate MKK4 to activate JNK and MKK3/6 to activate p38 MAPK (Yamashita et al., 2008). Putting the above mechanisms in doubt, a recent study reported that the activation of p38 MAPK does not involve TAK1 but rather MAP3K4 and 10 (Sapkota, 2013). Nonetheless, TGF-ß induced activation of JNK and p38 MAP kinases has been reported to play crucial roles in apoptosis (Edlund et al., 2003), EMT (Yamashita et al., 2008), regulation of cyskeletal rearrangement (Bakin et al., 2002) as well as transcription (Sapkota, 2013).

The BMP induced activation of JNK and p38 MAPK has not been reported extensively, compared to TGF-ß. Although the biochemical mechanisms are poorly defined, BMP-induced activation of JNK and p38 MAPK has been reported to play crucial roles in apoptosis and during *Xenopus* development (Kimura et al., 2000, Shibuya et al., 1998). Further investigation is needed to shed light on the exact molecular mechanisms on how BMP and TGF-ß cytokines regulate MAPK signalling.

1.5.2 Regulation of RhoA by BMP and TGF-ß ligands

RhoA belongs to the Rho GTPase enzyme family, which is key in the regulation of cytoskeletal dynamics such as cell migration, adhesion and EMT (Heasman and Ridley, 2008). Out of the Rho GTPase family, RhoA, Rac and Cdc42 are most extensively studied (Sit and Manser, 2011). The switch in Rho GTPases from inactive (GDP-bound) to an active (GTP-bound)

from is regulated by GTPase-activating proteins (GAPs), guanine-nucleotide-exchange factors (GEFs) and guanine nucleotide-dissociation inhibitors (GIDs) (Bishop and Hall, 2000).

The TGF-ß induced active type I and II receptor complex has been shown to bind to PAR6 in tight junctions, resulting in its phosphorylation by type II receptor kinase. PAR6 together with SMURF1, which is recruited by phosphorylated PAR6, binds to RhoA and leads to its ubiquitylation followed by proteasomal degradation. Dissociation of RhoA in tight junctions in response to TGF-ß ligands is associated with separation of tight junctions, a key event in TGF-ß induced EMT (Ozdamar et al., 2005). More recently, this pathway has been linked to BMP signalling, where it was reported that both TGF-ß and BMP cytokines are able to induce EMT via the PAR6/SMURF1/RhoA signalling cascade, albeit involving TGF-ß receptor type III .(Sanchez and Barnett, 2012, Townsend et al., 2011).

1.5.3 Regulation of the PI3-kinase signalling cascade by BMP and TGF-ß cytokines

Upon TGF-ß ligand stimulation, type I receptor kinase associates with the phosphatidylinositide 3 kinase (PI3K) via its regulatory subunit p85 (Yi et al., 2005). This association subsequently leads to the activation of AKT by PI3K. AKT is a downstream mediator of PI3K signalling and is phosphorylated by 3-phosphoinositide-dependent protein kinase 1 (PDK1) and mammalian target of rapamycin complex 1 (mTORC1). TGF-ß activation of PI3K, AKT and subsequent mediators such as mTORC1 and S6 kinase (S6K), was reported to induce changes in protein synthesis, that ultimately

led to TGF-ß induced EMT (Lamouille and Derynck, 2007). More recently, mTOR complex 2 has also been implicated in TGF-ß mediated EMT by a similar mechanism (Lamouille et al., 2012). BMP ligands were also reported to induce the phosphorylation of AKT. PI3K mediated activation of NFκB was reported to be induced by BMP ligands, which resulted in the inhibition of CASPASES and subsequently in the prevention of apoptosis in chondrocytes (Sugimori et al., 2005). In a similar cell system, BMP mediated PI3K activity was also reported to activate NFκB signalling (Fong et al., 2008). However, the molecular mechanism of PI3K activation by BMP ligands remains to be defined.

1.6 Aberrant BMP and TGF-ß signalling in human diseases

Due to the global impact of BMP and TGF-ß signalling pathways, it is not surprising that the malfunction of specific components of these pathways can have severe outcomes. Overexpression of BMP and TGF-ß cytokines and mutations of multiple pathway components are linked to many somatic and hereditary disorders. These include diseases that range from immune and cardiovascular disorders to cancer progression and metastasis. In this chapter, I summarise some of the most common disorders related to BMP and TGF-ß signalling.

1.6.1 Aberrant BMP and TGF-ß signalling in hereditary diseases

1.6.1.1 Ligand related diseases

One of the most studied autosomal dominant disorders related to TGF-ß signalling is the Marfan syndrome. It occurs in approximately 1 in every 4000 individuals. It is a connective tissue disease, that was linked to mutations in *FBN1* gene (Dietz et al., 1991). *FBN1* encodes FIBRILLIN1, an important extra-cellular matrix glycoprotein required for the formation of elastic fibres in connective tissue (Kielty et al., 2002). FIBRILLIN1 binds to TGF-ß cytokines and inhibits TGF-ß signalling. Mutations in FIBRILLIN1, which result in lower levels of FIBRILLIN1 expression, leads to increased TGF-ß signalling, leading to the failure of vascular system and lung disorders (Neptune et al., 2003).

Mutations in the *NOG* gene, which are reported to cause partial loss of NOGGIN function, are associated with a disorder called Brachydactyly Type B (BTB). The hypothesis is that NOGGIN partially fails in controlling the BMP signalling pathway especially during the development of hands and feet resulting in abnormally fused finger and toe joints (Lehmann et al., 2007).

Persistent Müllerian duct syndrome (PMDS) is an autosomal recessive congenital disease characterised by development of female organs in males. PMDS type I is caused by mis-regulation of AMH cytokines, leading to developmental disorders during embryogenesis (Belville et al., 1999). The expression of AMH is required during normal embryogenesis in order to

prevent the development of female organs like uterus in males. Usually the levels of AHM are not sufficient in patients with PMDS type I to prevent the development of female organs (Josso et al., 2005).

1.6.1.2 Disorders related to intracellular TGF-ß and BMP pathway components

Some of the hereditary diseases are linked to mutations in type I and type II receptor kinases. PMDS type II is one such example, as it is also known to be caused by mutations in AHM type II receptor (Imbeaud et al., 1996). Marfan syndrome has also been described to result from mutations in TGF-ß type I and type II receptor kinases (Matyas et al., 2006).

Other diseases known to be caused by aberrant TGF-ß or BMP cell membrane receptors include the Loeys-Dietz syndrome (LDS) and hereditary haemorrhagic telangiectasia (HHT) (Loeys et al., 2005, Abdalla and Letarte, 2006, Johnson et al., 1996). LDS has been associated with inactivating mutations in TGF-ß receptor type I and II. Some of the LDS patient phenotypes are similar to those seen in patients with Marfan syndrome, as LDS patients can suffer from aortic rupture (Dietz et al., 2005). Patients with HHT have developmental disorders in blood vessels in skin and internal organs that can lead to bleeding (Govani and Shovlin, 2009). HHT has been linked to mutations in ALK1 and its co-receptor endoglin (Abdalla and Letarte, 2006, Johnson et al., 1996).

Furthermore, inactivating mutations in TGF-ß receptor type I gene *TGFBR1* have been associated with multiple self-healing squamous epithelioma (MSSE). MSSE is an autosomal dominant disorder that displays aggressive and invading skin tumours that spontaneously self-heal within a few weeks (Goudie et al., 2011).

The most studied hereditary disorder associated with SMAD proteins is Juvenile polyposis syndrome (JPS). Juvenile polyposis describes the formation of spontaneous polyps in the gastrointestinal tract in young children. Autosomal dominant mutations of SMAD4 and ALK3 have been reported in patients with JPS (Sayed et al., 2002, Howe et al., 1998).

1.6.2 The role of BMP and TGF-ß signalling pathways in cancer

Not all disorders that have been linked to BMP and TGF-ß signalling components are hereditary as aberrant signalling in somatic cells, as a result of mutations or epigenetic changes, are often associated with cancer. BMP and TGF-ß signalling in normal epithelial cells controls proliferation, causes growth arrest and can induce apoptosis. Thus it acts as a tumour suppressor (Massague, 2008, Inman, 2011, Ikushima and Miyazono, 2010, Wakefield and Hill, 2013). The crucial steps in cancer development driven by TGF-ß and BMP signalling are that cancerous cells and tumours develop mechanisms that turn BMP and TGF-ß signalling from tumour suppressors to tumour promoters. Some mutations in key signalling components render the pathways inactive thereby losing the cytostatic potential. Other more subtle mutations of certain components not only inactivate the growth inhibitory effects of TGF-ß but also enhance tumour traits, such as epithelial to

mesenchymal transition and induction or angiogenesis, that promote tumour progression (Inman, 2011, Massague, 2008).

In normal cells, TGF-ß signalling controls and limits proliferation by regulating the expression of CDK inhibitors such as p15, p21 or p27 (Siegel and Massague, 2003). In order to evade the growth inhibition of TGF-ß signalling, inactivating mutations of the TGF-ß type I and II receptor kinases or SMAD4 are found in many cancers (Ikushima and Miyazono, 2010, Xu and Pasche, 2007, Goggins et al., 1998, Schutte et al., 1996). SMAD4 has long been known as a tumour suppressor as it has been reported to be mutated in ~50% of pancreatic tumours (Hahn et al., 1996).

Loss of SMAD4 expression or its mutation and mutations of BMP receptor type I play important role in colorectal cancer in order to evade the growth inhibitory effects of TGF-ß and BMP signalling (Zhang et al., 2010, Kodach et al., 2007). In contrast other cancers, such as certain types of aggressive breast cancer, have been reported to exploit TGF-ß signalling to enhance their metastatic ability (Massague, 2008). MDA-MB-231 breast cancer cells have been reported to require SMAD4 expression for metastasis (Deckers et al., 2006).

The role of BMP signalling pathways in cancer in general has not been covered as extensively as the TGF-ß signalling pathway in terms of number of research reports. However it is clear that BMP signalling plays a crucial role in many different cancers and impacts cancer progression. Nonetheless, the role of BMP signalling, especially the BMP antagonists, in cancer remains

elusive (Singh and Morris, 2010, Wakefield and Hill, 2013). Bone metastasis is the most common secondary tumour site in prostate cancer progression and these are accompanied by aberrant BMP signalling (Ye et al., 2007). Prostate cancer is usually dependent on androgen receptor (AR) signalling. Therefore the androgen-deprivation therapy (ADT) is often used to treat prostate cancer. Once the cancer becomes resistant to ADT at latter stages, the cancer becomes more aggressive and the mortality rates are increased (Klotz, 2000, Labrie et al., 2004). Interestingly, the proliferative inhibition by the BMP signalling pathway was reported to be diminished in androgen insensitive compared to sensitive prostate cancer cell lines (Brubaker et al., 2004, Ide et al., 1997). A direct link between AR and BMP signalling has also been reported. Linker phosphorylated SMAD1 was shown to interact to AR in response to androgen or BMP in androgen sensitive prostate cancer cells (Qiu et al., 2007).

1.7 Aims of the thesis

The fundamental steps in the TGF-ß and BMP signalling pathway, as described above, have been well established. However, many aspects of the signalling pathways pertaining to their regulation are still not completely defined. In order to identify novel regulators of BMP signalling and understand the molecular mechanisms by which BMP signalling is regulated in cells, a proteomic approach was undertaken to identify interactors of SMADs. FAM83G/PAWS1 was identified as a novel Protein Associated With SMAD1. The first aim of my thesis is to characterise the role of FAM83G/PAWS1 in regulating BMP signalling and its potential impact on other signalling networks.

Specific small molecule inhibitors of type I BMP and TGF-ß receptors are routinely employed to dissect the TGF-ß and BMP pathways and are useful in characterising the roles of novel pathway regulators. Furthermore selective small molecule inhibitors have therapeutic potential to control diseases caused by aberrant TGF-ß and BMP signalling. However, it is critical to establish the specificities and potencies of small molecule inhibitors against their intended targets. For the second aim of my thesis, I characterise the specificities and potencies of the most commonly employed small molecule inhibitors of the TGF-ß and BMP pathways.

2 Materials and Methods

2.1 Materials

2.1.1 Reagents

Reagent	Source
1 Kb Plus DNA Ladder	Life Technologies Inc
A-83-01	Tocris Bioscience
Acetic acid	BDH Chemicals Ltd.
Acetone	BDH Chemicals Ltd.
Acetonitrile (HPLC grade)	Rathburn Chemicals
Acrylamide:bis-acrylamide (40% (w/v) 29:1)	Flowgen Bioscience
Adenosine 5'-triphosphate (ATP)	Roche
agarose (electrophoresis grade)	Life Technologies Inc
ammonium persulphate	Sigma-Aldrich
ampicillin	Sigma-Aldrich
Blasticidin	Life Technologies Inc
BMP-2	R&D Systems
bromophenol blue	Sigma-Aldrich
Colloidal Coomassie Blue staining kit	Life Technologies Inc
Complete protease inhibitor cocktail tablets	Roche
Coomassie brilliant blue G-250	Sigma-Aldrich
Coomassie protein assay reagent (Bradford reagent)	Pierce
dimethyl sulphoxide (DMSO)	Sigma-Aldrich
Dithiobis succunimidyl propionate (DSP)	Thermo Scientific
dithiothreitol (DTT)	Sigma-Aldrich
Dorsomorphin	Sigma-Aldrich
Dulbecco's modified Eagle medium (DMEM)	Life Technologies Inc
Dulbecco's phosphate buffered saline (PBS)	Life Technologies Inc
Ethanol	BDH Chemicals Ltd.
FLAG-agarose	Sigma-Aldrich
foetal bovine serum (FBS)	Sigma-Aldrich
G418	Life Technologies Inc
GFP-Trap agarose beads	Chromotek
Glycerol	BDH Chemicals Ltd.
HA-agarose	Sigma-Aldrich

Reagent	Source
Hygromycin-B	Life Technologies Inc
IgG–free BSA	Jackson Immunoresearch
Immobilon Western chemiluminescent HRP substrate (ECL)	Merck-Millipore
Isopropanol	BDH Chemicals Ltd.
LDN-193189	Stemgent
L-glutamine	Life Technologies Inc
LY-364947	Sigma-Aldrich
Magnesium acetate	BDH Chemicals Ltd.
Manganese chloride	BDH Chemicals Ltd.
Methanol	BDH Chemicals Ltd.
Microcystin-LR	Life Technologies Inc
NE-PER Nuclear and Cytoplasmic Extraction Kit	Thermo Scientific
Nitrocellulose membranes	Schleicher and Schuell
NuPAGE MOPS running buffer (20x)	Life Technologies Inc
NuPAGE Novex 4-12% Bis-Tris polyacrylamide gels	Life Technologies Inc
Opti-MEM	Life Technologies Inc
Penicillin/streptomycin	Life Technologies Inc
Plasmid Maxi kit	Qiagen
polyethylene glycol sorbitan monolaurate (Tween-20)	Sigma-Aldrich
polyethylenimine (PEI)	Sigma-Aldrich
Polyvinylidene fluoride (PVDF) membrane	Merck-Millipore
Ponceau S solution	Sigma-Aldrich
Prestained See Blue protein markers for SDS-PAGE	BioRad
ProLong Gold mounting reagent	Life Technologies Inc
Protein G Sepharose	Life Technologies Inc
puromycin dihydrochloride	Sigma-Aldrich
RNeasy kit	Qiagen
SB-431542	Sigma-Aldrich
SB-505124	Sigma-Aldrich
Skimmed milk powder	Premier Brands
Sodium acetate	BDH Chemicals Ltd.
Sodium chloride	BDH Chemicals Ltd.
Sodium dodecyl sulphate	BDH Chemicals Ltd.
Sodium ethylenediaminetetraacetate (EDTA)	BDH Chemicals Ltd.
ß-mercaptoethanol (biochemical grade)	Sigma-Aldrich
Sucrose	BDH Chemicals Ltd.
Superscript VILO cDNA kit	Life Technologies Inc

Reagent	Source
SuperSignal West Pico Chemiluminescent Substrate	Thermo Scientific
SYBR green	BioRad
SYBR® Safe	Life Technologies Inc
tetramethylethylenediamine (TEMED)	Sigma-Aldrich
TGFß1	R&D Systems
t-octylphenoxypolyethoxyethanol (Triton) X-100	Sigma-Aldrich
Transfectin	BioRad
tris (hydroxymethyl) methylamine (Tris)	BDH Chemicals Ltd.
Trypsin Gold mass spectrometry grade	Promega
Trypsin-EDTA	Life Technologies Inc
urea	Sigma-Aldrich
Zeocin	Life Technologies Inc

Table 2-1 Reagents used in this thesis

2.1.2 Buffers and solutions

Polyethylenimine (PEI): 1mg/ml PEI in 25mM HEPES pH7.5.

TBS-Tween (TBS-T): 50 mM Tris/HCl pH 7.5, 0.15M NaCl and 0.25% (v/v) Tween-20.

Buffer A: 50mM Tris/HCl pH 7.5, 0.1mM EGTA and 0.1% (v/v) ß-ME.

TAE Buffer: 40mM Tris-Acetate pH 8, 1mM EDTA.

DNA loading dye: 20 mM EDTA pH 8, 50% (v/v) glycerol, 0.05% (w/v) bromophenol blue.

5x SDS Sample Buffer: 5% (w/v) SDS, 5% (v/v) ß-ME, 50mM Tris/HCl pH 6.8, 6.5% (v/v) glycerol and 0.02% (w/v) bromophenol blue.

SDS-PAGE Buffer: 25mM Tris/HCl pH 8.3, 192mM glycine, 0.1% SDS (v/v).

SDS.Transfer Buffer: 25mM Tris/HCl pH 8.3, 192mM glycine, 20% (v/v) methanol.

Luria Bertani broth plus Ampicillin (LB-Amp):

1% (w/v) tryptone peptone, 0.5% (w/v) yeast extrac, 86mM NaCl, 100 µg/ml Ampicillin after autoclaving for 20 min

LB-Amp plates: 1% (w/v) tryptone peptone, 0.5% (w/v) yeast extrac, 86mM NaCl, 2% (w/v) bacto-agar 100 µg/ml Ampicillin after autoclaving for 20 min

Gel filtration buffer: 150mM NaCl, 50mM Tris/HCl pH 7.5, 0.03% (v/v) Brij35. Bacterial lysis buffer: 25mM HEPES pH 7.6, 10% glycerol (v/v), 0.1mM EDTA, 150mM KCl, 1mM DTT, 1mM PMSF, 1 tablet of Complete protease inhibitor per 50ml lysis buffer.

Kinase assay buffer: 50mM Tris/HCl pH 7.5, 0.1% ß-mercaptoethanol, 0.1 EGTA, 10 mM $MgCl_2$, 0.5 µM Microcystein-LR

Lysis buffer: 50mM Tris/HCl pH 7.4, 0.27M sucrose, 150mM NaCl, 1mM EDTA pH 8.0, 1mM EGTA pH 8.0, 1mM sodium orthovanadate, 10mM sodium ß-glycerophosphate, 50mM sodium fluoride, 5mM sodium pyrophosphate, 1% v/v) Triton X-100, 0.5% (v/v) Nonidet P-40, 0.1% (v/v) ß-mercaptoethanol (ß-ME) and complete protease inhibitors.

Lysis buffer with DSP cross-linking agent:

40mM HEPES pH 7.4, 120mM NaCl, 1mM EDTA pH 8.0, 10mM sodium ß-glcerophosphate, 50mM sodium fluoride, 1mM sodium orthovanadate, 5mM sodium pyrophosphate, 1% (v/v) Triton X-100, complete protease inhibitors, 2.5mg/ml DSP added drop wise immediately prior to usage.

2.1.3 Plasmids

Mammalian expression constructs encoding human SMAD1, SMAD2, SMAD3, SMAD4, SMAD5, SMAD6, SMAD7, SMAD8, FAM83G/PAWS1, CULLIN3 and various truncation or point mutants of these genes (Table 2-2) were cloned into either pCMV5 or pcDNAFrtTO (Life Technologies, Paisley, U.K) vectors with N-terminal FLAG, haemagglutinin (HA) or green fluorescent protein (GFP)-tags. Untagged FAM83G/PAWS1 and various point mutants were in addition cloned into pBABE-puro. pCMV-Gag-Pol and pCMV-VSVG constructs were purchased from Cell Biolabs Inc. All plasmids used in this study are listed in Table 2-2.

For bacterial expression, constructs encoding N-terminal GST-tagged FAM83G/PAWS1, SMAD1, SMAD2 and mutants of these genes were cloned into pGex6p vector and subsequently transformed into BL21 cells. All constructs, unless stated otherwise, used in this thesis were generated the cloning team at the DSTT (Table 2-2). For baculoviral expression, constructs encoding N- or C-terminal GST-or 6x HIS tagged FAM83G/PAWS1, ALK5 and mutants of these genes were cloned into pFB GST-expression vectors. All DNA constructs employed were verified by DNA sequencing, performed by DNA Sequencing & Services (MRC PPU, College of Life Sciences, University of Dundee, Scotland, www.dnaseq.co.uk) using Applied Biosystems Big-Dye Ver 3.1 chemistry on an Applied Biosystems model 3730 automated capillary DNA.

DU number	Plasmid	Source
DU33273	**pCMV5-FLAG-1 PAWS1**	Thomas Macartney
DU19263	**pCMV5-HA-1 SMAD1**	Thomas Macartney
DU19305	**pCMV5-HA-1 SMAD2**	Thomas Macartney
DU19396	**pCMV5-HA-1 SMAD3**	Thomas Macartney
DU19308	**pCMV5-HA-1 SMAD4**	Thomas Macartney
DU19310	**pCMV5-HA-1 SMAD5**	Thomas Macartney
DU19604	**pCMV5-HA-1 SMAD6**	Thomas Macartney
DU19220	**pCMV5-HA-1 SMAD7**	Thomas Macartney
DU19568	**pCMV5-HA-1 SMAD8**	Thomas Macartney
	pCMV5-HA-1 SMAD1 MH1	Gopal Sapkota
	pCMV5-HA-1 SMAD1 MH1+Linker	Gopal Sapkota
	pCMV5-HA-1 SMAD1 Linker	Gopal Sapkota
	pCMV5-HA-1 SMAD1 MH2	Gopal Sapkota
DU33272	**pcDNA5-FRT/TO-GFP PAWS1**	Thomas Macartney
DU33460	**pBabe.puro PAWS1**	Thomas Macartney
DU33461	**pBabe.puro PAWS1 S610A**	Thomas Macartney
DU19338	**pcDNA5-FRT/TO-GFP SMAD4**	Thomas Macartney
	pBabe.puro Control	Thomas Macartney
DU19269	**pGEX6P-1-SMAD1**	Thomas Macartney
DU19395	**pGEX6P-1-SMAD2**	Thomas Macartney
DU19440	**pGEX6P-1-PAWS1 (523-end)**	Thomas Macartney
DU33233	**pGEX6P-1-PAWS1 (523-end) S610A**	Thomas Macartney
DU33235	**pGEX6P-1-PAWS1 (523-end) S613/14/16A**	Thomas Macartney
DU42168	**pBabe.puro mPAWS1**	Simone Weidlich
DU33547	**pFB GST ALK4 T204D 200-end**	Thomas Macartney
DU33574	**pFB GST ALK5 T204D 200-end**	Thomas Macartney
DU33022	**pGEX6P-1-PAWS1 (753-815)**	Thomas Macartney

Table 2-2 Plasmids used in this thesis

2.1.4 qRT-PCR Primers & siRNA oligonucleotide sequences

Human qRT-PCR primers were designed by PerlPrimer® and ordered from Life technologies and are listed in Table 2-3. *siRNA* oligonucleotides were purchased from Qiagen and are listed in Table 2-4.

Target	Sequence (5'-3')
GAPDH	F- TGCACCACCAACTGCTTAGC R- GGCATGGACTGTGGTCATGAG,
HPRTI	F- TGACACTGGCAAAACAATGCA R- GGTCCTTTTCACCAGCAAGCT

Target	Sequence (5'-3')
PAWS1	F- CACAGAAGGTGATAGCTGTG R- ACTTGACGTTACTCTCATCCA
FOXO4	F- TTGGAGAACCTGGAGTGTGACA R- AAGCTTCCAGGCATGACTCAG
ID1	F- AGGCTGGATGCAGTTAAGGG R- GGTCCTTTTCACCAGCAAGCT
NEDD9	F- GCTCTATCAAGTGCCAAACCC, R- GGTTCCCCCAATGCTTCTCT)
ASNS	F- AACTGCTGCTTTGGATTTCAC R- GCTGTTGCATCTTCTTATGGT
BMPR2	F- TGGAACATACCGTTTCTGCT R- GAATGAGGTGGACTGAGTGG
TGFBI	F- ATCACCAACAACATCCAGCA R- CCGTTACCTTCAAGCATCGT,
FST	F- GATCTTGCAACTCCATTTCGG R- GGCTATGTCAACACTGAACAC,
TGFBR2	F- GCTGTATGGAGAAAGAATGACGA R- ACAGGAACACATGAAGAAAGTC,
TSC22D1	F- CTATCAGTGGTGACAGTGGG. R- TTCACTAGATCCATAGCTTGCTC
WASF3	F- CATGCTGAAGACATATTTGGTGAG R- TCCTGTAGTGAGACCTCTTCC
CCNA1	F- CCCTATGCTGGTAGATTCATCTC R- GTGCCTTATTTCAGCTTCCCT
NPY1R	F- GTGGAGTTCGGCTTTAAGGA R- TGAACTGAACAATCCTCTTTGG
BEX1	F- TAGGCCCAGGAGTAATGGAG R- CCTACGATTTCCTCTAGGCAC
CKAP2	F- GGTCTGAGGAAGTTCTATCTTGG R- TTCTTTGCTCTTTGAATGCGG
MMP1	F- TAAAGACAGATTCTACATGCGC R- GTATCCGTGTAGCACATTCTG
LRP4	F- GGATTGCCAAGACTCAAGGA R- CAAGACAAATGGATGTTCTCTAGG,
ARHGAP44	F- AGGCTCTATGGAATGCTTGTG R- GTAATGTTCCCTTCTGCTTGTG,
TPX2	F- CCAAAGAAGATGAGGAAGAGGA R- AGAATCAAACGAGAAAGGGCA,
PDGFRA	F- GGAGAAGTGAAAGGCAAAGG. R- CAGCACATTCGTAATCTCCAC
PDZRN3	F- ACAGGATTATTGAGGTCAACGG R- ATGTTCAAAGGTGATGTCGGT
GTF2F2	F- GGATTGCCAAGACTCAAGGA R- CAAGACAAATGGATGTTCTCTAGG
MLLT11	F- TTGATAACAGGAAGCTATGAGGG R- TTGTAGGTGGCTGTATCTGAC
AR	F- CCTGGCTTCCGCAACTTACAC R- GGACTTGTGCATGCGGTACTC
MMP13	F- CAGTCTTTCTTCGGCTTAGAGG R- GGGTGTAATTCACAATTCTGTAGG

Table 2-3 qRT-PCR primers used in this thesis

Target	Sequence (5'-3')
PAWS1-1	AAGATGATGACGACTACGTAA
PAWS1-2	CCGGGCTAGCGTCTACATGCA
FOXO4	CCCGACCAGAGAUCGCUAA

Table 2-4 siRNA used in this thesis

2.1.5 Antibodies

Antibodies raised in sheep or rabbit (Table 2-5) using standard protocols of the Division of Signal Transduction and Therapy (DSTT), School of Life Sciences, University of Dundee. The antibodies were affinity purified on CH-Sepharose covalently coupled to the antigens used to raise the antibodies. For the purification of phospho-specific antibodies, the antibodies purified on the column containing the phosphopeptide immunogen were passed through a peptide column made with the non-phosphorylated form of the peptide immunogen. The antibodies that did not bind to the non-phosphorylated peptide column were collected and used.

Antibody	Company	Product ref	Source	Ab Dilution	Ab Conditions
Flag-M2 HRP	Sigma	A 8592	mouse	1:2000	Milk
GFP	Cell Signaling	#2555	rabbit	1:2000	Milk
HA HRP	Roche	12 013 819 001	rat	1:2000	Milk
GAPDH	Cell Signaling	#2118	rabbit	1:5000	Milk
LAMIN A/C	Cell Signaling	#2032	rabbit	1:1000	Milk
P-SMAD1/5/8	Cell Signaling	#9511	rabbit	1:1000	Milk
p-SMAD2	Cell Signaling	#3101	rabbit	1:1000	Milk
p-SMAD3	Rockland Ind.	600-401-919	rabbit	1:2000	Milk

Antibody	Company	Product ref	Source	Ab Dilution	Ab Conditions
Cullin3	DSTT	S347D	sheep	1:1000	Milk
SMAD2/3	Cell Signaling	#3102	rabbit	1:1000	Milk
Cyclin A	Cell Signaling	#4656	mouse	1:1000	Milk
SMAD4	Cell Signaling	#9515	rabbit	1:1000	Milk
Cyclin D	Cell Signaling	#2922	rabbit	1:1000	Milk
p44/42 MAPK	Cell Signaling	#9102	rabbit	1:1000	Milk
Cyclin E	Cell Signaling	#4132	rabbit	1:1000	Milk
PLK1	Cell Signaling	#4513	rabbit	1:1000	Milk
Fibronectin	Sigma	F3648	rabbit	1:2000	Milk
P-p38	Cell Signaling	#9211	rabbit	1:1000	Milk
p38	Cell Signaling	#9212	rabbit	1:1000	Milk
E-cadherin	Cell Signaling	#3195	rabbit	1:1000	Milk
FAM83G/PAWS1	DSTT	S876C	sheep	1:1000	Milk
SMAD1	DSTT	S618C	sheep	1:1000	Milk
P-FAM83G/PASW1	DSTT	R2783	rabbit	1:1000	Milk
P-SMAD1 S206	Cell Signaling	#5753	rabbit	1:500	Milk

Table 2-5 Antibodies used in this thesis

2.1.6 Proteins and Enzymes

N- or C-terminal GST- or 6x His-tagged FAM83G/PAWS1, SMAD1, SMAD2 and various mutants of these proteins were all expressed and purified by the Protein Production Team (DSTT) (Table 2-2). N-terminal GST-tagged ALK2, ALK3 and ALK6 were purchased from Carna Biosciences.

2.2 Methods

2.2.1 Cell culture

Human Keratinocytes (HaCaT), breast cancer MDA-MB231, osteosarcoma U2OS, HEK293, colon carcinoma RKO, breast cancer MCF7, human myeloid leukemia KBM-7, HeLa and prostate cancer PC3 cells were cultured at 37°C in a humidified incubator with 5% CO_2 in Dulbecco's modified Eagle's medium (DMEM) supplemented with 10% (v/v) foetal bovine serum (FBS), 100units/ml penicillin, 100µg/ml streptomycin and 2mM L-glutamine (standard medium). HEK293 T-Rex cells (Life Technologies) were grown in standard medium plus the addition of 15µg/ml Blasticidin and 100µg/ml zeocin (both Life Technologies). PC3 put-back cell lines were grown in standard medium plus the addition of 2 µg/ml puromycin. All cells, unless stated otherwise, were grown in 10-cm plates with 10ml of media solution covering them. When cells were passaged, the culture medium was removed and they were washed once with sterile Dulbecco's phosphate buffered saline (PBS). 1 to 3ml of sterile trypsin/EDTA was added per plate (depending on cell type) to disassociate them from the plate surface. The plates were then returned to a 37ºC incubator for 5-25 minutes, depending on the adherence of the cell line. Detached cells were re-suspended in 10 ml of standard media. The cell suspension was carefully pipettes up and down several times to prevent cell clumps. The cell suspension was subsequently used to seed the desired number of new plates.

2.2.2 Cell transfections

Cells were grown to a confluency of about 50-60% and then transfected with plasmids using 25µl of 1mg/ml polyethylenimine (PEI, Polysciences) in 1ml DMEM with a maximum of 10µg plasmid DNA. The transfection mix was vortexed for 15 seconds before incubation at room temperature (RT) for 15 minutes. The transfection mix was then carefully added to the cells. 16h after the transfection, the media was replaced with fresh media and cells were lysed 48h post transfection, if not stated otherwise. *SiRNA* was transfected using Transfectin (BioRad). A total of 300pmols of *siRNA* oligonucleotides was used for a 10 cm plate. The cells were transfected directly at the time of seeding during passaging. The transfected cells were lysed at 48h after the transfection. The oligonucleotide sequences of the *siRNA*'s are listed in Table 2-4.

2.2.3 Generation of cell lines stably expressing pBABE-puromycin constructs

A retroviral system was used to generate cell lines that stably express a protein at comparable levels to endogenous protein expression. Retroviral pBABE-puromycin control vector (1 µg each) or vectors encoding human or mouse untagged FAM83G/PAWS1 or FAM83G/PAWS1 S610A were co-expressed with CMV-Gag/Pol (0.9µg) and CMV-VSVG (0.1µg) constructs in HEK-293T cells. Retroviruses were collected 48h-post transfection from the culture media by filtering it through 0.25 µm filters into sterile falcon tubes. PC3 or NMuMG cells, plated at ~40% confluent for 24-h, were infected by transferring the filtered retroviruses directly onto the cells together with 8

µg/ml Polybrene reagent. The cells were cultured in selection medium containing puromycin (2 µg/ml) for selection of infected cells, 24h after infection. Immunoblots using cell extracts with a PAWS1 antibody was used to verify the expression of infected cells.

2.2.4 Generation of tetracycline inducible Flp-IN® HEK293 and U2OS cells stably integrated with N-terminally GFP-tagged proteins

FLP-In T-Rex HEK293 or U2OS cell lines (Life Technologies) were used to generate stably expressing tetracycline inducible GFP-FAM83G/PAWS1 cell lines. These cells were maintained as described in section 2.2.1. The antibiotics zeocin and blasticidin were added to the media to select for the FLP recombination target (FRT) sites and tetracycline repressor sequence, respectively. 2 passages before the transfection, cells were split into 10 cm plates containing standard medium and grown to a confluence of about 70%. Transfections were performed using PEI with 1µg pcDNA5FRT GFP-FAM83G/PAWS1 and 9µg of pOG44 plasmid (Life Technologies). pOG44 encodes the FLP recombinase that leads to site specific recombination of the sequence of interest. 24h after transfection the medium was replaced with fresh DMEM plus the addition of 15µg/ml blasticidin and 50µg/ml hygromycin-B. Hygromycin-B selection is to ensure the correct integration of the sequence of interest. This selection media was changed at least every four days until cell colonies were visible under the microscope. To test the correct expression of GFP-FAM83G/PAWS1, the cells were treated with 20 ng/ml doxycycline for a time course of 4h to 24h and the expression assessed by fluorescence microscopy and immunoblotting.

2.2.5 Cell lysis

Cells were lysed in 4°C cold lysis buffer (50mM Tris/HCl pH 7.4, 0.27M sucrose, 150mM NaCl, 1mM EDTA pH 8.0, 1mM EGTA pH 8.0, 1mM sodium orthovanadate, 10mM sodium ß-glycerophosphate, 50mM sodium fluoride, 5mM sodium pyrophosphate, 1% (v/v) Triton X-100, 0.5% (v/v) Nonidet P-40, 0.1% (v/v) ß-mercaptoethanol (ß-ME), 1µg/ml microcystin-LR and complete protease inhibitors (Roche). When the chemical cross-linking agent Dithiobis (succinimidyl propionate) (DSP; Thermo Scientific) was used, cells were lysed in 4°C cold HEPES lysis buffer (40mM HEPES pH 7.4, 120mM NaCl, 1mM EDTA pH 8.0, 10mM sodium pyrophosphate, 50mM sodium fluoride, 1mM sodium orthovanadate, 5mM sodium pyrophosphate, 1% (v/v) Triton X-100, complete protease inhibitors) containing 2.5mg/ml DSP, which was added just before usage. Cell extracts were subsequently incubated at 4°C for 30min before DSP was quenched with 1M Tris/HCl pH 7.5 at a final concentration of 0.2M. Cell extracts were further incubated for 30min at 4°C before subsequent usage. Extracts were boiled for 5min in 1x sodium dodecyl sulphate (SDS) sample buffer containing either 1% ß-mercaptoethanol or 50mM dithiothreitol (DTT).

2.2.6 Protein concentration determination

The concentration of proteins in cell extracts was determined using the Bradford method (Bradford, 1976). This assay is done by extrapolating the protein concentration from a standard curve determined with known concentration of protein standards. This was performed with a BSA standard solution with dilutions ranging from 0.1 mg/ml to 5 mg/ml. The standards

were diluted in millipore water in order to get to a final volume of 0.1ml. These solutions were subsequently mixed with 0.9ml Bradford reagent (Thermo Scientific) in 1.5 ml plastic cuvettes. The final mixture was incubated for at least 5 minutes at RT. The measurement of all the standards and samples was done using a photospectrometer with a wavelength of 595 nm after it has been normalised to a blank probe containing only 0.1ml distilled water and 0.9ml Bradford reagent. 1 to 2 µl of the extracts were diluted in distilled water to a final volume of 0.1ml and mixed again with 0.9ml Bradford reagent as before. If needed, an additional dilution was done to maintain the absorbance of each sample within the linear range of the Bradford asaay (Absorbance at 595nm between 0.1 and 0.7). All Bradford measurements were performed in duplicate.

2.2.7 Immunoprecipitation

To minimise unspecific binding of proteins to the solid phase resins, the cleared extracts were subjected to pre-clearing by incubating with the appropriate resin (agarose or protein-G Sepharose) for 1h at 4°C prior to immunprecipitation (IP). The pre-cleared extracts were then subjected to IPs with anti-FLAG or anti-HA agarose beads (Sigma-Aldrich), GFP-Trap agarose beads (Chromotek) or appropriate pre-immune IgG or antibodies coupled to protein G-Sepharose beads. For standard IPs, 1 to 2 mg of the cell extract protein was incubated with the appropriate resin. Large scale endogenous IPs and proteomic fingerprinting generally were done using >50 mg of cell extract proteins. IPs were performed for up to 4 h at 4°C with constant shaking. Then the beads were collected by centrifugation at 5000 rpm for 1 min and the supernatant was removed (an aliquot was collected to detect the

efficiency of immune-depletion of the appropriate target). The beads were washed twice with lysis buffer containing 0.5 M NaCl and 0.1% (v/v) ß-mercaptoethanol and twice with Buffer A (50 mM Tris/HCl pH 7.4, 0.1 mM EGTA and 0.1% (v/v) ß-mercaptoethanol) at 4°C. The IPs were reconstituted in 50 µl Buffer A and 1x SDS sample buffer with 1% (v/v) ß-mercaptoethanol and boiled for 5 min prior to SDS-PAGE.

2.2.8 Conjugation of antibodies to protein G Agarose and Sepharose

The required volumes of protein G-Agarose/Sepharose beads were washed twice in PBS (1 ml) and the final volume was adjusted to 50% (v/v) slurry in PBS prior to antibody conjugation. For each IP, 2-5 µg of the antibody was added to 20 µl of protein G Agarose or Sepharose beads slurry. This mixture was left on a shaker at 4°C to allow conjugation of the antibodies to the protein-G beads. After 1h, the beads were washed twice in PBS and re-suspended as 50% (v/v) slurry. The antibody coupled bead slurry was then ready to be used for IPs.

2.2.9 Subcellular Fractionation

Cells were grown to about 60 to 70 % confluency, prior to separation into nuclear and cytosolic fractions. The fractionation was performed using the Nuclear and Cytoplasmic Extraction Kit (Thermo Scientific) following the manufacturer's instruction manual, except that the lysis buffers were supplemented with complete protease inhibitor tablets (Roche) to prevent protein degradation. Subcellular fractions were reduced with 1x SDS sample

buffer containing 1% (v/v) ß-mercaptoethanol and boiled for 5 min prior to analysis by immunoblotting.

2.2.10 Size exclusion chromatography

The AKTA Explorer was operated according to manufacturer's instructions using the Unicorn 4.1 software. All buffers and extracts were sterile filtered before loading onto the column. Extracts from HaCaT cells treated with or without BMP-2 (25 ng/ml) or TGF-ß (50 pM) for 1 h prior to lysis, were cleared by centrifugation and further cleared through Spin-X columns. 1 mg of protein extract was subjected to separation through a Superose™ 10/300 GL Column (GE Health Care), which was washed and equilibrated with three column volumes of degassed gel filtration buffer (150 mM NaCl, 50 mM Tris/HCl pH 7.5, 0.03% (v/v) Brij35). 32 fractions of 0.2 ml each were collected at a flow-rate of 0.15 ml/min. The eluted fractions were reduced with 1x SDS sample buffer containing 1% (v/v) ß-mercaptoethanol and boiled for 5 minutes at 95°C before SDS-PAGE and immunoblot analysis were performed.

2.2.11 Cell migration assay

The PC3 Control, PC3 PAWS1 or PC3 PAWS1 S610A cells were seeded with 80 % confluency into migration inserts (Ibidi) and left growing for 36 h. Afterwards the inserts were removed, the cells were serum starved for 4 h and stimulated with or without BMP (25 ng/ml). Cellular migration was monitored in a 37 °C humidified chamber supplied with 5 % CO2 using an

Eclipse Ti live cell imaging microscope (Nikon Corp.) with pictures taken every 2 minutes for 24 h.

2.2.12 *In vitro* kinase assays of FAM83G/PAWS1 with ALK receptors

For each kinase assay, 20 µl reactions were set up consisting of 150 ng of kinase (GST-ALK2, GST-ALK3 or GST-ALK6; Carna Biosciences) and 2 µg substrate protein (GST-SMAD1, GST-SMAD2, GST-PAWS1(523-end) or other mutants of PAWS1 as indicated) in a buffer containing 50 mM TrisHCl pH 7.5, 0.1% ß-mercaptoethanol, 0.1 mM EGTA, 10 mM $MgCl_2$, 0.5 µM Microcystein-LR and 0.1 mM γ^{32}P-ATP (500 cpm/pmole). All assays were performed at 30°C for 30 minutes and stopped by adding 1X SDS sample buffer containing 1% ß-mercaptoethanol and heating at 95°C for 5 minutes. The samples were resolved by SDS-PAGE and the gels were stained with Coomassie Blue and dried. The radioactivity was analysed by autoradiography. For the identification of the phospho-residues within PAWS1 see section 2.2.16.3.

2.2.13 Specificity kinase panel

All protein kinases in the specificity panel were expressed, purified and assayed at The National Centre for Protein Kinase Profiling (http://www.kinase-screen.mrc.ac.uk/) as previously described (Bain et al., 2007). The assays were carried out robotically at RT (21 °C) and were linear with respect to time and enzyme concentration under all conditions used. The assays were performed for 30 min using Multi drop Micro reagent dispensers (Thermo Electron Corporation, Waltham, MA, U.S.A.) in a 96-well format. The

concentration of magnesium acetate in the assays was 10 mM and [γ-32 P]ATP (~800 cpm/pmol)was used at 5μM for ABL, Aurora A, CK2α, CLK2, DAPK1, DYRK3, EF2K, EIF2AK3, ERK1, ERK8, GSK3ß, HER4, HIPK2, IGF-1R, IKKß, IRAK1, IRR, JAK2, MARK3, MKK1, MKK2, p38αMAPK, p38γMAPK, PAK2, PAK5, PIM3,PKBα,PKCζ,PRAK, RIPK2, TAK1, TLK1andZAP70, 20μMfor AuroraB, BRK, BRSK1, CAMKKß, CDK2-Cyclin A, CHK1, CHK2, CK1δ, CSK, EPH-B1, EPH-B2, EPH-B3, ERK2, FGF-R1, GCK, HIPK1, HIPK3, IR, IRAK4, JNK1, JNK2, JNK3, LKB1, MAPKAP-K2, MAPKAP-K3, MARK1, MARK2, MEKK1, MLK3, MNK1, MSK1, MST4, NEK2α,OSR1, p38δMAPK, PAK4, PAK6, PDK1, PIM1, PIM2, PKA, PKCγ, PKD1, PLK1, PRK2, ROCK2, RSK1, SGK1, SmMLCK, SYK, TAO1, TIE2, TrkA, TTK, VEG-FR and YES1. 50μM were used for AMPK, ASK1, BRSK2, BTK, CAMK1, DYRK1A, DYRK2, EPH-A2, EPH-A4, EPH-B4, IKKε,Lck,MARK4,MELK, MINK1, MKK6, MLK1, MNK2, MPSK1, MST2, NEK6, NUAK1, p38ßMAPK, PHK, PKBß,PKCα, RSK2, S6K1, Src, SRPK1, STK33 and TBK1 in order to be at or below the K_m for ATP for each enzyme. For kinase assays with CK1 isoforms, 300μM CK1-peptide KRRRALS*VASLPGL (where S* is phosphor Serine) was used as the substrate.

2.2.14 SDS-PAGE separation of proteins

Two different SDS-PAGE systems were used for this study. NuPAGE 4-12% Bis-Tris pre-cast gels (Life Technologies) were used for mass spectrometry applications and for autoradiography after kinase assays. For all other experiments, the ATTO self-assemble gel system for gel electrophoresis was employed (ATTO, Japan). The SDS-PAGE gels were

assembled by first pouring the SDS-PAGE gel mix (a solution containing 0.375 M Tris/HCl pH 8.8, 0.1% (w/v) SDS, 10% (w/v) acrylamide and 0.075% (w/v) ammonium persulphate) to which polymerisation was initiated by the addition of 0.1% (v/v) tetramethylethylenediamine (TEMED) just prior to pouring. 100 % ethanol was then pipetted on top of the gel gently to level the surface and extract bubbles. After at least 20 minutes of polymerisation the ethanol was removed and a stacking gel (0.125 M Tris/HCl pH 6.8, 0.1% (w/v) SDS, 4% (w/v) acrylamide, 0.075% (w/v) ammonium persulphate and finally 0.1% (v/v) TEMED) was poured immediately on top of the pre-set SDS-PAGE gel. A 12-well comb was inserted into the stacking gel prior to its polymerisation. Life Technologies 4-12% Bis-Tris gels were run using Novex NuPAGE 3-[N-morpholino] propane sulphonic acid (MOPS) running buffer. ATTO gels were run using running buffer which contained 25 mM Tris/HCl pH 8.3, 192 mM glycine and 0.1% (v/v) SDS. Unless stated otherwise 20 µg of proteins was loaded for gel electrophoresis. The gel electrophoresis was performed at a constant voltage of 200V for 1h for the Novex gels and 180V for 1h and 25 minutes for ATTO gels.

2.2.15 Coomassie Blue Protein staining of gels

After SDS-PAGE, protein separation could be visualised by in gel staining of the proteins using colloidal Coomassie Blue staining solution (Life Technologies). Gels were stained using the manufacture's protocol for 1h to overnight, depending on the staining level that was needed, at RT with constant shaking on a rocking platform. To destain the gel, deionised water was used with several changes of water until the background staining was reduced and the protein bands were visible.

2.2.16 Mass spectrometry

2.2.16.1 In gel digestion of proteins

All preparation steps for mass spectrometry analysis, unless stated otherwise, were performed under a laminar flow hood (Model A3VB, Bassaire Limited) to minimize contamination of the samples. Accordingly clean disposable scalpels were used to excise the protein bands of interest from Coomassie-stained SDS-PAGE gel. Gel pieces were sequentially washed with 0.5 ml 50% acetonitrile (ACN), 100 mM NH_4HCO_3 and finally in 50% ACN and 50 mM NH_4HCO_3. All washes were performed by shaking for 10 minutes and aspirating the supernatant after each wash. In order to reduce the disulphide bonds, the excised gel bands were first reduced with 10 mM DTT in 100 mM NH_4HCO_3 for 45 min at 65°C and then alkylated by incubation with 50 mM iodoacetamide in 100 mM NH_4HCO_3 for 30 min at RT with constant agitation. To destain the gel pieces completely, they were washed repeatedly with 100 mM NH_4HCO_3 until Coomassie was not visible and subsequently with 50% ACN and 50 mM NH_4HCO_3. Then 0.3 ml ACN was used per gel piece for 15 min at RT. Subsequently the ACN was removed and the dehydrated gel pieces were dried completely in a SpeedVac. To digest the proteins in the gel pieces, 30 µl of 25 mM Triethylammonium bicarbonate containing Trypsin (5 µg/ml) was added to the gel pieces and incubated for 30 minutes at 30°C. Then 170 µl of deionised water was added and the digestion allowed to proceed overnight at 30°C with constant shaking. The following morning 200 µl of ACN was added to the digest and incubated at RT for 15 min. The supernatant was transferred to clean, keratin-free, Eppendorf tubes and subsequently SpeedVac-ed to

complete dryness. In the meantime, 100 µl 50% ACN/2.5% formic acid was added to the remaining gel pieces to maximise the peptide recovery. When the first SpeedVac was complete, the supernatant from the gel pieces was combined with the dried extraction and the sample were SpeedVaced to complete dryness. Peptide samples were stored at -20°C prior to analysis by Mass spectrometry.

2.2.16.2 Protein mass fingerprinting

The digested peptides (see 2.2.15.1) were reconstituted in 5% ACN and 0.1% formic acid and afterwards injected into a nano liquid chomatography system coupled to a LTQ-orbitrap mass spectrometer (Thermo Scientific). The obtained data files (raw files) were converted to MSM files that were afterwards submitted to the in-house Mascot server. The matching database was the IPI human database and the oxidation of methionine was specified as a variable modification. Peptide tolerance was 20ppm for precursor ions and 1.0Da for fragment ions (MSMS tolerance). Liquid chromatography-mass spectrometry (LC-MS) analysis was performed in the in-house mass spectrometry facility by Dr. David Campbell and Mr Robert Gourlay.

2.2.16.3 Identification of phosphorylated peptides

The phosphorylated FAM83G/PAWS1 protein (see section 2.2.12) was digested as described above (see section 2.2.16.1). The dried peptides were reconstituted in 5 % ACN and 0.1 % trifluoroacetic acid (TFA) before injected

into a 218TP5215 C_{18} column that was equilibrated with 0.1 % TFA for reverse phase HPLC run. The column was developed with a linear ACN gradient at a flow rate of 0.2 ml/min and fractions of 100 µl were collected. The major eluting peptides were analysed by LTQ-orbitrap mass spectrometer (Thermo Scientific). The peptides were also coupled to Sequelon-AA membrane and subjected to solid-phase Edman degradation as previously described (Campbell and Morrice, 2002). The HPLC, LTQ-orbitrap mass spectrometry and Edman degradation was performed by Mr. Robert Gourlay.

2.2.17 Immunoblotting analysis

Following resolution of extracts and IPs by SDS-PAGE (see section 2.2.14), samples were transferred onto nitrocellulose or methanol activated polyvinylidene fluoride (PVDF) membranes. This was performed using a Mini-Cell (BioRad) transfer system at 90V for 1.5 h in 1X transfer buffer (25mM Tris/HCl pH 8.3, 192mM glycine, 20% (v/v) methanol). Efficiency of the transfer was assessed by visualising the blue molecular weight markers or by staining the membranes with PonceauS solution. The transferred membranes were blocked in TBS-T containing either dried non-fat milk (5% (w/v)) or IgG-free BSA (5% (w/v)), depending on the primary antibody. In both cases, blocking was done for 1 h at RT. The primary antibodies were diluted in 5 ml of TBS-T containing either dried non-fat milk (5% (w/v) or IgG-free BSA (5% (w/v)) and added to the membranes for 16 h at 4°C with constant agitation to ensure an even access across the membranes. Membranes were then washed 4x5 minutes with TBS-T, before being incubated with the HRP-conjugated secondary antibodies for 1 h at RT under constant agitation. All

secondary antibodies were used at 1:10000 dilutions in TBS-T containing 5% (w/v) dried non-fat milk. The membranes were then washed 4x5 minutes in TBS-T. Detection was performed by using enhanced chemiluminescence reagent (ECL) (incubated for 3 minutes) followed by exposure on the Medical X-Ray Film in the dark and development of the film using an SRX-101A automatic film processor (Konica Minolta).

2.2.18 Generation of antibody

Derived peptides from human FAM83G/PAWS1 (amino acids ranging from 715-815), P-FAM83G/PAWS1 S610 (amino acids 603-613) as well as polypeptides of SMAD1 (amino acids 144-268), SMAD2 (amino acids 87-107), SMAD3 (amino acids 158-178) and CULLIN3 (amino acids 544-end) were N-terminal GST-tagged. These polypeptides were then used as antigens for antibody production by injection into sheep (all peptides except P-FAM83G/PAWS1 S610) or rabbit (P-FAM83G/PAWS1 S610). The antigens were emulsified, prior to the injection, in Freund's adjuvant. A pre-immune bleed was taken on the same day as the first injection of antigen. Each animal was immunised every 28 days up to a total of 4 injections. Seven days after injections two, three and four a blood sample was collected. These were called bleed 1 to 3. Each bleed had to clot at 4°C overnight. Afterwards, the antiserum was decanted though glass wool, after centrifugation for 1h at 1500g at 4°C, and was stored at -20°C. Antisera were raised in sheep or rabbit at Scottish National Blood Transfusion Service (Penicuik). In order to purify the serum, it was heated for 20min at 56°C and then filtered through a 0.45 µm filter. The anti-serum was subsequently diluted 1:1 in 50mM Tris/HCl pH 7.5, 2% Triton X-100 and in order or minimse the cross reactivity of the

antibodies present in the anti-serum with GST, the GST antibodies were depleted using activated CH Sepharose beads coupled to GST. The GST cleared flow-through was affinity purified against the given antigen. The antibodies were first eluted in 50mM glycine pH 2.5 before being dialyzed overnight in PBS. All in-house antibodies used in this thesis were generated and purified by the DSTT antibody production team, as described above. The coordination of the antibody production is done by Dr. H. McLauchlan and Dr. J. Hastie (DSTT/University of Dundee).

2.2.19 Double thymidine block for cell cycle arrest

The cells were seeded at about 20% confluency before treated with 2 nM thymidine for 16 h. Afterwards the cells were washed twice with PBS and left growing in standard medium for 10 h before treated again with 2nM thymidine for further 16 h. Finally, the cells were washed three times with PBS and given standard medium afterwards in order to be subsequently harvested at indicated time points for FACS and immunoblotting analysis. The cells were harvested by using standard trypsinisation as described in section 2.2.1, and then resuspended in 10 ml of ice-cold PBS. 9 ml where spun down at 1000 rpm for 5 min before being processed for cell lysis and subsequent immunoblotting analysis as described above. The remaining 1 ml was resuspended with ice-cold 70% (v/v) ethanol while vortexed. Samples were then stored at -20 °C until or immediately washed twice in PBS with 1% (w/v) BSA before resuspensed in 300 µl PBS containing propidium iodide (50 µg/ml), ribonuclease A (50 µg/ml) and TritonX-100 (0.1% v/v). Samples were subsequently incubated at room temperature for 20 min in the dark before analysis by flow cytometry on a Beckman FACS Calibur Flow. Cells were

gated on the flow cytometer using forward scatter and side scatter parameters (linear scale), DNA was detected in the FL2-H channel (linear). FL2-W and FL2-A were used to distinguish single cells. Cell numbers in different cell cycle stages were measured on FlowJo using the Dean-Jett-Fox method (Fox, 1980).

2.2.20 Fluorescence microscopy

U20S cell stably expressing GFP-PAWS1 were seeded onto glass chamber slides and were allowed to grow for 24 h, while the expression of GFP-PAWS1 was induced by doxycycline. The cells were stimulated with BMP-2 (25 ng/ml) or TGFß (50 pM) for 45 min before fixation with 4% paraformaldehyde for 10 minutes at RT. The cells were then washed 3 times with PBS and once with deionised water before Prolong Gold mounting medium (Life Technologies), which contained the nuclear stain 4',6-diamidino-2-phenylindole (DAPI), was added and a coverslip mounted onto the chamber slides. The mounted slides were left to dry in the dark for at least 2 h. Flourescence images were analysed using a Deltavision Core Restoration microscope (Applied Precision, USA).

2.2.21 DNA and RNA concentration measurements

In order to measure the concentrations of isolated DNA or RNA in aqueous solution, the NanoDrop spectrophotometer (Life Technologies) was used. It was calibrated using nuclease free water. The absorbance measurements were done at 260 nm according to the manufacturer’s instructions.

2.2.22 Real time quantitative reverse transcription PCR (qRT-PCR)

cDNA was made using the SuperScript cDNA kit (Life Technologies) from 1 µg of the isolated total RNA using the RNeasy kit (Qiagen), both used as stated in the manufacturers protocols. qRT-PCR reactions were performed either using a 96-well plate or 384-well plate format. When 96-well format was used, the reactions were performed in triplicates, where each 20 µl reaction included forward and reverse primers (0.5 µM each), 50% SYBR Green (BioRad) and cDNA (2.5% of reverse transcriptase reaction). When the 384-well format was used the reactions where performed in quadruplicates (10 µl each), with forward and reverse primers (0.5 µM each), 50% SYBR Green (BioRad) and cDNA (2.5% of reverse transcriptase reaction) in a CFX 384 Real time System qRT-PCR machine (BioRad). In both cases all the data presented in the thesis represent at least three independent biological replicates.

The data was normalised to the geometrical mean of two housekeeping genes (GAPDH and HPRTI) and the $2^{(-\Delta\Delta C(T))}$ method (Livak and Schmittgen, 2001) was used to analyse the qRT-PCR data in Microsoft Excel. The graphical visualisation and statistical analysis was done using GraphPad Prism 5

2.2.23 Statistical analysis and representation of results

The data is presented as the mean ± SD. Statistical significance of differences between experimental groups was assessed using the two-way analysis of variance (ANOVA) test with Bonferroni post tests. Differences in

means were considered significant if the p-value was smaller than 0.05. Differences with $p<0.05$ were indicated as "*", $p<0.005$ were indicated as "**" and $p<0.001$ were indicated as "***".

All results shown in this thesis are representatives of independent biological replicate experiments that have been performed at least 3 times if not indicated otherwise.

2.2.24 DNA and RNA agarose gels

The size and the purity of DNA PCR products and the RNA quality for the RNA sequencing were assessed by electrophoresis on 1% agarose gels. Each gel contained a 1:1000 dilution of SYBR Safe nucleotide gel stain (Life Technologies). Gels were submerged in 1x TAE running buffer using an agarose gel tank. Between 100 and 500ng of DNA and RNA, respectively was loaded onto a gel together with DNA loading dye. 500 ng of a 1 kbp DNA ladder (Life Technologies) was used as a marker. Gels were run at 100V for approximately 20 to 25 minutes. The stained nucleotide complexes were visualised using a UV transilluminator.

2.2.25 RNA-sequencing

1 µg of total RNA, isolated with the RNeasy kit (Qiagen), was used to generate libraries using Illuminia's TruSeq RNA kit according to the manufacturer's instructions. Indexed adapters were ligated to the ends of the cDNAs in order to perform single end multiplex sequencing on Illumina's HiSeq2000 platform. Reads were mapped to the human genome using CLC

Genomics Workbench v 5.0. Mapped reads were subsequently analysed for differential expression using Avadis® NGS software, Version 1.3.0, Build 163982 (Strand Scientific Intelligence, Inc., San Francisco, CA, USA). The analysis of RNAseq data was performed by Dr. Kevin Dingwell (MRC NIMR, London).

2.2.26 Plasmid transformation, amplification and isolation

For transformation of plasmids on to competent *E. coli* DH5α cells, cells stored at -80°C were thawed slowly on ice. Approximately 10 ng of plasmid DNA was added to the cell suspension and mixed gently by tapping. After 2 min incubation on ice, the cells were subjected to heat-shock at 42°C for 1 minute to facilitate DNA uptake. The cells were then placed on ice for 2 min. Finally, the cells were plated onto LB/100µg/ml ampicillin agar plates and incubated for 16 h at 37 °C.

One transformed colony was used to inoculate 250 ml LB/100 µg/ml Amp media. This culture was left growing overnight at 37°C under constant shaking. The culture was harvested by centrifugation at 3,000 rpm for 10 min at 4°C in a J-6 Beckman centrifuge. The plasmid DNA was then isolated using the Qiagen DNA Maxi Kit according to the manufacturer's instructions. Bacteria from 250 ml log phase cultures typically yielded between 500 ng and 1000 ng of plasmid DNA.

2.2.27 Purification of GST-tagged FAM83G/PAWS1 from *E.coli*

The bacterial expression vector (pGEX6T) encoding wild type or various truncation mutants of GST-PAWS1 were transformed into BL21 *E.coli* strain. A single colony of transformed bacteria was added to 50 ml LB/100 µg/ml Amp medium and incubated overnight at 37°C in a shaking incubator, to generate a starter culture. This culture was then added to 1 L LB/100 µg/ml Amp medium. The bacterial growth was monitored by measuring the optical density (OD) of the culture medium at 600 nm. Once the OD reached 0.5, the expression of the GST-tagged protein was induced using 0.1 mM isopropyl ß-D-1-thiogalactopyranoside (IPTG). After 16 h of further growth at 16°C, bacteria were harvested by centrifugation in a Beckman J6 rotor at 4000 rpm for 20 min at 4°C. The pellet was re-suspended in 30 ml bacterial lysis buffer (25mM HEPES pH 7.6, 10% glycerol (v/v), 0.1mM EDTA, 150mM KCl, 1mM DTT, 1mM PMSF plus 1 tablet of Complete protease inhibitor for each 50 ml of lysis buffer). The bacterial lysis was facilitated by sonication (4x45 s bursts at 4°C). If the isolation was not continued immediately, the extracts were snap frozen in liquid nitrogen and stored at -80°C. Subsequently the extracts were centrifuged at 20000 g for 20 min at 4°C. 1 ml equilibrated Glutathione Sepharose 4B (GSH-Sepharose) beads per 500ml of original culture were added to the cleared extracts and incubated for 1 h at 4°C in a shaking platform. The beads were collected afterwards by centrifugation at 3000 rpm for 15 min at 4°C. After removal of the supernatant, the beads were pipetted onto new tubes. The beads were washed five times with bacterial lysis buffer containing 0.5 M NaCl and twice with buffer A. The proteins were eluted by adding an equal volume of glutathione elution buffer to the beads and incubate this mixture for 5 minutes

at 4°C. The eluate was collected before a second elution was done using 50% of the bead volume. Both eluates were combined and dialysed using 1 L of buffer A on a Slide-A-Lyzer Cassette (Thermo Scientific) for 16 h at 4°C. The protein concentration of the purified proteins was determined (see 2.2. 6) before they were aliquoted, snap frozen in liquid nitrogen and stored at -80°C.

2.2.28 *Xenopus laevis* embryo manipulations

Xenopus laevis embryos were generated by *in vitro* fertilization and staged according to Nieuwkoop and Faber (Nieuwkoop and Faber, 1994). Microinjections were carried out in 4% Ficoll in 75% Normal Amphibian Medium (Manning et al.), and when they reached stage 8, they were transferred to 10% NAM. RNA for injections was synthesized *in vitro* using the MessageMachine kit (Ambion) according to the manufacturer's instructions. For axis duplication assays, mRNA was injected into a single ventral blastomere at the 4 cell stage. Secondary axes were scored at stage 32 and were classed as complete if the second axis had eyes and a cement gland.

3 The role of FAM83G/PAWS1 in BMP signalling and beyond

3.1 Introduction

The basic mechanisms of the canonical BMP pathway are well established: binding of BMP ligands to their corresponding receptors leads to the phosphorylation of SMAD1, 5 and 8 transcription factors. This leads to their association with SMAD4 and translocation to the nucleus, where they regulate the transcription of target genes. Yet the outcome of cellular responses to BMP cytokines is cell type and context dependent. Complex mechanisms have evolved to control and regulate the fate of BMP signals in cells in different biological contexts. Multiple signalling networks modulate BMP signalling by providing regulatory inputs at each step of the pathway. While many regulatory inputs have been reported, gaps remain in our understanding of the full scope of regulation. SMAD proteins, as key intracellular mediators of BMP signalling, are prominent for regulatory inputs from other proteins or signalling networks.

A proteomic approach was undertaken to identify interactors of SMAD1 fragments. From this screen, FAM83G was identified as a novel interactor of FLAG-SMAD1 fragment consisting of the linker and MH2 domains. Interestingly, no cellular functions of FAM83G have been reported. Therefore, I set out to investigate the biochemical mechanisms by which FAM83G could potentially regulate BMP signalling.

3.1.1 Family with sequence similarity member 83 (FAM83A-H)

The family with sequence similarity 83 (FAM83) consists of 8 different members (FAM83A-H). They all share sequence similarity within the domain of unknown function 1669 (DUF1669), which is located towards the N-terminus of the protein (Figure 3-1). The DUF1669 contains a putative phospholipase D active site motif (PLDc). Sequence alignment of members of the FAM83 protein family revealed that they share between 32 and 48% protein sequence similarity within the DUF1669 domain. Outside the DUF1669 domain, the different FAM83 class members are very divergent and show no obvious protein sequence similarities (Figure 3-1).

FAM83A was recently identified from a breast cancer cell overexpression screen for proteins whose expression resulted in resistance to EGF receptor tyrosine kinase inhibitors (EGFR-TKI) (Lee et al., 2012). Cells with high levels of FAM83A were found to have increased proliferation and invasion rates as well as resistance to EGFR-TKI. In contrast, depletion of FAM83A inhibited tumour proliferation in mice and significantly inhibited the malignant nature of cancer cells to EGFR-TKI susceptible phenotype (Lee et al., 2012).

FAM83B was also reported as a potential oncogene, using a validation-based insertional mutagenesis (VBIM) approach, whereby it was found to drive the transformation of human mammary epithelial cells (Cipriano et al., 2012). Cipriano and colleagues demonstrated that the expression of FAM83B, like FAM83A, was linked to tumour growth and EGFR-TKI resistance. FAM83A was found to be highly expressed in a variety

of different tumours and linked to poor prognosis in cancer patients (Cipriano et al., 2012)

Because FAM83A and B were both reported to play a role in EGFR-TKI resistance and cancer progression, it was hypothesized that FAM83 members could comprise a novel oncogene family that could potentially be targeted for drug discovery (Grant, 2012, Cipriano et al., 2012, Lee et al., 2012).

FAM83D or CHICA has been reported to associate with the mitotic spindle apparatus, and interact with the spindle protein KID (Santamaria et al., 2008). It was shown to be cell cycle regulated and phosphorylated. Depletion of FAM83D from cells resulted in shorter spindle assembly and spindle misalignment (Santamaria et al., 2008).

FAM83H is associated with the autosomal dominant hypocalcified amelogenesis imperfecta disease. Amelogenesis imperfecta (AI) is a group of diverse inherited disorders that cause dental enamel defects, whereby the calcification of the enamel is abnormal (Lee et al., 2008). Although several reports have shown the relationship between AI and mutations in FAM83H, there is still complete lack of insights into the biochemical properties by which FAM83H is involved in amelogenesis (Kweon et al., 2013, Lee et al., 2011, Ding et al., 2009, Hyun et al., 2009, Lee et al., 2009, Wright et al., 2009, Hart et al., 2009, Lee et al., 2008, Kim et al., 2008). The calcification defect phenotypes of FAM83H mutations are potentially interesting as they imply potential defects in BMP signalling in tooth development.

The other members of the FAM83 family, FAM83C, E, F and G remain to be characterised and as of yet there are no reports describing their function or links to any diseases.

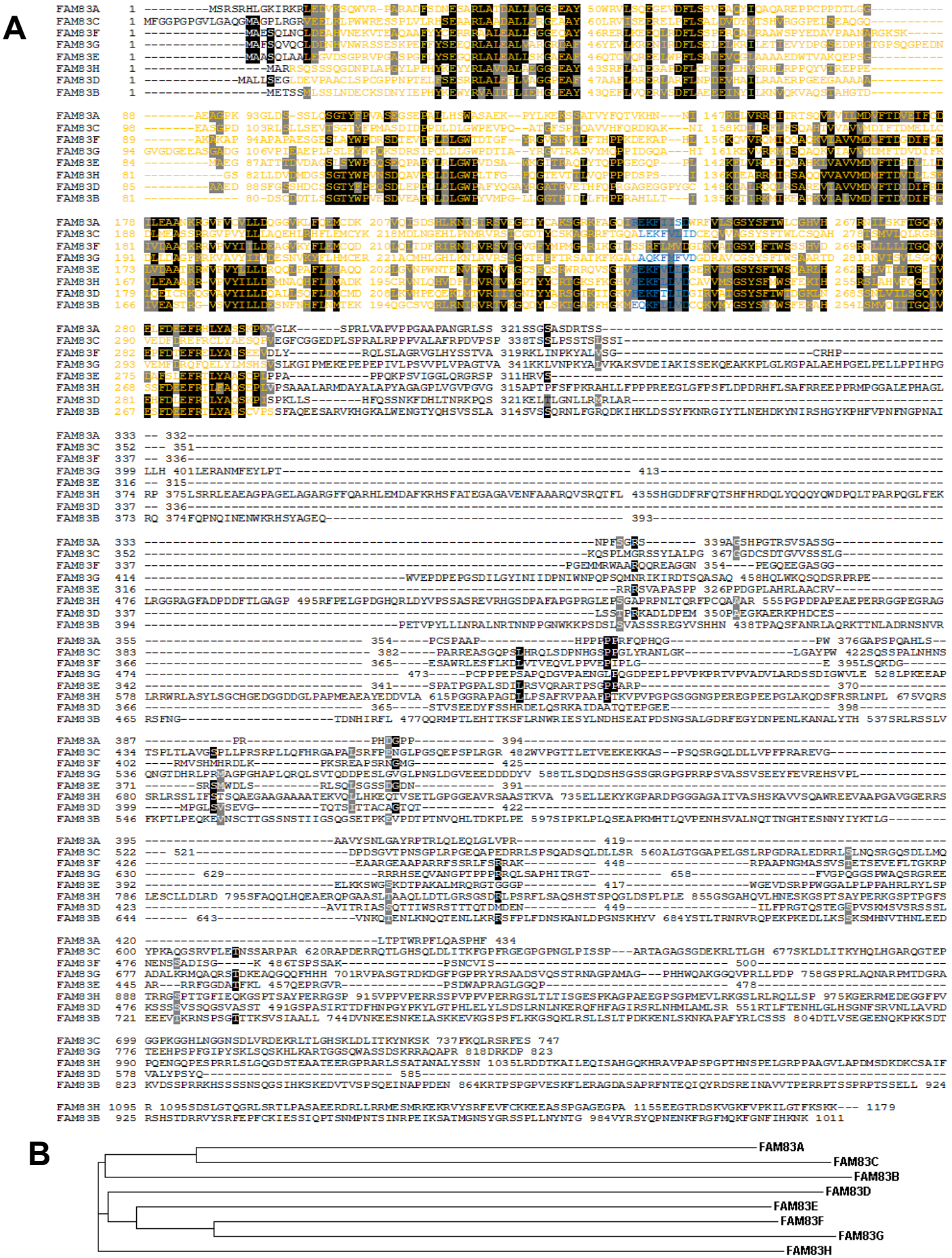

Figure 3-1 The FAM83 (A-H) family of proteins

(A) Sequence alignment of amino acids of theFAM83 family members using BoxShade server. Conserved amino acids are presented in black boxes while similar residues are in grey boxes. Amino acids in yellow indicate the conserved DUF1669 domain and amino acids in blue indicate the putative PLDc motif. **(B)** Phylogenetic tree of FAM83A-H generated using ClustalW.

3.1.1.1 FAM83G/PAWS1

The human family with sequence similarity member 83G (FAM83G) is 823 amino acid long protein that is encoded by the *FAM83G* gene located on chromosome 17p11.2. Apart from the domain of unknown function 1669 (DUF1669; amino acids 9-310) in its N-terminal region (Figure 3-2), there are no other known domains within FAM83G. The DUF1669 domain contains a putative phospholipase D active site motif (PLDc; Figure 3-2).

In humans FAM83G is most closely related to FAM83F (Figure 3-23B) FAM83G is highly conserved in mammals and closely related to chimpanzee (Figure 3-3A and B). *Xenopus laevis* FAM83G shares 45% overall amino acid identity, whereby the N-terminus is highly conserved. Although the C-terminus is diverse, there are some regions that are highly conserved (Figure 3-3A and Table 3-1)

The biochemical roles of FAM83G in cells and organisms are unknown. To date there is only one short report, which was published only very recently, describing the wooly (*wly*) phenotype in mice (Radden et al., 2013). The authors demonstrate that in these mice there was a deletion of 955 bp from the genomic DNA transcribing the *FAM83G* gene, resulting in a frame shift mutation predicted to lead to a shortened *FAM83G* gene. The FAM83G protein expression in these mice was not investigated (Radden et al., 2013). One report identified FAM83G as an interactor of CIN85. In this study, the SH3 domain of CIN85 was used as bait to identify novel SH3 domain binding proteins (Havrylov et al., 2009).

Several putative phosphorylation sites on FAM83G have been reported ((Figure 3-2) (Christensen et al., 2010, Dephoure et al., 2008, Rigbolt et al., 2011, Shiromizu et al., 2013, Van Hoof et al., 2009)). All of these phosphorylation sites have been identified by mass spectrometry and none have been confirmed by other techniques, albeit all of the listed phosphorylation sites have been reported by more than one group. Furthermore no kinases that mediate the phosphorylation have been assigned for each phosphorylation site.

Using the Sanger Institute cancer COSMIC database for gene mutations in cancer patients and cells, I have generated a map of point mutations in FAM83G (Figure 3-32) that are reported for various cancers (http://cancer.sanger.ac.uk/cosmic/gene/overview?ln=FAM83G).

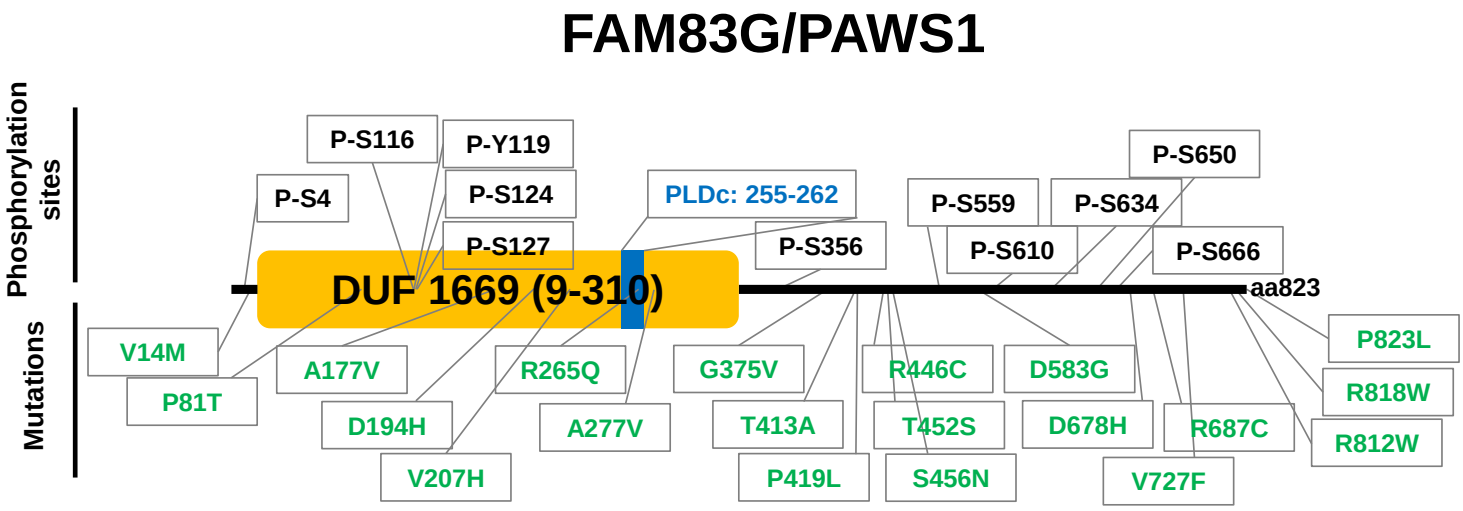

Figure 3-2 Schematic diagram of FAM83G/PAWS1

Schematic diagram of FAM83G/PAWS1 protein showing all reported phosphorylation sites (black). All the point mutations included in the Sanger Institute COSMIC database for FAM83G/PAWS1 in cancer cell lines and patient samples are indicated (Groppe et al.). The DUF1669 domain (yellow) and the putative PLDc domain (blue) are also indicated.

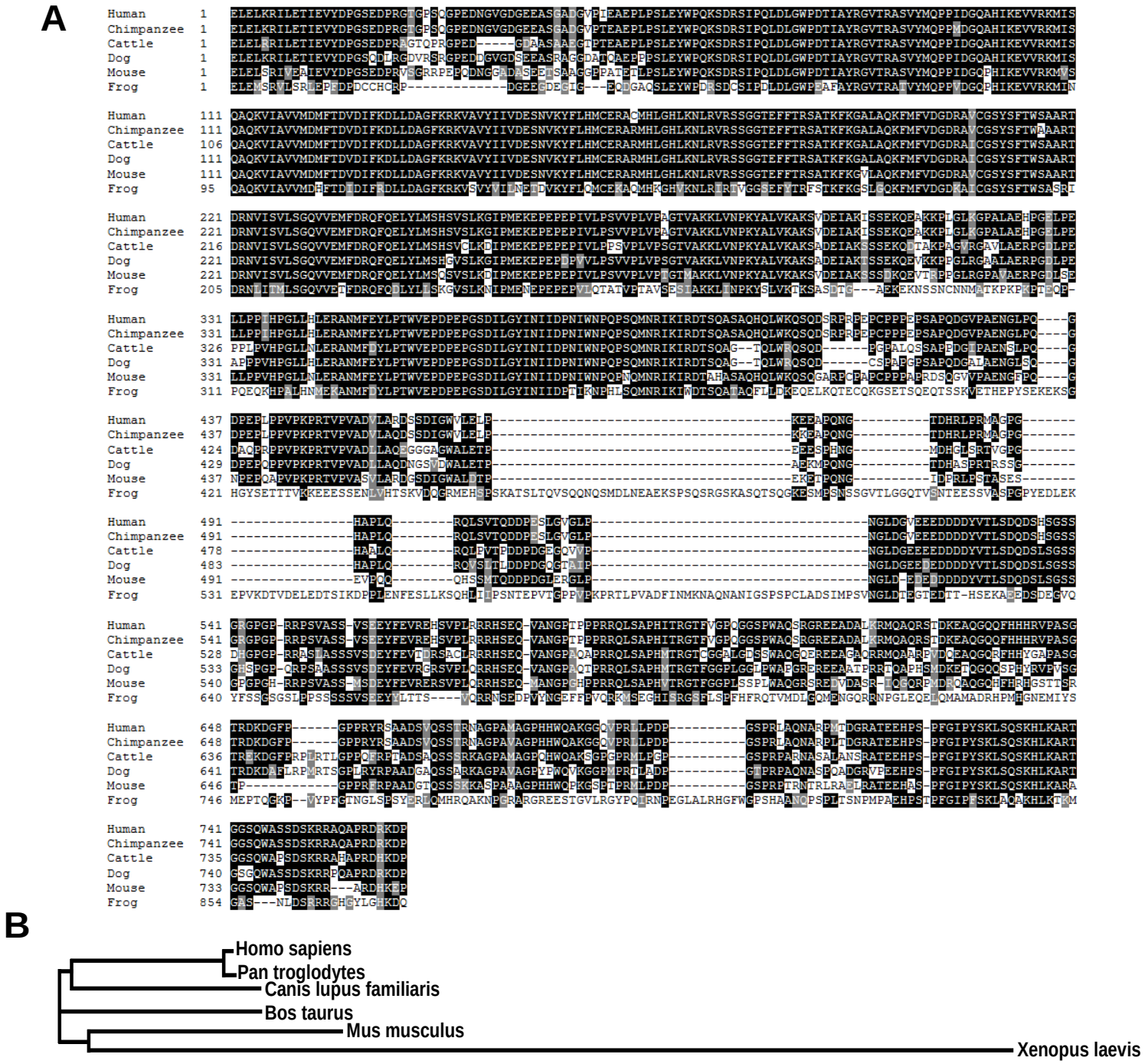

Figure 3-3 FAM83G/PAWS1 is conserved in vertebrates

(**A**) Amino acid sequence alignment of FAM83G/PAWS1 in different species using BoxShade server. Conserved amino acids are presented in black boxes and similar amino acids in grey boxes. (**B**) Phylogenetic tree of FAM83G/PAWS1 in different species generated using ClustalW.

Organism	amino acid sequence identity	Protein length in amino acids
Human (*Homo sapiens*)	100%	823
Chimpanzee (*Pan troglodytes*)	99.00%	823
Dog (*Canis lupus familiaris*)	83.10%	822
Cattle (*Bos taurus*)	81.60%	817
Mouse (*Mus musculus*)	80.70%	812
Frog (*Xenopus laevis*)	45.30%	933

Table 3-1 Summary of the analysis of FAM83G/PAWS1 protein sequence similarity and length in different species

3.1.2 The interplay between BMP and Wnt signalling during early *Xenopus* development

Xenopus laevis, the African clawed frog is an established experimental model to study vertebrate embryogenesis. Its development is very tightly regulated whereby the fertilised egg develops into a complete organism. Nieuwkoop and Faber divided *Xenopus* develpment into 50 different stages, the initial cleavage stages that results in the formation of the blastula, which subsequently undergoes gastrulation followed by the initiation of neurulation and organogenesis. Axis elongation occurs during the tailbud stages that eventually develops into an independently feeding tadpole (Nieuwkoop and Faber, 1994). Two important and extensively studied signalling pathways in this context are the BMP and Wnt pathways (Hoppler and Moon, 1998).

3.1.2.1 Wnt signalling pathway

The Wnt signal transduction pathway can be divided into canonical (ß-catenin-dependent) Wnt signalling pathway, non-canonical planar cell polarity (PCP) Wnt signalling pathway and non-canonical Wnt/calcium signalling pathway (Rao and Kuhl, 2010). The focus of this thesis, in respect to Wnt signalling, concentrates on the canonical Wnt signalling pathway. Canonical Wnt signalling starts with Wnt ligands binding to the extra-cellular binding domain of their corresponding transmembrane G-protein coupled receptors ((Figure 3-4(Schulte and Bryja, 2007)). These receptors are called Fizzled receptors (Fz) and together with co-receptors LRP 5/6 are activated when they bind Wnt ligands (Kestler and Kuhl, 2008). The canonical Wnt pathway is defined by the intracellular signal transducer protein ß-catenin. ß-catenin

is, in the absence of Wnt ligands, constitutively phosphorylated and ubiquitylated and subsequently degraded by the proteasome (MacDonald et al., 2009). ß-catenin is phosphorylated by the “destruction complex” comprising AXIN, APC, GSK3, CK1α and PP2A that leads to its recognition by the E3 ubiquitin ligase ß-TrCP (Stamos and Weis, 2013). Binding of Wnt ligands to the receptors, leads to the breakdown of the destruction complex by trapping the complex at the plasma membrane (Kestler and Kuhl, 2008). This leads to the accumulation of ß-catenin in the cytosol which subsequently translocates to the nucleus, where it drives transcription by binding to the TCF/LEF family of factors (DasGupta and Fuchs, 1999). Active Wnt signalling has been reported to co-regulate adult tissue homeostasis and is of high importance in *Xenopus* axis specification and development (Logan and Nusse, 2004). Tight spatial and temporal regulation of Wnt signalling is especially important during embryogenesis. Therefore specific antagonists, like DKK, WIF1, SFRP and others have evolved that can block Wnt signalling (Logan and Nusse, 2004).

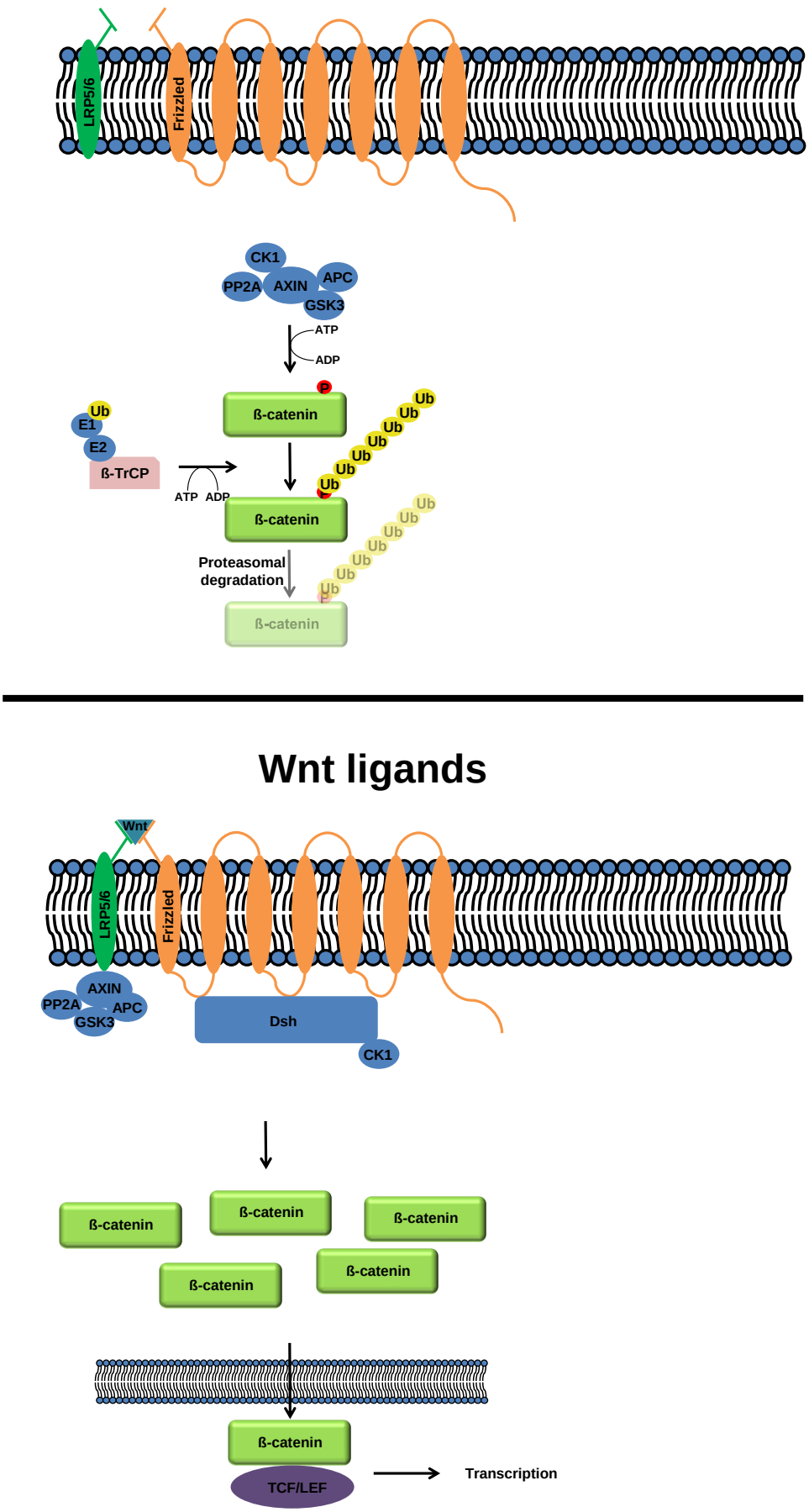

Figure 3-4 A schematic overview of the canonical Wnt signalling pathway

Top panel illustrates the intracellular canonical Wnt signalling cascade that leads to the degradation of ß-catenin in the absence of Wnt ligands. Lower panel illustrates the intracellular canonical signalling cascade in the presence of Wnt ligands.

3.1.2.2 Early Xenopus embryogenesis

Sperm entry at the animal pole of the egg initiates an internal reorganisation of the yolk driven by microtubules (Rowning et al., 1997). This is called cortical rotation and is characterised by the first patterning of the dorso-ventral (D-V) axis. The D-V axis patterning is initiated by the relocalisation of maternal Wnt pathway components like Dsh from the vegetal pole (opposite of the animal pole) towards the dorsal side of the embryo (Miller et al., 1999, Itoh et al., 1998). This, in turn, leads to ß-catenin stabilisation and subsequent nuclear translocation in the whole dorsal region of the embryo (Schneider et al., 1996).

In the early blastula stage, the vegetal side expresses other signalling molecules like maternal VegT, which belongs to the TGF-ß signalling pathway. This leads to the induction of NODAL associated protein expression (XNRs). This NODAL signal induction is further enhanced by ß-catenin driven signalling on the vegetal-dorsal side (Nieuwkoop center), leading to a NODAL signalling gradient along the vegetal embryo side, which is now referred to as the endoderm (Figure 3-5 (Takahashi et al., 2000, Agius et al., 2000). Vegetal NODAL signalling induces mesoderm formation, high NODAL in the dorsal-mesoderm induces the Spemann organizer while low NODAL signalling defines the ventral-mesoderm formation that later gives rise to the ventral signalling center (Figure 3-5 (De Robertis and Kuroda, 2004)). Furthermore, ß-catenin signalling in the dorsal animal side leads to the expression of BMP antagonists like NOGGIN and CHORDIN, that later play a role in the development of the central nervous system (CNS) (Wessely et al.,

2001). These defined signalling processes described above restructure the embryo during the blastula by inducing the formation of the three germ layers: ectoderm (animal/anterior side), mesoderm and endoderm (vegetal/posterior side), each of which later forms different tissues and organs (De Robertis and Kuroda, 2004, Blitz et al., 2006).

During gastrulation the D-V axis pattering is further defined by the two opposing signalling centers at the ventral (Ventral centre) and dorsal sides (Spemann organizer, (Hamburger, 1988)). Whereas the ventral centre expresses the BMP and BMP related cytokines, in the Spemann organizer antagonists of BMP and also Wnt signalling pathways like CHORDIN, NOGGIN, DKK1 and CERBERUS among many others are expressed (Figure 3-5 (De Robertis and Kuroda, 2004)) . This leads to a gradient of BMP signalling along the D-V axis and a gradient of Wnt signalling along the anterior-posterior (A-P) axis (Eivers et al., 2008). The inhibition of both Wnt and BMP signalling at the dorsal side is important for the development of the CNS and the induction of head structures (De Robertis and Kuroda, 2004, Kiecker and Niehrs, 2001). CERBERUS, a powerful antagonist of both signalling pathways, has been shown to induce head structures when expressed ectopically (Glinka et al., 1997).

Taken together BMP and Wnt signalling pathways are key pathways during *Xenopus* embryogenesis and are of special interest because of their defining dorso-ventral and anterior-postirior axis pattering ability.

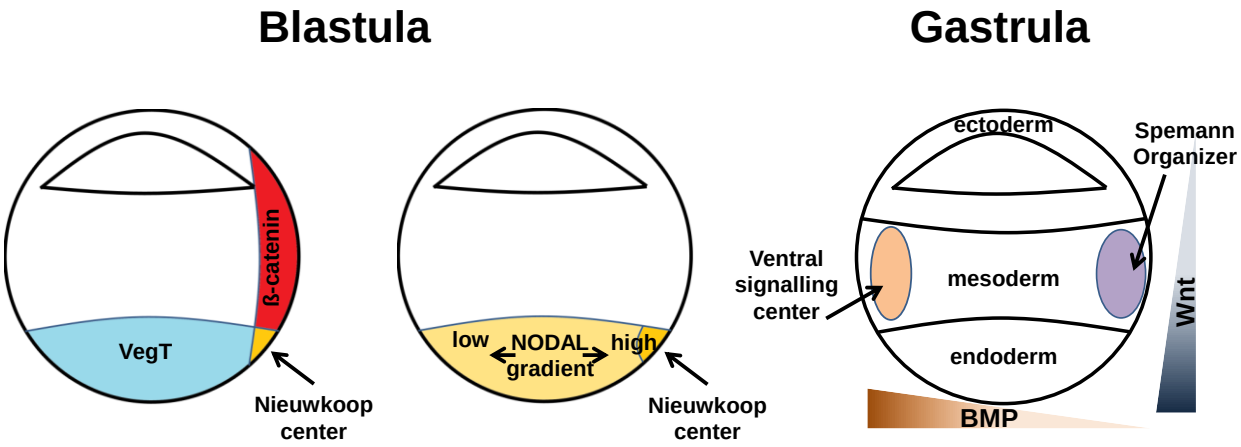

Figure 3-5 Organisation in early *Xenopus* embryo

Schematic overview of the *Xenopus laevis* embryogenesis from the blastula to gastrula (adapted from (De Robertis and Kuroda, 2004)). ß-catenin signalling on the dorsal side and VegT signalling at the vegetal side leads to the formation of the Nieuwkoop centre at the intersection. NODAL signalling in the vegetal pole induces mesoderm formation. High NODAL signalling is needed for the induction of the Spemann Organizer at the dorsal-mesoderm and low NODAL signalling is needed for the formation of the ventral signalling centre.

3.2 Results

3.2.1 A proteomic approach identifies FAM83G/PAWS1 as a novel interactor of SMAD1

In order to uncover novel regulators of the BMP pathway, a proteomic approach was undertaken to identify interactors of SMAD1. For this, a N-terminally FLAG-tagged SMAD1 fragment consisting of the linker and MH2 domains or empty FLAG control was expressed in HEK293 cells and immunoprecipitated with anti-FLAG antibody (Figure 3-6A). Subsequently these immunoprecipitates (IPs) were incubated with cleared HeLa extracts. The immunoprecipitated proteins were resolved by SDS-PAGE and stained with Coomassie. The gel pieces covering the whole lane were excised and digested with trypsin for identification by mass fingerprinting (Figure 3-6B and C). The proteins identified as interactors of FLAG-SMAD1[L+MH2] IPs but not the control FLAG IPs included LEMD3, SMURF2 and SMAD4, all previously reported to be interacting partners of SMAD1 ((Pan et al., 2005, Zhang et al., 2001) (Figure 3-6C)). Interestingly a previously uncharacterised protein called FAM83G was also identified as a novel interactor of FLAG-SMAD1[L+MH2] but not control FLAG IPs (Figure 3-6C). I have renamed this protein as PAWS1 (Protein Associated With SMAD1). Therefore, from here on the protein will be referred to as PAWS1.

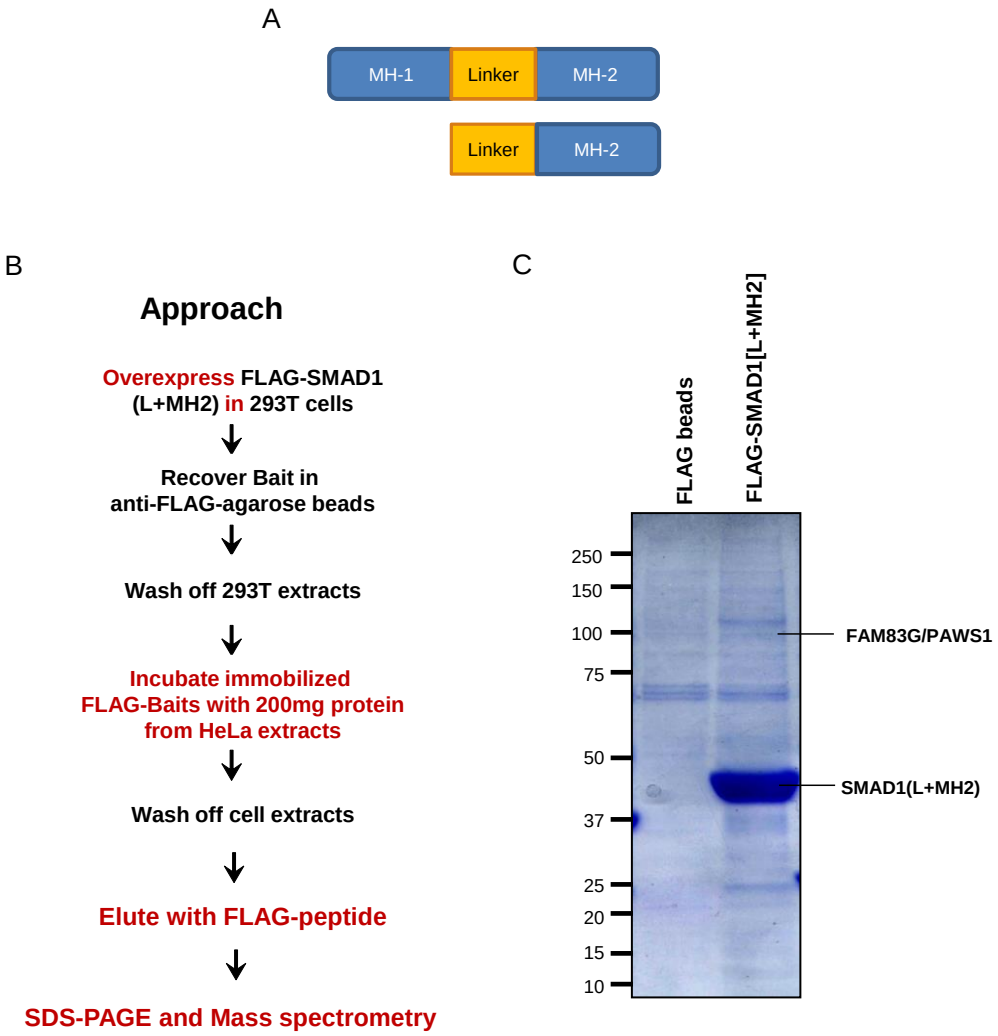

Figure 3-6 Proteomic approach to identify novel SMAD1 interacting proteins

(A) Schematic diagram of SMAD1 comprising the MH1, the linker and the MH2 domains in the upper panel. The bottom panel shows a truncation version of SMAD1 comprising the linker and MH2 domains. **(B)** Overview of the proteomic approach undertaken. **(C)** Coomassie stained gel in which the eluted proteins after FLAG immunoprecipitation were resolved.

3.2.2 Analysis of interaction between PAWS1 and SMADs

The interaction between PAWS1 and SMAD1 was analysed using an N-terminal FLAG-tagged mammalian expression construct of PAWS1 (FLAG-PAWS1) and different N-terminally HA-tagged SMAD constructs. These constructs were co-expressed in HEK293T cells to determine the specificity of the interaction between PAWS1 and SMAD proteins. HA-SMAD1 was detected in the FLAG-PAWS1 IPs, but HA-SMADs 2 or 3 were not (Figure 3-7A and B). Although HA-SMADs 5 and 8 did not appear to be detected in FLAG-PAWS1 IPs, their expression was much lower compared to other SMADs (Figure 3-7A and B). Co-SMAD HA-SMAD4 and inhibitory SMAD, HA-SMAD7 were not detected in FLAG-PAWS1 IPs (Figure 3-7B). As BMP and TGF-ß can induce phosphorylation of R-SMAD proteins, it was important to test whether this phosphorylation could alter the association of PAWS1 to any of these R-SMADs. FLAG-PAWS1 was co-transfected with HA-SMAD1, HA-SMAD3 or HA-vector control in HEK293T cells. These cells were treated with or without BMP or TGF-ß and the cell extracts were subjected to a FLAG IPs. As expected, HA-SMAD1 was detected in FLAG-PAWS1 IPs. BMP treatment slightly enhanced the interaction between PAWS1 and HA-SMAD1 (Figure 3-7C). Treating cells with or without TGF-ß did not alter the lack of association between HA-SMAD3 and FLAG-PAWS1 (Figure 3-7C).

To investigate if PAWS1 interacts with SMAD1 at the endogenous level, extracts from HaCaT cells were used to IP SMAD1. Endogenous PAWS1 was detected in SMAD1 IPs but not pre-immune IgG IPs employed as control (Figure 3-7E). Using the crosslinking agent DSP in extracts prior to SMAD1 IP did not further enhance this interaction (Figure 3-7D). To ensure

that PAWS1 detected in SMAD1 IPs was not a contaminant, PAWS1 expression was depleted by siRNA in HaCaT cells. SMAD1 IPs from these extracts were not able to pull down PAWS1 (Figure 3-7E). Consistent with the interaction between PAWS1 and SMAD1 at the endogenous level, endogenous SMAD1 was detected in PAWS1 IPs from HaCaT extracts. However, endogenous SMAD2 or SMAD3 was not detected in PAWS1 IPs (Figure 3-7F). Treatment of these cells with or without BMP or TGF-ß , did not significantly alter the binding of PAWS1 with SMAD1 or induce binding with SMAD2 and SMAD3 (Figure 3-7F).

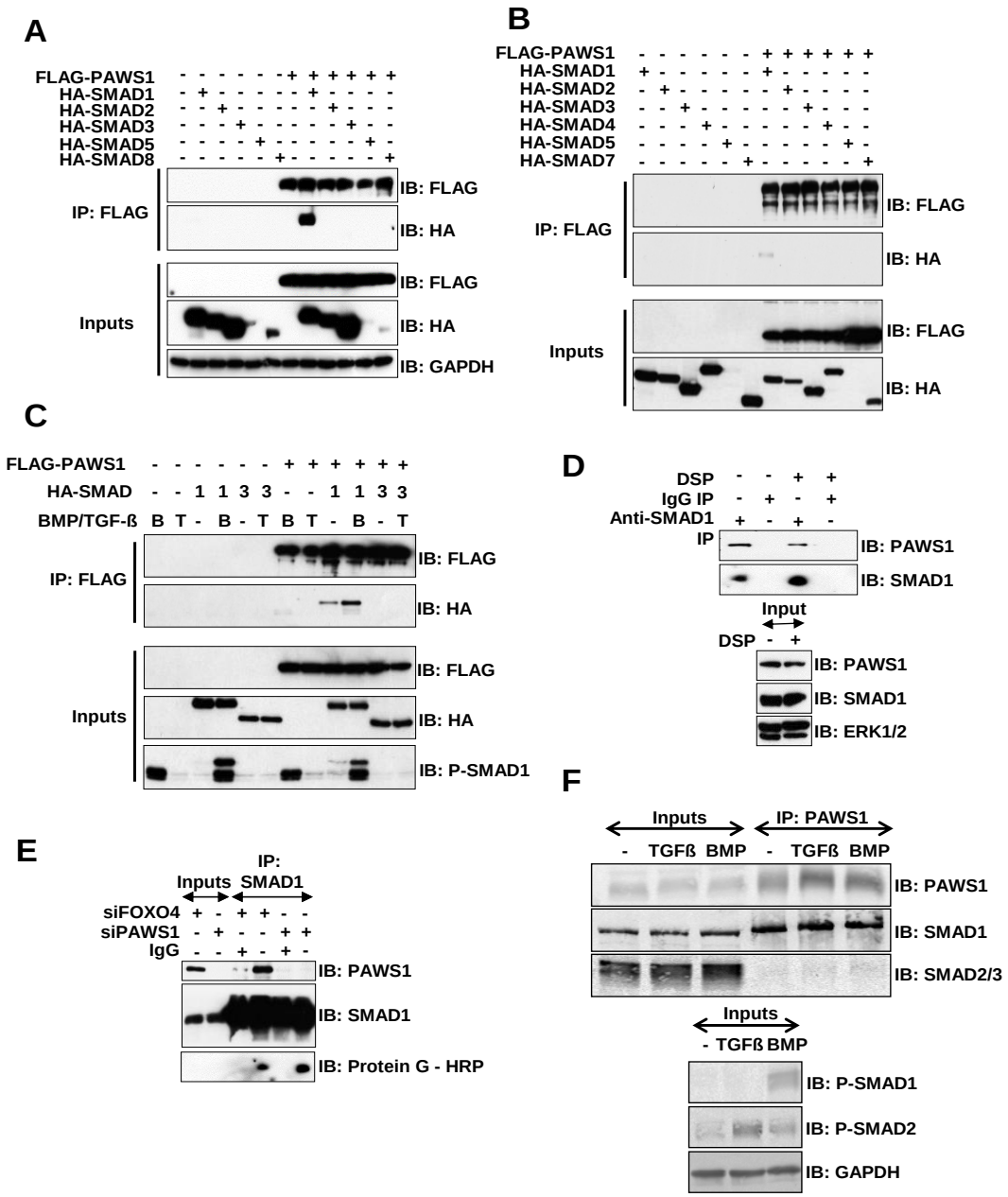

Figure 3-7 PAWS1 interacts with SMAD1

(A) HEK293 cells were transfected with FLAG-PAWS1 or indicated HA-tagged SMADs 48 h prior to lysis. Cell extracts were subjected to FLAG immunoprecipitation. Extracts and IPs were subjected to SDS-PAGE before an immunoblotting analysis using the indicated antibodies. **(B)** Same as (A) except HA-SMAD4 and 7 were included. **(C)** FLAG-PAWS1 and HA-tagged SMAD1 or SMAD3 were co-transfected in HEK293 cells 48 h prior to cell lysis. The cells were treated with or without BMP-2 (25 ng/ml) or TGF-ß (50 pM) 1 h prior to cell lysis. FLAG immunoprecipitation was performed and the IPs as well as the extracts were subjected to SDS-PAGE before an immunoblotting analysis using the indicated antibodies was performed. **(D)** HaCaT cells were lysed in the presence or absence of the protein crosslinking agent DSP. Cell extracts were used for immunoprecipitations with either sheep IgG or anti-SMAD1 antibodies. IPs and inputs were subjected to SDS-PAGE before analysis by immunoblotting using indicated antibodies. **(E)** HaCaT cells were transfected with *siRNA* against FOXO4 as a control or against PAWS1 (300 pmoles each per 10-cm dish) 48 h prior to lysis. Cell extracts were subjected to immunoprecipitation with either sheep IgG or anti-SMAD1 antibodies. IPs and inputs were subjected to SDS-PAGE prior to immunoblotting analysis using the indicated antibodies. **(F)** HaCaT cells were treated with or without TGF-ß (50 pmoles) or BMP-2 (25 ng/ml) for 1 h prior to lysis. Cell extracts were subjected to immunoprecipitation with anti-PAWS1 antibody. IPs and extract inputs were subjected to SDS-PAGE and subsequently analysed by immunonblotting using the indicated antibodies.

3.2.3 Mapping interaction domains on SMAD1 and PAWS1

In order to map the interaction between PAWS1 and the functional domains of SMAD1, FLAG-PAWS1 was co-expressed with N-terminal HA-tagged SMAD1 truncation fragments comprising the MH1, the MH2, the linker domain or combinations of these domains in HEK293T cells (Figure 3-8A). As expected, FLAG-PAWS1 IPs displayed interaction with the full-length HA-SMAD1 (Figure 3-8B). Among the HA-SMAD1 truncated domains, the MH2 domain of SMAD1 interacted with FLAG-PAWS1, however there truncated MH2 domain also interacted with the FLAG-beads. The MH1 and the linker domains or the combination of these (MH1+Linker domains) did not interact with PAWS1 (Figure 3-8B). Nonetheless, these results are not sufficient to confidently suggest that the MH2 domain is sufficient to mediate the interaction between SMAD1 and PAWS1. No clear domain could be mapped within PAWS1 that could mediate the interaction with SMAD1.

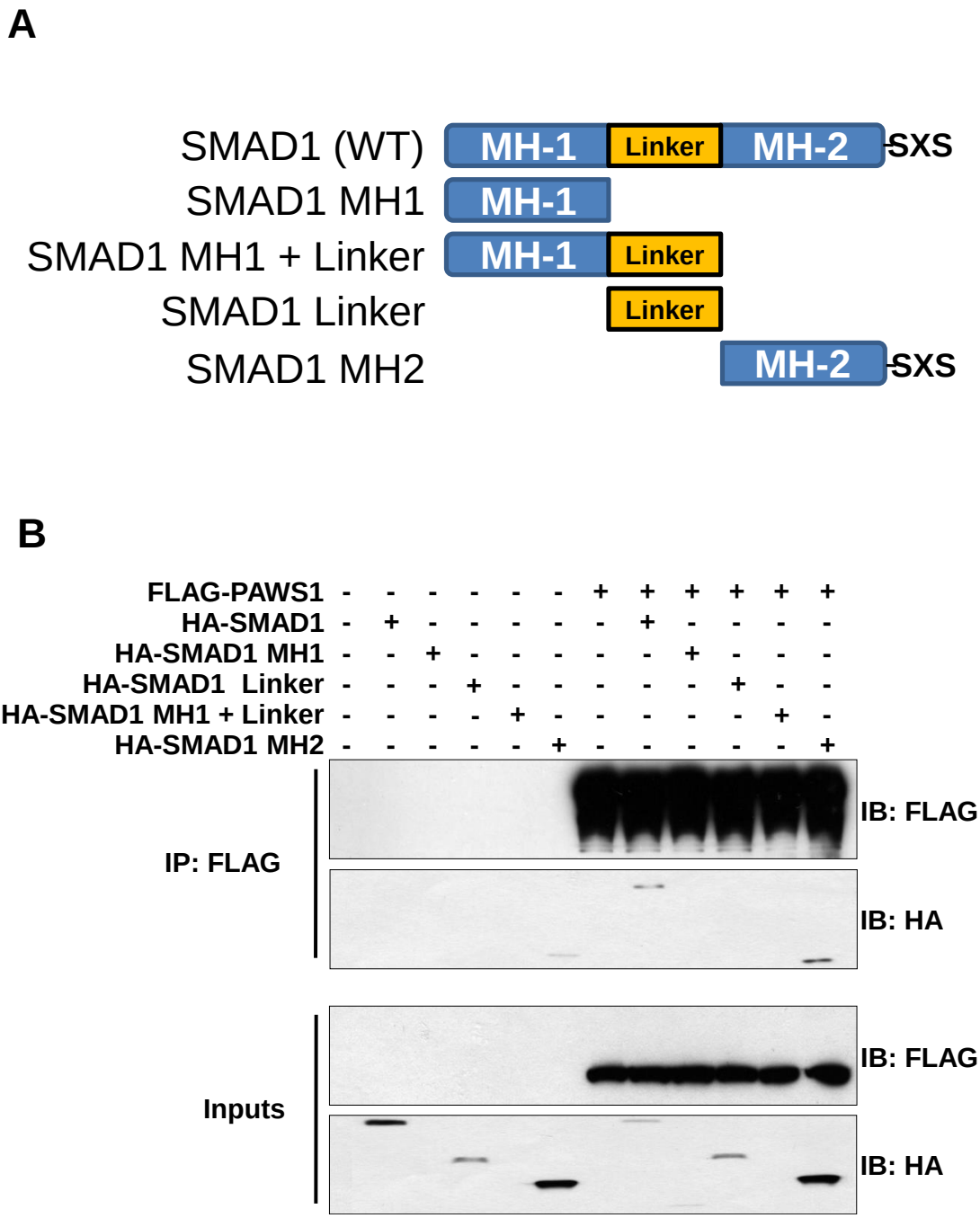

Figure 3-8 Mapping the interaction domains between SMAD1 and PAWS1

(A) Schematic representation of the wild-type SMAD1 together with the indicated domain truncations of SMAD1. **(B)** HEK293 cells were co-transfected with FLAG-PAWS1 and the indicated HA-tagged truncation versions of SMAD1 48 h prior to lysis. Extracts were used for anti-FLAG immunoprecipitation and subsequently IPs and extract inputs were subjected to SDS-PAGE before analysis by immunoblotting using the indicated antibodies.

3.2.4 SMAD1 linker phosphorylation does not impact PAWS1 interaction

The linker domain of SMAD1 is known to be phosphorylated by MAPKs like ERK1/2, p38 MAPK and JNK as well as CDK8/9. These phosphorylation events have been reported to occur at Ser187, Ser195, Ser206 and Ser214. To test if the linker phosphorylation interferes with SMAD1 binding to PAWS1, HA-SMAD1 or HA-SMAD1 EPSM mutant, where the four linker domain serine residues were mutated to alanine to prevent phosphorylation (Figure 3-9A), were co-expressed with FLAG-PAWS1 in HEK293 cells. The cells were treated with or without BMP. FLAG IPs from the cell extracts displayed a robust interaction with either the wild-type HA-SMAD1 or the HA-SMAD1 EPSM mutant (Figure 3-9B). The linker domain phosphorylation at Ser206 in SMAD1 was evaluated by the phospho-linker antibody (P-SMAD1 S206). The difference detected in the linker phosphorylation intensity in the presence or absence of FLAG-PAWS1 was consistent with the lower levels of HA-SMAD1 when co-expressed with FLAG-PAWS1 (Figure 3-9B).

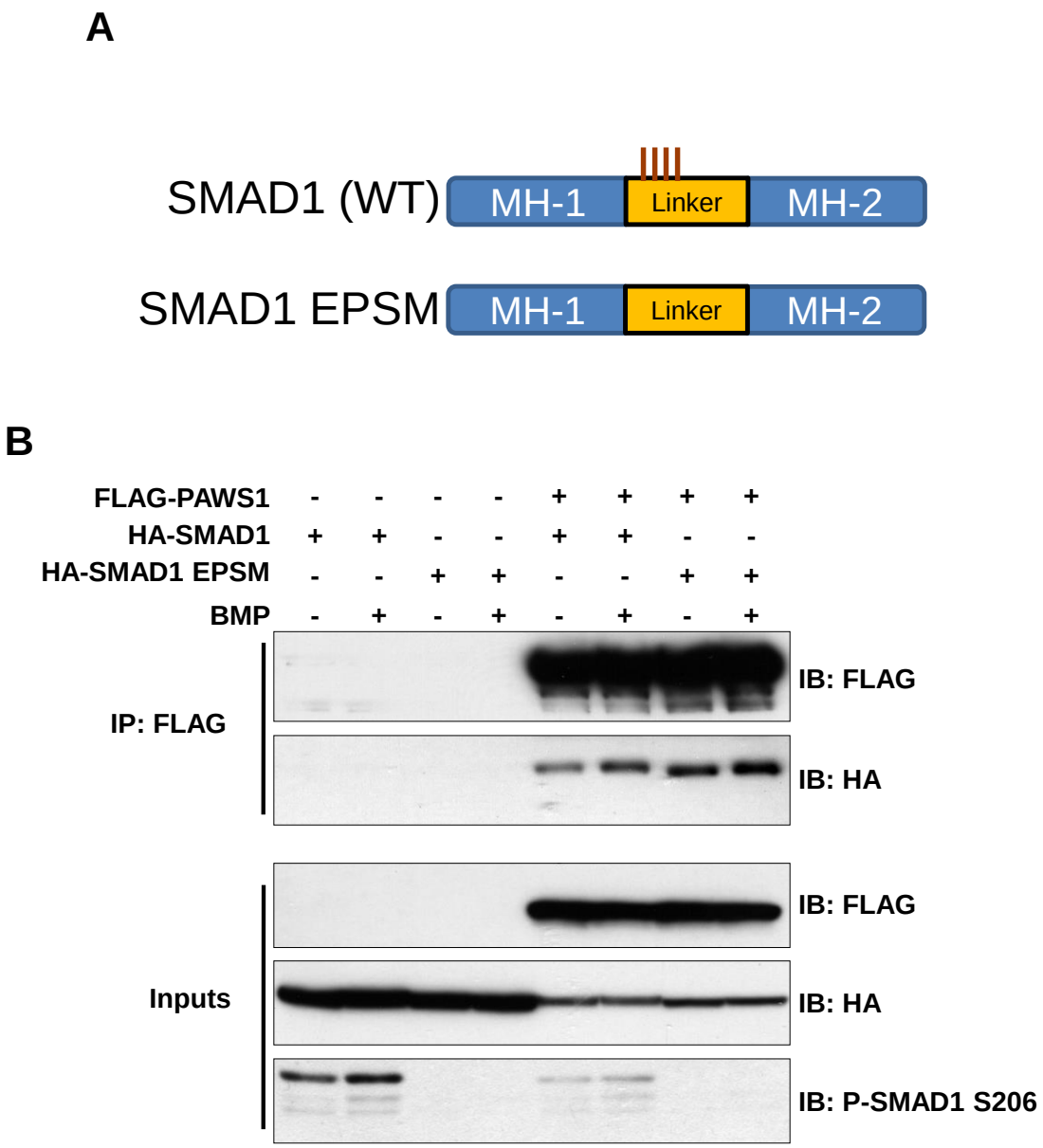

Figure 3-9 SMAD1 linker phosphorylation does not impact association with PAWS1

(A) Schematic representation of the SMAD1 wild-type protein (top) and the SMAD1 phospho-linker mutant, SMAD1 EPSM (bottom). **(B)** HEK293 cells were co-transfected with or without FLAG-PAWS1 and HA-SMAD1 or HA-SMAD1 EPSM 48 h prior to lysis. The cells were treated with or without BMP-2 (25 ng/ml) for 1 h prior to lysis. Extracts were used for anti-FLAG immunoprecipitation. The IPs and extract inputs were subjected to SDS-PAGE and subsequently analysed by immunoblotting using the indicated antibodies.

3.2.5 PAWS1 co-elutes with SMAD1 in a size exclusion chromatography

The robust endogenous interaction between PAWS1 and SMAD1 prompted me to investigate if they form a macromolecular complex. To address this, cell extracts from HaCaT cells treated with or without BMP or TGF-ß, were subjected to separation by size-exclusion chromatography in a Superose™ 6 Column. 32 fractions were collected (Figure 3-10). Under basal unstimulated conditions, SMAD1 and SMAD2/3 predominantly eluted in fractions X-Z which by and large corresponds to their native molecular masses (around 50-55 kDa) (Figure 3-10A). Stimulating the cells with BMP, which induces the posphorylation of SMAD1, resulted in a slight shift in the elution of phospho-SMAD1 towards higher molecular weight fractions (Fractions V-W; Figure 3-10B). Additionally phospho-SMAD1 also eluted at its predicted molecular weight (Fractions X-Z; Figure 3-10B). TGF-ß stimulation, which induces the phosphorylation of SMAD2/3, caused a significant change in the elution profile of phospho-SMAD2/3. The majority of phospho-SMAD2/3 eluted in fractions T-Y, which is significantly higher than their predicted molecular weights (Figure 3-10C).

Consistent with the canonical TGF-ß signalling implicated in the complex formation between phosphorylated R-SMADs and the co-SMAD4, TGFß-induced phospho-SMAD2/3 and BMP-induced phospho-SMAD1 eluted in overlapping fractions with SMAD4 (Fractions T-X; Figure 3-10B and C). Interestingly, the elution profile of SMAD4 was unchanged under all stimulation conditions and represented a higher than predicted monomeric molecular weight (Figure 3-10A, B and C). A portion of phospho-SMAD1 was

detected in fractions O&P corresponding to molecular weights greater than 670 kDa under all conditions, albeit to a greater extent under BMP stimulation. This overlaps with the elution profile of PAWS1 (Figure 3-10A, B and C). Total SMAD1 was confirmed in these fractions by immunoblotting SMAD1 IPs from these fractions (Figure 3-10D). The PAWS1 elution profile did not overlap with SMADs 2, 3 and 4. Interestingly BMP caused a slight shift in the elution proflie of PAWS1 towards lower molecular weight fractions (Figure 3-10A, B and C).

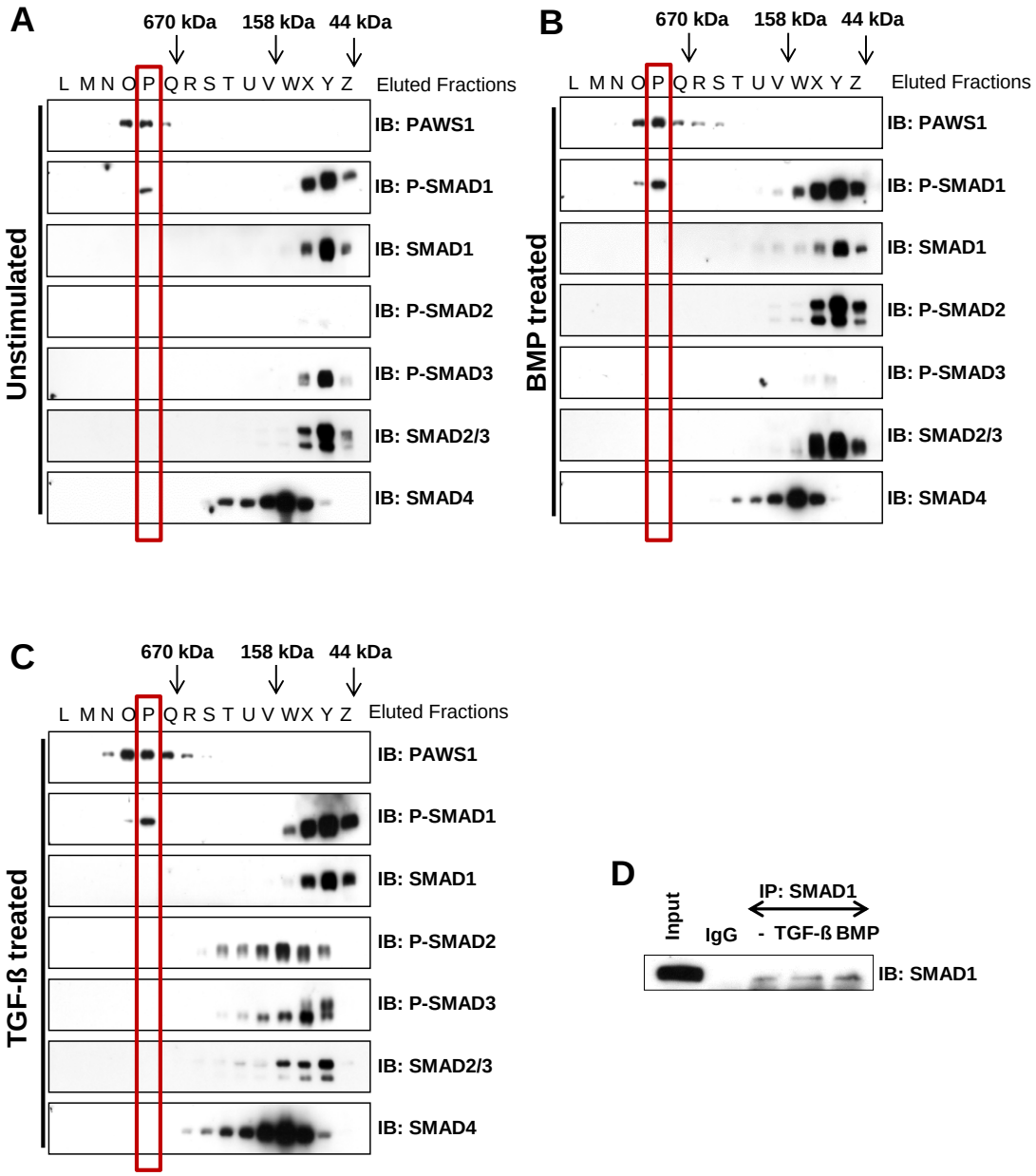

Figure 3-10 Size exclusion chromatography

(A) Unstimulated HaCaT cell extracts were fractionated by gel filtration chromatography on a Superose™ 10/300 GL Column (GE Health Care). 5 µl each of recovered fractions were resolved by SDS-PAGE and subsequently analysed by immunoblotting using the indicating antibodies. **(B)** Same as A except the cells were treated with BMP (25 ng/ml) for 1 h prior to lysis **(C)** Same as A except the cells were treated with TGFß (50 pM) for 1 h prior to lysis. **(D)** Inputs and SMAD1-immunoprecipitations from gel filtration chromatography fraction 16 were analysed by immunoblotting using SMAD1 antibody.

3.2.6 SMAD4 independent interaction between SMAD1 and PAWS1

To assess if PAWS1 affects SMAD1 association with SMAD4, a HEK293 cell line stably expressing GFP-SMAD4 under tetracycline induction was used. The expression of GFP-SMAD4 was induced by doxycycline and the cells were transfected with HA-SMAD1, FLAG-PAWS1 or both and treated with or without BMP. In the absence of FLAG-PAWS1 overexpression, GFP-SMAD4 IPs pulled down HA-SMAD1 predominantly upon BMP treatment (Figure 3-11). This association was slightly reduced when FLAG-PAWS1 was co-expressed with HA-SMAD1. However, under these conditions, the levels of HA-SMAD1 in extracts were significantly lower than when HA-SMAD1 was overexpressed in the absence of FLAG-PAWS1. GFP-SMAD4 did not pull down FLAG-PAWS1 in the presence or absence of HA-SMAD1 (Figure 3-11).

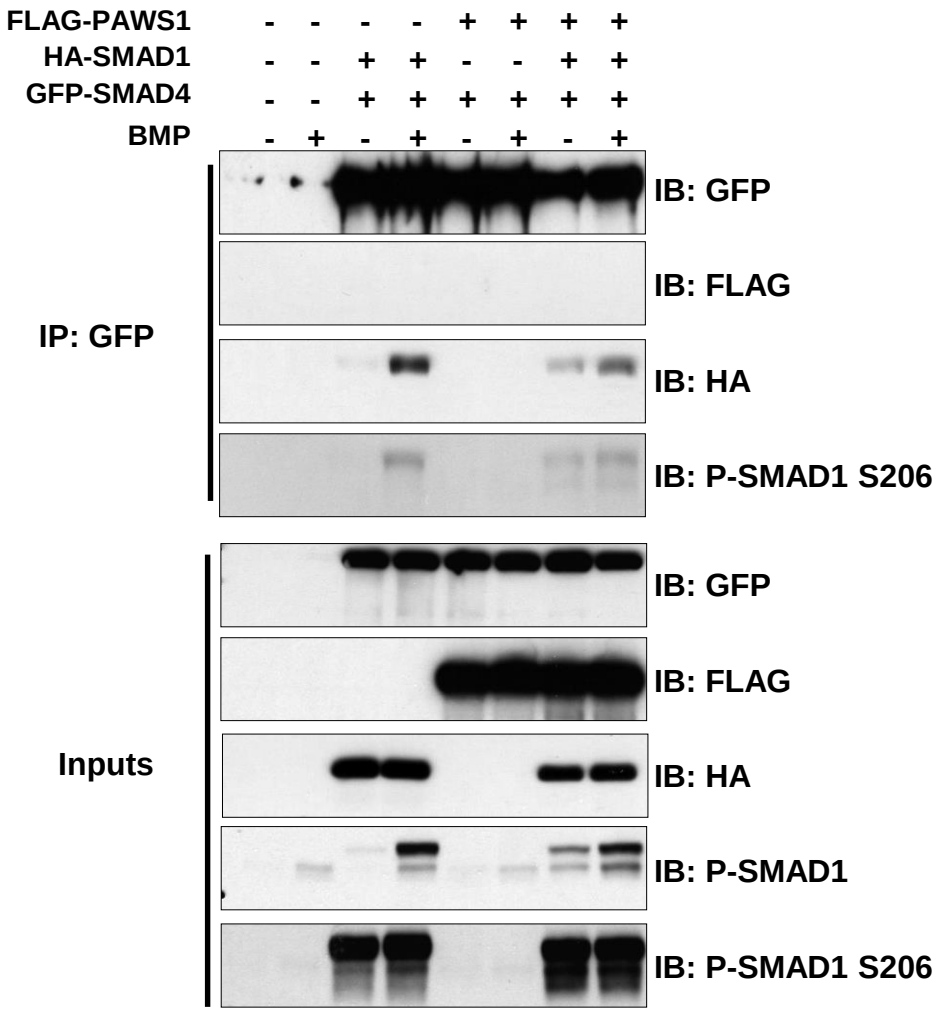

Figure 3-11 The impact of PAWS1 on SMAD1:SMAD4 interaction

HEK293 cells stably expressing tetracycline inducible GFP-SMAD4 were co-transfected with or without FLAG-PAWS1 and HA-SMAD1 48 h prior to lysis. The expression of GFP-SMAD4 was induced for 24 h prior to lysis with 20 ng/ml doxycycline. The cells were treated with or without BMP-2 (25 ng/ml) for 1 h prior to lysis. Extracts were used for GFP-Trap immunoprecipitation. The IPs and extract inputs were subjected to SDS-PAGE and subsequently analysed by immunoblotting using the indicated antibodies.

3.2.7 PAWS1 expression in various mouse tissues and different cell lines

PAWS1 expression in tissues and cell lines has not been characterised previously. Therefore, I analysed its expression in different mouse tissues as well as in various cell lines routinely used in the lab by immunoblotting. High levels of PAWS1 protein expression at predicted molecular weight were detected in tissue extracts derived from liver, adipose and pancreatic tissue (Figure 3-12A). PAWS1 expression, albeit to a lesser extent, was also detected in brain, lung, kidney and thymus tissue extracts (Figure 3-12A, high exposure). Additionally the anti-PAWS1 antibody also cross-reacted with higher than predicted molecular weight proteins in brain and liver tissue extracts (Figure 3-12A). PAWS1 expression could not be detected in heart, skeletal muscle, testis, epididymis and ovary tissue extracts (Figure 3-12A).

PAWS1 expression at the predicted molecular weight was detected by immunoblotting in several human cell lines including breast cancer MDA-MB231, osteosarcoma U2OS, HEK293, colon carcinoma RKO, human keratinocyte HaCaT, HeLa, breast cancer MCF7 and human myeloid leukaemia KBM-7 (Figure 3-12B). Endogenous PAWS1 protein expression was absent in prostate cancer cell line PC3 (Figure 3-12B).

Furthermore the expression was tested in the NCI-60 cancer cell line panel. PAWS1 protein expression was observed to be absent in 30 out of the 54 cell lines employed in the panel. However, SMAD1 expression did not

appear to mirror the expression profile of PAWS1 in the tissue and cell extracts (Figure 3-12).

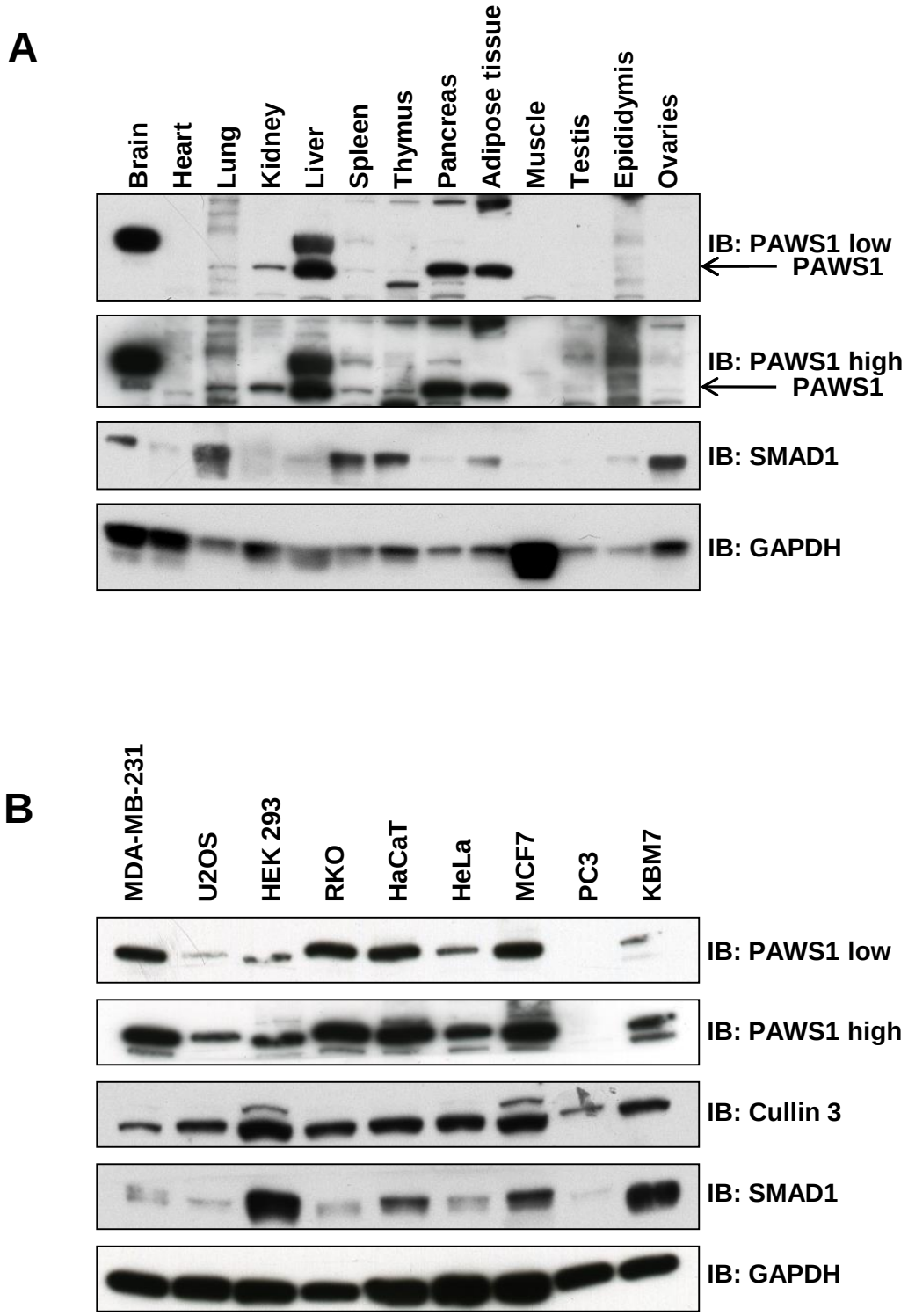

Figure 3-12 PAWS1 protein expression in tissues and cells

(A) Indicated mouse tissues were lysed and the extracts were subjected to SDS-PAGE. The subsequent immunoblotting analysis was performed using the indicated antibodies. **(B)** Extracts from different routinely used cell lines were analysed by immunoblotting for the protein expression of PAWS1. Immunoblotting analysis was performed using the indicating antibodies.

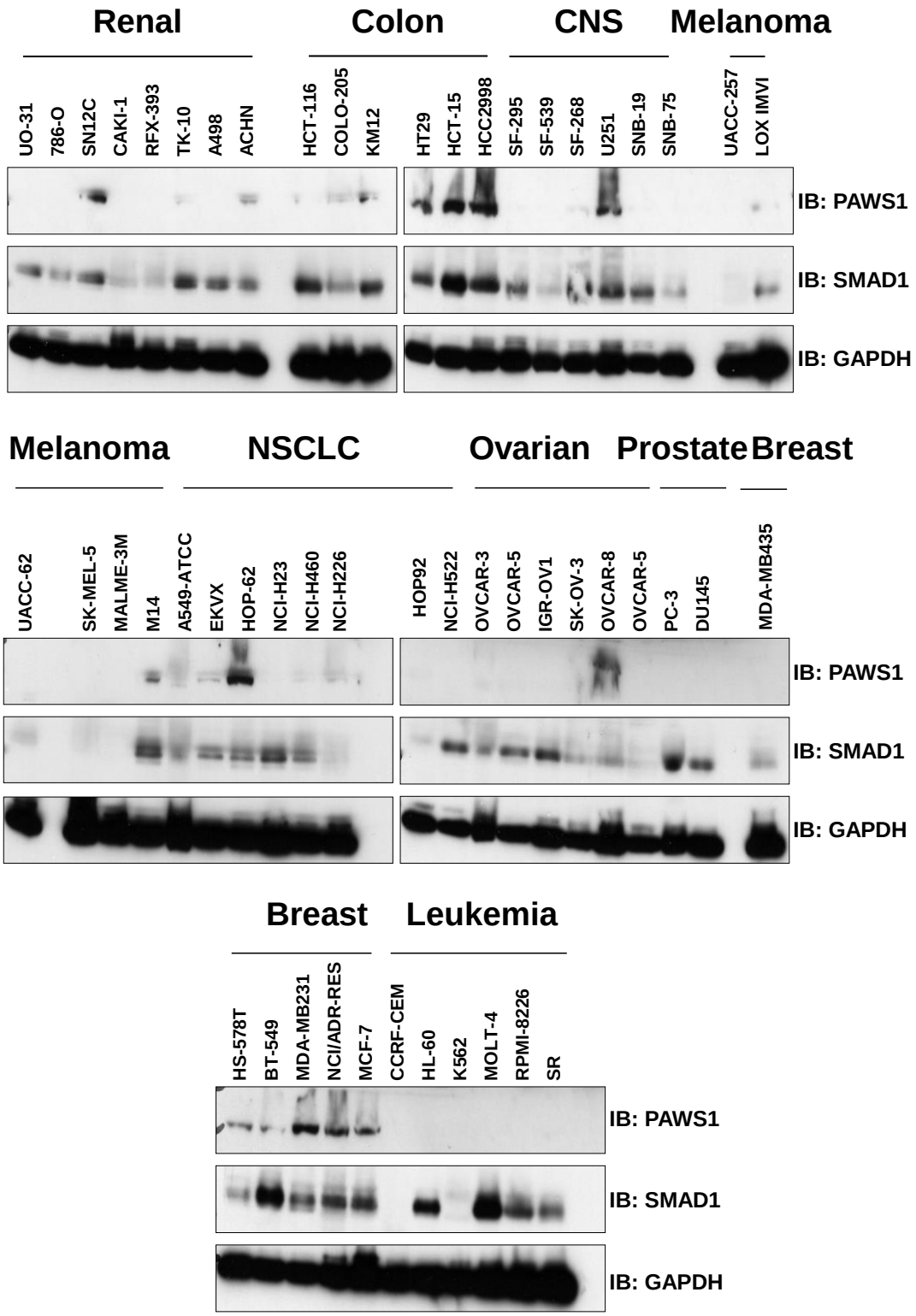

Figure 3-13 PAWS1 protein expression in the NCI-60 cancer cell line panel

Extracts from the NCI-60 panel of cancer cell lines were resolved by SDS-PAGE and subsequently analysed by immunoblotting using the indicated antibodies.

3.2.8 Sub-cellular localisation of PAWS1

As the sub-cellular localisation of PAWS1 in cells is unknown, I analysed its localisation by sub-cellular fractionation and immunofluorescence approaches.

HaCaT cells treated with or without BMP and TGF-ß were separated into cytosolic and nuclear fractions. Under all conditions, PAWS1 was detected predominantly in the cytosolic fractions. However upon BMP treatment a portion of PAWS1 was detected in the nuclear fraction. As expected, phospho-SMAD1 and phospho-SMAD2 were mainly detected in the nuclear fractions upon BMP and TGF-ß stimulations respectively (Figure 3-14A). Lamin A/C and GAPDH were used as controls and were detected in the nuclear and cytosolic fractions respectively (Figure 3-14A).

Fractionating cells for immunoblot analysis has limitations when it comes to assessing the precise sub-cellular localisation and co-localisation of proteins. Immunofluorescence studies on endogenous proteins are essential for robust conclusions on protein localisation. I tested all available anti-PAWS1 antibodies for immunofluorescence studies using PC3 cells that lack endogenous PAWS1 expression or PC3 cells restored with PAWS1 expression (Figure 3-15A). There was no differential fluorescence in these cells with any of the antibodies, indicating that they were unsuitable for endogenous immunofluorescence studies. I therefore looked at the intracellular localisation of GFP-PAWS1 stably expressed in U2OS cells. While GFP-PAWS1 fluorescence was observed in both cytosolic and nuclear compartments, the fluorescence was more pronounced in the cytosol and

nuclear periphery (Figure 3-14B). Treating the cells with BMP did not change the GFP-fluorescence intensities in either the nucleus or the cytosol (Figure 3-14B).

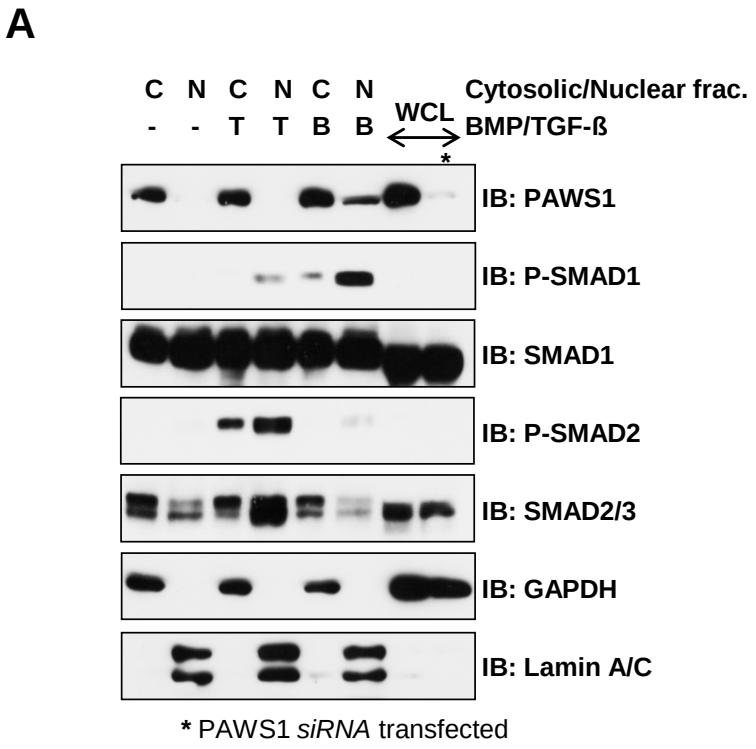

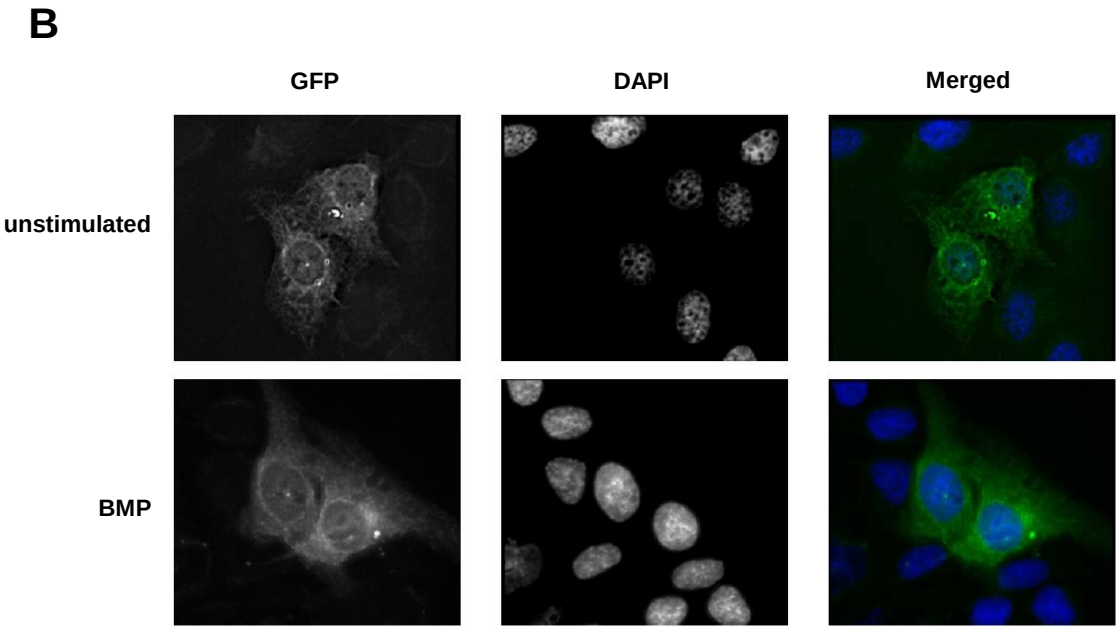

Figure 3-14 Subcellular localisation of PAWS1:

(A) HaCaT cells were treated with or without BMP (25 ng/ml) or TGFß (50 pM) for 1 h prior to separation into indicated subcellular fractions. Fractions or whole cell extract (WCL) were resolved by SDS-PAGE and analysed by immunoblotting using the indicated antibodies. GAPDH and Lamin A/C were used as cytosolic and nuclear controls respectively. **(B)** U2OS cells stably expressing GFP-tagged PAWS1 cultured on glass chamber slides were treated with or without BMP (25 ng/ml) for 1 h prior to fixation with 4% paraformaldehyde. Fluorescence was analysed using a Deltavision Core Restoration microscope. DAPI staining was used to detect the nuclei.

3.2.9 Re-introduction of PAWS1 in PC3 cells does not alter BMP induced phosphorylation of SMAD1

To investigate the impact of PAWS1 on canonical BMP signalling, I used PC3 cells that lack endogenous expression of PAWS1. Using a retroviral infection approach, I stably reintegrated either a control vector (PC Control) or a vector encoding the human *PAWS1* gene (PC3 PAWS1) into the cells. PC3 PAWS1 cells displayed PAWS1 protein expression that was comparable to the endogenous PAWS1 expression observed in HEK293 and HaCaT cells, whereas PC Control cells did not express PAWS1 (Figure 3-15A). A BMP time course experiment in PC Control and PC3 PAWS1 cells was performed to investigate the effect of PAWS1 on BMP-induced phosphorylation of SMAD1 (Figure 3-15B). Independent of the cell type, BMP induced the phosphorylation of SMAD1 within 15 min., reaching maximal level by 1 h and falling thereafter (Figure 3-15B). Reintroducing PAWS1 in PC3 cells did not significantly alter the kinetics or the extent of BMP-induced SMAD1 phosphorylation or the levels of SMAD1 protein compared to the PC Control cells (Figure 3-15B). Cells were also treated with increasing amounts of BMP to investigate if PAWS1 impacts the BMP threshold in PC3 cells (Figure 3-15C). No significant differences were observed between the two cell types at all applied doses of BMP (Figure 3-15C).

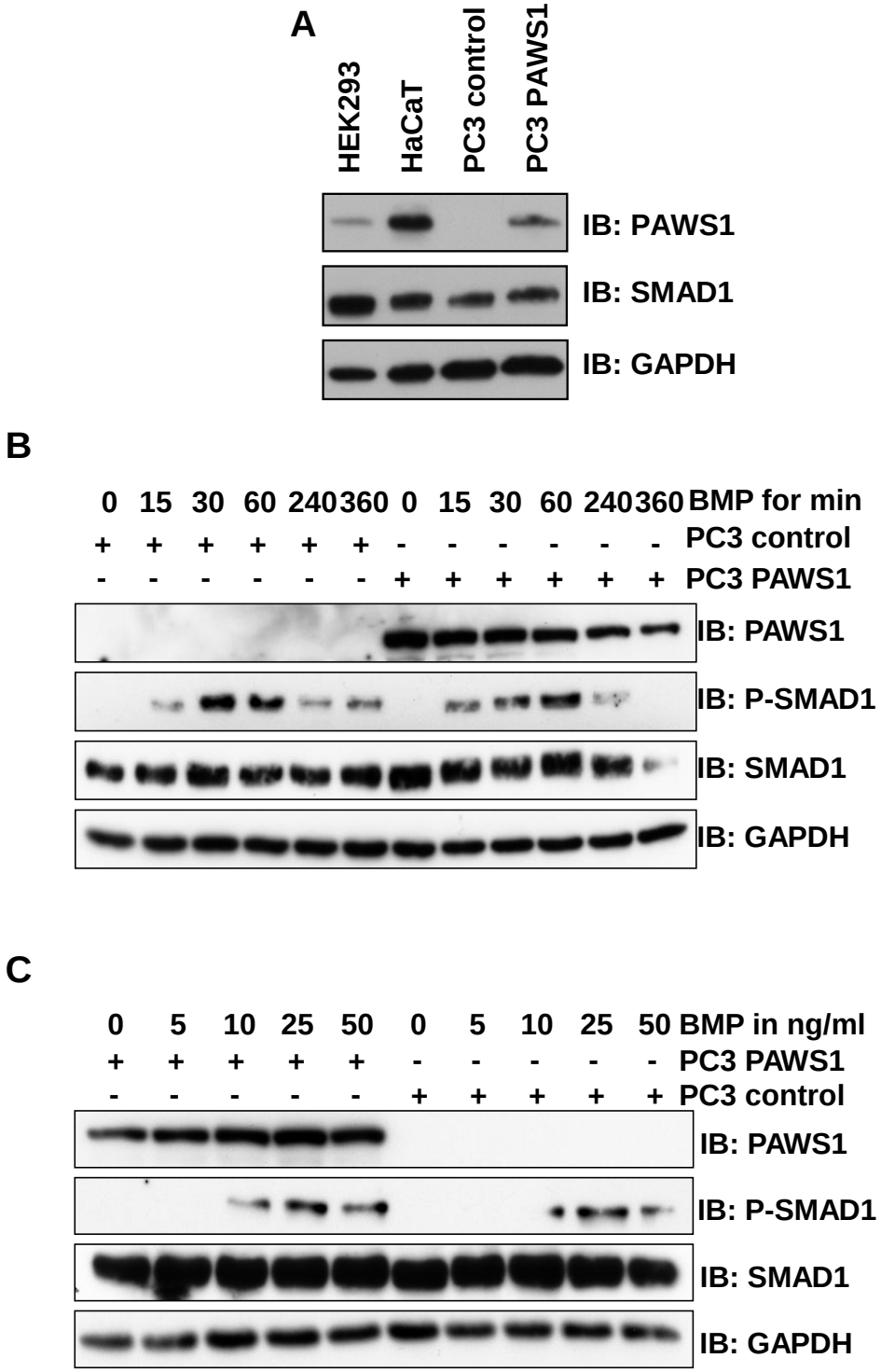

Figure 3-15 The effect of PAWS1 on BMP-induced SMAD1 phosphorylation

(A) HaCaT cells or PC3 cells stably integrated with a control vector (PC Control) or a vector encoding wild type PAWS1 (PC3-PAWS1) were lysed. Extracts were resolved by SDS-PAGE and analysed by immunoblotting using the indicated antibodies. **(B)** PC Control and PC3-PAWS1 cells were treated with BMP-2 (25 ng/ml) for the indicated time (h) prior to lysis. Extracts were resolved by SDS-PAGE and analysed by immunoblotting using the indicated antibodies. **(C)** PC Control and PC3-PAWS1 cells were treated with the indicated concentrations of BMP-2 for 1 h prior to lysis. Extracts were resolved by SDS-PAGE and analysed by immunoblotting using the indicated antibodies.

3.2.10 Size exclusion chromatography of PC Control and PC3 PAWS1 cells

In order to test if the reintroduced PAWS1 in PC3 cells elutes in similar fractions to the endogenous PAWS1 in HaCaT cells (Figure 3-10), PC3 PAWS1 and PC Control cell extracts were used in a similar size exclusion chromatography experiment. PC3 PAWS1 or Control cells were treated with or without BMP and the extracts were resolved by gel filtration chromatography using a Superose™ 6 Column (see section 0). 32 fractions were collected and analysed by immunoblotting. When PAWS1 was present in PC3 cells, it was detected in fractions M-O for unstimulated cell extracts and in fractions M-R in BMP stimulated fractions (Figure 3-16A upper panel). This corresponds to a macromolecular complex bigger than 670 kDa in size. A faint signal corresponding to tail-phosphorylated SMAD1 (P-SMAD1) was detected only in fraction N in the unstimulated cell extract, whereas it was detected in fractions N and O and also in fractions S-X in BMP stimulated cell extracts (Figure 3-16A lower panel).

PC Control cells, that lack the expression of PAWS1, were also fractionated in the same manner. As expected, PAWS1 could not be detected in any fraction, independent of the BMP treatment. Phosphorylated SMAD1 could be detected in fractions N and O in unstimulated cells. Upon BMP stimulation, P-SMAD1 was detected in fractions N and O and, additionally, fractions R-X (Figure 3-16B).

The elution profile of PAWS1 using PC3 PAWS1 cells is comparable to the endogenous PAWS1 elution profile observed in HaCaT cells (Figure

3-10). However, the distribution pattern of fractionated P-SMAD1 in PC3 PAWS1 cells shows no significant difference when compared to the fractionation pattern of P-SMAD1 in PC Control cells (Figure 3-16).

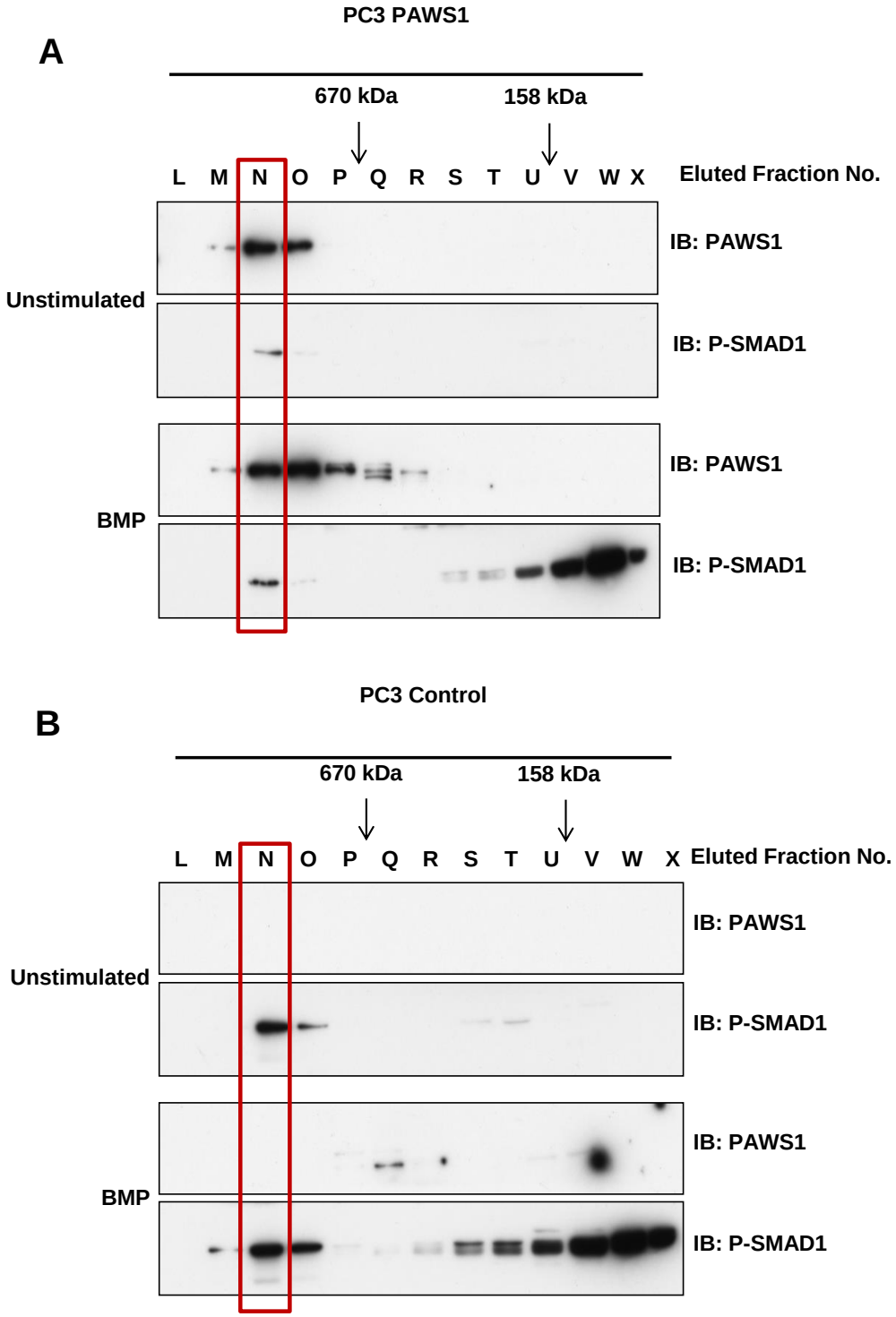

Figure 3-16 Size exclusion chromatography using PC Control of PC3 PAWS1 cells

(A) Unstimulated or BMP-2 (25 ng/ml) treated PC3 PAWS1 cell extracts were fractionated by gel filtration chromatography on a Superose™ 10/300 GL Column (GE Health Care). 5 µl each of recovered fractions were resolved by SDS-PAGE and subsequently analysed by immunoblotting using the indicating antibodies. **(B)** Same as A except that PC Control cells were used.

3.2.11 *In vitro* phosphorylation of FAM83G/PAWS1 by ALK receptor kinases

The observation that BMP treatment leads to partial nuclear localisation of PAWS1 (Figure 3-14) and a portion of phosphorylated SMAD1 elutes in the same fractions with PAWS1 (Figure 3-10 and Figure 3-16), prompted me to evaluate whether BMP could also induce a post translational modification within PAWS1. To investigate this, I generated a HEK293 cell line stably integrated with a single copy of GFP-PAWS1 under a tetracycline repressor (see section 2.2.4). After 24 h tetracycline induction (1 µg/ml), the cells were treated with or without BMP. Subsequently the GFP IPs from these cells were analysed for phosphorylation sites by mass spectrometry (Figure 3-17A). Interestingly, a triply phosphorylated peptide corresponding to residues 608-623 (RPSVASSVSEEYFEVR) of human PAWS1 was identified (Figure 3-17A). This internal SS(V/M)S motif identified in PAWS1 is not only conserved across different species but identical to the C-terminal SS(V/M)S activation motif within SMAD proteins (Figure 3-17A). The triphospho peptide was identified from cells treated with BMP. While the mass spectrometric analysis was able to establish Serine 610 as one of the phosphorylation sites, it was unable to precisely establish the two remaining phosphorylation residues within this peptide.

Despite the failure to map the precise BMP-induced phosphorylation residues within the SSVS motif in PAWS1 by mass-spectrometry, based on the above observations, I predicted that PAWS1 could be a novel target for the BMP type I receptor kinase (BMPR1A/ALK3). To date, there are no non-SMAD substrates reported for ALK3 or any other ALK. To test this

hypothesis, I set up an *in vitro* kinase assay in the presence of $^{\gamma 32}$P-ATP using a GST-tagged PAWS1 (523-end) fragment as a substrate for ALK3. PAWS1 was phosphorylated *in vitro* by ALK3 (Figure 3-17B). GST-SMAD1, which was used as a positive control, was also phosphorylated by ALK3, while GST-SMAD2, used as a negative control, was not phosphorylated by ALK3 (Figure 3-17B). Other BMP activated type I receptors, ALK2 and ALK6, also phosphorylated GST-PAWS1(523-end) *in vitro* and this phosphorylation was efficiently blocked by LDN-193189, an inhibitor of BMP activated ALKs (1, 2, 3 & 6) (Figure 3-17C).

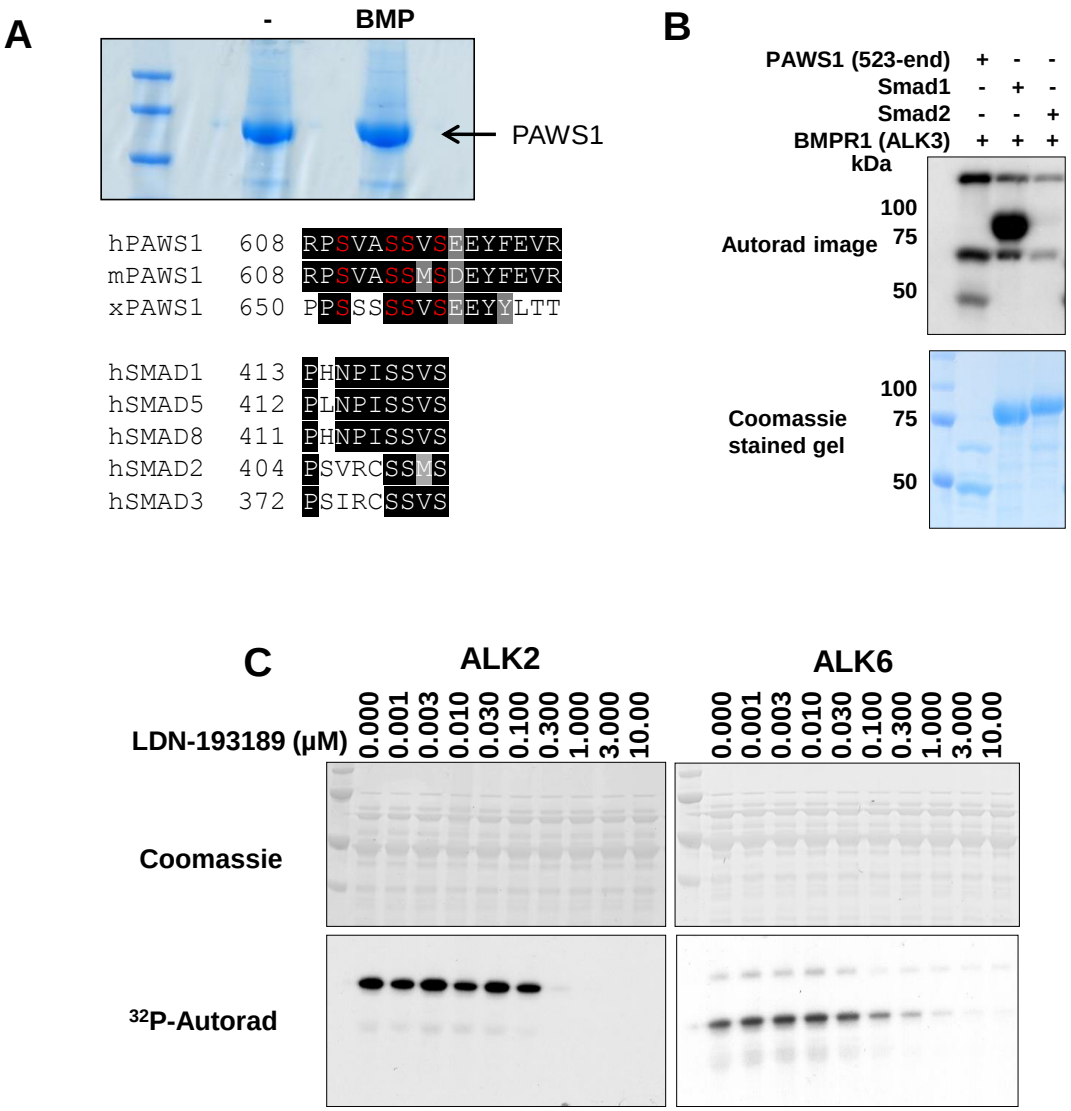

Figure 3-17 Phosphorylation of PAWS1 by BMPR1 (ALK3)

(A) GFP IPs from HEK293 cells stably expressing GFP-PAWS1 treated with or without BMP-2 (25 ng/ml) were resolved by SDS-PAGE. The gel was Coomassie stained and bands representing GFP-PAWS1 excised and digested with trypsin. The phospho-peptides were identified by mass spectrometry. The sequence alignment of the PAWS1 tri-phospho peptide identified upon BMP treatment with other vertebrates is shown. Also shown for comparison is the sequence alignment of the SXS motif in different R-SMADs. h: human; m: mouse; x: *Xenopus laevis* **(B)** Kinase assays were set up with BMPR1 (ALK3) using GST-SMAD1, GST-SMAD2 and GST-PAWS1 (523-end) as substrates using $^{\gamma 32}$P-ATP (500 cpm/pmole) as described in methods section 2.2.12. Samples were resolved by SDS-PAGE, the gel was Coomassie stained and radioactivity was analysed by autoradiography. **(C)** Kinase assays were performed with ALK2 or ALK6 and PAWS1 in the presence of the indicated concentration of LDN-193189. Samples were resolved by SDS-PAGE. Subsequently the gels were Coomassie stained, dried and analysed by ^{32}P autoradiography

3.2.12 Mapping ALK3 phosphorylation sites in PAWS1

I set out to map the *in vitro* ALK3 phosphorylation sites within PAWS1 by a combination of mass spectrometry and solid-phase Edman sequencing. GST-PAWS1(523-end) was phosphorylated by ALK3 using $^{\gamma 32}$P-ATP. $^{\gamma 32}$P-labelled GST-PAWS1(523-end) was digested with trypsin and the resulting peptides were separated by chromatography on a C18 column. Three $^{\gamma 32}$P-labelled peaks, one major (P1) and two minor (P2 & P3), were observed eluting at 26%, 25% and 24% acetonitrile respectively (Figure 3-18A). For P1, ^{32}P radioactivity was released after the third cycle after Edman degradation (Figure 3-18C). The molecular mass of this peak as determined by mass spectrometry (961.4382 Da) was identical to that expected for a tryptic phospho-peptide comprising residues 608–623 with a single phosphorylation modification. Taken together, these results imply that ALK3 phosphorylates PAWS1 at Ser610. For the second peak, P2, the ^{32}P radioactivity was released after the seventh and the ninth cycles after Edman degradation, indicating phosphorylation at Ser614 and Ser616 of PAWS1 (Figure 3-18B). For Peak 3 (P3) the material was insufficient for mass spectrometric and Edman degradation analysis of potential phosphorylation sites within peak P3 (Figure 3-18A). These results taken together show that ALK3 phosphorylates PAWS1 predominantly at Ser610 but can also phosphorylate Ser614 and Ser616 *in vitro.* Consistent with this observation, when Ser610 was mutated to Ala, the phosphorylation of GST-PAWS1(523-end) by ALK3 *in vitro* was almost completely abolished (Figure 3-18D). On the other hand, mutation of Ser613, Ser614 and Ser616 to Ala resulted in a significant but not complete inhibition of phosphorylation of GST-PAWS1(523-end) by ALK3 *in vitro* (Figure 3-18D).

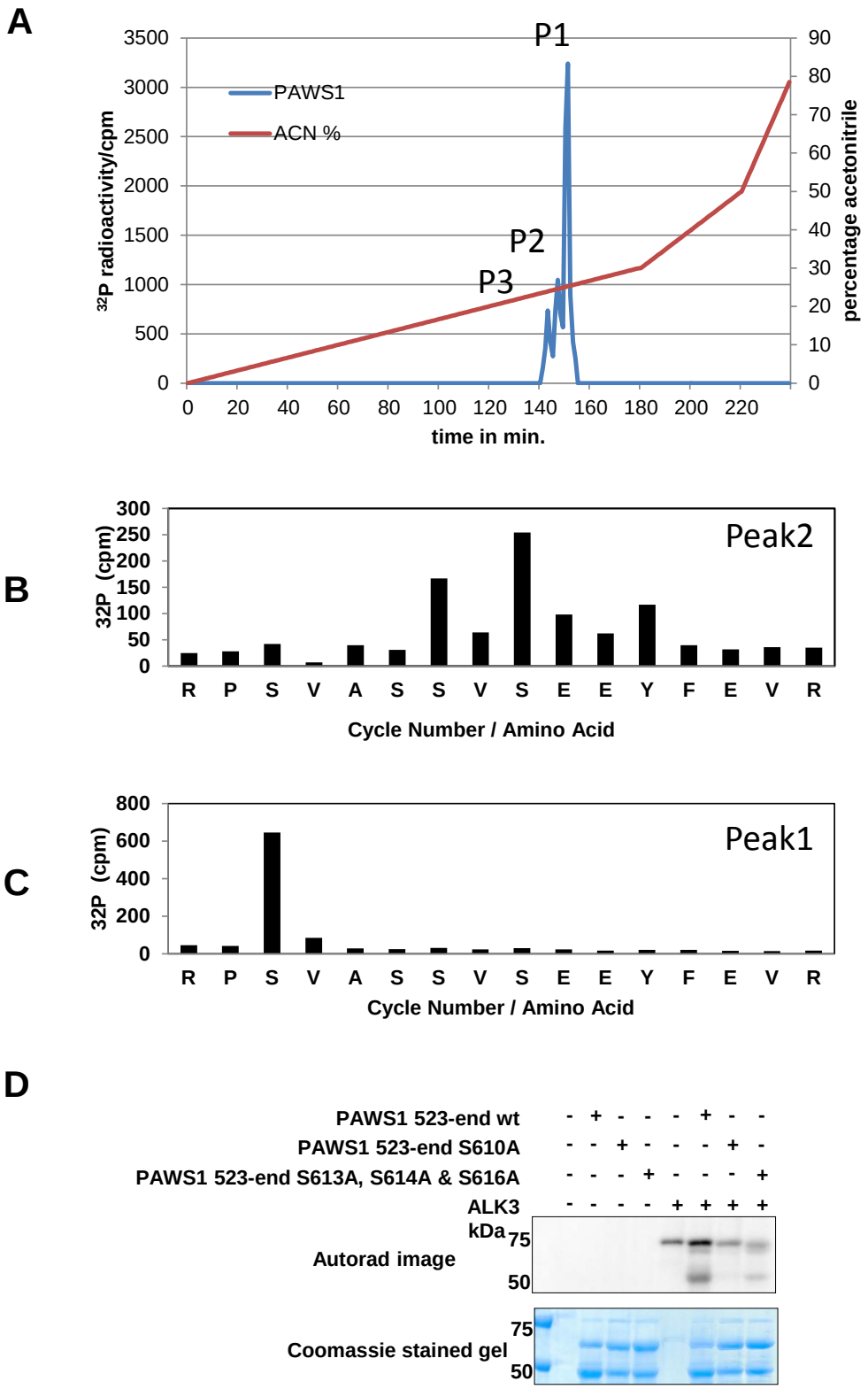

Figure 3-18 Mapping ALK3 phosphorylation sites in PAWS1

(A) GST-PAWS1(523-end) phosphorylated by BMPR1 (ALK3) as described in methods section 2.2.12 was excised, digested with trypsin and resolved by HPLC on a C_{18} column on an increasing acetonitrile gradient as indicated. Three peaks (P1-3) of ^{32}P release were observed. Analysis of the phospho-peptide in peak P1 revealed a mass of 961.4382. **(B)** Solid-phase sequencing of peak P2 revealed the release of ^{32}P radioactivity after the seventh and ninth cycles of Edman degradation. **(C)** Solid-phase sequencing of peak P1 revealed the release of ^{32}P radioactivity after the third cycle of Edman degradation. **(D)** BMPR1 (ALK3) was incubated in a kinase assay with GST-PAWS1(523-end), GST-PAWS1(523-end) S610A or GST-PAWS1(523-end) S613A, S614A and S616A as substrates. Samples were resolved by SDS-PAGE. Subsequently the gels were Coomassie stained, dried and analysed by ^{32}P autoradiography.

3.2.13 PAWS1 is phosphorylated upon BMP stimulation in cells

To further elucidate the role of Ser610 in PAWS1, I generated PC3 cell line stably integrated with a PAWS1-Ser610Ala mutation (PC3 PAWS1 S610A). I also generated an antibody against PAWS1 phosphorylated at Ser610 (P-PAWS1) (see section 2.2.18). Using these tools, I investigated the nature and role of BMP induced phosphorylation of PAWS1 at Ser610 in cells. In PC3 PAWS1 cells, stimulation with BMP but not control or TGF-ß, resulted in the phosphorylation of PAWS1 at Ser610 as detected by the P-PAWS1 antibody (Figure 3-19A). In contrast, stimulation of PC Control cells or PC3 PAWS1 S610A cells with BMP did not result in the detection of PAWS1 phosphorylation at Ser610 (Figure 3-19A). These results not only confirm the specificity of P-PAWS1 antibody but indicate that BMP induces phosphorylation of PAWS1 at Ser610. The re-introduction of wild type or the Ser610Ala mutant PAWS1 in PC3 cells did not significantly alter the levels of BMP induced phosphorylation of SMAD1 (Figure 3-19A and Figure 3-15). Next, I also investigated whether BMP could induce the phosphorylation of endogenous PAWS1 at Ser610 in HaCaT cells. PAWS1 phosphorylation at Ser610 was detected in HaCaT cell extracts treated with BMP. This was inhibited by LDN-193189, a potent albeit non-selective ALK3 inhibitor (Figure 3-19B). Furthermore, I assessed the kinetics of BMP induced PAWS1 phosphorylation at Ser610. The BMP-induced phosphorylation of PAWS1 at Ser610 mirrored the kinetics of SMAD1 tail phosphorylation (Figure 3-19C).

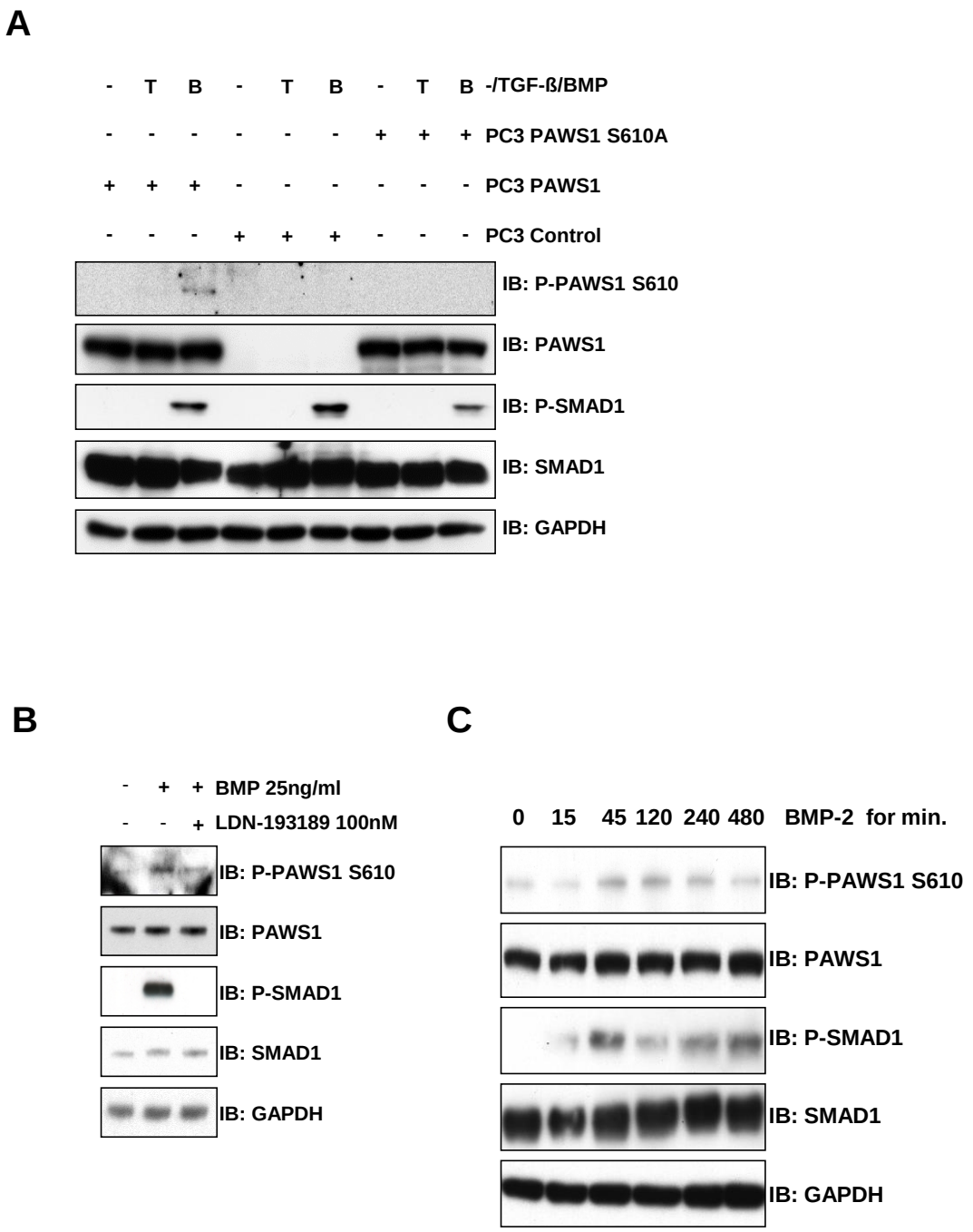

Figure 3-19 PAWS1 is phosphorylated at Ser610 upon BMP stimulation in cells

(A) PC3 Ccontol, PC3 PAWS1 or PC3 PAWS1 S610A cells were treated with BMP-2 (25 ng/ml), TGF-ß (50 pM) or left untreated for 1 h prior to lysis. Extract were resolved by SDS-PAGE and immunoblotted with the indicated antibodies **(B)** HaCaT cells were left unstimulated or stimulated with BMP-2 (25 ng/ml) with or without LDN193189 (100 nM) for 1 h prior to lysis. PAWS1 was immunoprecipitated from cell extracts (1 mg protein) using anti-PAWS1 antibody. PAWS1 IPs or extract inputs were resolved by SDS-PAGE and immunoblotted with the indicated antibodies. **(C)** HaCaT cells were treated with BMP-2 (25 ng/ml) for the indicated time prior to lysis. Extracts were resolved by SDS-PAGE and analysed by immunoblotting using the indicated antibodies.

3.2.14 PAWS1 regulates the expression of some non-canonical BMP target genes

Both SMAD4-dependent (canonical) and independent (non-canonical) modes of TGF-ß signalling have been reported to control the transcription of distinct target genes (Derynck and Zhang, 2003). *ID1* is a prominent example for a BMP target gene reported to be SMAD4 dependent (Miyazono and Miyazawa, 2002). However, in cells lacking endogenous SMAD4 expression, BMP stimulation can still induce the transcription of many different target genes, including NEDD9 and ASNS (Deng et al., 2009).

Because PAWS1 can form a complex with SMAD1 independently of SMAD4 (Figure 3-10 and Figure 3-11), I hypothesised that the transcription of SMAD4-independent BMP target genes could be regulated by PAWS1. In order to test this hypothesis, I used PC Control and PC3 PAWS1 cells. I also included the PC3 PAWS1 S610A mutant cell line to test whether the BMP-induced phosphorylation of PAWS1 affected the transcription of these genes. In PC3 PAWS1 cells, BMP induced the expression of NEDD9 and ASNS, two SMAD4-independent BMP-target genes ((Deng et al., 2009)Figure 3-20 A and B)). Interestingly, in PC3 Control or PC3 PAWS1 S610A cells, BMP-induced expression of NEDD9 and ASNS was not induced (Figure 3-20A and B). This would suggest that the phosphorylation of PAWS1 at Ser610 in response to BMP is important for the transcription of these genes. The expression of the BMP receptor type 2 gene (BMPR2) was unchanged in PC3 PAWS1 or PC3 PAWS1 S610A cells, when compared to PC Control cells (Figure 3-20C). Finally, I also investigated whether phosphorylation of PAWS1 Ser610 impacts the ability of PAWS1 to interact with SMAD1. Both

wild-type PAWS1 and PAWS1 S610A mutant expressed in PC3 cells interacted with endogenous SMAD1 with similar affinities (Figure 3-20D).

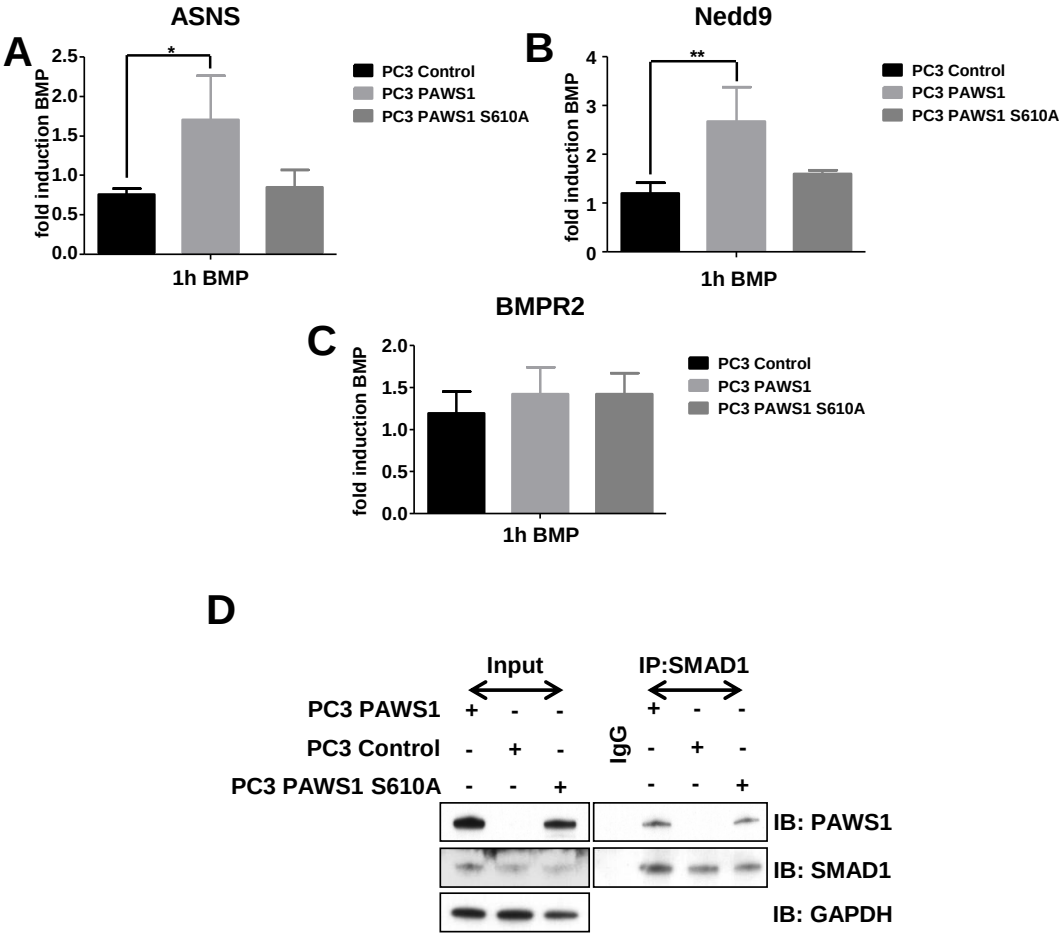

Figure 3-20 The role of PAWS1 in the BMP pathway

(A-C) PC3 Contol, PC3 PAWS1 or PC3 PAWS1 S610A cells were treated with BMP-2 (25 ng/ml) or left untreated for 6 h prior to RNA isolation. The relative expression of the indicated genes was analysed by qRT-PCR as described in the methods (see section 2.2.22). The results are presented as fold change in gene expression relative to unstimulated controls. Data are represented as mean of three biological replicates and error bars indicate standard deviation (n=3). **(D)** PC3 Contol, PC3 PAWS1 or PC3 PAWS1 S610A cells were lysed and PAWS1 was immunoprecipitated from cell extracts using anti-PAWS1 antibody. IgG was used as a control. PAWS1 IPs or extract inputs were resolved by SDS-PAGE and immunoblotted with the indicated antibodies.

3.2.15 Biased qRT-PCR array of TGF-ß signalling components and TGF-ß signalling targets in PC3 cells

In order to evaluate whether the restoration of PAWS1 expression in PC3 cells regulates the expression of 155 transcripts known to be TGF-ß and BMP pathway components or targets, I performed quantitative real-time (qRT) PCR macroarrays (Sabiosciences). I identified 35 genes in which the change in expression was more than 2 fold upon restoration of PAWS1 in both untreated and BMP treated PC3 cells (Figure 3-21, Table 3-2 and Table 3-3). Among these, 15 genes were low expression genes (qRT-PCR cycle above 30 (Table 3-3)) and 20 high to medium expression genes (qRT-PCR cycle below 30 (Table 3-2)). Of the high expression genes, only 3 genes (CDKN1A, HEY1 and INHA) appeared to be BMP-inducible, albeit the fold change was small (Table 3-2 second row).

Next I sought to verify the observed changes in gene expression from the macroarray by qRT-PCR. In PC Control or PAWS1 cells treated with or without BMP, using a similar set up as for the macroarray, I confirmed that PAWS1 expression augmented the expression of TGFBI, FST and TGFBR2 while it diminished the expression of AR and TSC22D (Figure 3-22A). ID1 expression, which serves as a control for BMP stimulation, was not significantly altered between PC Control and PC3 PAWS1 cells. All other genes from the macroarray displaying significant changes in expression between PC Control and PAWS1 were found to be false positive.

Furthermore, to ensure that the expression changes of the genes were directly dependent on PAWS1 expression in PC3 cells, I analysed the

expression of FST and TGFBI in HaCaT cells by qRT-PCR upon *RNAi*-mediated depletion of PAWS1, which results in ~80% reduction in PAWS1 protein expression (Figure 3-22B). PAWS1 depletion in HaCaT cells results in repression of FST and TGFBI expression (Figure 3-22C), confirming the results from PC Control and PAWS1 cells. I also investigated whether BMP affected the expression of these genes. I found that stimulation of cells with BMP did not alter the expression of FST, TGFBI, AR, TGFBR2 and TSC22D in both PC Control or PC3 PAWS1 cells (Figure 3-22A). Consistent with this, BMP stimulation did not affect the expression of FST and TGFBI in HaCaT cells expressing *control or PAWS1 siRNAs* (Figure 3-22C). Taken together these results imply that PAWS1 can regulate the expression of some genes that have been previously described as being components of the TGF-ß and BMP pathways, albeit independently of BMP stimulation.

A

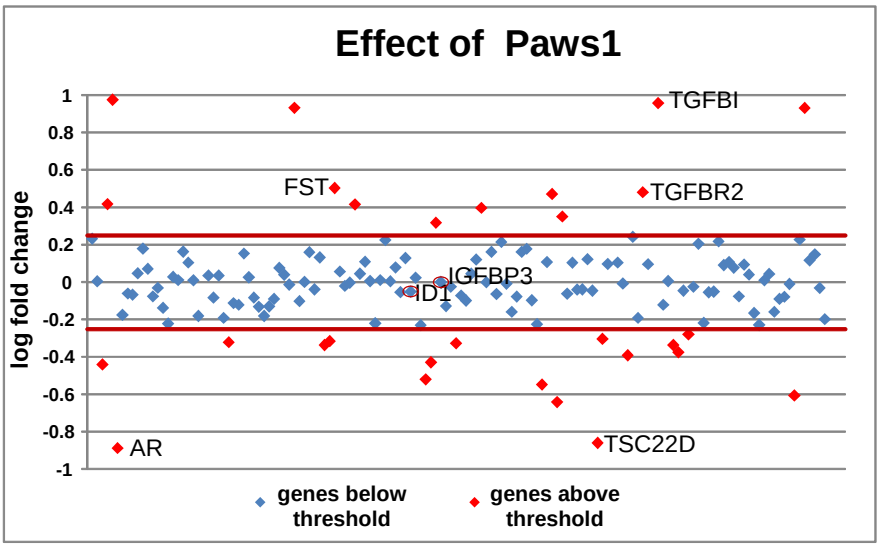

B

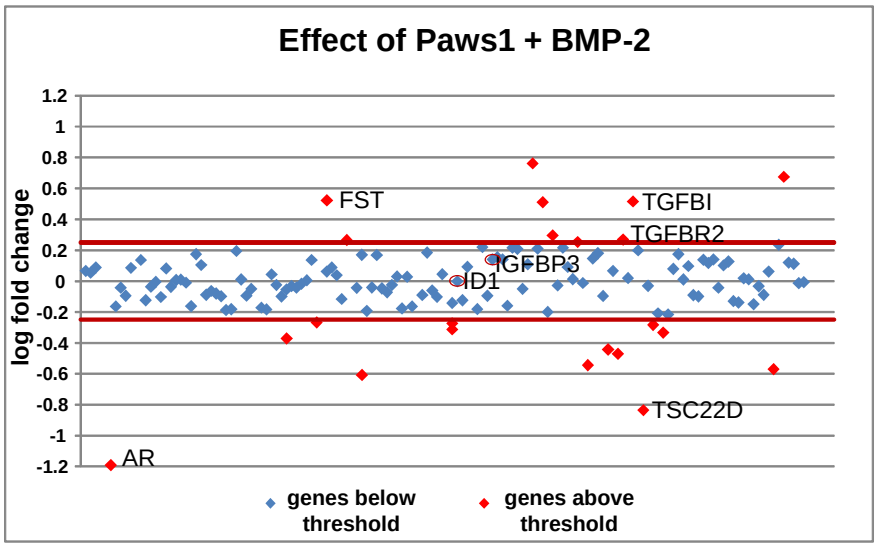

Figure 3-21 PAWS1 impacts the expression of multiple genes in the TGF-ß/BMP pathway independent of BMP treatment

(A) Scatter plots of log fold change in gene expression in PC3 PAWS1 over PC Control cells of 150 TGF-ß/BMP pathway components or target genes analysed by qRT-PCR. Each dot represents the expression of a single gene. **(B)** Same as A but cells were treated with BMP-2 (25 ng/ml) for 6 h prior to lysis.

High expression genes (<30 cycles)		
	Effect of PAWS1	Effect of PAWS1 + BMP
	Fold change	
TGFBI	8.53	4.73
FST	3.02	3.27
BMP6	2.96	3.23
TGFBR2	2.61	2.40
PDGFA	2.60	1.84
MECOM	1.74	1.85
INHBA	-1.91	-1.65
MYC	-2.04	-1.86
FOS	-2.10	
SNAI1	-2.13	-2.06
IGFBP3	-2.17	-1.93
MSX2	-2.17	-1.86
IL6	-2.38	
DLX2	-2.47	-2.97
SERPINE1	-3.69	-6.04
TSC22D1	-4.05	-3.37
AR	-7.74	-15.62
CDKN1A		1.79
HEY1		-1.86
INHA		-2.17

Table 3-2 High expression genes that are regulated by PAWS1

Genes identified with the macroarray whose expression changed at least 2-fold upon PAWS1 expression. All genes represented in this table were identified by qRT-PCR with an expression below the cycle 30 threshold in PC Control and PC3 PAWS1 cells. Red indicates upregulation and blue indicates downregulation in gene expression.

Low expression genes (>30 cycles)		
	Effect of PAWS1	Effect of PAWS1 + BMP
	Fold change	
AIPL1	8.53	4.73
GSC	3.02	3.27
IL10	2.96	3.23
MYOD1	2.61	2.40
AGT	2.60	1.84
BMPER	1.74	1.85
CHRD	-1.91	-1.65
SHH	-2.04	-1.86
ACVRL1	-2.10	
BMP3	-2.13	-2.06
BMP7	-2.17	-1.93
CER1	-2.17	-1.86
GDF6	-2.38	
BDNF	-2.47	-2.97
COL3A1	-3.69	-6.04

Table 3-3 Low expression genes that are regulated by PAWS1

Genes identified from the macroarray whose expression changed at least 2-fold upon PAWS1 expression. All genes represented in this table were identified by qRT-PCR with an expression above the cycle 30 threshold in PC Control and PC3 PAWS1 cells. Red indicates upregulation and blue indicates downregulation in gene expression.

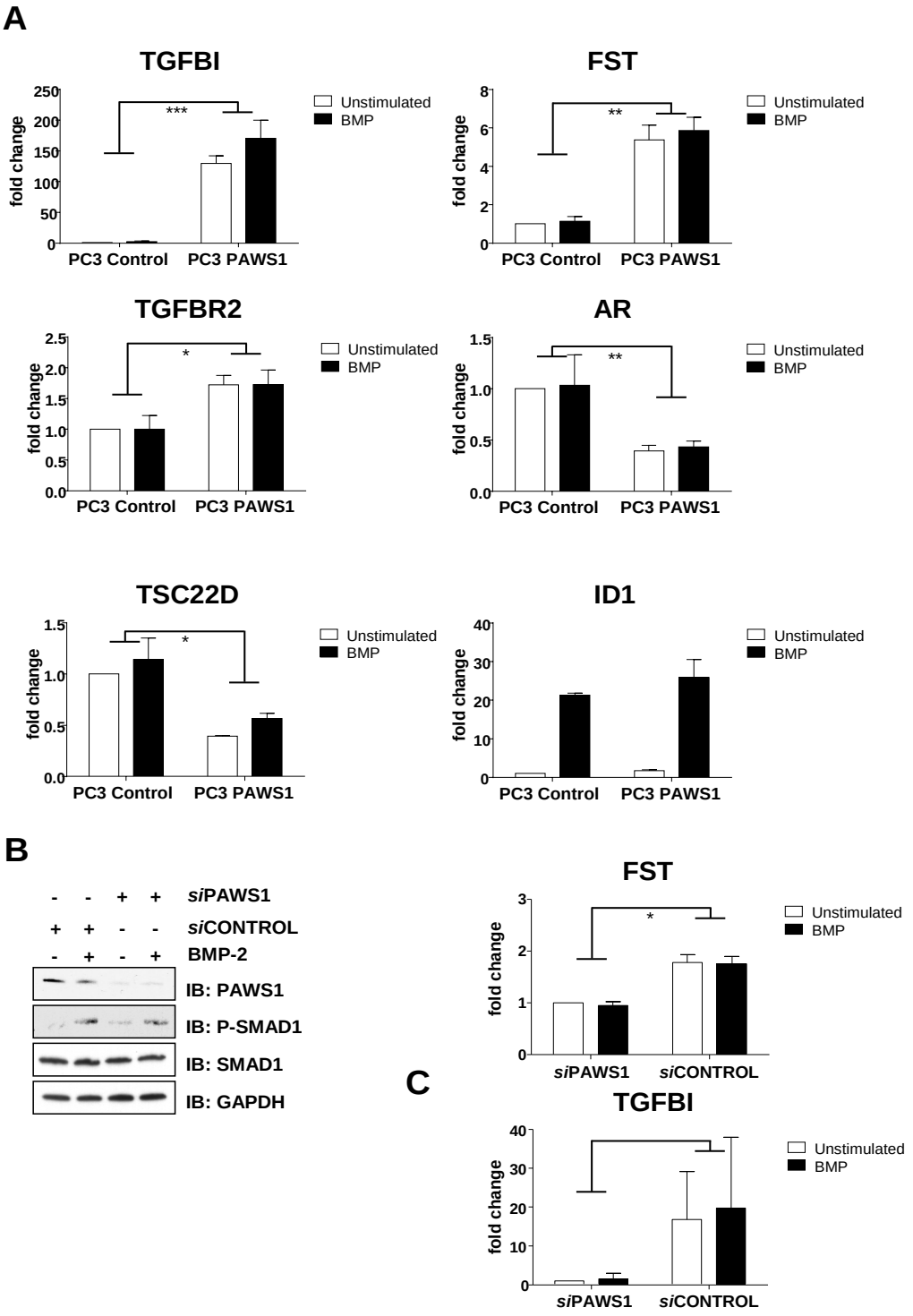

Figure 3-22 PAWS1 impacts the expression of multiple genes in the TGF-ß/BMP pathways independent of BMP treatment

(A) PC3 PAWS1 or PC Control cells were treated with or without BMP-2 (25 ng/ml) for 6 h prior to lysis. RNA was extracted and the cDNA synthesized. The expression of the genes was analysed by qRT-PCR. The results show the fold change in gene expression relative to the levels observed for unstimulated PC Control cells. Data are represented as mean of three biological repeats and error bars indicate standard deviation (n=3). **(B)** PAWS1 depleted HaCaT cells *(siPAWS1)* or HaCaT cells expressing FOXO4 *siRNA (siCONTROL)* were lysed. Extracts were resolved by SDS-PAGE and immunoblotted with the indicated antibodies. **(C)** PAWS1 depleted HaCaT cells *(siPAWS1)* or HaCaT cells expressing FOXO4 *siRNA (siCONTROL)* were treated with or without BMP-2 (25 ng/ml) for 6 h prior to lysis. RNA was extracted and the cDNA synthesized. The expression of FST and TGFBI genes was analysed by qRT-PCR. The results respresent the fold change in gene expression relative to the levels observed for unstimulated *siPAWS1* HaCaT cells. Data are represented as mean of three biological repeats and error bars indicate standard deviation (n=3).

3.2.16 Analysis of global PAWS1-dependent gene expression by RNA sequencing

The macroarray (Figure 3-21) described above was limited with respect to the gene number (155 genes) and it was biased towards TGF-ß and BMP pathway components and target genes. Therefore, I decided to undertake a transcriptomic approach to identify candidate genes that might be regulated by PAWS1 globally. In order to do this, our lab initiated collaboration with Prof. Jim Smith (MRC NIMR, London). I isolated RNA from PC Control and PC3 PAWS1 cells treated without or with BMP for 3 h and 16 h in triplicates. The quality of the RNA was verified by running 0.5 µg of each RNA sample on 1% agarose gel prior to RNA seq. (Figure 3-23). Dr. Kevin Dingwell in Prof. Smith's laboratory performed RNA sequencing analysis on the isolated RNAs. We identified more than 800 genes that changed expression as a result of PAWS1 expression in PC3 cells (Appendix Table 1). Out of these 800 genes, more than 300 changed expression by more than 2 fold (Appendix Table 1). To validate the identified genes, I employed the qRT-PCR approach and out of 30 genes randomly picked from 50 top hits, I verified the differential expression caused by PAWS1 for 19 genes (Figure 3-24 and Figure 3-25). Among these, 7 were up-regulated (Figure 3-24) and 12 were down-regulated upon PAWS1 expression (Figure 3-25).

Stimulating the cells with BMP for 3 or 16 h prior to RNA isolation did not yield many genes for which expression was dependent on both PAWS1 and BMP stimulation. However, ASNS was one of the genes that displayed a slight change in expression (Appendix Table 3).

Furthermore, in order to gain confidence that the observed changes in gene expression are indeed regulated by PAWS1, an *RNAi* approach using HaCaT cells as described above was used alongside the PC Control/PAWS1 cells. RNA was isolated from PC Control, PC3 PAWS1 and HaCaT cells expressing *siPAWS1* or *siControl* that were treated with or without BMP. The isolated RNA was analysed by qRT-PCR for some of the PAWS1 target genes (Figure 3-26). As expected the expression of BEX1, CCNA1, GTF2F2 and ASNS was reduced by PAWS1 expression in PC3 cells (Figure 3-26 left panel). In contrast, in HaCaT cells expressing PAWS1 siRNA, the expression of these genes was enhanced compared to cells that expressed control *siRNA* (Figure 3-26 right panel). The treatment of BMP did not significantly alter the expression these genes in either cell system (Figure 3-26).

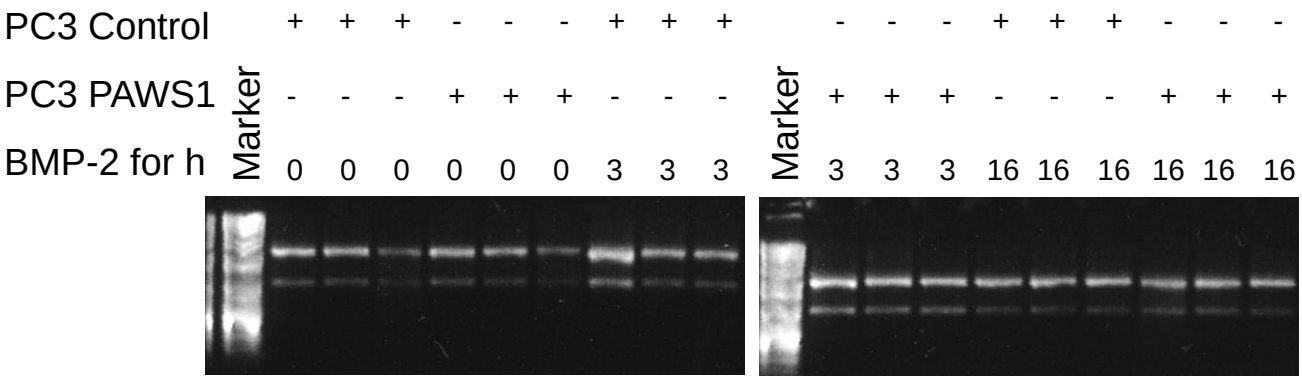

Figure 3-23 PAWS1 regulated genes in PC3 cells identified by RNA sequencing

RNA isolated from PC Control and PC3 PAWS1 cells treated with BMP-2 (25 ng/ml) for the indicated time points prior to isolation of RNA. 250 ng of isolated RNA was resolved on a 1% agarose gel to test its quality prior to an RNA sequencing analysis.

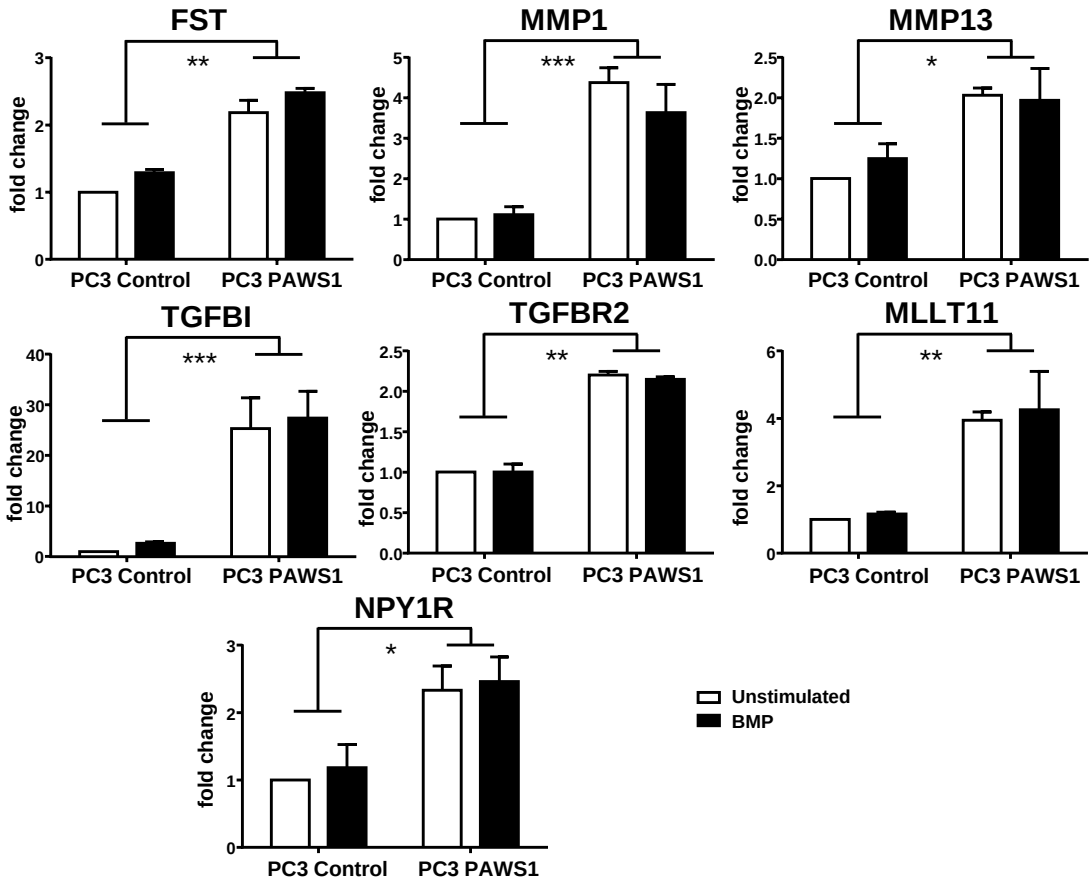

Figure 3-24 Genes that are upregulated by PAWS1 expression

PC Control and PC3 PAWS1 cells were treated with or without BMP-2 (25 ng/ml) for 3 h prior to RNA isolation. RNA was extracted and the cDNA synthesized. The expression of the genes was analysed by qRT-PCR. The results represent fold change in gene expression relative to the levels observed for unstimulated PC Control cells. Data are represented as mean of three biological repeats and error bars indicate standard deviation (n=3).

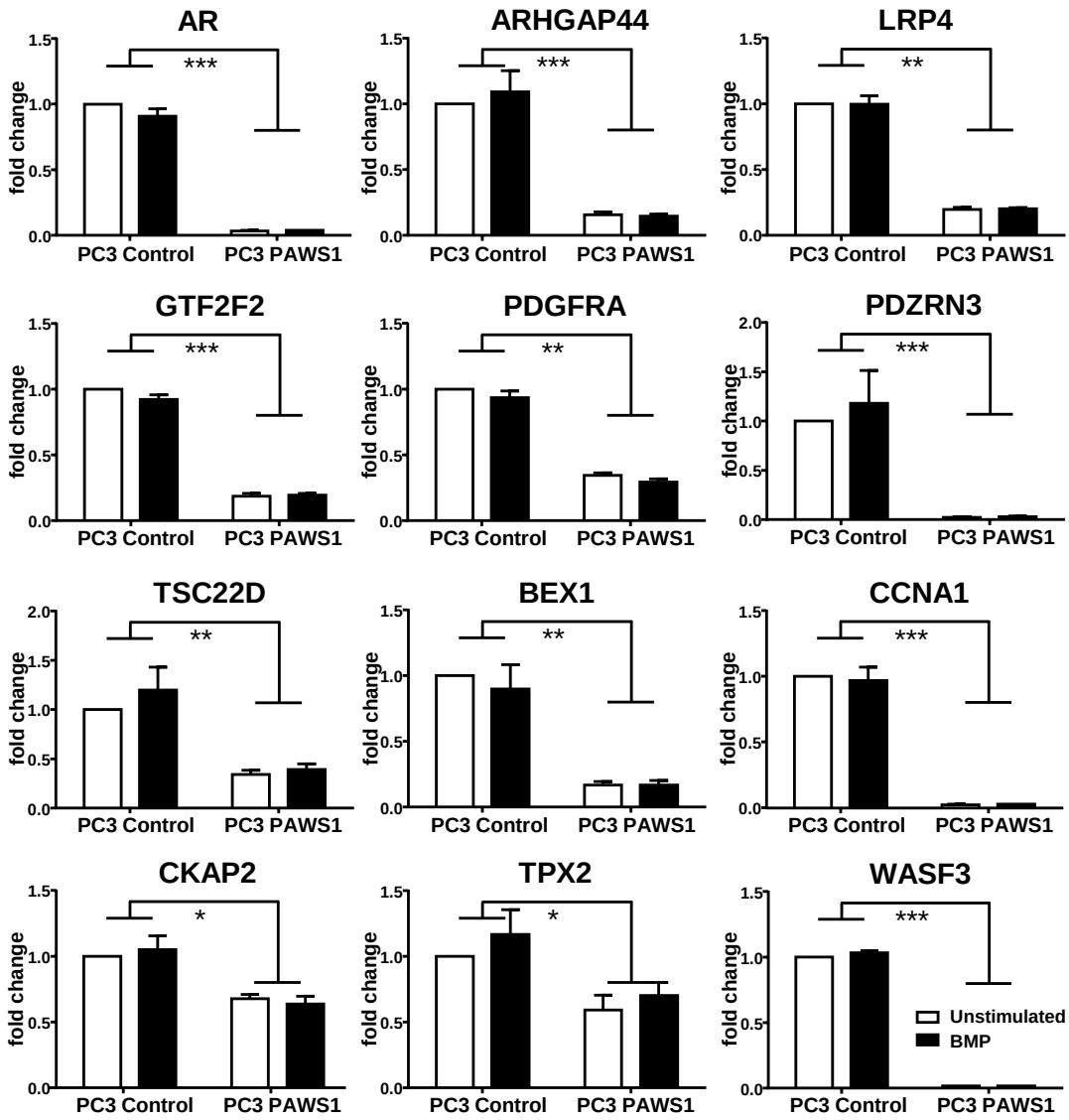

Figure 3-25 Genes that are downregulated by PAWS1 expression

PC Control and PC3 PAWS1 cells were treated with or without BMP-2 (25 ng/ml) for 3 h prior to RNA isolation. RNA was extracted and the cDNA synthesized. The expression of the genes was analysed by qRT-PCR. The results represent fold change in gene expression relative to the levels observed for unstimulated PC Control cells. Data are represented as mean of three biological repeats and error bars indicate standard deviation (n=3).

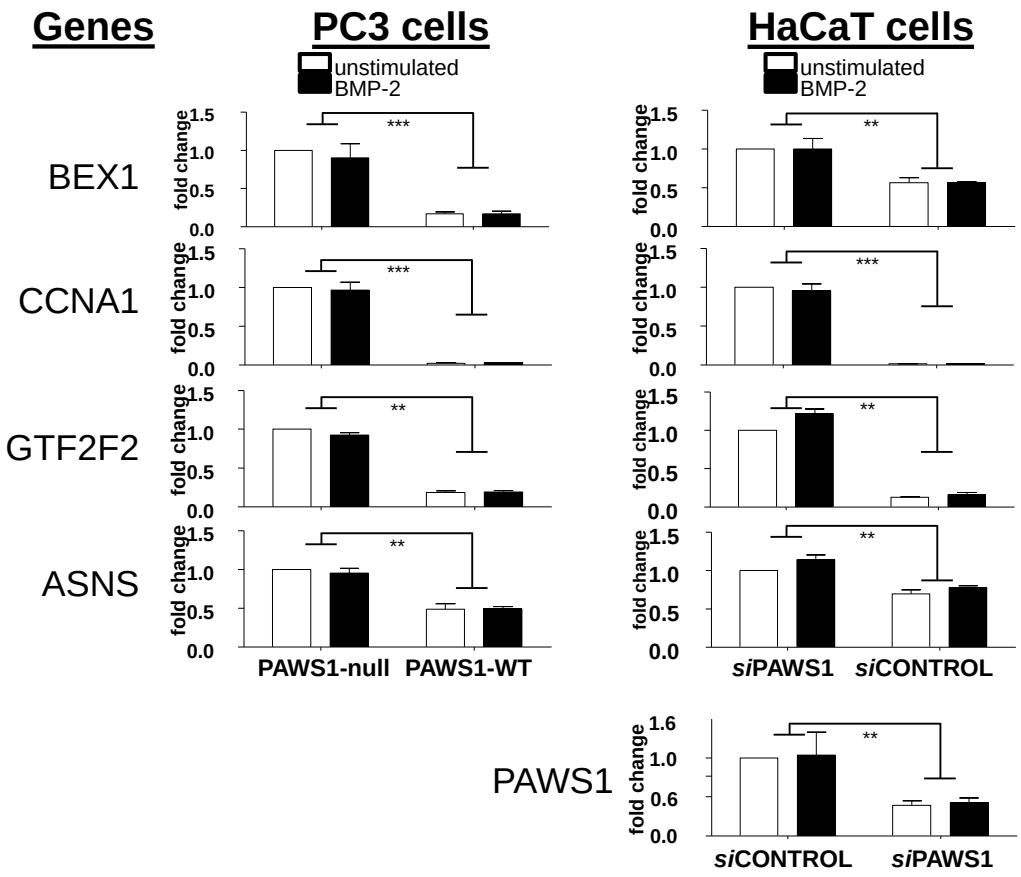

Figure 3-26 PAWS1 dependent genes in PC3 cells are also controlled by PAWS1 in HaCaT cells

PC Control, PC3 PAWS1 or HaCaT cells transfected with *siRNA* against PAWS1 or FOXO4 (control) were treated with or without BMP-2 (25 ng/ml) for 3 h prior to RNA isolation. RNA was extracted and the cDNA synthesized. The expression of the indicated genes was analysed by qRT-PCR. The results represent fold change in gene expression relative to the levels observed for unstimulated PC Control cells or HaCaT cells depleted of PAWS1 respectively. Data are represented as mean of three biological repeats and error bars indicate standard deviation (n=3).

3.2.17 The role of PAWS1 in epithelial to mesenchymal transition

Epithelial to mesenchymal transition is an important process in embryogenesis and plays a role in adult tissue wound healing. It has also been implicated in cancer progression and metastasis (Kalluri and Weinberg, 2009). EMT is a multistep cellular process that can be induced in many cell types by TGF-ß stimulation. It has been reported that TGF-ß stimulation induces EMT through the induction of SNAIL, TWIST and SLUG (Xu et al., 2009). SNAIL and SLUG induction leads to down-regulation of E-cadherin, a cell-cell adhesion marker, which in turn leads to loss of cell-cell contact. TWIST has been reported to be an oncogene (Ansieau et al., 2008). Because PAWS1 regulates the expression of a number of TGF-ß pathway components and target genes, including TGFBR2, FST and SNAIL, I investigated whether PAWS1 played a role in TGF-ß induced EMT using NMuMG cells. NMuMGs are mouse mammary epithelial cells, which have been previously used to study TGF-ß induced EMT (Wrana et al., 1994).

Interestingly PAWS1 expression is absent in NMuMG cells. NMuMG cells were infected with retroviruses containing either an empty vector with puromycin resistance (NMuMG Control; Figure 3-27A) or wild-type mouse PAWS1 (NMuMG PAWS1 Figure 3-27B). The cells were selected with puromycin for 4 days before treating them with or without TGF-ß or with TGF-ß plus the addition of SB-505124 (1 µM), a potent TGFBR1 inhibitor, for 24 or 48 h (Figure 3-27). Control Cells treated with TGF-ß undergo a rapid EMT, noticeable even after 24 h by the longitudinal/epithelial shape and by the loss of cell-cell contact (Figure 3-27A). This is inhibited by SB-505124, as there is no visible difference between untreated and TGF-ß plus SB-505124

treatment (Figure 3-27A). On the other hand, if the NMuMG PAWS1 cells are used, there is no obvious difference compared to NMuMG Control cells for any treatment (Figure 3-27A and B). However, in order to verify the morphological observations biochemically, the same cells (Figure 3-27A and B) were used for immunobloting analysis (Figure 3-27C) with antibodies against Fibronectin and E-cadherin. Increased Fibronectin levels were observed upon TGF-ß stimulation while changes in E-cadherin levels were not detected (Figure 3-27C). No significant differences between the NMuMG Control and NMuMG PAWS1 cells were observed, suggesting that PAWS1 is probably not involved in EMT.

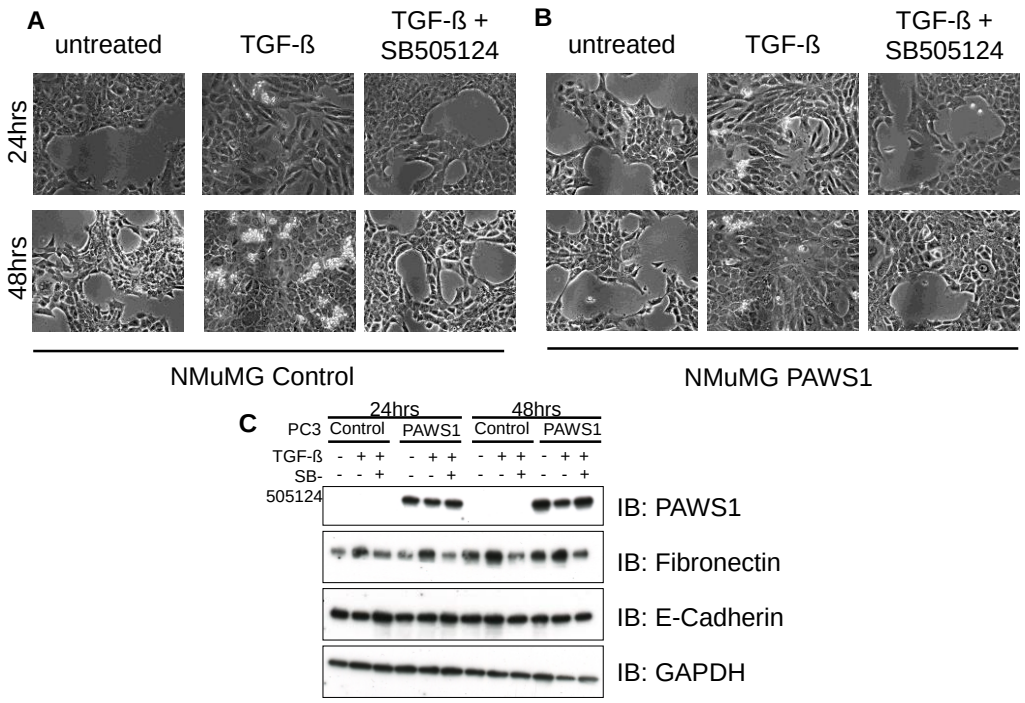

Figure 3-27 Role of PAWS1 in EMT

(A) NMuMG cells stably expressing an empty puromycin resistance vector were left untreated or treated with TGF-ß (75 pM) with or without SB505124 (1 µM) for 24 and 48 h, respectively. **(B)** Same as A, except that NMuMG cells stably expressing mouse PAWS1 were used. **(C)** Cell extracts from A and B were subjected to SDS-PAGE and subsequently analysed by immunoblotting using the indicated antibodies.

3.2.18 The role of PAWS1 in cellular migration

One of the PAWS1 target genes, NEDD9, has been implicated in cellular migration (Zhong et al., 2012, Ahn et al., 2012). TGF-ß and BMP pathways are known to be involved in cellular migration (Platten et al., 2000, Inai et al., 2008). Therefore, I tested whether PAWS1 impacts cellular migration. In order to do this, PC Control, PC3 PAWS1 or PC3 PAWS1 S610A cells were cultured to confluency in adjacent chambers of inserts separated by a small fixed-sized spacer. When the inserts were removed, a uniform gap was formed. Cellular migration onto the gap was monitored by live cell imaging for 24 h (1 frame every 2 minutes). At the 18 h time point, the gap is filled by cells to about 80 to 90 % in PC Control cells (Figure 3-28). This is also observed for PC3 PAWS1 and PC3 PAWS1 S610A cells (Figure 3-28). Therefore, it appears that there was no significant impact on lateral migration of these three cell types. The movement of individual cells onto the gap as seen on live cell imaging movies appeared to be slightly different in different cell types. However these observations were hard to quantify because of the disorderly nature of individual cell movements within the gap (supplementary movies 1-6).Treatment of all cell types with BMP did not significantly alter the nature of cellular migration onto the gap (Figure 3-28, supplementary movies 1-6).

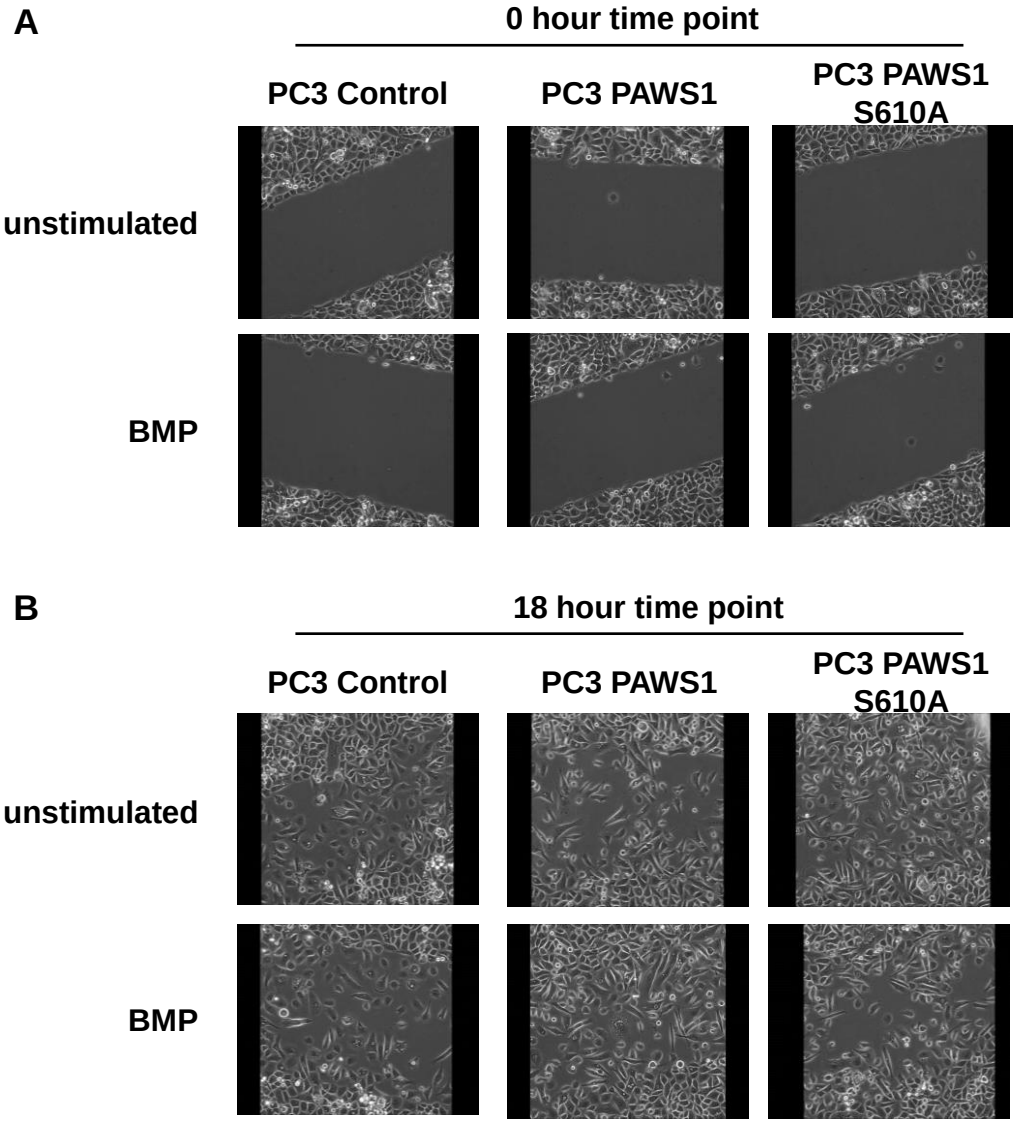

Figure 3-28 The role of PAWS1 in lateral migration

(A) PC Control, PC3 PAWS1 and PC3 PAWS1 S610A cells were plated to confluence in migration chambers as described in methods. Images were taken at time 0 when cells were left unstimulated or stimulated with BMP-2 (25 ng/ml). **(B)** Images of cells in A were taken at 18 h time point.

3.2.19 Identification of PAWS1 interactors by mass fingerprinting

As the biochemical roles of PAWS1 remain largely uncharacterised, in order to get insights into the possible roles of PAWS1 in cells, I employed a proteomic approach to identify interactors of GFP-PAWS1 from cells stably expreesing GFP-PAWS1. Any identified interacting partners could help define functional roles of PAWS1 in cells.

Stable, tetracycline inducible GFP or GFP-PAWS1 HEK293 cells (see section 2.2.4) were treated with doxycycline for up to 24 h (Figure 3-29A). The expression of GFP-PAWS1 was increased upon doxycycline treatment in a time-dependent manner (Figure 3-29A). For identification of GFP-PAWS1 interactors by mass spectrometry, GFP or GFP-PAWS1 HEK293 cells were treated for 24 h with doxycycline, and treated with or without BMP prior to lysis. The GFP IPs from extracts were resolved by SDS-PAGE, which was stained by colloidal coomassie, and proteins in the entire lanes excised and analysed by mass spectrometry (Figure 3-29B).

The identified proteins are listed in Appendix (Table 4), sorted according to their identification confidence score (called PEP score). The list of GFP-PAWS1 interactors was compared against the list of GFP-interactors as well as common contaminants collected over time from multiple similar experiments performed in the lab and the contaminants were removed from this list. One of the top scoring interactors was CULLIN3, the key component of the CUL3-E3 ubiquitin ligase complex ((Petroski and Deshaies, 2005), Appendix Table 4). More importantly, other components of the complex such as the unique adaptor protein KLHL13 or KLHL15 and the essential ring box

protein RBX1 were also identified ((Sumara et al., 2007) Appendix Table 4). Another protein shown to be interacting with PAWS1 was CD2AP, a poorly characterised protein that has been previously linked to TGF-ß signalling (Xavier et al., 2009). SMADs were also identified as PAWS1-interacting proteins (Appendix Table 4). Stimulating the cells with BMP did not alter the interactors identified for GFP-PAWS1 IPs.

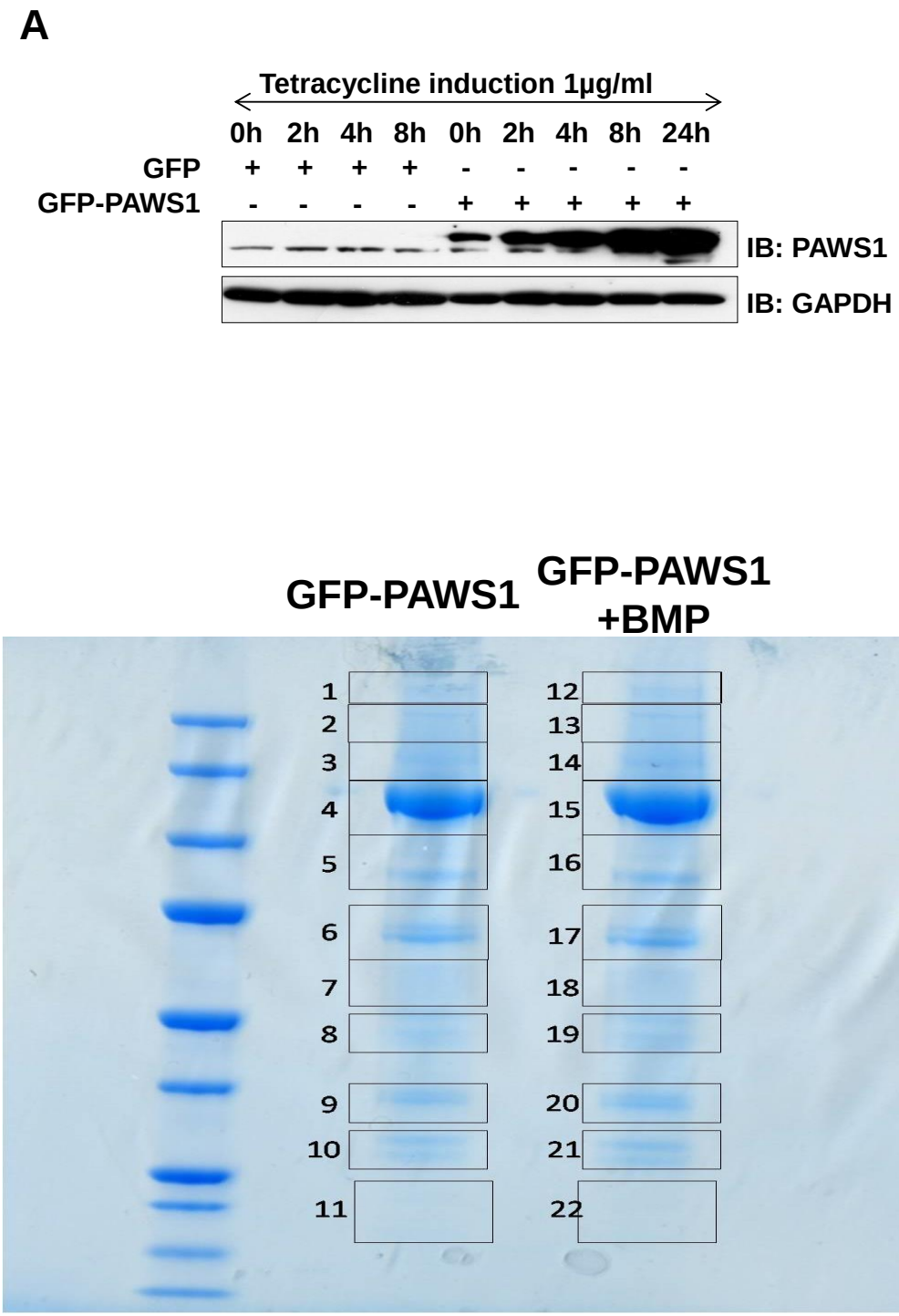

Figure 3-29 Identification of PAWS1 interactors by mass spectrometry

(A) HEK293 cells stably integrated with tetracycline inducible GFP or GFP-PAWS1 were lysed following induction by tetracycline (1 µg/ml) for the indicated times. Extracts were resolved by SDS-PAGE and analysed by immunoblotting for PAWS1 protein levels. **(B)** HEK293 cells stably expressing GFP-PAWS1 were treated with or without BMP-2 (25 ng/ml) for 1 h prior to lysis. Cell extracts were subjected to immunoprecipitation using GFP-Trap beads and IPs were resolved by SDS-PAGE gel electrophoresis. The gel was stained with Coomassie and the numbered boxes indicating individual gel pieces were excised, trypsinised and analysed by mass spectrometry.

3.2.20 PAWS1 interacts with CULLIN3 at the endogenous level

To verify the observations from mass spectrometry on the interaction between PAWS1 and CULIN3 (CUL3) at the endogenous level, PAWS1 was immunoprecipitated from HaCaT cell extracts. PAWS1 IPs were subjected to SDS-PAGE and immonoblotted with anti-CUL3 antibody. Both neddylated and un-neddylated forms of CUL3 were identified in PAWS1 IPs but not in pre-immune IgG IPs employed as control (Figure 3-30A). Furthermore I demonstrate that CUL3 and PAWS1 elute in overlapping fractions when HaCaT extracts were resolved by a size exclusion chromatography (Figure 3-30B).

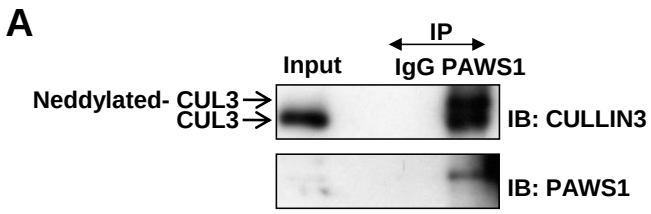

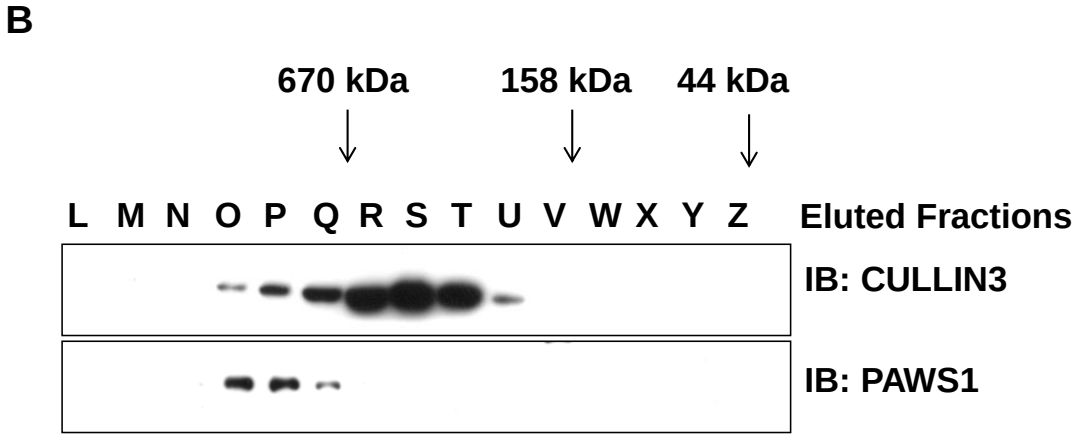

Figure 3-30 Interaction between PAWS1 and CULLIN3

(A) HaCaT cells were lysed and extracts were subjected to immunoprecipitation with either IgG (control) or anti-PAWS1 antibodies. Extracts and IPs were resolved by SDS-PAGE and subsequently analysed by immunoblotting using the indicated antibodies. **(B)** Unstimulated HaCaT cell extracts were fractionated by gel filtration chromatography on a Superose™ 10/300 GL Column (GE Health Care). 5 µl each of recovered fractions were resolved by SDS-PAGE and subsequently analysed by immunoblotting using the indicated antibodies.

3.2.21 Tracking PAWS1 protein levels during cell cycle

I have shown above that PAWS1 interacts with CUL3 and potentially forms a complex (Figure 3-30). CUL3 is implicated in the regulation of the cell cycle, whereby it mediates the ubiquitylation of AURORA B marking it for proteasomal degradation (Sumara and Peter, 2007, Sumara et al., 2007). In order to investigate whether CUL3 regulates PAWS1 in a similar manner, I tested the expression of PAWS1 during the cell cycle.

HaCaT cells were synchronised by treating the cells twice with thymidine (see section 2.2.19). This leads to a cell cycle arrest in the G_1/S border because excess thymidine in a dividing cells generates negative feedback on the production of deoxycytidine triphosphate and prevents the progression of the cells in the cell cycle. This is reversible and cells released after thymidine block progress through the cell cycle in a synchronised manner. U2OS cells were released from thymidine block and harvested at 2 h intervals, with the first harvest at 1 h after release. The cells were analysed by fluorescence activated cell sorting (FACS) according to their DNA content. This allows for the assessment of synchronous progression through the cell cycle (Figure 3-31A and B). As shown in Figure 3-31, the cell cycle arrest in G_1/S was successful and the majority of the cells progress synchronised through the cell cycle. This was also confirmed by assessing the levels of Cyclins A, D and E that are reported to be cell cycle regulated (Johnson and Walker, 1999) by immunoblotting extracts collected at fixed time points after release (Figure 3-31C). Under these conditions, PAWS1 is uniformly expressed throughout the different stages of cell cycle (Figure 3-31A top

panel). Therefore, PAWS1 expression appears not to be cell cycle regulated (Figure 3-31).

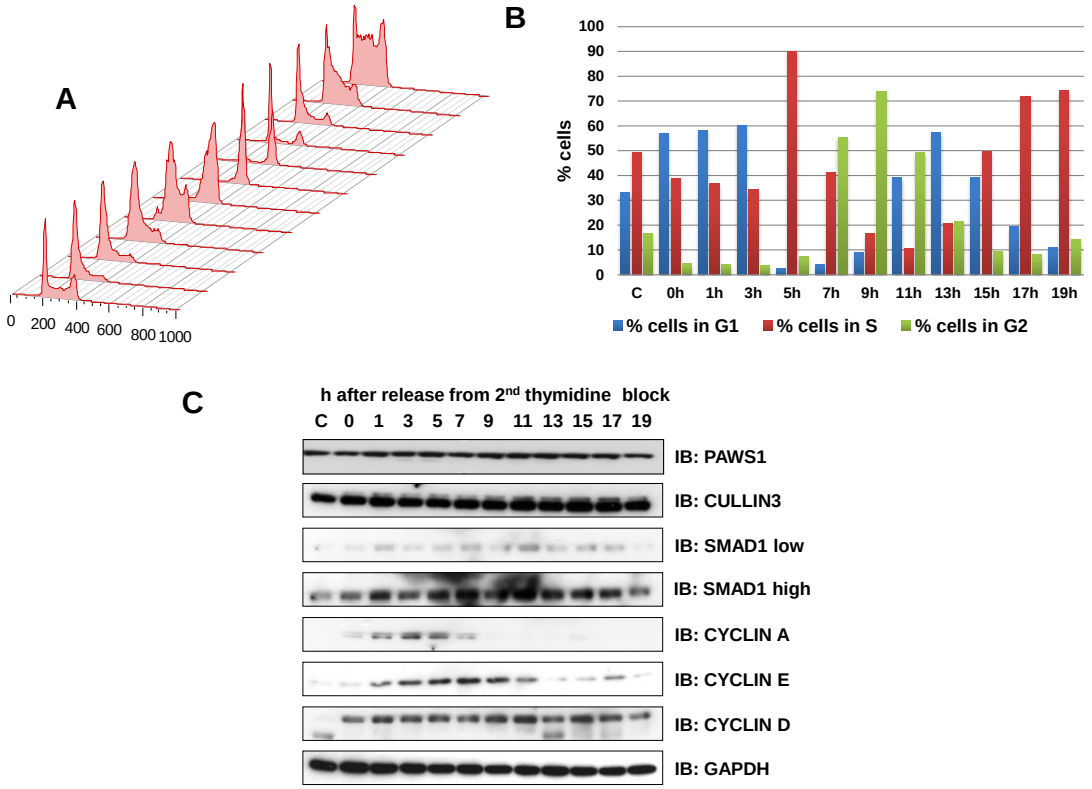

Figure 3-31 PAWS1 expression during cell cycle

(A) HaCaT cells were treated with thymidine (2 mM) for 16 h, washed, left for 10 h and treated again with thymidine (2mM) for 16 h. FACS profile of the HaCaT cells showing the cell cycle distribution at the indicated time points after thymidine release. **(B)** Graph representing the percentage of cells in an indicated cell cycle state at the given time point. **(C)** Cells were lysed at the indicated time points after thymidine release and extracts subjected to SDS-PAGE prior to analysis by immunoblotting using the indicated antibodies.

3.2.22 The role PAWS1 expression in *Xenopus laevis* development

The BMP signalling pathway, among others, is a very important pathway in *Xenopus* development and has been extensively studied (see section 3.1.2). SMAD1, being the intracellular transducer of BMP ligands, has been established as an interactor of PAWS1 in this thesis. Therefore, in order to gain insight on the role of PAWS1 in vertebrate development, we collaborated with Dr. Kevin Dingwell in the laboratory of Prof. Jim Smith (MRC NIMR London). Dr. Kevin Dingwell injected *X.laevis* PAWS1 mRNA into the ventral side of 4 cell embryos (Figure 3-32A). The injected embryos showed complete duplication of axis at tailbud stages (Figure 3-32C). Given the limited role for PAWS1 in the BMP-induced phosphorylation of SMAD1 and transcription of downstream target genes, the axis duplication caused by PAWS1 could be unrelated to its role in the BMP pathway. Consistent with this, a similar phenotype is observed by injecting xWnt8 into the embryo (Figure 3-32D). The uninjected embryos displayed a normal developmental phenotype (Figure 3-32A). In all, more than 70% of embryos injected with PAWS1 mRNA (250 pg) displayed the axis duplication phenotype and a further 10% showed a partial axis duplication (Figure 3-32E and F). This was comparable to the phenotypes observed when xWnt8 (5 pg) was injected in embryos (Figure 3-32E and F).

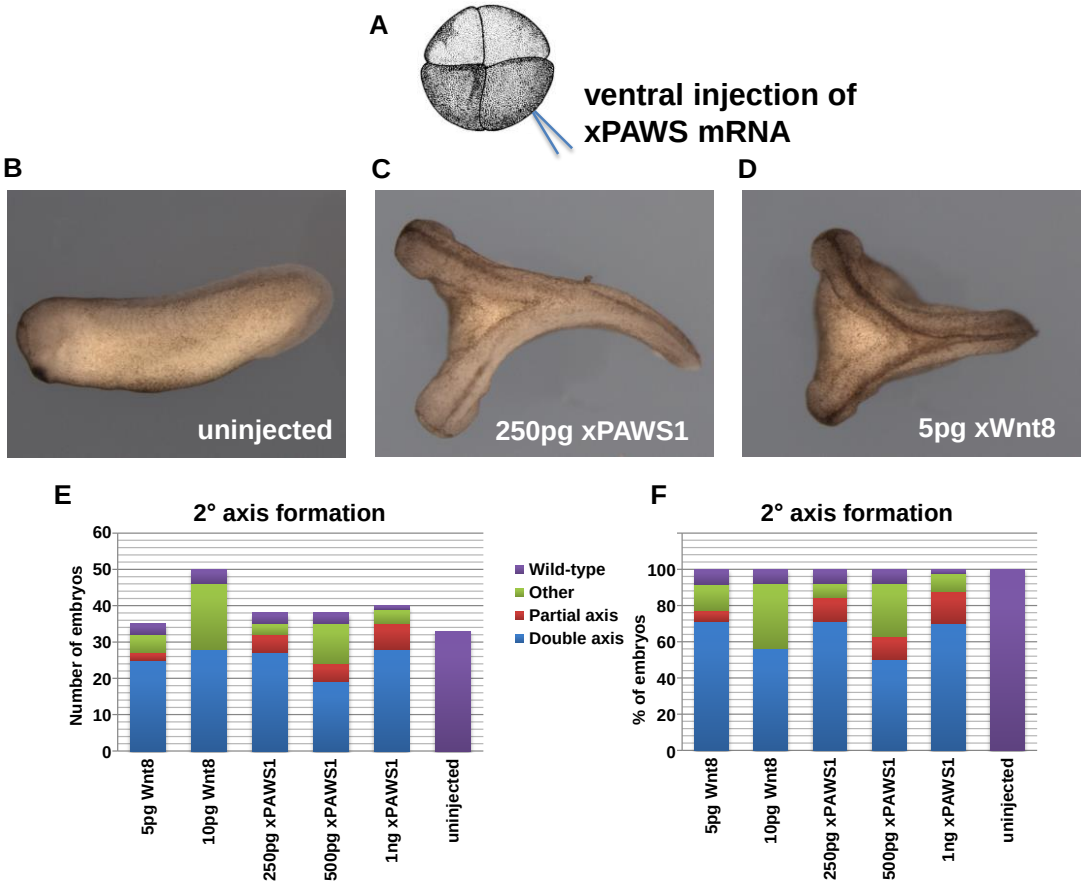

Figure 3-32 The impact of PAWS1 on *X. laevis* embryogenesis

(A) Schematic representation of strategy employed to inject xPAWS1 mRNA. **(B)** Uninjected **(C)** 250 pg xPAWS1 mRNA injected or **(D)** 5 pg xWnt8 mRNA injected embryos were imaged at tadpole stage. **(E)** Graph representing the total number of phenotypes observed for injected embryos at tadpole stage. **(F)** Graph representing the percentage of the different phenotypes observed in (E).

3.3 Discussion

In this chapter I discuss the role of PAWS1 as a novel player in the BMP pathway and beyond. I have shown that PAWS1 forms a SMAD4-independent complex with SMAD1 and identify PAWS1 as the first non-SMAD substrate for type I BMP receptor kinases. Furthermore, I demonstrate that PAWS1 regulates the expression of some BMP-dependent SMAD4-independent target genes as well as a large number of BMP-independent target genes. This indicates a potential non-canonical, SMAD4-independent SMAD1-dependent, BMP signalling pathway.

3.3.1 PAWS1 selectively interacts with SMAD1 and not with SMAD2/3

PAWS1 selectively interacts with SMAD1 but not SMAD2 or SMAD3 unlike reported before (Brown et al., 2008). Despite the fact that R-SMADs are very similar (Shi and Massague, 2003), the selective binding of PAWS1 to SMAD1 is intriguing (Figure 3-7). The linker region that connects the MH1 and MH2 domains of R-SMADs is the least conserved domain (Massague, 2003). However, SMAD1-linker does not mediate the interaction with PAWS1, nor does the linker phosphorylation of SMAD1 affect its interaction with PAWS1 (Figure 3-8 and Figure 3-9). I demonstrate that MH2 domain of SMAD1 is sufficient to mediate the interaction with PAWS1 (Figure 3-8). Because the MH2 domains across the R-SMADs are very similar, the selectivity of SMAD1 interaction to PAWS1 could be determined by the accessibility of MH2 domain within SMAD1 structural conformation. I was unable to determine the minimal domain within PAWS1 that mediated the interaction with SMAD1. A crystal structure of the PAWS1-SMAD1 complex

would address the selective nature of the complex as well as the interaction interface. Alternatively, yeast two-Hybrid screen employing random mutagenesis approach would be appropriate to identify the exact amino acid sequence that mediates the interaction between PAWS1 and SMAD1.

Treatment of cells with TGF-ß or BMP ligands leads to the phosphorylation of R-SMADs at the C-terminal SXS motif within the MH2 domain (Shi and Massague, 2003). Phosphorylated R-SMADs bind the co-SMAD4 and form an active complex (ten Dijke and Hill, 2004). SMAD4 is not detected in PAWS1 IPs (Figure 3-7). Furthermore, in control or BMP treated extracts, PAWS1 forms a unique complex with a small proportion of SMAD1 that does not include SMAD4 (Figure 3-10). Further evidence suggests that SMAD1 binds either SMAD4 or PAWS1, as GFP-SMAD4 under conditions where it binds to HA-SMAD1 still fails to interact with FLAG-PAWS1 (Figure 3-11). Consistent with the above observations, GFP-PAWS1 IPs in the presence or absence of BMP treatment fail to pull down SMAD4 (Figure 3-29, Appendix Table 4). The SMAD4-independent interaction between PAWS1 and SMAD1 suggests a non-canonical function of this complex within the BMP pathway, despite the fact that the majority of SMAD1 still forms a canonical complex with SMAD4 upon BMP treatment (Figure 3-10). On the other hand, PAWS1 and SMAD4 may compete for access to SMAD1. This has to be investigated further.

The high molecular weight (>670 kDa) co-elution of PAWS1 and P-SMAD1 in a gel filtration assay implies that there are potentially more proteins contributing to the PAWS1:SMAD1 macromolecular complex as the

combined molecular weight of SMAD1 and PAWS1 is 140 kDa. Furthermore, as full-length PAWS1 did not express in bacteria, it is not known whether recombinant PAWS1 and SMAD1 associate directly. Identification of all the components of the PAWS1:SMAD1 complex could provide us with important functional insight. Even in the absence of PAWS1, P-SMAD1 was still detected in a high molecular weight fraction in a gel filtration assay (Figure 3-16). This could mean that there are other proteins that could substitute the place of PAWS1, possibly the members from the FAM83 family. Because PAWS1 elutes in the same high molecular weight fractions after size exclusion chromatography in PC3 PAWS1 cells compared to HaCaT cells (Figure 3-10 and Figure 3-16), it is likely that PAWS1 re-introduced in PC3 PAWS1 cells forms functional complexes.

The interaction between PAWS1 and SMAD1 in cell extracts is independent of stimulation with BMP or TGF-ß cytokines (Figure 3-7). However, when cells are treated with BMP, more P-SMAD1 was observed in overlapping fractions with PAWS1 upon size exclusion chromatography (Figure 3-10 and Figure 3-16). It is possible that posttranslational modifications of either SMAD1 or PAWS1 could impact on their interaction, although none have been identified yet. Immunoprecipitation interaction assays and gel filtration chromatography were performed on cell extracts, which allow for soluble proteins to spontaneously interact and potentially form macromolecular complexes. Therefore it is essential to confirm interactions between endogenous proteins by performing co-localisation studies in cells.

3.3.2 The impact of PAWS1 on BMP signalling

Because PAWS1 was identified, and verified, as an interactor of SMAD1, I investigated its role in the BMP pathway. The manipulation of PAWS1 protein expression does not influence the kinetics or threshold of BMP induced phosphorylation of SMAD1 (Figure 3-15). Furthermore, PAWS1 does not alter the expression of the SMAD4-dependent BMP target gene *ID1*. These results, together with the observation that PAWS1 forms a complex with SMAD1 independently of SMAD4, imply a unique role for PAWS1 in the BMP pathway. A microarray analysis on the expression of BMP-target genes in SMAD4-deficient SW480 cells revealed that BMP still induced the expression multiple genes including NEDD9 and ASNS (Deng et al., 2009). Interestingly, the BMP-dependent expression of NEDD9 and ASNS was lost in PC Control cells (Figure 3-20). After re-introduction of wild type PAWS1 (PC3 PAWS1), BMP was able to induce the expression of both NEDD9 and ASNS in these cells. BMP-induced phosphorylation of PAWS1 at Ser610 is necessary for the expression of these genes as the re-introduction of PAWS1 S610A (PC3 PAWS1 S610A) mutant did not rescue the expression of NEDD9 and ASNS in response to BMP (Figure 3-20). NEDD9 has previously been linked to TGF-ß signalling and it was shown that the binding to SMAD3 led to its degradation (Liu et al., 2000, Zheng and McKeown-Longo, 2002). Furthermore, the role of NEDD9 in FAK and SRC signalling has been studied extensively, whereby NEDD9 plays a role in integrin-dependent adhesion and cellular migration (Fashena et al., 2002, O'Neill and Golemis, 2001, van Seventer et al., 2001). More recently, NEDD9 was shown to impact cancer progression by facilitating the invasion and metastasis of cancer cells (Ahn et al., 2012). Misregulated ASNS expression has also been

linked with many cancers (Cui et al., 2007, Scian et al., 2004). It will be important to further investigate if these events can be linked to abnormal BMP signalling and whether PAWS1 plays a central role in the regulation of NEDD9 and ASNS expression and NEDD9/ASNS-dependent homeostasis of cells.

3.3.3 PAWS1 is the first non-SMAD protein substrate for a type I BMP receptor kinase

Nuclear accumulation of phospho-SMAD complexes upon BMP treatment is fundamental to transcriptional responses controlled by BMP. Even in the absence of SMAD4, BMP can induce the nuclear localization of phospho-SMAD1 (Liu et al., 1997). It was therefore quite interesting to observe that a small portion of PAWS1 was detected in the nuclear fractions upon BMP treatment from cell extracts fractionated into nuclear and cytosolic compartments (Figure 3-14). Even though a robust immunofluorescence study to look at the endogenous PAWS1 localisation in intact cells is necessary to complement the nuclear localisation, upon overexpression of PAWS1, some nuclear localisation was observed, albeit independently of BMP treatment (Figure 3-14). At this time, immunofluorescence of endogenous PAWS1 has not been possible due to the unavailability of suitable antibodies. Nonetheless, the observation of endogenous PAWS1 in nuclear fractions upon BMP treatment prompted me to evaluate possible mechanisms of PAWS1 localisation.

It is possible that by association with SMAD1, PAWS1 could translocate to the nucleus under conditions that SMAD1 does. However, the

determinants of PAWS1:SMAD1 association are not yet known to test this in cells. Alternatively, PAWS1 could be modified by type I BMP receptors (ALKs2, 3 & 6). Consistent with this, rather intriguingly, a triphospho-peptide was repeatedly observed in PAWS1 IPs from BMP-treated extracts. The observed phospho-peptide identified contained a SXS motif that is conserved in species (Figure 3-3) and identical to the motif in SMAD1 that is phosphorylated by the type I BMP receptor kinase (ALK3) (Figure 3-17). The phosphorylation motif in PAWS1 is internally located compared to the C-terminal location of the SSXS motif in SMAD1. To date, no non-SMAD substrates for type I BMP receptor kinases (ALKs 1, 2, 3 and 6) have been reported. I was able to demonstrate that BMPR1 (ALK3) phosphorylated PAWS1 at Ser610, Ser614 and Ser616 *in vitro*. Although I predicted that Ser614 and Ser616 (equivalent to the *SVS* motif in SMAD1) would be the major ALK3 phosphorylation sites, it was rather surprising that Ser610 (a SV motif) was the major ALK3 *in vitro* phosphorylation site on PAWS1 (Figure 3-18). Consistent with this, mutating Ser610 to Ala significantly inhibited the phosphorylation of PAWS1 by ALK3 *in vitro* (Figure 3-18). This indicates that SXS motif may not be absolutely necessary for ALK3, or possibly other ALKs, to phosphorylate potential substrates *in vitro*. Furthermore, ALK3 could phosphorylate a Ser residue, which is followed by Val, *in vitro*. However, despite the fact that SMAD3 SXS motif is identical to SMAD1, ALK3 does not phosphorylate SMAD3. This clearly implies that specific substrate-kinase interactions are probably essential for a kinase to phosphorylate its target.

I was able to demonstrate that PAWS1 is phosphorylated at Ser610 in response to BMP in cells (Figure 3-19). These findings imply for the first time

that type I BMP receptor kinases have substrates other than SMADs in cells, although the precise roles of BMP induced phosphorylation needs to be investigated further and could also potentially be extended to other type I TGF-ß receptor kinases. Indeed, knockout studies in mice demonstrate that the loss of ALKs 2, 3 or 6 expression results in distinct phenotypes that cannot be fully explained by phenotypes observed following the loss in expression of SMADs 1, 5 or 8 (Chang et al., 1999, Clarke et al., 2001, Fukuda et al., 2006, Hester et al., 2005, Komatsu et al., 2007, Sun et al., 2007, Tremblay et al., 2001). These observations imply that depending on the biological context, different type I BMP receptor kinases could signal in a unique way by phosphorylating distinct non-SMAD substrates.

3.3.4 The impact of PAWS1 beyond BMP signalling

To further characterise the role of PAWS1 in cells, I undertook a qRT-PCR macroarray to analyse the changes in gene expression caused by PAWS1. I identified and verified several genes in the TGF-ß and BMP pathway that displayed differential expression patterns upon PAWS1 re-introduction in PC3 cells, independent of ligand treatment. The PAWS1-dependent expression of some of these genes was also verified in HaCaT cells upon *RNAi*-mediated depletion of PAWS1 (Figure 3-22). Clearly PAWS1 appears to control the expression of many genes independently of BMP signalling. Therefore a global transcriptomic analysis of genes affected by PAWS1 was performed by RNA sequencing in order to yield clues to its possible biochemical roles beyond the BMP pathway.

This RNA seq. analysis not only confirmed the differentially expressed genes including AR, TSC22D, FST, TGFBI and TGFBR2 that were identified from qRT-PCR macroarray but also revealed about 800 differentially expressed genes upon PAWS1 expression in PC3 cells (Figure 3-22 and Appendix Table 1). Out of these 800, 300 were differentially expressed with more than 2-fold (Appendix Table 1). TGFBR2 and FST are important components of the TGF-ß signalling pathway (Shi and Massague, 2003), while TSC22D, AR and TGFBI have also been linked to TGF-ß signalling (Choi et al., 2005, Kang et al., 2001, Thapa et al., 2007). This would imply that PAWS1 potentially could play a role in TGF-ß signalling, albeit it does not appear to bind to SMAD2 or SMAD3 nor does it impact on TGF-ß induced EMT in NMuMG cells (Figure 3-7 and Figure 3-27). The possible role for PAWS1 in the TGF-ß pathway has not been investigated yet. TGFBI, which is

involved in binding of integrin to ECM proteins like collagen, where it has been reported to activate a variety of cell functions including proliferation, migration and differentiation (Kim et al., 2000). The regulation of TGFBI expression by PAWS1 in PC3 cancer cells is interesting as misregulation of TGFBI has been linked to cancer progression (Calaf et al., 2008, Ivanov et al., 2008, Kitahara et al., 2001, Schneider et al., 2002). Similarly, PAWS1-dependent down-regulation of AR in PC3, a prostate cancer cell line is interesting. Although PC3 cells were first reported to be AR-negative, they were later shown to express AR (Alimirah et al., 2006). AR plays important roles in normal prostate development as well as certain prostate cancers, where it has been reported to influence cancer progression (Heinlein and Chang, 2004). When I analysed the protein expression in the NCI-60 panel of cancer cell lines, endogenous PAWS1 expression was not detectable in 30 out of the 54 tested cell lines (Figure 3-13) These findings, together with potential pathogenic mutations of PAWS1 reported in cancer patients (Figure 3-2), suggest that PAWS1 could be implicated in certain cancers. Whether the loss of PAWS1 in cancer is causative or a consequence remains elusive.

Other genes verified to be differentially expressed include MMP1, MMP13, WASF3 and ARHGAP44, 4 genes that have been associated in cell morphology and motility. Whereas the matrix metalloproteinases 1 and 13 (MMP1 and MMP13) were up-regulated upon PAWS1 re-expression, WASF3 and ARGAPG4 were down-regulated (Figure 3-24 and Figure 3-25). MMPs are secreted proteins that degrade extracellular matrix (ECM) and WASF3 is an important protein in the SCAR/WAVE complex that activates the ARP2/3 complex and thereby regulate actin structure assembly (Suetsugu et al.,

1999, Takenawa and Suetsugu, 2007, Kahari and Saarialho-Kere, 1999). ARGAP44 is a RhoGAP that also has been implicated in the formation of apical microvilli by interactin with the CD317 intergin cell surface receptor (Rollason et al., 2009). Despite the fact that PAWS1 impacts on the the expression of these genes which are reported to be involved in the cellular migration, including NEDD9, PAWS1 re-expression did not significantly impact in PC3 cell lateral migration (Figure 3-28). Still, this assay was only analysing 2D cell migration on a stiff plastic surface. In order to further evaluate the impact of PAWS1 on PC3 cell migration, cells would have to be analysed in a 3D environment employing a more physiological environment.

PDGFRA, a tyrosine receptor kinase, PDZRN3, an E3 RING ubiquitin ligase, LRP4, which has been linked to Wnt signalling and the two genes, NPY1R and BEX1, linked to the nervous system and brain have all been validated to be differentially regulated upon PAWS1 expression (Figure 3-24 and Figure 3-25) (Foltz et al., 2006, Li et al., 2010, Silva et al., 2005). BEX1 and BEX2 have been reported as potential tumour suppressor genes in glioblastoma (Foltz et al., 2006), whereas PDGFRA has been reported to be involved in many aspects of cellular homeostasis as well as development and glioblastoma (Ozawa et al., 2010, Williams, 1989). Whether PAWS1 expression, which was observed to be absent in many glioma cell lines in the NCI-60 cancer cell line panel (Figure 3-13) can be linked to glioblastomas still remains to be investigated.

Taken these observations together, it is likely that PAWS1 has many more functions, in part or completely, independently of BMP signalling. As the

PAWS1-dependent genes discussed above are only a small subset of the 800 genes that are potentially regulated by PAWS1, it is likely that PAWS1 exerts control over other aspects of cellular homeostasis (Appendix Table 1). Furthermore, I observed that BMP stimulation in PC3 cells led to significant changes in expression of only a limited number of genes (Appendix Tables 2 and 3). On the other hand, moderate changes in gene expression resulting from BMP treatment might be sufficient to cause phenotypic changes in the cells. Therefore, these genes might not be considered as BMP target genes or are beyond the limitations of the RNA seq. to be analysed. This could be true for PAWS1-dependent target genes as well.

CD2AP, which was identified as an interacting protein of PAWS1 with the highest score by mass fingerprinting (Appendix Table 4), was recently published to impact EGFR signalling together with another protein called CIN85 (Minegishi et al., 2013). CIN85 was also identified as an interacting protein of PAWS1 by mass fingerprinting ((Havrylov et al., 2009) and Appendix Table 4)). CD2AP and CIN85 have been reported to control the levels of HER2, a tyrosine kinase receptor, which could be important for tumours that overexpress HER2 (Minegishi et al., 2013). Moreover two other member of the FAM83 family, FAM83A and FAM83B, have also recently been linked to EGFR-tyrosine kinase inhibitor (EGFR-TKI) resistance (Cipriano et al., 2012, Lee et al., 2012). Whether PAWS1 plays a role EGFR signalling or EGFR-TKI resistance still has to be investigated but given the results mentioned above, it cannot be ruled out.

PAWS1 expression was observed in many mouse tissues potentially indicating a broad role for PAWS1 in different tissue types and contexts (Figure 3-12). However, PAWS1 protein expression was absent in mouse ovaries and testis, suggesting that PAWS1 expression is potentially not required for meiosis. PAWS1 expression appears to be absent in muscle tissues (Figure 3-12).

3.3.5 Possible roles for PAWS1:CULLIN3 interaction

The CULLIN E3 ligase complex consists of CULLIN3 (CUL3), the RING E3 ligase RBX1 and the BTB domain substrate specific adaptor proteins (Petroski and Deshaies, 2005, Pintard et al., 2004). CUL3 acts as a scaffold protein, whereby its C-terminus binds RBX1 and the BTB domain adapter proteins bind towards the N-terminus. In order to activate the CULLIN3 E3 ligase complex, it has to be conjugated with NEDD8 at the conserved lysine residue within CUL3 (Saha and Deshaies, 2008). This process is called neddylation and induces a conformational change, bringing the RBX1 E3 ligase in close proximity with its substrate bound to its BTB domain containing adaptor (Duda et al., 2008).

CUL3 knock-out mice have been reported to be embryonically lethal (Singer et al., 1999). Furthermore, CULLIN3 E3 ligase complex has been reported to be involved in regulation of mitosis, in part by initiating the degradation of AURORA B (Sumara et al., 2007). AURORA B is a kinase that localises to centromeres during mitosis and regulates proper kinetochore assembly (Gorbsky, 2004). More recently AURORA A was also reported to be ubiqutylated by the CULLIN3 E3 ligase complex (Moghe et al., 2012).

Interestingly, AURORA A has been reported to be activated, rather than degraded, by ubiquitylation in this report (Moghe et al., 2012). AURORA A activation is important for entry into mitosis (Marumoto et al., 2005) whereby it activates PLK1 and, in turn, CDK1 (Macurek et al., 2008, Seki et al., 2008). Cyclin dependent kinases (CDKs) regulate the transition from one cell cycle stage to the next one (G_1-S-G_2-M). They in turn are activated by their corresponding cyclin proteins (Vermeulen et al., 2003a, Vermeulen et al., 2003b). Interestingly one of the cylins, Cyclin A1 (CCNA1) was verified to be significantly down-regulated by PAWS1 expression, both in PC3 and HaCaT cells (Figure 3-26). Another protein, TPX2, was reported to bind and target AURORA A to the mitotic spindle and was down-regulated upon PAWS1 expression in PC3 cells (Figure 3-25), (Kufer et al., 2002).

Interestingly, in PAWS1 IPs I identified not only CUL3 but also many of the components of the CULLIN3 E3 ligase complex, including KLHL13 and 15, COP9 and RBX1 (Appendix Table 4). Moreover, PAWS1 binds to CUL3, preferentially the neddylated (activated) form of CUL3, in HaCaT cell extracts (Figure 3-30). Interestingly, another member of the FAM83 family, FAM83D, also known as CHICA, has been reported to be associated with cell cycle progression, as it localises to the mitotic spindle (Santamaria et al., 2008). In order to test if PAWS1 is regulated during cell cycle, I synchronised HaCaT cells in the G1/S phase but neither CUL3 nor PAWS1 protein expression appears to be cell cycle regulated (Figure 3-31). This potentially implies that, at least in HaCaT cells, it is more likely that PAWS1 impacts on CUL3 rather than PAWS1 being a target for CUL3-mediated ubiquitylation and degradation. Evidence that PAWS1 might be regulated by post-translation

changes instead of its expression being altered comes from a large scale mass spectrometry analysis of mitotic phosphorylation sites, where Ser666 in PAWS1 was reported to by phosphorylated (Dephoure et al., 2008). The above discussed results suggest that PAWS1 could be implicated in cell cycle regulation and/or progression, albeit more research has to be done to directly link PAWS1 to the cell cycle.

3.3.6 Biochemical roles for PAWS1

One major drawback to studying PAWS1 as a regulator of BMP signalling is the lack of insight into its function. The amino-acid sequence analysis shows that the N-terminal domain of PAWS1 comprises a conserved domain of unknown function (DUF1669; Pfam PF07894) that displays similarities to known phospholipase D (PLD) active site motif (PLDc_2; Pfam PF13091) (Figure 3-1). PLD catalyses the hydrolysis of phosphatidylcholine into phosphatidic acid (PA) and choline. PA and its derivate diacylglycerol (DAG) are powerful second messenger molecules, involved in the activation of many signalling and metabolic pathways (Merida et al., 2008). When the key His (H) residue within the active-site PLD motif (HxKx4D) is mutated to Ala (A), the PLD activity is abolished (Gottlin et al., 1998, Xie et al., 1998). In PAWS1, Ala is present in place of the key His, suggesting that PAWS1 with its pseudo-PLD motif is unlikely to possess PLD activity. Nonetheless, it has not been confirmed experimentally whether PAWS1 possesses PLD activity. The DUF1669 is present within the entire FAM83 family (A-H), albeit only FAM83D displays the reported amino-acid sequence (HxKx4D) (Figure 3-1). A recent report showed that FAM83A, that has an Arg (R) instead of the His (H) has no PLD activity (Lee et al., 2012). Despite the likely lack of PLD

catalytic activity, PAWS1 could potentially interact with phospho-lipids and/or other PLDs or act as a scaffolding protein to control the signalling pathways downstream of PLDs. Identifying the precise molecular roles of PAWS1 will be critical to test how BMP stimulation and the association with SMAD1 can impact the biochemical properties of PAWS1.

3.3.7 The impact of PAWS1 in embryogenesis

Because PAWS1 interacts with SMAD1 and impacts the expression of a large number of genes, including some in BMP signalling, I assessed its role during *Xenopus* embryogenesis in collaboration with Dr. K. Dingwell (Prof. J. Smith's laboratory at MRC NIMR, London). During *Xenopus laevis* embryogenesis the interplay between BMP and Wnt signalling has been well characterised (De Robertis and Kuroda, 2004). Activation of the Wnt pathway by microinjection of xWnt8 or ß-catenin RNA was shown to induce a secondary axis (Figure 3-32 (Du et al., 1995, Sokol et al., 1991, Molenaar et al., 1996)). In contrast, CHORDIN, an antagonist of BMP signalling is reported to induce a partial secondary axis (Sasai et al., 1994). xPAWS1 mRNA microinjection in the ventral zone of the embryos induces a complete duplication of the axis, including cement glands, in the embryo (Figure 3-32). This suggested that PAWS1 could potentially impact BMP as well as other signalling networks, such as the Wnt signalling pathway during development. Nonetheless, this complete axis duplication phenotype indicates the morphogenic potential of PAWS1 in embryogenesis. The observations that expression of up to 800 genes is potentially regulated by PAWS1 in cells are consistent with the dramatic impact during embryogenesis. The precise molecular mechanisms by which PAWS1 causes axis duplication in *X. laevis*

embryogenesis are unknown and are still under investigation. Nonetheless, Dr. Dingwell was able to confirm the duplication of axis phenotype of xPAWS1 by using human PAWS1, suggesting that xPAWS1 is indeed the ortholog to human PAWS1.

The evidence collected thus far implies that, unlike BMP-antagonists such as CHORDIN, PAWS1 does not inhibit canonical BMP-signalling. To assess the mechanisms by which PAWS1 causes axis duplication, I investigated its possible role in regulating the Wnt signalling. Initial evidence that PAWS1 could impact Wnt signalling stems from the observation that PAWS1 expression is linked to the regulation of LRP4 and LGR5 expression (Figure 3-25 and Appendix Table 1). LRP4, which has been discussed before, and LGR5 are components of the Wnt pathway in humans. LGR5 is a G protein-coupled receptor that mediates Wnt signalling (Carmon et al., 2012). Furthermore, PAWS1 also interacts with CULLIN3, which has been implicated in the regulation of Wnt pathway during axis elongation (Angers et al., 2006). PAWS1 could potentially mediate a signalling crosstalk between BMP and Wnt signalling. One such mechanism could be by proteins such as PDZRN3. The expression of E3 RING ubiquitin ligase PDZRN3 is regulated by PAWS1 (Figure 3-25). Honda and colleagues reported that the BMP induced differentiation of C2C12 cells into osteoblasts is regulated by PDZRN3, which inhibits Wnt signalling (Honda et al., 2010). To test whether PAWS1 impacts on osteoblast differentitation in C2C12 cells, one could employ an alkaline phosphatase assay, which indirectly measures the osteoblast differentiation (Katagiri et al., 1994) upon PAWS1 expression. Rather unfortunately, the PC3 cells employed to study the role of PAWS1 in

this thesis have been reported to overexpress DICKKOPF, a Wnt antagonist (Kawano et al., 2006) and therefore were unsuitable for the analysis of Wnt pathway. Further investigations are needed to dissect the role of PAWS1 in Wnt signalling.

Very recently, a report describing a mouse phenotype was linked to mis-expression of PAWS1 (Radden et al., 2013). Radden and colleagues demonstrated that a mutation in PAWS1 that leads to a substantially smaller version of PAWS1 in mice results a wooly (*wly*) phenotype (Radden et al., 2013). However, no function of PAWS1 or concluding evidence that the mis-expression of PAWS1 caused this phenotype was presented in this report (Radden et al., 2013). To further elucidate the physiological role PAWS1, conditional PAWS1 knockout (PAWS1 -/-) mice are being generated. These knock-out mice as well as possible knock-in mice where phospho-site mutations or mutations reported in cancer (Figure 3-2) would shed light on yet undiscovered functions and roles of PAWS1.

4 The specificities of small molecule inhibitors of the TGF-ß and BMP pathways

4.1 Introduction

Targeted disruption of specific TGF-ß signalling components provides potential therapeutic opportunities. Protein kinases have proven to be very promising drug discovery targets for intervention by small molecule inhibitors (Cohen, 2002, Dancey and Sausville, 2003). The availability of selective small molecule inhibitors of these protein kinases is potentially very useful for many therapeutic applications. The selective inhibitors are also efficient and cost-effective tools for inhibiting the target protein kinases in cells, tissues and whole organisms to study the physiological roles of these kinases.

Over the past decade, BMP and TGF-ß type I receptor serine threonine protein kinases have been targeted, led primarily by pharmaceutical industry, for the development of small molecule inhibitors (Seoane, 2008). From these efforts, several inhibitors have been reported to selectively target TGF-ß or BMP type I receptors. SB-431542 (Callahan et al., 2002, Sumara and Peter, 2007, Laping et al., 2002), SB-505124 (DaCosta Byfield et al., 2004), SB-525334 (Laping et al., 2002), LY-364947 (Peng et al., 2005, Sawyer et al., 2003), LY-2157299 (Bueno et al., 2008), A-83-01 (Tojo et al., 2005), GW-6604 (de Gouville et al., 2005) and SD-208 (Uhl et al., 2004) have all been reported as potent and selective inhibitors of TGF-ß activated ALKs (ALK4, 5 and 7) (Figure 4-1). The development of small molecule inhibitors of the BMP ALKs has lagged behind significantly

compared to the TGF-ß ALKs. Compound C, renamed Dorsomorphin (Yu et al., 2008b) and its derivative LDN-193189 (Cuny et al., 2008, Yu et al., 2008a) have been reported as potent and selective inhibitors of the BMP ALKs 2, 3 and 6 (Figure 4-1). All these compounds are described as selective inhibitors of specific ALKs (either ALKs 1, 2, 3 and 6 or ALKs 4, 5 and 7). However, comprehensive specificity tests against other protein kinases have only been reported for Compound C (Bain et al., 2007). In this chapter I present the specificities and potencies of the four most commonly used small molecule inhibitors of the type I TGF-ß receptor kinases (SB-431542, SB-505124, LY-364947 and A-83-01) and type I BMP receptor kinases (Dorsomorphin, LDN-193189 and K02288) (Figure 4-1). These chemical inhibitors are profiled against a large panel of up to 123 protein kinases, which covers 23% of the human kinome. Identifying and characterizing small molecule inhibitors of the TGF-ß signalling pathway would be very beneficial for researchers as well as clinicians.

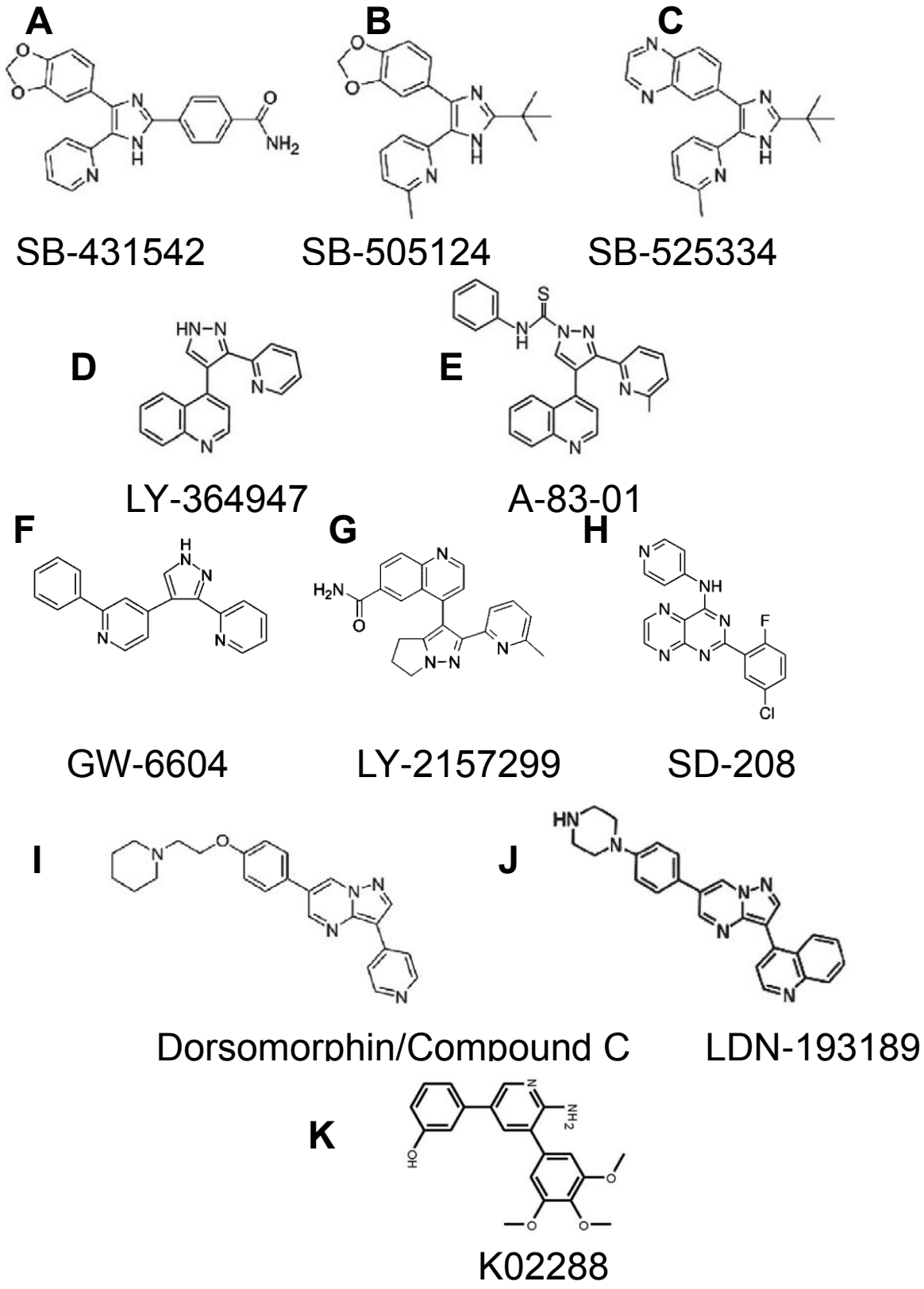

Figure 4-1 Chemical structures of the small molecule inhibitors of the TGF-ß (A–H) and BMP (I and K) pathways.

4.1.1 TGF-ß pathway specific inhibitors

4.1.1.1 SB-431542

SB-431542 (Figure 4-1) is a pyridine based small molecule inhibitor, which was originally engineered from a p38 mitogen-activated protein kinase (MAPK) imidazole inhibitor class library screen, as a potent ATP competitive inhibitor of ALK5. It inhibits ALK5 *in vitro* with an IC_{50} of 0.094 µM (Callahan et al., 2002, Laping et al., 2002). The first specificity test was performed by Inman and colleagues (Inman et al., 2002), who demonstrated that in addition to ALK5, it also inhibited ALK4 and ALK7 very potently in cells expressing constitutively active forms of the ALKs. Phosphorylation of SMAD2 was used as readout. It was also shown that SB-431542 did not inhibit BMP-induced phosphorylation of SMADs 1, 5 and 8. SB-431542 has been subsequently used by many researchers to dissect the TGF-ß pathway and is the most commonly used inhibitor used to block the TGF-ß pathway in cells and organisms. Although there have been two reports demonstrating the potency and specificity of SB-431542, a comprehensive characterisation of SB-431542 specificity has not been reported.

4.1.1.2 SB-505124

SB-505124 (Figure 4-1) evolved from the same programme that developed the closely related ATP competitive ALK5 inhibitor SB-431542 (DaCosta Byfield et al., 2004). Like SB-431542, it was shown to inhibit ALK4, ALK5 and ALK7 (DaCosta Byfield et al., 2004). DaCosta Byfield and

colleagues showed that SB-505124 does not inhibit constitutively active ALK1, 2, 3 and 6, as measured by their ability to induce phosphorylation of SMADs 1, 5 and 8 in COS1 cells. Furthermore, it was demonstrated that concentrations of up to 100 µM SB-505124 were not cytotoxic in a cell based XTT viability assay. The effect of SB-505124 against a limited panel of non-ALK kinases was also tested and at high concentration (10 µM) it was shown to inhibit p38 MAPKα (DaCosta Byfield et al., 2004). Nonetheless SB-505124 has not been profiled against a comprehensive panel comprising a large number of kinases.

4.1.1.3 LY-364947

LY-364947 (Figure 4-1) is a pyrazole based small molecule, which was engineered from diheteroaryl-substituted pyrazole using a structure–activity relationship (Christensen et al.) development approach. Diheteroaryl-substituted pyrazole was identified from a large cell based small molecule inhibitor screen to identify TGF-ß pathway inhibitors (Sawyer et al., 2003). LY-364947 was initially described as a cell permeable, ATP-competitive inhibitor of ALK5 (Peng et al., 2005, Sawyer et al., 2003). *In vitro*, it inhibited ALK5 with an IC_{50} of 0.058 µM. It was shown to inhibit TGF-ß induced phosphorylation of SMAD2 in cells ((Peng et al., 2005), Table 4-1A). None of these reports provided a comprehensive potency and specificity profiles for this compound.

4.1.1.4 A-83-01

A-83-01 (Figure 4-1) was derived from LY-364947 and is therefore structurally related to it (Figure 4-1). It was initially developed as an inhibitor of ALK5 using a cell-based CAGA-Luciferase reporter assay but has also been shown to inhibit ALK4 and 7 (Tojo et al., 2005). A-83-01 inhibited TGF-ß induced CAGA-Luciferase reporter activity in Mv1Lu lung epithelial cells with an IC_{50} of 12 nM ((Tojo et al., 2005), Table 4-1A). However, a detailed kinetic analysis of A-83-01 potency and its ability to inhibit different ALKs or other kinases has not been reported.

A

Assay	SB4-31542	SB-505124	LY-364947	A-83-01
TGF-ß induced p-SMAD2	~0.5-1 µM[1]	~0.25 µM[4]	0.135 µM[5]	N/A
ALK4 *in vitro* kinase	0.14 µM[2]	0.129 µM[4]	N/A	N/A
ALK5 *in vitro* kinase	0.094 µM[3]	0.047 µM[4]	0.058 µM[5]	N/A
CAGA-Luc assay in cells	0.25 µM[4]	0.1 µM[4]	N/A	N/A
CAGA-Luc with caALK4	0.75 µM[1]	N/A	N/A	0.045 µM[6]
CAGA-Luc with caALK5	0.5 µM[1]	N/A	N/A	0.012 µM[6]
CAGA-Luc with caALK7	1-2 µM[1]	N/A	N/A	0.0075 µM[6]

B

Assay	Dorsomorphin	LDN-193189
BMP induced P-SMAD1/5/8	0.47 µM[7]	0.005 µM[8]
BRE-Luc with caALK2	0.20 µM[7]	0.005 µM[9]
BRE-Luc with caALK3	0.50 µM[7]	0.03 µM[9]
BRE-Luc with caALK6	5-10 µM[7]	0.15 µM[9]

Table 4-1 Summary of the reported potencies of inhibitors of TGF-ß and BMP pathways

(A) IC_{50} values for the inhibitors of the TGF-ß pathway for the indicated assays. Abbreviations: TGF-ß induced P-SMAD2, TGF-ß induced phosphorylation of SMAD2 in cells as detected by immunoblotting; CAGA-Luc in cells, CAGA-Luciferase Reporter Activity dependent on TGF-ß signalling measured in a cell-based assay; ca, constitutively active; N/A, not available. **(B)** IC_{50} values for the inhibitors of the BMP pathway for the indicated assays. Abbreviations: BMP induced P-SMAD1/5/8, BMP induced phosphorylation of SMADs1/5/8 in cells as detected by immunoblotting; ca, constitutively active. BRE-Luc, BMP-Responsive Luciferase reporter activity measured in a cell-based assay.

[1] (Sumara and Peter, 2007); [2] (Laping et al., 2002); [3] (Callahan et al., 2002); [4](DaCosta Byfield et al., 2004): [5] (Peng et al., 2005); [6] (Tojo et al., 2005); [7](Yu et al., 2008b); [8] (Cuny et al., 2008); [9] (Yu et al., 2008a)

4.1.2 BMP pathway specific inhibitors

4.1.2.1 Dorsomorphin/Compound C

In vertebrates BMP signalling is important in defining the dorso-ventral (DV) axis. Inhibition of the BMP pathway results in dorsalised axis patterning in embryos (see section 3.1.2, (Nguyen et al., 1998)). A high throughput small molecule inhibitor screen in zebrafish embryos identified Compound C as an inhibitor of the BMP pathway, because it led to dorsalisation phenotype in zebrafish embryos (Yu et al., 2008b). Subsequently Compound C was renamed Dorsomorphin (Figure 4-1) and described as being a selective small molecule inhibitor of the BMP pathway (Yu et al., 2008b). Dorsomorphin was reported to inhibit the constitutively active ALK2, ALK3 and ALK6 in cells, as measured by the inhibition of BMP Responsive Element (BRE)-Luciferase reporter assay with IC_{50} values of 0.2 μM, 0.5 μM and 5 to 10 μM respectively ((Yu et al., 2008b), Table 4-1B).

Compound C (Dorsomorphin) has previously been described as a selective small molecule inhibitor of the AMP activated protein kinase (AMPK) (Zhou et al., 2001). Although used extensively as an AMPK inhibitor, a comprehensive specificity study profiling Compound C against a panel of 70 protein kinases showed that it inhibited a range of other kinases, including ERK8, MNK1, PHK, MELK, DYRK isoforms, HIPK2, Src and Lck with similar or greater potency than AMPK (Bain et al., 2007). This extremely useful specificity information of Compound C has not been mentioned by the reports describing Dorsomorphin as a specific inhibitor of the BMP pathway

(Boergermann et al., 2010, Hao et al., 2008, Hong and Yu, 2009, Yu et al., 2008b).

4.1.2.2 LDN-193189

Using Dorsomorphin as a template, LDN-193189 was engineered primarily by replacing the 4-pyridine ring with 4-quinoline (Figure 4-1, (Cuny et al., 2008)). As a result the new compound (LDN-193189) had improved potency over Dorsomorphin as a BMP pathway inhibitor (Cuny et al., 2008). This was demonstrated in rat pulmonary artery smooth muscle cells (rPASMC), as LDN-193189 inhibited BMP-4-induced phosphorylation of SMADs1, 5 and 8 with an IC_{50} value of 5 nM. This is a 94-fold improvement when compared to the IC_{50} value of 470 nM for Dorsomorphin (Cuny et al., 2008). LDN-193189 has been subsequently shown to inhibit the BRE-Luciferase reporter activity driven by constitutively active ALK2, ALK3 and ALK6 with IC_{50} values of 5 nM, 30 nM and 150 nM respectively. On the other hand LDN-193189 inhibited ALK4, ALK5 and ALK7 with IC_{50} values greater than 500 nM (Yu et al., 2008a). Nonetheless there is no report available that describes the specificities and potencies of LDN-193189 against a comprehensive number of protein kinases

4.2 Results

4.2.1 Specificities of small molecule inhibitors of the TGF-ß pathway

4.2.1.1 Specificities and potencies of SB-431542 and SB-505124

To investigate the ability of both SB-431542 and SB-505124 to inhibit the activity of a panel of over 105 protein kinases, both compounds were assayed at two different concentrations (0.1 and 1 μM) (Figure 4-2). At both concentrations, SB-431542 and SB-505124 inhibited ALK5 activity *in vitro* but did not inhibit ALK3 (Figure 4-2A and B, Figure 4-5A and B). At 1μM, SB-431542 inhibited ALK5 but also RIPK2 and CK1δ by 77% and 70% respectively. Furthermore p38αMAPK was inhibited by 30% (Figure 4-2A). At lower concentration of 0.1μM, SB-431542 still inhibited RIPK2 and CK1δ by 33% and 29% respectively (Figure 4-2A). Similarly at 1μM, SB-505124 inhibited RIPK2 by about 72% and p38α MAPK by 49% but did not inhibit CK1δ (Figure 4-2B). At 0.1μM, SB-505124 inhibited RIPK2 by 18% but CK1δ and p38αMAPK were not inhibited (Figure 4-2B). Both concentrations of either of the two compounds did not significantly inhibit the activity of any other kinase used in the *in vitro* panel (Figure 4-2). Because SB-431542 could inhibit CK1δ at 1 μM (Figure 4-2A), it was investigated if both SB-431542 and SB-505124 could inhibit other CK1 isoforms *in vitro*. SB-431542 inhibited CK1α, CK1δ and CK1ε isoforms with IC_{50} values of 1.34μM, 0.92μM and 0.38μM respectively but it did not inhibit CK1γ (Table 4-2). SB-505124 inhibited CK1α, CK1δ and CK1ε isoforms with IC_{50}s of 19.44μM, 3.38μM and 1.60μM respectively and did not inhibit CK1γ (Table 4-2Table 4-2).

Furthermore, SB-431542 and SB-505124 inhibited RIPK2 with IC_{50} of 0.41μM and 0.35μM respectively (Table 4-2).

SB-431542 inhibits TGF-ß-induced phosphorylation of SMAD2 with an IC_{50} value of ~2.5 μM (Figure 4-6). The TGF-ß-induced phosphorylation of SMADs 1, 5 and 8 was only modestly affected at concentrations higher than 1 μM and BMP-2-induced phosphorylation of SMADs 1, 5 and 8 was not inhibited by SB-431542 (Figure 4-6B).

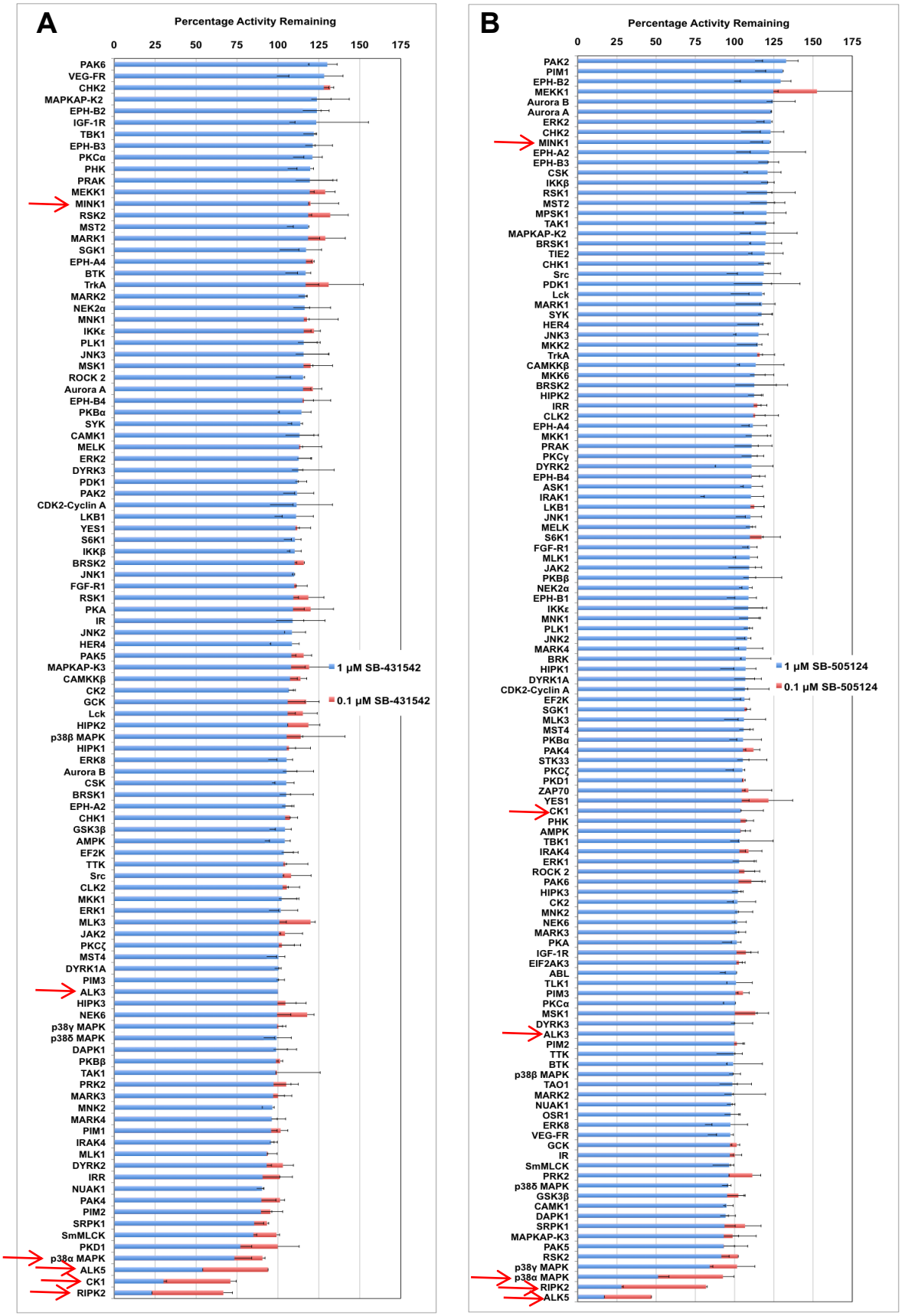

Figure 4-2 The specificities of TGF-ß pathway inhibitors

The specificity of **(A)** SB-431542, **(B)** SB-505124 at the indicated concentrations was profiled against a panel of up to 123 protein kinases. The results are presented as bars indicating percentage activity remaining for each kinase (averages of two duplicate determinations) in the presence of the indicated concentration of the inhibitor compared with a control lacking the inhibitor ± standard deviation. The results are ranked according to the percentage activity remaining when the assays were performed in the presence of the indicated inhibitors at 1 μM. Protein kinases referred to in results section 4.2.1.1 are indicated by red arrows. Abbreviations for the protein kinases can be found in the abbreviation list.

Kinase	SB-431542	SB-505124	LY-364947	A-83-01	LDN-193189
RIPK2	0.41 µM	0.35 µM	0.11 µM	0.10 µM	0.025 µM
CK1α	1.34 µM	19.44 µM	2.27 µM	15.66 µM	3.61 µM
CK1δ	0.92 µM	3.38 µM	0.22 µM	3.42 µM	0.92 µM
CK1ε	0.38 µM	1.60 µM	1.34 µM	4.59 µM	14.24 µM
CK1γ	>100 µM	>100 µM	43.97 µM	28.55 µM	98.92 µM
GCK	>100 µM	>100 µM	7.91 µM	2.22 µM	0.08 µM

Table 4-2 Potencies of small molecules developed as TGF-ß and BMP pathway inhibitors against some other kinases

IC_{50} values were determined from multiple assays carried out at ten different inhibitor concentrations *in vitro*.

4.2.1.2 Specificities and potencies of LY-364947 and A-83-01

When profiled against 123 protein kinases (Figure 4-3A), LY-364947 at a concentration of 1μM inhibited ALK5, RIPK2, VEGF-R, CK1δ and MINK1 activity by greater than 50%. If the concentration is increased to 10 μM, LY-364947, additionally inhibited the following kinases by more than 50%: p38αMAPK, PKD1, GCK, BRK, Lck, TAK1, YES1, FGF-R1 and p38ß MAPK. LY-364947 inhibited RIPK2 and CK1δ with IC_{50} of 0.11 μM and 0.22 μM respectively (Table 4-2). LY-364947 inhibited CK1α, CK1ε and CK1γ isoforms with IC_{50} values of 2.27 μM, 1.34 μM and 44 μM respectively (Table 4-2).

A-83-01, which is structurally related to LY-364947 (Figure 4-1), was also used in an *in vitro* kinase assay against a panel of 107 kinases at concentrations of 1 μM and 0.1 μM (Figure 4-3B). At 1 μM, A-83-01 inhibited ALK5, VEG-FR, RIPK2, MINK1, p38α MAPK, PKD1 and FGF-R1 by greater than 50% (Figure 4-3B). At concentrations of 0.1μM, MINK1, p38α MAPK and FGF-R1 were inhibited by more than 30% while ALK5, VEG-FR, RIPK2 were still inhibited by more than 50% (Figure 4-3B). A-83-01 was able to only moderately inhibit the activity of CK1 isoforms. The IC_{50} values of CK1α, CK1δ, CK1ε and CK1γ were 15.66 μM, 3.42 μM, 4.59 μM and 29 μM respectively (Table 4-2).

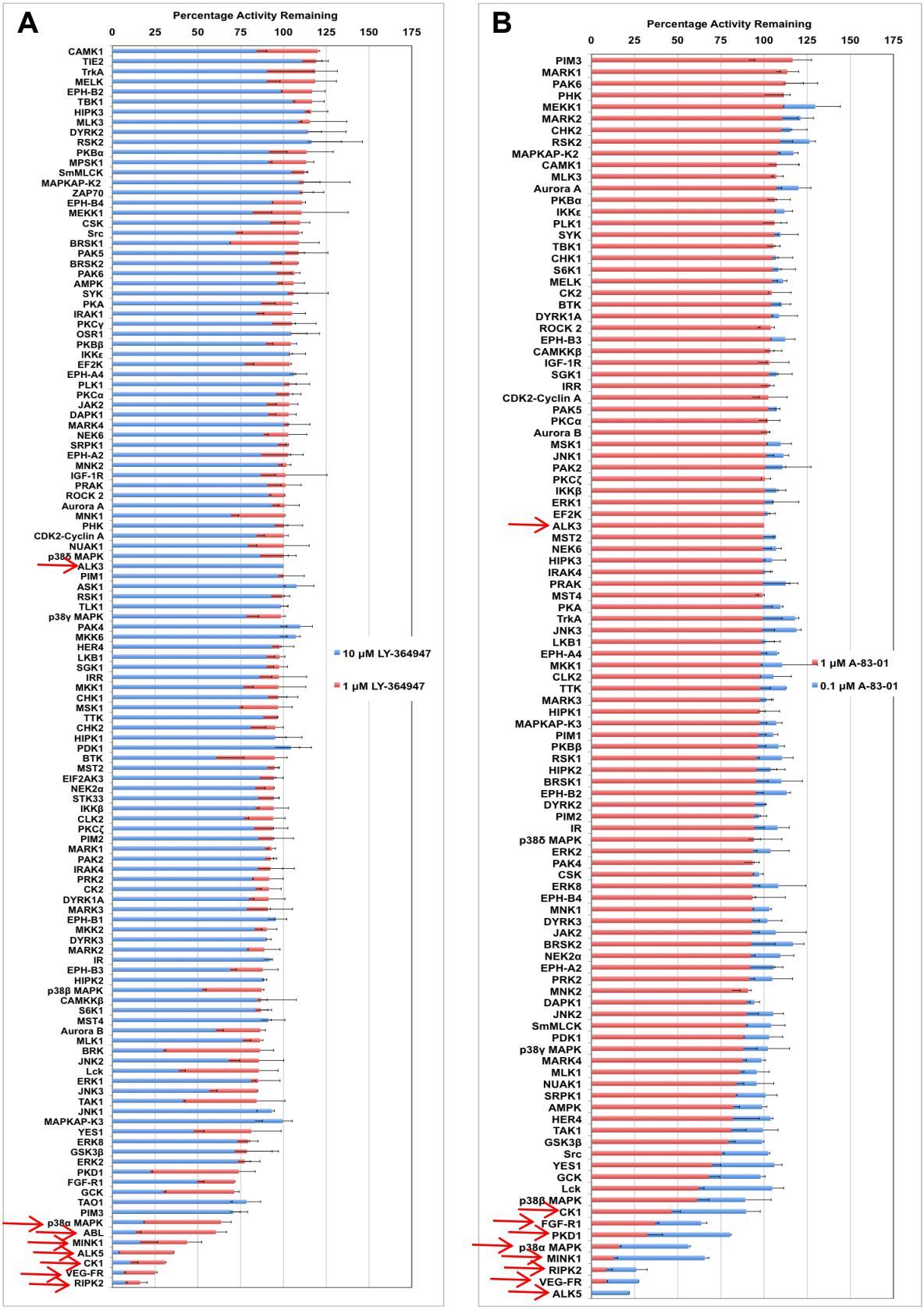

Figure 4-3 The specificities of TGF-ß pathway inhibitors

The specificity of **(A)** LY-364947, **(B)** A-83-01 at the indicated concentrations was profiled against a panel of up to 123 protein kinases. The results are presented as bars indicating percentage activity remaining for each kinase (averages of two duplicate determinations) in the presence of the indicated concentration of the inhibitor compared with a control lacking the inhibitor ± standard deviation. The results are ranked according to the percentage activity remaining when the assays were performed in the presence of the indicated inhibitors at 1 µM. Protein kinases referred to in results section 4.2.1.2 are indicated by red arrows. Abbreviations for the protein kinases can be found in the abbreviation list.

4.2.2 Specificities of small molecule inhibitors of the BMP pathway

4.2.2.1 Specificity of Dorsomorphin (Compound C) as a BMP pathway inhibitor

The specificity and the potency of Dorsomorphin was profiled at three different concentrations (10, 1 and 0.1 μM) against a panel of 119 protein kinases (Figure 4-4A). At a concentration of 10 μM, Dorsomorphin inhibited the activities of 64 out of the 119 kinases by greater than 50%. At concentrations of 1 μM, Dorsomorphin inhibited the activities of 34 out of 119 kinases more potently than it inhibited AMPK and by more than 50% (Figure 4-4A). Even at concentrations of 0.1 μM, it inhibited VEGF-R, ERK8, GCK, CLK2, DYRK1A, PHK, ABL, NUAK1, PRK2 and YES1 by more than 50% (Figure 4-4A). Dorsomorphin inhibited ALK3 *in vitro* with an IC_{50} value of about 1 μM while ALK5 was not inhibited (Figure 4-5C).

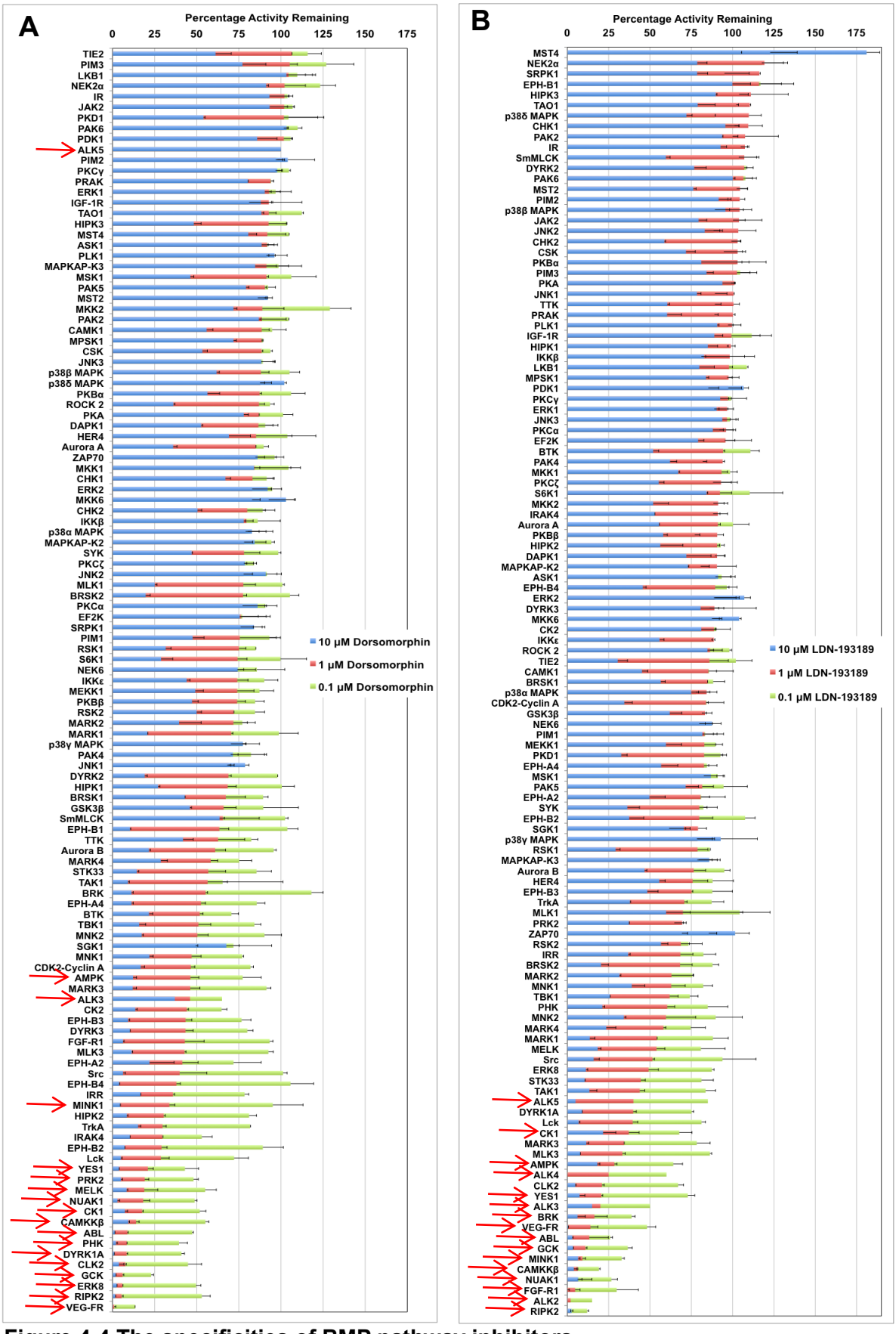

Figure 4-4 The specificities of BMP pathway inhibitors

(A) Dorsomorphin and **(B)** LDN-193189 were assayed against a panel of up to 121 kinases at the indicated concentrations. The results are presented as bars indicating percentage activity remaining for each kinase (averages of two duplicate determinations) in the presence of the indicated concentration of the inhibitor compared with a control lacking the inhibitor ± standard deviation. The results are ranked according to the percentage activity remaining when the assays were performed in the presence of the indicated inhibitors at 1 μM. Protein kinases referred to in Results section 4.2.2 are indicated by red arrows.

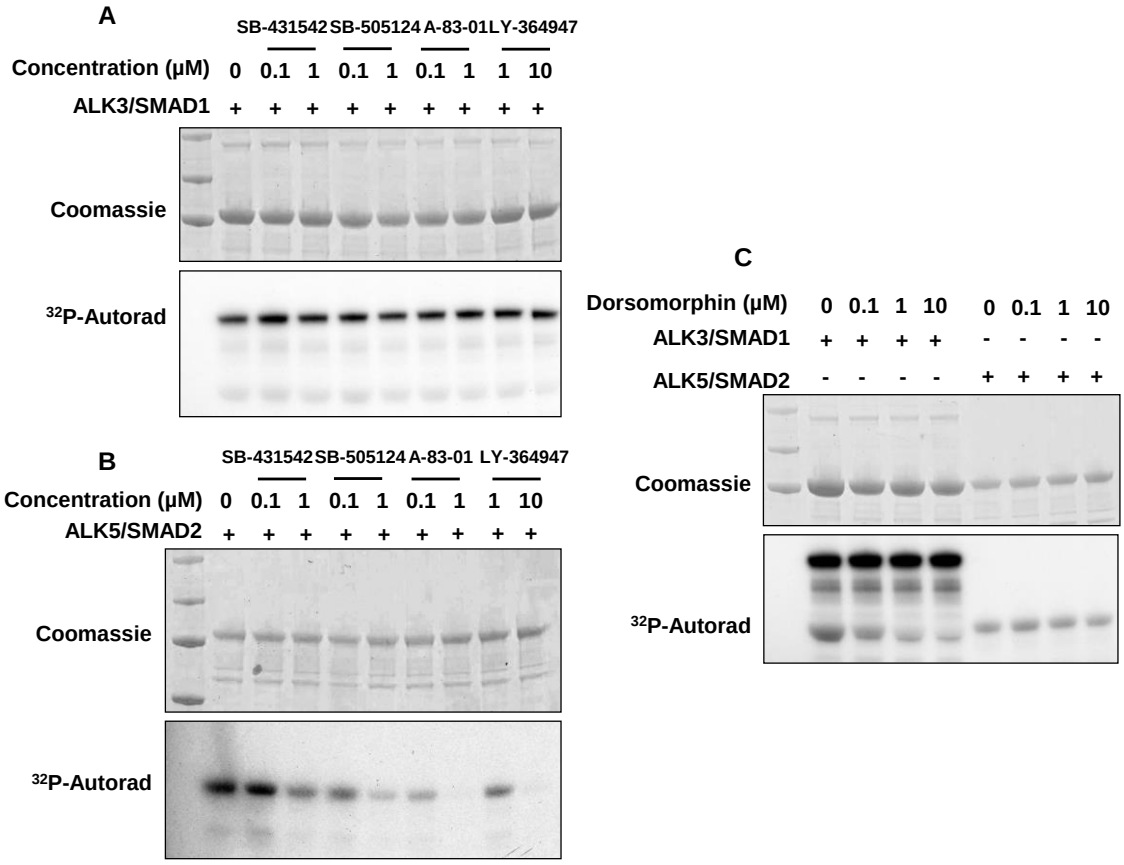

Figure 4-5 Inhibition of ALK3 and ALK5 by inhibitors of the TGF-ß and BMP pathways

(A) Kinase assay with ALK3 as described in section 2.2.12, in the presence or absence of the indicated concentrations of TGF-ß pathway inhibitors SB-431542, SB-505124, LY-364947 and A-83-01. The assay samples were resolved by SDS-PAGE, and the gels were Coomassie-stained, dried and analysed by ^{32}P autoradiography. For percentage activity remaining determinations, Coomassie stained bands corresponding to substrate proteins were excised, ^{32}P-incorporation measured and the resulting radioactivity (cpm) used as a percentage of control. **(B)** Same as (A) but using ALK5 instead of ALK3. **(C)** As above, except that ALK3 and ALK5 were assayed in the presence or absence of the indicated concentrations of Dorsomorphin.

4.2.2.2 Specificity of LDN-193189 as a BMP pathway inhibitor

LDN-193189 was derived from Dorsomorphin in order to improve potency against the BMP pathway (Cuny et al., 2008). In HaCaT cells, LDN-193189 inhibits BMP-2-induced phosphorylation of SMADs 1, 5 and 8 with an IC_{50} value of ~0.005 µM (Figure 4-6A). The TGF-ß (50 pM) induced phosphorylation of SMAD2 was only modestly affected at concentrations higher than 3 µM, although TGF-ß induced phosphorylation of SMADs 1, 5 and 8 was inhibited at a dose of around 0.3 µM LDN-193189 (Figure 4-6B). Subsequently, I investigated the inhibitory effect of LDN-193189 against the activity of various ALKs using *in vitro* kinase assays (Figure 4-7). LDN-193189 inhibited the ability of ALK2 to phosphorylate GST-SMAD1 *in vitro* with an IC_{50} value of 45 nM, while ALK2 autophosphorylation was inhibited with an IC_{50} of 30 nM (Figure 4-7A). LDN-193189 inhibited the ability of ALK3 to phosphorylate SMAD1 under these conditions with an IC_{50} value of 100 nM, although even at 3 µM, ALK3 activity could not be completely inhibited (Figure 4-7B). BMPRII is essential for the activity of ALK3 *in vitro* but its auto-phosphorylation was not affected by LDN-193189 (Figure 4-7B). LDN-193189 inhibited the activity of ALK4 and ALK5, although with higher IC_{50} values of 0.3 µM and 0.5 µM respectively (Figure 4-7C and D).

Because the off target effects of LDN-193189 towards other protein kinases have not been described previously, the specificity and potency of LDN-193189 at three different concentrations was assayed against a panel of 121 protein kinases (Figure 4-4B). From the resulting data, it is evident that the specificity and potency profile for LDN-193189 was similar to that of

Dorsomorphin (compare Figure 4-4A and B). At a concentration of 10 μM, LDN-193189 inhibited 44 out of the 121 kinases by more than 50% (Figure 4-4B). At 1 μM, LDN-193189 still inhibited 24 out of the total 121 protein kinases by more than 50%. Even at 0.1 μM, LDN-193189 inhibited RIPK2, FGF-R1, NUAK1, CAMKKß, MINK1, GCK, VEG-FR and BRK by greater than 50% (Figure 4-4B).

When tested *in vitro*, LDN-193189 inhibits RIPK2 and GCK with IC_{50} values of 0.025 μM and 0.08 μM respectively. These values are comparable to those calculated for inhibition of ALK2 and ALK3 by LDN-193189 using *in vitro* kinase assays (Table 4-2, Figure 4-7A and B).

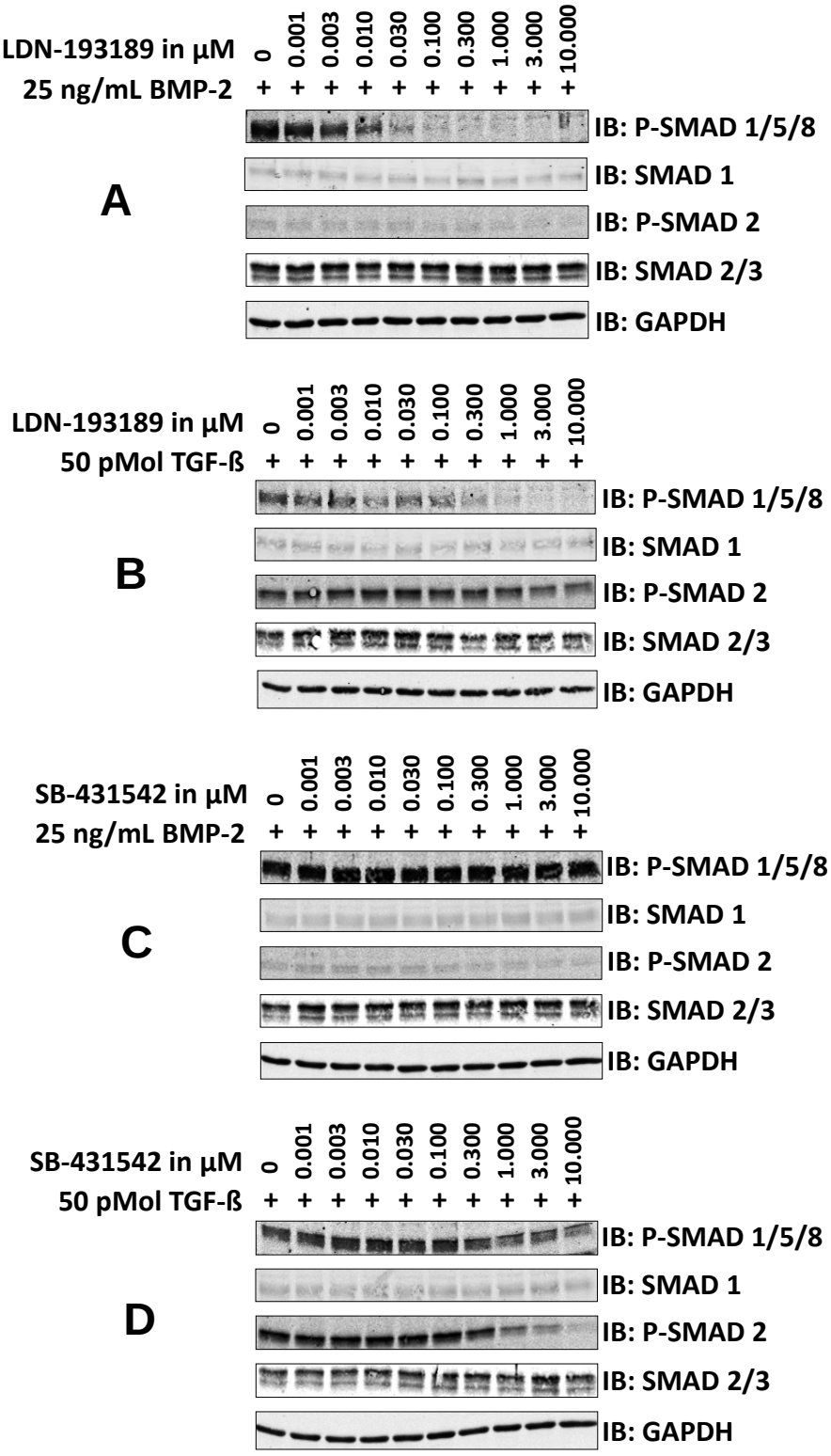

Figure 4-6 Inhibition of TGF-ß and BMP pathways by LDN-193189 and SB-431542

(A) Serum-starved HaCaT cells were treated with the indicated concentrations of LDN-193189 for 2 h and then treated with BMP-2 (25 ng/ml) for 1 h prior to lysis. Extracts were resolved by SDS-PAGE and transferred to nitrocellulose membranes, which were analysed by immunoblotting using the indicated antibodies. **(B)** Same as A but cells were treated with TGF-ß (50 pM) for 1 h prior to lysis. **(C)** Same as A, but indicated concentrations of SB-431542 were used for 3 h prior to lysis. **(D)** Same as C, but cells were treated with TGF-ß (50 pM) 1 h prior to lysis.

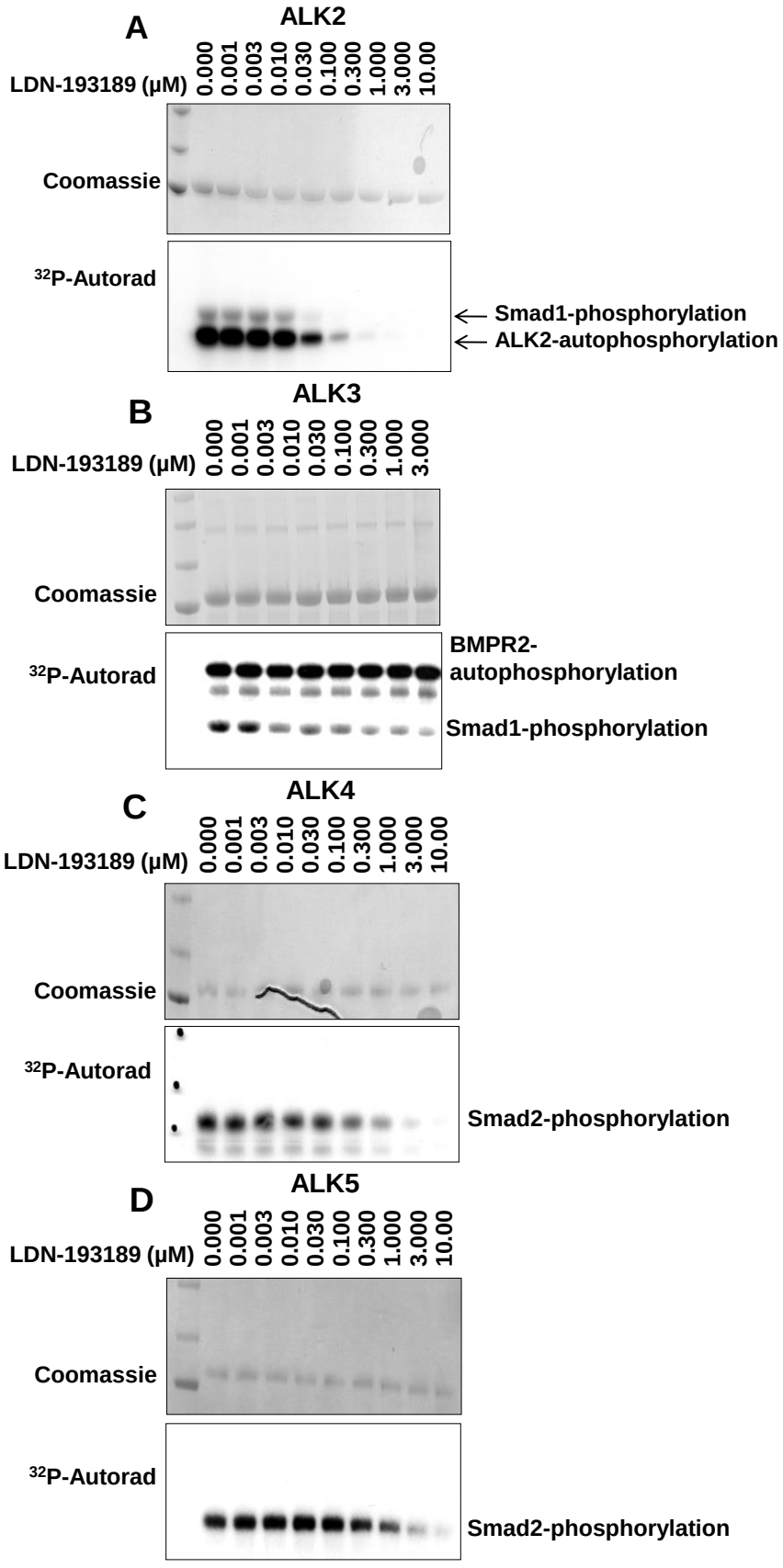

Figure 4-7 LDN-193189 inhibits ALK2 and ALK3 in vitro

(A) Kinase assay with ALK2 as described in section 2.2.12, in the absence or presence of the indicated concentrations of LDN-193189. The assay samples were resolved by SDS-PAGE, and the gels were Coomassie-stained, dried and analysed by ^{32}P autoradiography. For IC_{50} determinations, Coomassie stained bands corresponding to substrate proteins were excised, ^{32}P-incorporation measured and the resulting radioactivity (cpm) plotted against concentrations of LDN-193189 used. **(B)** Same as A, except that ALK3 was used. **(C)** Same as A, except that ALK4 was used. **(D)** Same as A, except that ALK5 was used.

4.2.3 Inhibition of RIPK2 by LDN-193189 in RAW macrophage cells

As shown before, RIPK2, a member of the receptor interacting protein (RIP) family of protein kinases, was inhibited potently *in vitro* by LDN-193189 (Table 4-2). To test whether LDN-193189 can inhibit RIPK2 in cells at concentrations sufficient to inhibit BMP signalling (Figure 4-6A), RAW macrophage cells were used. These cells were treated with the peptidoglycan-related agonist D-glutamyl-meso-diaminopimelic acid (meso-DAP), which leads to the phosphorylation of ERK1/2 (Figure 4-8). This phosphorylation was inhibited when cells were treated with 0.1 μM or 10μM LDN-193189 (Figure 4-8).

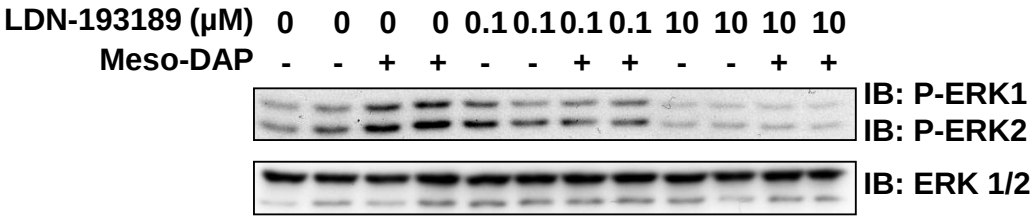

Figure 4-8 Inhibition of the NOD-RIPK2 pathway by LDN-193189

RAW 264.7 cells were treated with indicated concentrations of LDN-193189 for 2 h prior to treatment of cells with 15 μM Meso-DAP for 1 h before lysis. Extracts were resolved by SDS-PAGE and analysed by immunoblotting using the indicated antibodies.

4.3 Discussion

In this study, I have established the *in vitro* specificities of some of the most commonly used small molecule inhibitors of the TGF-ß and BMP pathways against a panel of up to 123 protein kinases. This represents almost a quarter of the human kinome. The results obtained indicate many potential off-target effects for these small molecule inhibitors, when they are used to assess the physiological roles of TGF-ß and BMP pathways by inhibition of the type I receptors (ALKs). Therefore, any potential impact on the activity of the TGF-ß and BMP pathways observed by using any of these small molecule inhibitors should be interpreted with caution. If any of these inhibitors are used to inhibit the TGF-ß and BMP pathways, either in cell culture-based assays or whole animal studies, it is recommended that the minimum effective concentrations against the intended targets are used. It is also recommended that this minimal effective concentration is determined for each assay individually, in order to minimise the potential unwanted off-target effects. As mentioned above, the specificity of the small molecule inhibitors was only profiled against 23% of all human kinases. Hence, these inhibitors could potentially inhibit other kinases that could not be included in this study. Nonetheless, this study does provide vital information for researchers when deciding on which inhibitor to use for any particular assay.

4.3.1 Inhibitors of the TGF-ß pathway

Active TGF-ß signalling has been implicated in numerous diseases (see section 1.6), including the development of fibrotic sclerosis of multiple organs like heart, kidney, lungs, liver and skin (Border and Noble, 1994,

Bottinger and Bitzer, 2002, Gu et al., 2007). TGF-ß signalling is also strongly associated with cancer progression and metastasis (see section 1.6; (Massague, 2008, Padua and Massague, 2009)). As a result, TGF-ß signalling components, have been targeted for the development of small molecule kinase inhibitors (mainly targeting ALK5), ligand binding antibodies or antisense oligonucleotides by major pharmaceutical industries (Callahan et al., 2002, Sawyer et al., 2003, Seoane, 2008). Several TGF-ß pathway inhibitors have entered pre-clinical and clinical trials to treat fibrosis and advanced metastatic cancers (Seoane, 2008). The outcome of these trails are mixed (Seoane, 2008). One possible explanation is that these inhibitors block TGF-ß signalling globally and therefore unwanted side effects occur. Another likely explanation is that all compounds used could also impact other pathways and thereby create unwanted off-target effects. Therefore it is important to use chemical inhibitors that are highly specific to a specific target in order to minimise unwanted off-target effects that could have undesired consequences for the whole organism.

While both SB-431542 and SB-505124 are relatively selective inhibitors of ALKs 4, 5 and 7, SB-505124 is the more potent inhibitor of ALK4, 5 and 7 and inhibits CK1 isoforms less potently than SB-431542 ((DaCosta Byfield et al., 2004), Table 4-1A, Table 4-2). Furthermore, in cell-based assays, SB-505124 was reported to be less cytotoxic than SB-431542 (DaCosta Byfield et al., 2004). Both, SB-431542 and SB-505124 inhibit RIPK2 with similar IC_{50} values (Table 4-2) and both have also been reported to inhibit p38α MAPK at high concentrations with IC_{50} values above 10 µM (DaCosta Byfield et al., 2004, Sumara and Peter, 2007). SB-525334, which is

structurally very closely related to SB-505124 (Figure 4-1), has been reported to be around 3-fold more potent in inhibiting ALK5 and around 2-fold more potant in inhibiting ALK4 compared to SB-505124 (Grygielko et al., 2005). However, as it has not been used as extensively as other ALK5 inhibitors, it was not included in this study. Although A-83-01 showed to be the most potent ALK5 inhibitor *in vitro* (Figure 4-5B), at concentrations sufficient to inhibit ALK5, it also inhibited RIPK2, MINK1, VEGF-R, p38α MAPK, PKD1 and FGF-R1 potently. LY-364947, a less potent inhibitor of ALK5 compared to A-83-01, also inhibited RIPK2, MINK1, VEGF-R and CK1 isoforms potently (Figure 4-3A and B).

Based on the discussions above on specificities and potencies of the four small molecule inhibitors of the TGF-ß pathway used in this study, the use of SB-505124 over SB-431542, at or below 1μM, as an inhibitor of ALKs 4, 5 and 7 in cell-based assays is recommended. If LY-364947 or A-83-01 is used as a TGF-ß pathway inhibitor, the potential off-target effects have to be considered with caution.

To date, there are no small molecule inhibitors of the TGF-ß pathway that can selectively inhibit ALK4, 5 or 7. All five discussed inhibitors in this study show no significant selectivity between these ALKs. On the other hand, knockout mouse models of ALK4, ALK5 or ALK7 display unique phenotypes (Itoh et al., 2009, Jornvall et al., 2004). Whereas knocking out ALK4 and ALK5 is embryonically lethal and the mice die at around E9.5 and E10.5 respectively (Gu et al., 1998, Jornvall et al., 2004), ALK7 knockout mice are viable and fertile (Jornvall et al., 2004). This emphasises the need for ALK-

specific inhibitors to further dissect the roles of individual ALKs in cells. Targeting selective ALKs might also be beneficial for treating specific diseases, where individual ALKs might be responsible for driving a particular disease state.

4.3.2 Inhibitors of the BMP pathway

BMP signalling plays critical roles during embryogenesis and in controlling the fate of various progenitor cell populations including embryonic stem cells and hematopoietic stem cells. BMP signalling is also important in skeletogenesis (Chen et al., 2004, De Robertis and Kuroda, 2004, Li and Cao, 2006, Varga and Wrana, 2005). While the efforts of the pharmaceutical companies have focussed on developing small molecule inhibitors of the TGF-ß pathway, the development of small molecule inhibitors of the BMP pathway has largely lagged behind. The selective small molecule inhibitors of the BMP pathway would be useful in dissecting and understanding the physiological roles of BMP signalling in different cellular contexts. ALKs 2, 3 and 6 are ubiquitously expressed and mediate BMP signals in most cells and tissues. ALK1 is unique in that it is mainly reported to be expressed in endothelial cells and has been reported to phosphorylate SMAD1 in response to BMP and TGF-ß ligands (Oh et al., 2000, Wrighton et al., 2009). Aberrant BMP signalling has been reported to play a role in heterotopic ossification, where ALK6 is mutated to a constitutively active form (Yu et al., 2008a). Similarly overexpression of certain BMP ligands and activation of downstream signalling has been reported in some cancers (Blanco Calvo et al., 2009). Having a potent and specific small molecule inhibitor of BMP activated ALKs could therefore be of clinical benefit against these diseases.

Dorsomorphin, and its derivative LDN-193189 were reported as selective and potent inhibitors of BMP signalling (Cuny et al., 2008, Yu et al., 2008a, Yu et al., 2008b). Subsequently, both compounds have been widely used *in vitro*, in cell-based assays and also in whole organisms to study the BMP pathway and its physiological roles. In this study the specificities of Dorsomorphin and LDN-193189 have been profiled against a panel of up to 121 protein kinases *in vitro* (Figure 4-4A and B). When compared to the best TGF-ß pathway inhibitors, Dorsomorphin and LDN-193189, are rather non-specific inhibitors of the BMP pathway as they inhibit a number of other protein kinases potently (Figure 4-4). Some of the off-target effects of using Dorsomorphin at concentrations sufficient to inhibit BMP signalling have been demonstrated before and in this study and it is likely that many more exist ((Bain et al., 2007, Cannon et al., 2010), Figure 4-4A). Therefore, using Dorsomorphin as a small molecule inhibitor for the BMP pathway should be avoided.

LDN-193189 on the other hand is a very potent inhibitor of BMP signalling, inhibiting BMP-induced phosphorylation of Smad1 in cells with an IC_{50} of 5 nM ((Cuny et al., 2008, Yu et al., 2008a), Figure 4-6A). ALK2 and ALK3 were inhibited *in vitro* by LDN-193189 with IC_{50} values of 30–45 nM and 100 nM respectively (Figure 4-7A and B). Interestingly, these IC_{50} values are substantially higher when compared to those obtained from inhibiting the BMP pathway in cells (Figure 4-6A). A possible explanation would be that LDN-193189 binds very efficiently, maybe allosterically, to the BMP-activated ALKs in cells. However, the crystal structures of LDN-193189 in complex with the kinase domain of ALK1 revealed that LDN-193189 binds to the ATP-

binding pocket of the ALK1 kinase domain (http://www.thesgc.org/structures/structure_description/3MY0/). It is also possible that the inhibitory effects of LDN-193189 to block BMP signalling very potently could be only partly dependent on the direct effects of LDN-193189 on ALKs and partly also on the off-target effects on other kinases. These kinases could impact on both the activation and activity of ALKs or the access of ALKs to their substrates or a combination of these possibilities. This is not unlikely because LDN-193189 inhibited a large number of other kinases very potently *in vitro* (Figure 4-4B). While LDN-193189 shows much improved potencies against BMP ALKs 2 and 3 compared to Dorsomorphin, its potency against many other kinases did not change to a large extent (Figure 4-4). The usage of LDN-193189 as an inhibitor of the BMP pathway in cells or whole organisms should be considered with caution, knowing its ability to inhibit other kinases, notably RIPK2, FGF-R1, NUAK1, CAMKKß, MINK1, GCK, VEG-FR and BRK and possibly many more. RIPK2 for example is implicated in NOD1 and NOD2 signalling and activates MAP Kinases (Figure 4-8), NFκB signalling, as well as the mediation of inflammatory responses. In cells, NOD1 and NOD2 can sense peptidoglycan-related molecules from bacteria that have entered the cell and evaded immune recognition via Toll-like receptors at the cell membrane (Inohara et al., 2005). Therefore inhibiting RIPK2 in whole organisms could lead to unwanted side effects by, for example, affecting the immune system.

Nonetheless due to its potency as a BMP pathway inhibitor, LDN-193189 provides a very good platform to design derivatives that could enhance its selectivity for BMP-activated ALKs. Evidently, Dorsomorphin is

not a good candidate for a selective inhibitor of the BMP pathway. In zebrafish, Dorsomorphin, when used at sufficient concentrations to block BMP signalling, it strongly inhibited intersegmental vessel formation by inhibiting VEGF-R2 (Cannon et al., 2010). This is only one example, demonstrating the potential off-target effects when using a non-specific inhibitor. DMH1, a Dorsomorphin analogue was reported as being very specific to BMP signalling and displaying no off-target effects against VEG-FR (Hao, J 2009). However, there is no comprehensive study of DMH1 against a substantial panel of kinases that Dorsomorphin and LDN-193189 inhibit potently to prove its specificity. Very recently a study described K02288 (Figure 4-1) as being a specific and potent small molecule inhibitor of BMP signalling (Sanvitale et al., 2013). K02288 was designed as an inhibitor of ALK2 but also possess activity against ALK1, ALK6 and to a lesser extend ALK3. The potencies compared to LDN-193189 against ALK1 and ALK2 are similar, whereas LDN-193189 inhibits ALK3 more potently and K02288 inhibits ALK6 more potently. K02288 inhibition of BMP-mediated SMAD1/5/8 phosphorylation was reported to be 10-fold lower compared to LDN-193189 (Sanvitale et al., 2013). Although the specificity was shown to be improved compared to LDN-193189 when the compounds were assayed against 200 human kinases, RIPK2, NUAK1, CAMKKß, GCK and GCKR, all inhibited by LDN-193189, were not tested. Testing specificity against these kinases may yet prove K02288 a more selective inhibitor of the BMP pathway.

References

ABDALLA, S. A. & LETARTE, M. 2006. Hereditary haemorrhagic telangiectasia: current views on genetics and mechanisms of disease. *J Med Genet,* 43**,** 97-110.

AGIUS, E., OELGESCHLAGER, M., WESSELY, O., KEMP, C. & DE ROBERTIS, E. M. 2000. Endodermal Nodal-related signals and mesoderm induction in Xenopus. *Development,* 127**,** 1173-83.

AGRICOLA, E., RANDALL, R. A., GAARENSTROOM, T., DUPONT, S. & HILL, C. S. 2011. Recruitment of TIF1gamma to chromatin via its PHD finger-bromodomain activates its ubiquitin ligase and transcriptional repressor activities. *Mol Cell,* 43**,** 85-96.

AHN, J., SANZ-MORENO, V. & MARSHALL, C. J. 2012. The metastasis gene NEDD9 product acts through integrin beta3 and Src to promote mesenchymal motility and inhibit amoeboid motility. *J Cell Sci,* 125**,** 1814-26.

AKHURST, R. J. & HATA, A. 2012. Targeting the TGFbeta signalling pathway in disease. *Nat Rev Drug Discov,* 11**,** 790-811.

AL-SALIHI, M. A., HERHAUS, L. & SAPKOTA, G. P. 2012. Regulation of the transforming growth factor beta pathway by reversible ubiquitylation. *Open Biol,* 2**,** 120082.

ALARCON, C., ZAROMYTIDOU, A. I., XI, Q., GAO, S., YU, J., FUJISAWA, S., BARLAS, A., MILLER, A. N., MANOVA-TODOROVA, K., MACIAS, M. J., SAPKOTA, G., PAN, D. & MASSAGUE, J. 2009. Nuclear CDKs drive Smad transcriptional activation and turnover in BMP and TGF-beta pathways. *Cell,* 139**,** 757-69.

ALIMIRAH, F., CHEN, J., BASRAWALA, Z., XIN, H. & CHOUBEY, D. 2006. DU-145 and PC-3 human prostate cancer cell lines express androgen receptor: implications for the androgen receptor functions and regulation. *FEBS Lett,* 580**,** 2294-300.

ANNES, J. P., MUNGER, J. S. & RIFKIN, D. B. 2003. Making sense of latent TGFbeta activation. *J Cell Sci,* 116**,** 217-24.

ANSIEAU, S., BASTID, J., DOREAU, A., MOREL, A. P., BOUCHET, B. P., THOMAS, C., FAUVET, F., PUISIEUX, I., DOGLIONI, C., PICCININ, S., MAESTRO, R., VOELTZEL, T., SELMI, A., VALSESIA-WITTMANN, S., CARON DE FROMENTEL, C. & PUISIEUX, A. 2008. Induction of EMT by twist proteins as a collateral effect of tumor-promoting inactivation of premature senescence. *Cancer Cell,* 14**,** 79-89.

ARAGON, E., GOERNER, N., ZAROMYTIDOU, A. I., XI, Q., ESCOBEDO, A., MASSAGUE, J. & MACIAS, M. J. 2011. A Smad action turnover switch operated by WW domain readers of a phosphoserine code. *Genes Dev,* 25**,** 1275-88.

BAI, Y., YANG, C., HU, K., ELLY, C. & LIU, Y. C. 2004. Itch E3 ligase-mediated regulation of TGF-beta signaling by modulating smad2 phosphorylation. *Mol Cell,* 15**,** 825-31.

BAIN, J., PLATER, L., ELLIOTT, M., SHPIRO, N., HASTIE, C. J., MCLAUCHLAN, H., KLEVERNIC, I., ARTHUR, J. S., ALESSI, D. R. & COHEN, P. 2007. The selectivity of protein kinase inhibitors: a further update. *Biochem J,* 408**,** 297-315.

BAKIN, A. V., RINEHART, C., TOMLINSON, A. K. & ARTEAGA, C. L. 2002. p38 mitogen-activated protein kinase is required for TGFbeta-mediated fibroblastic transdifferentiation and cell migration. *J Cell Sci,* 115**,** 3193-206.

BECK, S. E. & CARETHERS, J. M. 2007. BMP suppresses PTEN expression via RAS/ERK signaling. *Cancer Biol Ther,* 6**,** 1313-7.

BELVILLE, C., JOSSO, N. & PICARD, J. Y. 1999. Persistence of Mullerian derivatives in males. *Am J Med Genet,* 89**,** 218-23.

BISHOP, A. L. & HALL, A. 2000. Rho GTPases and their effector proteins. *Biochem J,* 348 Pt 2**,** 241-55.

BLANCO CALVO, M., BOLOS FERNANDEZ, V., MEDINA VILLAAMIL, V., APARICIO GALLEGO, G., DIAZ PRADO, S. & GRANDE PULIDO, E. 2009. Biology of BMP signalling and cancer. *Clin Transl Oncol,* 11**,** 126-37.

BLITZ, I. L., ANDELFINGER, G. & HORB, M. E. 2006. Germ layers to organs: using Xenopus to study "later" development. *Semin Cell Dev Biol,* 17**,** 133-45.

BOERGERMANN, J. H., KOPF, J., YU, P. B. & KNAUS, P. 2010. Dorsomorphin and LDN-193189 inhibit BMP-mediated Smad, p38 and Akt signalling in C2C12 cells. *Int J Biochem Cell Biol,* 42**,** 1802-7.

BORDER, W. A. & NOBLE, N. A. 1994. Transforming growth factor beta in tissue fibrosis. *N Engl J Med,* 331**,** 1286-92.

BOTTINGER, E. P. & BITZER, M. 2002. TGF-beta signaling in renal disease. *J Am Soc Nephrol,* 13**,** 2600-10.

BRADFORD, M. M. 1976. A rapid and sensitive method for the quantitation of microgram quantities of protein utilizing the principle of protein-dye binding. *Anal Biochem,* 72**,** 248-54.

BROWN, K. A., HAM, A. J., CLARK, C. N., MELLER, N., LAW, B. K., CHYTIL, A., CHENG, N., PIETENPOL, J. A. & MOSES, H. L. 2008. Identification of novel Smad2 and Smad3 associated proteins in response to TGF-beta1. *J Cell Biochem,* 105**,** 596-611.

BRUBAKER, K. D., COREY, E., BROWN, L. G. & VESSELLA, R. L. 2004. Bone morphogenetic protein signaling in prostate cancer cell lines. *J Cell Biochem,* 91**,** 151-60.

BRUCE, D. L. & SAPKOTA, G. P. 2012. Phosphatases in SMAD regulation. *FEBS Lett,* 586**,** 1897-905.

BUENO, L., DE ALWIS, D. P., PITOU, C., YINGLING, J., LAHN, M., GLATT, S. & TROCONIZ, I. F. 2008. Semi-mechanistic modelling of the tumour growth inhibitory effects of LY2157299, a new type I receptor TGF-beta kinase antagonist, in mice. *Eur J Cancer,* 44**,** 142-50.

CALAF, G. M., ECHIBURU-CHAU, C., ZHAO, Y. L. & HEI, T. K. 2008. BigH3 protein expression as a marker for breast cancer. *Int J Mol Med,* 21**,** 561-8.

CALLAHAN, J. F., BURGESS, J. L., FORNWALD, J. A., GASTER, L. M., HARLING, J. D., HARRINGTON, F. P., HEER, J., KWON, C., LEHR, R., MATHUR, A., OLSON, B. A., WEINSTOCK, J. & LAPING, N. J. 2002. Identification of novel inhibitors of the transforming growth factor beta1 (TGF-beta1) type 1 receptor (ALK5). *J Med Chem,* 45**,** 999-1001.

CAMPBELL, D. G. & MORRICE, N. A. 2002. Identification of protein phosphorylation sites by a combination of mass spectrometry and solid phase Edman sequencing. *J Biomol Tech,* 13**,** 119-30.

CANNON, J. E., UPTON, P. D., SMITH, J. C. & MORRELL, N. W. 2010. Intersegmental vessel formation in zebrafish: requirement for VEGF but not BMP signalling revealed by selective and non-selective BMP antagonists. *Br J Pharmacol,* 161**,** 140-9.

CARMON, K. S., LIN, Q., GONG, X., THOMAS, A. & LIU, Q. 2012. LGR5 interacts and cointernalizes with Wnt receptors to modulate Wnt/beta-catenin signaling. *Mol Cell Biol,* 32**,** 2054-64.

CHAI, J., WU, J. W., YAN, N., MASSAGUE, J., PAVLETICH, N. P. & SHI, Y. 2003. Features of a Smad3 MH1-DNA complex. Roles of water and zinc in DNA binding. *J Biol Chem,* 278**,** 20327-31.

CHANG, H., HUYLEBROECK, D., VERSCHUEREN, K., GUO, Q., MATZUK, M. M. & ZWIJSEN, A. 1999. Smad5 knockout mice die at mid-gestation due to multiple embryonic and extraembryonic defects. *Development,* 126**,** 1631-42.

CHEN, D., ZHAO, M. & MUNDY, G. R. 2004. Bone morphogenetic proteins. *Growth Factors,* 22**,** 233-41.

CHEN, H. B., SHEN, J., IP, Y. T. & XU, L. 2006a. Identification of phosphatases for Smad in the BMP/DPP pathway. *Genes Dev,* 20**,** 648-53.

CHEN, N. X., DUAN, D., O'NEILL, K. D. & MOE, S. M. 2006b. High glucose increases the expression of Cbfa1 and BMP-2 and enhances the calcification of vascular smooth muscle cells. *Nephrol Dial Transplant,* 21**,** 3435-42.

CHEN, X. & XU, L. 2011. Mechanism and regulation of nucleocytoplasmic trafficking of smad. *Cell Biosci,* 1**,** 40.

CHOI, S. J., MOON, J. H., AHN, Y. W., AHN, J. H., KIM, D. U. & HAN, T. H. 2005. Tsc-22 enhances TGF-beta signaling by associating with Smad4 and induces erythroid cell differentiation. *Mol Cell Biochem,* 271**,** 23-8.

CHRISTENSEN, G. L., KELSTRUP, C. D., LYNGSO, C., SARWAR, U., BOGEBO, R., SHEIKH, S. P., GAMMELTOFT, S., OLSEN, J. V. & HANSEN, J. L. 2010. Quantitative phosphoproteomics dissection of seven-transmembrane receptor signaling using full and biased agonists. *Mol Cell Proteomics,* 9**,** 1540-53.

CIPRIANO, R., GRAHAM, J., MISKIMEN, K. L., BRYSON, B. L., BRUNTZ, R. C., SCOTT, S. A., BROWN, H. A., STARK, G. R. & JACKSON, M. W. 2012. FAM83B mediates EGFR- and RAS-driven oncogenic transformation. *J Clin Invest,* 122**,** 3197-210.

CLARKE, T. R., HOSHIYA, Y., YI, S. E., LIU, X., LYONS, K. M. & DONAHOE, P. K. 2001. Mullerian inhibiting substance signaling uses a bone morphogenetic protein (BMP)-like pathway mediated by ALK2 and induces SMAD6 expression. *Mol Endocrinol,* 15**,** 946-59.

COHEN, P. 2002. Protein kinases--the major drug targets of the twenty-first century? *Nat Rev Drug Discov,* 1**,** 309-15.

CONSTAM, D. B. & ROBERTSON, E. J. 1999. Regulation of bone morphogenetic protein activity by pro domains and proprotein convertases. *J Cell Biol,* 144**,** 139-49.

CUI, H., DARMANIN, S., NATSUISAKA, M., KONDO, T., ASAKA, M., SHINDOH, M., HIGASHINO, F., HAMURO, J., OKADA, F., KOBAYASHI, M., NAKAGAWA, K. & KOIDE, H. 2007. Enhanced expression of asparagine synthetase under glucose-deprived conditions protects pancreatic cancer cells from apoptosis induced by glucose deprivation and cisplatin. *Cancer Res,* 67**,** 3345-55.

CUI, Y., JEAN, F., THOMAS, G. & CHRISTIAN, J. L. 1998. BMP-4 is proteolytically activated by furin and/or PC6 during vertebrate embryonic development. *EMBO J,* 17**,** 4735-43.

CUNY, G. D., YU, P. B., LAHA, J. K., XING, X., LIU, J. F., LAI, C. S., DENG, D. Y., SACHIDANANDAN, C., BLOCH, K. D. & PETERSON, R. T.

2008. Structure-activity relationship study of bone morphogenetic protein (BMP) signaling inhibitors. *Bioorg Med Chem Lett,* 18**,** 4388-92.

DACOSTA BYFIELD, S., MAJOR, C., LAPING, N. J. & ROBERTS, A. B. 2004. SB-505124 is a selective inhibitor of transforming growth factor-beta type I receptors ALK4, ALK5, and ALK7. *Mol Pharmacol,* 65**,** 744-52.

DALY, A. C., RANDALL, R. A. & HILL, C. S. 2008. Transforming growth factor beta-induced Smad1/5 phosphorylation in epithelial cells is mediated by novel receptor complexes and is essential for anchorage-independent growth. *Mol Cell Biol,* 28**,** 6889-902.

DANCEY, J. & SAUSVILLE, E. A. 2003. Issues and progress with protein kinase inhibitors for cancer treatment. *Nat Rev Drug Discov,* 2**,** 296-313.

DASGUPTA, R. & FUCHS, E. 1999. Multiple roles for activated LEF/TCF transcription complexes during hair follicle development and differentiation. *Development,* 126**,** 4557-68.

DAVIES, M., ROBINSON, M., SMITH, E., HUNTLEY, S., PRIME, S. & PATERSON, I. 2005. Induction of an epithelial to mesenchymal transition in human immortal and malignant keratinocytes by TGF-beta1 involves MAPK, Smad and AP-1 signalling pathways. *J Cell Biochem,* 95**,** 918-31.

DE GOUVILLE, A. C., BOULLAY, V., KRYSA, G., PILOT, J., BRUSQ, J. M., LORIOLLE, F., GAUTHIER, J. M., PAPWORTH, S. A., LAROZE, A., GELLIBERT, F. & HUET, S. 2005. Inhibition of TGF-beta signaling by an ALK5 inhibitor protects rats from dimethylnitrosamine-induced liver fibrosis. *Br J Pharmacol,* 145**,** 166-77.

DE ROBERTIS, E. M. & KURODA, H. 2004. Dorsal-ventral patterning and neural induction in Xenopus embryos. *Annu Rev Cell Dev Biol,* 20**,** 285-308.

DECKERS, M., VAN DINTHER, M., BUIJS, J., QUE, I., LOWIK, C., VAN DER PLUIJM, G. & TEN DIJKE, P. 2006. The tumor suppressor Smad4 is required for transforming growth factor beta-induced epithelial to mesenchymal transition and bone metastasis of breast cancer cells. *Cancer Res,* 66**,** 2202-9.

DENG, H., RAVIKUMAR, T. S. & YANG, W. L. 2009. Overexpression of bone morphogenetic protein 4 enhances the invasiveness of Smad4-deficient human colorectal cancer cells. *Cancer Lett,* 281**,** 220-31.

DENNLER, S., HUET, S. & GAUTHIER, J. M. 1999. A short amino-acid sequence in MH1 domain is responsible for functional differences between Smad2 and Smad3. *Oncogene,* 18**,** 1643-8.

DEPHOURE, N., ZHOU, C., VILLEN, J., BEAUSOLEIL, S. A., BAKALARSKI, C. E., ELLEDGE, S. J. & GYGI, S. P. 2008. A quantitative atlas of mitotic phosphorylation. *Proc Natl Acad Sci U S A,* 105**,** 10762-7.

DERYNCK, R. & MIYAZONO, K. H. 2007. *The TGF-[beta] family,* Cold Spring Harbor, N.Y., Cold Spring Harbor Laboratory Press.

DERYNCK, R. & ZHANG, Y. E. 2003. Smad-dependent and Smad-independent pathways in TGF-beta family signalling. *Nature,* 425**,** 577-84.

DIETZ, H. C., CUTTING, G. R., PYERITZ, R. E., MASLEN, C. L., SAKAI, L. Y., CORSON, G. M., PUFFENBERGER, E. G., HAMOSH, A., NANTHAKUMAR, E. J., CURRISTIN, S. M. & ET AL. 1991. Marfan syndrome caused by a recurrent de novo missense mutation in the fibrillin gene. *Nature,* 352**,** 337-9.

DIETZ, H. C., LOEYS, B., CARTA, L. & RAMIREZ, F. 2005. Recent progress towards a molecular understanding of Marfan syndrome. *Am J Med Genet C Semin Med Genet,* 139C**,** 4-9.

DING, Y., ESTRELLA, M. R., HU, Y. Y., CHAN, H. L., ZHANG, H. D., KIM, J. W., SIMMER, J. P. & HU, J. C. 2009. Fam83h is associated with intracellular vesicles and ADHCAI. *J Dent Res,* 88**,** 991-6.

DU, S. J., PURCELL, S. M., CHRISTIAN, J. L., MCGREW, L. L. & MOON, R. T. 1995. Identification of distinct classes and functional domains of Wnts through expression of wild-type and chimeric proteins in Xenopus embryos. *Mol Cell Biol,* 15**,** 2625-34.

DUBOIS, C. M., LAPRISE, M. H., BLANCHETTE, F., GENTRY, L. E. & LEDUC, R. 1995. Processing of transforming growth factor beta 1 precursor by human furin convertase. *J Biol Chem,* 270**,** 10618-24.

DUDA, D. M., BORG, L. A., SCOTT, D. C., HUNT, H. W., HAMMEL, M. & SCHULMAN, B. A. 2008. Structural insights into NEDD8 activation of cullin-RING ligases: conformational control of conjugation. *Cell,* 134**,** 995-1006.

DUPONT, S., ZACCHIGNA, L., CORDENONSI, M., SOLIGO, S., ADORNO, M., RUGGE, M. & PICCOLO, S. 2005. Germ-layer specification and control of cell growth by Ectodermin, a Smad4 ubiquitin ligase. *Cell,* 121**,** 87-99.

EBISAWA, T., FUKUCHI, M., MURAKAMI, G., CHIBA, T., TANAKA, K., IMAMURA, T. & MIYAZONO, K. 2001. Smurf1 interacts with transforming growth factor-beta type I receptor through Smad7 and induces receptor degradation. *J Biol Chem,* 276**,** 12477-80.

EDLUND, S., BU, S., SCHUSTER, N., ASPENSTROM, P., HEUCHEL, R., HELDIN, N. E., TEN DIJKE, P., HELDIN, C. H. & LANDSTROM, M. 2003. Transforming growth factor-beta1 (TGF-beta)-induced apoptosis

of prostate cancer cells involves Smad7-dependent activation of p38 by TGF-beta-activated kinase 1 and mitogen-activated protein kinase kinase 3. *Mol Biol Cell,* 14**,** 529-44.

EIVERS, E., FUENTEALBA, L. C. & DE ROBERTIS, E. M. 2008. Integrating positional information at the level of Smad1/5/8. *Curr Opin Genet Dev,* 18**,** 304-10.

FASHENA, S. J., EINARSON, M. B., O'NEILL, G. M., PATRIOTIS, C. & GOLEMIS, E. A. 2002. Dissection of HEF1-dependent functions in motility and transcriptional regulation. *J Cell Sci,* 115**,** 99-111.

FINELLI, M. J., MURPHY, K. J., CHEN, L. & ZOU, H. 2013. Differential Phosphorylation of Smad1 Integrates BMP and Neurotrophin Pathways through Erk/Dusp in Axon Development. *Cell Rep,* 3**,** 1592-606.

FOLTZ, G., RYU, G. Y., YOON, J. G., NELSON, T., FAHEY, J., FRAKES, A., LEE, H., FIELD, L., ZANDER, K., SIBENALLER, Z., RYKEN, T. C., VIBHAKAR, R., HOOD, L. & MADAN, A. 2006. Genome-wide analysis of epigenetic silencing identifies BEX1 and BEX2 as candidate tumor suppressor genes in malignant glioma. *Cancer Res,* 66**,** 6665-74.

FONG, Y. C., LI, T. M., WU, C. M., HSU, S. F., KAO, S. T., CHEN, R. J., LIN, C. C., LIU, S. C., WU, C. L. & TANG, C. H. 2008. BMP-2 increases migration of human chondrosarcoma cells via PI3K/Akt pathway. *J Cell Physiol,* 217**,** 846-55.

FOX, M. H. 1980. A model for the computer analysis of synchronous DNA distributions obtained by flow cytometry. *Cytometry,* 1**,** 71-7.

FUKUDA, T., SCOTT, G., KOMATSU, Y., ARAYA, R., KAWANO, M., RAY, M. K., YAMADA, M. & MISHINA, Y. 2006. Generation of a mouse with conditionally activated signaling through the BMP receptor, ALK2. *Genesis,* 44**,** 159-67.

GALLIHER-BECKLEY, A. J. & SCHIEMANN, W. P. 2008. Grb2 binding to Tyr284 in TbetaR-II is essential for mammary tumor growth and metastasis stimulated by TGF-beta. *Carcinogenesis,* 29**,** 244-51.

GAO, S., ALARCON, C., SAPKOTA, G., RAHMAN, S., CHEN, P. Y., GOERNER, N., MACIAS, M. J., ERDJUMENT-BROMAGE, H., TEMPST, P. & MASSAGUE, J. 2009. Ubiquitin ligase Nedd4L targets activated Smad2/3 to limit TGF-beta signaling. *Mol Cell,* 36**,** 457-68.

GLINKA, A., WU, W., ONICHTCHOUK, D., BLUMENSTOCK, C. & NIEHRS, C. 1997. Head induction by simultaneous repression of Bmp and Wnt signalling in Xenopus. *Nature,* 389**,** 517-9.

GOGGINS, M., SHEKHER, M., TURNACIOGLU, K., YEO, C. J., HRUBAN, R. H. & KERN, S. E. 1998. Genetic alterations of the transforming

growth factor beta receptor genes in pancreatic and biliary adenocarcinomas. *Cancer Res,* 58**,** 5329-32.

GORBSKY, G. J. 2004. Mitosis: MCAK under the aura of Aurora B. *Curr Biol,* 14**,** R346-8.

GOTTLIN, E. B., RUDOLPH, A. E., ZHAO, Y., MATTHEWS, H. R. & DIXON, J. E. 1998. Catalytic mechanism of the phospholipase D superfamily proceeds via a covalent phosphohistidine intermediate. *Proc Natl Acad Sci U S A,* 95**,** 9202-7.

GOUDIE, D. R., D'ALESSANDRO, M., MERRIMAN, B., LEE, H., SZEVERENYI, I., AVERY, S., O'CONNOR, B. D., NELSON, S. F., COATS, S. E., STEWART, A., CHRISTIE, L., PICHERT, G., FRIEDEL, J., HAYES, I., BURROWS, N., WHITTAKER, S., GERDES, A. M., BROESBY-OLSEN, S., FERGUSON-SMITH, M. A., VERMA, C., LUNNY, D. P., REVERSADE, B. & LANE, E. B. 2011. Multiple self-healing squamous epithelioma is caused by a disease-specific spectrum of mutations in TGFBR1. *Nat Genet,* 43**,** 365-9.

GOUMANS, M. J., VALDIMARSDOTTIR, G., ITOH, S., LEBRIN, F., LARSSON, J., MUMMERY, C., KARLSSON, S. & TEN DIJKE, P. 2003. Activin receptor-like kinase (ALK)1 is an antagonistic mediator of lateral TGFbeta/ALK5 signaling. *Mol Cell,* 12**,** 817-28.

GOVANI, F. S. & SHOVLIN, C. L. 2009. Hereditary haemorrhagic telangiectasia: a clinical and scientific review. *Eur J Hum Genet,* 17**,** 860-71.

GRANT, S. 2012. FAM83A and FAM83B: candidate oncogenes and TKI resistance mediators. *J Clin Invest,* 122**,** 3048-51.

GRIFFITH, D. L., KECK, P. C., SAMPATH, T. K., RUEGER, D. C. & CARLSON, W. D. 1996. Three-dimensional structure of recombinant human osteogenic protein 1: structural paradigm for the transforming growth factor beta superfamily. *Proc Natl Acad Sci U S A,* 93**,** 878-83.

GROPPE, J., GREENWALD, J., WIATER, E., RODRIGUEZ-LEON, J., ECONOMIDES, A. N., KWIATKOWSKI, W., AFFOLTER, M., VALE, W. W., IZPISUA BELMONTE, J. C. & CHOE, S. 2002. Structural basis of BMP signalling inhibition by the cystine knot protein Noggin. *Nature,* 420**,** 636-42.

GRYGIELKO, E. T., MARTIN, W. M., TWEED, C., THORNTON, P., HARLING, J., BROOKS, D. P. & LAPING, N. J. 2005. Inhibition of gene markers of fibrosis with a novel inhibitor of transforming growth factor-beta type I receptor kinase in puromycin-induced nephritis. *J Pharmacol Exp Ther,* 313**,** 943-51.

GU, L., ZHU, Y. J., YANG, X., GUO, Z. J., XU, W. B. & TIAN, X. L. 2007. Effect of TGF-beta/Smad signaling pathway on lung myofibroblast differentiation. *Acta Pharmacol Sin,* 28**,** 382-91.

GU, Z., NOMURA, M., SIMPSON, B. B., LEI, H., FEIJEN, A., VAN DEN EIJNDEN-VAN RAAIJ, J., DONAHOE, P. K. & LI, E. 1998. The type I activin receptor ActRIB is required for egg cylinder organization and gastrulation in the mouse. *Genes Dev,* 12**,** 844-57.

HAHN, S. A., SCHUTTE, M., HOQUE, A. T., MOSKALUK, C. A., DA COSTA, L. T., ROZENBLUM, E., WEINSTEIN, C. L., FISCHER, A., YEO, C. J., HRUBAN, R. H. & KERN, S. E. 1996. DPC4, a candidate tumor suppressor gene at human chromosome 18q21.1. *Science,* 271**,** 350-3.

HAMBURGER, V. 1988. *The heritage of experimental embryology : Hans Spemann and the organizer,* New York, Oxford University Press.

HAO, J., DALEO, M. A., MURPHY, C. K., YU, P. B., HO, J. N., HU, J., PETERSON, R. T., HATZOPOULOS, A. K. & HONG, C. C. 2008. Dorsomorphin, a selective small molecule inhibitor of BMP signaling, promotes cardiomyogenesis in embryonic stem cells. *PLoS One,* 3**,** e2904.

HART, P. S., BECERIK, S., COGULU, D., EMINGIL, G., OZDEMIR-OZENEN, D., HAN, S. T., SULIMA, P. P., FIRATLI, E. & HART, T. C. 2009. Novel FAM83H mutations in Turkish families with autosomal dominant hypocalcified amelogenesis imperfecta. *Clin Genet,* 75**,** 401-4.

HAVRYLOV, S., RZHEPETSKYY, Y., MALINOWSKA, A., DROBOT, L. & REDOWICZ, M. J. 2009. Proteins recruited by SH3 domains of Ruk/CIN85 adaptor identified by LC-MS/MS. *Proteome Sci,* 7**,** 21.

HE, W., DORN, D. C., ERDJUMENT-BROMAGE, H., TEMPST, P., MOORE, M. A. & MASSAGUE, J. 2006. Hematopoiesis controlled by distinct TIF1gamma and Smad4 branches of the TGFbeta pathway. *Cell,* 125**,** 929-41.

HEASMAN, S. J. & RIDLEY, A. J. 2008. Mammalian Rho GTPases: new insights into their functions from in vivo studies. *Nat Rev Mol Cell Biol,* 9**,** 690-701.

HEINLEIN, C. A. & CHANG, C. 2004. Androgen receptor in prostate cancer. *Endocr Rev,* 25**,** 276-308.

HESTER, M., THOMPSON, J. C., MILLS, J., LIU, Y., EL-HODIRI, H. M. & WEINSTEIN, M. 2005. Smad1 and Smad8 function similarly in mammalian central nervous system development. *Mol Cell Biol,* 25**,** 4683-92.

HILL, C. S. 2009. Nucleocytoplasmic shuttling of Smad proteins. *Cell Res,* 19**,** 36-46.

HINCK, A. P. 2012. Structural studies of the TGF-betas and their receptors - insights into evolution of the TGF-beta superfamily. *FEBS Lett,* 586**,** 1860-70.

HO, J., COCOLAKIS, E., DUMAS, V. M., POSNER, B. I., LAPORTE, S. A. & LEBRUN, J. J. 2005. The G protein-coupled receptor kinase-2 is a TGFbeta-inducible antagonist of TGFbeta signal transduction. *EMBO J,* 24**,** 3247-58.

HONDA, T., YAMAMOTO, H., ISHII, A. & INUI, M. 2010. PDZRN3 negatively regulates BMP-2-induced osteoblast differentiation through inhibition of Wnt signaling. *Mol Biol Cell,* 21**,** 3269-77.

HONG, C. C. & YU, P. B. 2009. Applications of small molecule BMP inhibitors in physiology and disease. *Cytokine Growth Factor Rev,* 20**,** 409-18.

HOPPLER, S. & MOON, R. T. 1998. BMP-2/-4 and Wnt-8 cooperatively pattern the Xenopus mesoderm. *Mech Dev,* 71**,** 119-29.

HOWE, J. R., ROTH, S., RINGOLD, J. C., SUMMERS, R. W., JARVINEN, H. J., SISTONEN, P., TOMLINSON, I. P., HOULSTON, R. S., BEVAN, S., MITROS, F. A., STONE, E. M. & AALTONEN, L. A. 1998. Mutations in the SMAD4/DPC4 gene in juvenile polyposis. *Science,* 280**,** 1086-8.

HYUN, H. K., LEE, S. K., LEE, K. E., KANG, H. Y., KIM, E. J., CHOUNG, P. H. & KIM, J. W. 2009. Identification of a novel FAM83H mutation and microhardness of an affected molar in autosomal dominant hypocalcified amelogenesis imperfecta. *Int Endod J,* 42**,** 1039-43.

IDE, H., YOSHIDA, T., MATSUMOTO, N., AOKI, K., OSADA, Y., SUGIMURA, T. & TERADA, M. 1997. Growth regulation of human prostate cancer cells by bone morphogenetic protein-2. *Cancer Res,* 57**,** 5022-7.

IKUSHIMA, H. & MIYAZONO, K. 2010. TGFbeta signalling: a complex web in cancer progression. *Nat Rev Cancer,* 10**,** 415-24.

IMBEAUD, S., BELVILLE, C., MESSIKA-ZEITOUN, L., REY, R., DI CLEMENTE, N., JOSSO, N. & PICARD, J. Y. 1996. A 27 base-pair deletion of the anti-mullerian type II receptor gene is the most common cause of the persistent mullerian duct syndrome. *Hum Mol Genet,* 5**,** 1269-77.

INAI, K., NORRIS, R. A., HOFFMAN, S., MARKWALD, R. R. & SUGI, Y. 2008. BMP-2 induces cell migration and periostin expression during atrioventricular valvulogenesis. *Dev Biol,* 315**,** 383-96.

INMAN, G. J. 2011. Switching TGFbeta from a tumor suppressor to a tumor promoter. *Curr Opin Genet Dev,* 21**,** 93-9.

INMAN, G. J., NICOLAS, F. J., CALLAHAN, J. F., HARLING, J. D., GASTER, L. M., REITH, A. D., LAPING, N. J. & HILL, C. S. 2002. SB-431542 is a potent and specific inhibitor of transforming growth factor-beta superfamily type I activin receptor-like kinase (ALK) receptors ALK4, ALK5, and ALK7. *Mol Pharmacol,* 62**,** 65-74.

INOHARA, CHAMAILLARD, MCDONALD, C. & NUNEZ, G. 2005. NOD-LRR proteins: role in host-microbial interactions and inflammatory disease. *Annu Rev Biochem,* 74**,** 355-83.

ITOH, F., ITOH, S., CARVALHO, R. L., ADACHI, T., EMA, M., GOUMANS, M. J., LARSSON, J., KARLSSON, S., TAKAHASHI, S., MUMMERY, C. L., DIJKE, P. T. & KATO, M. 2009. Poor vessel formation in embryos from knock-in mice expressing ALK5 with L45 loop mutation defective in Smad activation. *Lab Invest,* 89**,** 800-10.

ITOH, K., KRUPNIK, V. E. & SOKOL, S. Y. 1998. Axis determination in Xenopus involves biochemical interactions of axin, glycogen synthase kinase 3 and beta-catenin. *Curr Biol,* 8**,** 591-4.

IVANOV, S. V., IVANOVA, A. V., SALNIKOW, K., TIMOFEEVA, O., SUBRAMANIAM, M. & LERMAN, M. I. 2008. Two novel VHL targets, TGFBI (BIGH3) and its transactivator KLF10, are up-regulated in renal clear cell carcinoma and other tumors. *Biochem Biophys Res Commun,* 370**,** 536-40.

JOHNSON, D. G. & WALKER, C. L. 1999. Cyclins and cell cycle checkpoints. *Annu Rev Pharmacol Toxicol,* 39**,** 295-312.

JOHNSON, D. W., BERG, J. N., BALDWIN, M. A., GALLIONE, C. J., MARONDEL, I., YOON, S. J., STENZEL, T. T., SPEER, M., PERICAK-VANCE, M. A., DIAMOND, A., GUTTMACHER, A. E., JACKSON, C. E., ATTISANO, L., KUCHERLAPATI, R., PORTEOUS, M. E. & MARCHUK, D. A. 1996. Mutations in the activin receptor-like kinase 1 gene in hereditary haemorrhagic telangiectasia type 2. *Nat Genet,* 13**,** 189-95.

JORNVALL, H., REISSMANN, E., ANDERSSON, O., MEHRKASH, M. & IBANEZ, C. F. 2004. ALK7, a receptor for nodal, is dispensable for embryogenesis and left-right patterning in the mouse. *Mol Cell Biol,* 24**,** 9383-9.

JOSSO, N., BELVILLE, C., DI CLEMENTE, N. & PICARD, J. Y. 2005. AMH and AMH receptor defects in persistent Mullerian duct syndrome. *Hum Reprod Update,* 11**,** 351-6.

JUN, J. H., YOON, W. J., SEO, S. B., WOO, K. M., KIM, G. S., RYOO, H. M. & BAEK, J. H. 2010. BMP2-activated Erk/MAP kinase stabilizes Runx2 by increasing p300 levels and histone acetyltransferase activity. *J Biol Chem,* 285**,** 36410-9.

KAHARI, V. M. & SAARIALHO-KERE, U. 1999. Matrix metalloproteinases and their inhibitors in tumour growth and invasion. *Ann Med,* 31**,** 34-45.

KALLURI, R. & WEINBERG, R. A. 2009. The basics of epithelial-mesenchymal transition. *J Clin Invest,* 119**,** 1420-8.

KANG, H. Y., LIN, H. K., HU, Y. C., YEH, S., HUANG, K. E. & CHANG, C. 2001. From transforming growth factor-beta signaling to androgen action: identification of Smad3 as an androgen receptor coregulator in prostate cancer cells. *Proc Natl Acad Sci U S A,* 98**,** 3018-23.

KATAGIRI, T., IMADA, M., YANAI, T., SUDA, T., TAKAHASHI, N. & KAMIJO, R. 2002. Identification of a BMP-responsive element in Id1, the gene for inhibition of myogenesis. *Genes Cells,* 7**,** 949-60.

KATAGIRI, T., YAMAGUCHI, A., KOMAKI, M., ABE, E., TAKAHASHI, N., IKEDA, T., ROSEN, V., WOZNEY, J. M., FUJISAWA-SEHARA, A. & SUDA, T. 1994. Bone morphogenetic protein-2 converts the differentiation pathway of C2C12 myoblasts into the osteoblast lineage. *J Cell Biol,* 127**,** 1755-66.

KAVSAK, P., RASMUSSEN, R. K., CAUSING, C. G., BONNI, S., ZHU, H., THOMSEN, G. H. & WRANA, J. L. 2000. Smad7 binds to Smurf2 to form an E3 ubiquitin ligase that targets the TGF beta receptor for degradation. *Mol Cell,* 6**,** 1365-75.

KAWANO, Y., KITAOKA, M., HAMADA, Y., WALKER, M. M., WAXMAN, J. & KYPTA, R. M. 2006. Regulation of prostate cell growth and morphogenesis by Dickkopf-3. *Oncogene,* 25**,** 6528-37.

KESTLER, H. A. & KUHL, M. 2008. From individual Wnt pathways towards a Wnt signalling network. *Philos Trans R Soc Lond B Biol Sci,* 363**,** 1333-47.

KIECKER, C. & NIEHRS, C. 2001. A morphogen gradient of Wnt/beta-catenin signalling regulates anteroposterior neural patterning in Xenopus. *Development,* 128**,** 4189-201.

KIELTY, C. M., BALDOCK, C., LEE, D., ROCK, M. J., ASHWORTH, J. L. & SHUTTLEWORTH, C. A. 2002. Fibrillin: from microfibril assembly to biomechanical function. *Philos Trans R Soc Lond B Biol Sci,* 357**,** 207-17.

KIM, J. E., KIM, E. H., HAN, E. H., PARK, R. W., PARK, I. H., JUN, S. H., KIM, J. C., YOUNG, M. F. & KIM, I. S. 2000. A TGF-beta-inducible cell adhesion molecule, betaig-h3, is downregulated in melorheostosis and involved in osteogenesis. *J Cell Biochem,* 77**,** 169-78.

KIM, J. W., LEE, S. K., LEE, Z. H., PARK, J. C., LEE, K. E., LEE, M. H., PARK, J. T., SEO, B. M., HU, J. C. & SIMMER, J. P. 2008. FAM83H mutations in families with autosomal-dominant hypocalcified amelogenesis imperfecta. *Am J Hum Genet,* 82**,** 489-94.

KIMURA, N., MATSUO, R., SHIBUYA, H., NAKASHIMA, K. & TAGA, T. 2000. BMP2-induced apoptosis is mediated by activation of the TAK1-p38 kinase pathway that is negatively regulated by Smad6. *J Biol Chem,* 275**,** 17647-52.

KITAHARA, O., FURUKAWA, Y., TANAKA, T., KIHARA, C., ONO, K., YANAGAWA, R., NITA, M. E., TAKAGI, T., NAKAMURA, Y. & TSUNODA, T. 2001. Alterations of gene expression during colorectal carcinogenesis revealed by cDNA microarrays after laser-capture microdissection of tumor tissues and normal epithelia. *Cancer Res,* 61**,** 3544-9.

KLOTZ, L. 2000. Hormone therapy for patients with prostate carcinoma. *Cancer,* 88**,** 3009-14.

KNOCKAERT, M., SAPKOTA, G., ALARCON, C., MASSAGUE, J. & BRIVANLOU, A. H. 2006. Unique players in the BMP pathway: small C-terminal domain phosphatases dephosphorylate Smad1 to attenuate BMP signaling. *Proc Natl Acad Sci U S A,* 103**,** 11940-5.

KODACH, L. L., BLEUMING, S. A., PEPPELENBOSCH, M. P., HOMMES, D. W., VAN DEN BRINK, G. R. & HARDWICK, J. C. 2007. The effect of statins in colorectal cancer is mediated through the bone morphogenetic protein pathway. *Gastroenterology,* 133**,** 1272-81.

KOINUMA, D., SHINOZAKI, M., KOMURO, A., GOTO, K., SAITOH, M., HANYU, A., EBINA, M., NUKIWA, T., MIYAZAWA, K., IMAMURA, T. & MIYAZONO, K. 2003. Arkadia amplifies TGF-beta superfamily signalling through degradation of Smad7. *EMBO J,* 22**,** 6458-70.

KOMATSU, Y., SCOTT, G., NAGY, A., KAARTINEN, V. & MISHINA, Y. 2007. BMP type I receptor ALK2 is essential for proper patterning at late gastrulation during mouse embryogenesis. *Dev Dyn,* 236**,** 512-7.

KUFER, T. A., SILLJE, H. H., KORNER, R., GRUSS, O. J., MERALDI, P. & NIGG, E. A. 2002. Human TPX2 is required for targeting Aurora-A kinase to the spindle. *J Cell Biol,* 158**,** 617-23.

KWEON, Y. S., LEE, K. E., KO, J., HU, J. C., SIMMER, J. P. & KIM, J. W. 2013. Effects of Fam83h overexpression on enamel and dentine formation. *Arch Oral Biol*.

LABRIE, F., CUSAN, L., GOMEZ, J., LUU-THE, V., CANDAS, B., BELANGER, A. & LABRIE, C. 2004. Major impact of hormonal therapy in localized prostate cancer--death can already be an exception. *J Steroid Biochem Mol Biol,* 92**,** 327-44.

LAMOUILLE, S., CONNOLLY, E., SMYTH, J. W., AKHURST, R. J. & DERYNCK, R. 2012. TGF-beta-induced activation of mTOR complex 2 drives epithelial-mesenchymal transition and cell invasion. *J Cell Sci,* 125**,** 1259-73.

LAMOUILLE, S. & DERYNCK, R. 2007. Cell size and invasion in TGF-beta-induced epithelial to mesenchymal transition is regulated by activation of the mTOR pathway. *J Cell Biol,* 178**,** 437-51.

LAPING, N. J., GRYGIELKO, E., MATHUR, A., BUTTER, S., BOMBERGER, J., TWEED, C., MARTIN, W., FORNWALD, J., LEHR, R., HARLING, J., GASTER, L., CALLAHAN, J. F. & OLSON, B. A. 2002. Inhibition of transforming growth factor (TGF)-beta1-induced extracellular matrix with a novel inhibitor of the TGF-beta type I receptor kinase activity: SB-431542. *Mol Pharmacol,* 62**,** 58-64.

LARRAIN, J., BACHILLER, D., LU, B., AGIUS, E., PICCOLO, S. & DE ROBERTIS, E. M. 2000. BMP-binding modules in chordin: a model for signalling regulation in the extracellular space. *Development,* 127**,** 821-30.

LEE, M. J., LEE, S. K., LEE, K. E., KANG, H. Y., JUNG, H. S. & KIM, J. W. 2009. Expression patterns of the Fam83h gene during murine tooth development. *Arch Oral Biol,* 54**,** 846-50.

LEE, M. K., PARDOUX, C., HALL, M. C., LEE, P. S., WARBURTON, D., QING, J., SMITH, S. M. & DERYNCK, R. 2007. TGF-beta activates Erk MAP kinase signalling through direct phosphorylation of ShcA. *EMBO J,* 26**,** 3957-67.

LEE, S. K., HU, J. C., BARTLETT, J. D., LEE, K. E., LIN, B. P., SIMMER, J. P. & KIM, J. W. 2008. Mutational spectrum of FAM83H: the C-terminal portion is required for tooth enamel calcification. *Hum Mutat,* 29**,** E95-9.

LEE, S. K., LEE, K. E., JEONG, T. S., HWANG, Y. H., KIM, S., HU, J. C., SIMMER, J. P. & KIM, J. W. 2011. FAM83H mutations cause ADHCAI and alter intracellular protein localization. *J Dent Res,* 90**,** 377-81.

LEE, S. Y., MEIER, R., FURUTA, S., LENBURG, M. E., KENNY, P. A., XU, R. & BISSELL, M. J. 2012. FAM83A confers EGFR-TKI resistance in breast cancer cells and in mice. *J Clin Invest,* 122**,** 3211-20.

LEHMANN, K., SEEMANN, P., SILAN, F., GOECKE, T. O., IRGANG, S., KJAER, K. W., KJAERGAARD, S., MAHONEY, M. J., MORLOT, S., REISSNER, C., KERR, B., WILKIE, A. O. & MUNDLOS, S. 2007. A new subtype of brachydactyly type B caused by point mutations in the bone morphogenetic protein antagonist NOGGIN. *Am J Hum Genet,* 81**,** 388-96.

LEVY, L. & HILL, C. S. 2005. Smad4 dependency defines two classes of transforming growth factor {beta} (TGF-{beta}) target genes and distinguishes TGF-{beta}-induced epithelial-mesenchymal transition from its antiproliferative and migratory responses. *Mol Cell Biol,* 25**,** 8108-25.

LEVY, L., HOWELL, M., DAS, D., HARKIN, S., EPISKOPOU, V. & HILL, C. S. 2007. Arkadia activates Smad3/Smad4-dependent transcription by triggering signal-induced SnoN degradation. *Mol Cell Biol,* 27**,** 6068-83.

LI, L., XIN, H., XU, X., HUANG, M., ZHANG, X., CHEN, Y., ZHANG, S., FU, X. Y. & CHANG, Z. 2004. CHIP mediates degradation of Smad proteins and potentially regulates Smad-induced transcription. *Mol Cell Biol,* 24**,** 856-64.

LI, X. & CAO, X. 2006. BMP signaling and skeletogenesis. *Ann N Y Acad Sci,* 1068**,** 26-40.

LI, Y., PAWLIK, B., ELCIOGLU, N., AGLAN, M., KAYSERILI, H., YIGIT, G., PERCIN, F., GOODMAN, F., NURNBERG, G., CENANI, A., URQUHART, J., CHUNG, B. D., ISMAIL, S., AMR, K., ASLANGER, A. D., BECKER, C., NETZER, C., SCAMBLER, P., EYAID, W., HAMAMY, H., CLAYTON-SMITH, J., HENNEKAM, R., NURNBERG, P., HERZ, J., TEMTAMY, S. A. & WOLLNIK, B. 2010. LRP4 mutations alter Wnt/beta-catenin signaling and cause limb and kidney malformations in Cenani-Lenz syndrome. *Am J Hum Genet,* 86**,** 696-706.

LIN, X., LIANG, M. & FENG, X. H. 2000. Smurf2 is a ubiquitin E3 ligase mediating proteasome-dependent degradation of Smad2 in transforming growth factor-beta signaling. *J Biol Chem,* 275**,** 36818-22.

LIU, F., POUPONNOT, C. & MASSAGUE, J. 1997. Dual role of the Smad4/DPC4 tumor suppressor in TGFbeta-inducible transcriptional complexes. *Genes Dev,* 11**,** 3157-67.

LIU, X., ELIA, A. E., LAW, S. F., GOLEMIS, E. A., FARLEY, J. & WANG, T. 2000. A novel ability of Smad3 to regulate proteasomal degradation of a Cas family member HEF1. *EMBO J,* 19**,** 6759-69.

LIVAK, K. J. & SCHMITTGEN, T. D. 2001. Analysis of relative gene expression data using real-time quantitative PCR and the 2(-Delta Delta C(T)) Method. *Methods,* 25**,** 402-8.

LOEYS, B. L., CHEN, J., NEPTUNE, E. R., JUDGE, D. P., PODOWSKI, M., HOLM, T., MEYERS, J., LEITCH, C. C., KATSANIS, N., SHARIFI, N., XU, F. L., MYERS, L. A., SPEVAK, P. J., CAMERON, D. E., DE BACKER, J., HELLEMANS, J., CHEN, Y., DAVIS, E. C., WEBB, C. L., KRESS, W., COUCKE, P., RIFKIN, D. B., DE PAEPE, A. M. & DIETZ, H. C. 2005. A syndrome of altered cardiovascular, craniofacial, neurocognitive and skeletal development caused by mutations in TGFBR1 or TGFBR2. *Nat Genet,* 37**,** 275-81.

LOGAN, C. Y. & NUSSE, R. 2004. The Wnt signaling pathway in development and disease. *Annu Rev Cell Dev Biol,* 20**,** 781-810.

MACDONALD, B. T., TAMAI, K. & HE, X. 2009. Wnt/beta-catenin signaling: components, mechanisms, and diseases. *Dev Cell,* 17**,** 9-26.

MACUREK, L., LINDQVIST, A., LIM, D., LAMPSON, M. A., KLOMPMAKER, R., FREIRE, R., CLOUIN, C., TAYLOR, S. S., YAFFE, M. B. &

MEDEMA, R. H. 2008. Polo-like kinase-1 is activated by aurora A to promote checkpoint recovery. *Nature,* 455**,** 119-23.

MANNING, G., WHYTE, D. B., MARTINEZ, R., HUNTER, T. & SUDARSANAM, S. 2002. The protein kinase complement of the human genome. *Science,* 298**,** 1912-34.

MARUMOTO, T., ZHANG, D. & SAYA, H. 2005. Aurora-A - a guardian of poles. *Nat Rev Cancer,* 5**,** 42-50.

MASSAGUE, J. 2003. Integration of Smad and MAPK pathways: a link and a linker revisited. *Genes Dev,* 17**,** 2993-7.

MASSAGUE, J. 2008. TGFbeta in Cancer. *Cell,* 134**,** 215-30.

MASSAGUE, J. & CHEN, Y. G. 2000. Controlling TGF-beta signaling. *Genes Dev,* 14**,** 627-44.

MASSAGUE, J., SEOANE, J. & WOTTON, D. 2005. Smad transcription factors. *Genes Dev,* 19**,** 2783-810.

MATYAS, G., ARNOLD, E., CARREL, T., BAUMGARTNER, D., BOILEAU, C., BERGER, W. & STEINMANN, B. 2006. Identification and in silico analyses of novel TGFBR1 and TGFBR2 mutations in Marfan syndrome-related disorders. *Hum Mutat,* 27**,** 760-9.

MCMAHON, J. A., TAKADA, S., ZIMMERMAN, L. B., FAN, C. M., HARLAND, R. M. & MCMAHON, A. P. 1998. Noggin-mediated antagonism of BMP signaling is required for growth and patterning of the neural tube and somite. *Genes Dev,* 12**,** 1438-52.

MERIDA, I., AVILA-FLORES, A. & MERINO, E. 2008. Diacylglycerol kinases: at the hub of cell signalling. *Biochem J,* 409**,** 1-18.

MILLER, J. R., ROWNING, B. A., LARABELL, C. A., YANG-SNYDER, J. A., BATES, R. L. & MOON, R. T. 1999. Establishment of the dorsal-ventral axis in Xenopus embryos coincides with the dorsal enrichment of dishevelled that is dependent on cortical rotation. *J Cell Biol,* 146**,** 427-37.

MINEGISHI, Y., SHIBAGAKI, Y., MIZUTANI, A., FUJITA, K., TEZUKA, T., KINOSHITA, M., KURODA, M., HATTORI, S. & GOTOH, N. 2013. Adaptor protein complex of FRS2beta and CIN85/CD2AP provides a novel mechanism for ErbB2/HER2 protein downregulation. *Cancer Sci,* 104**,** 345-52.

MIYAZONO, K. & MIYAZAWA, K. 2002. Id: a target of BMP signaling. *Sci STKE,* 2002**,** pe40.

MOGHE, S., JIANG, F., MIURA, Y., CERNY, R. L., TSAI, M. Y. & FURUKAWA, M. 2012. The CUL3-KLHL18 ligase regulates mitotic entry and ubiquitylates Aurora-A. *Biol Open,* 1**,** 82-91.

MOLENAAR, M., VAN DE WETERING, M., OOSTERWEGEL, M., PETERSON-MADURO, J., GODSAVE, S., KORINEK, V., ROOSE, J., DESTREE, O. & CLEVERS, H. 1996. XTcf-3 transcription factor mediates beta-catenin-induced axis formation in Xenopus embryos. *Cell,* 86**,** 391-9.

MOUSTAKAS, A. & HELDIN, C. H. 2005. Non-Smad TGF-beta signals. *J Cell Sci,* 118**,** 3573-84.

NACHTIGAL, M. W. & INGRAHAM, H. A. 1996. Bioactivation of Mullerian inhibiting substance during gonadal development by a kex2/subtilisin-like endoprotease. *Proc Natl Acad Sci U S A,* 93**,** 7711-6.

NEPTUNE, E. R., FRISCHMEYER, P. A., ARKING, D. E., MYERS, L., BUNTON, T. E., GAYRAUD, B., RAMIREZ, F., SAKAI, L. Y. & DIETZ, H. C. 2003. Dysregulation of TGF-beta activation contributes to pathogenesis in Marfan syndrome. *Nat Genet,* 33**,** 407-11.

NGUYEN, V. H., SCHMID, B., TROUT, J., CONNORS, S. A., EKKER, M. & MULLINS, M. C. 1998. Ventral and lateral regions of the zebrafish gastrula, including the neural crest progenitors, are established by a bmp2b/swirl pathway of genes. *Dev Biol,* 199**,** 93-110.

NIEUWKOOP, P. D. & FABER, J. 1994. *Normal table of Xenopus laevis (Daudin) : a systematical and chronological survey of the development from the fertilized egg till the end of metamorphosis,* New York, Garland Pub.

O'NEILL, G. M. & GOLEMIS, E. A. 2001. Proteolysis of the docking protein HEF1 and implications for focal adhesion dynamics. *Mol Cell Biol,* 21**,** 5094-108.

OH, S. P., SEKI, T., GOSS, K. A., IMAMURA, T., YI, Y., DONAHOE, P. K., LI, L., MIYAZONO, K., TEN DIJKE, P., KIM, S. & LI, E. 2000. Activin receptor-like kinase 1 modulates transforming growth factor-beta 1 signaling in the regulation of angiogenesis. *Proc Natl Acad Sci U S A,* 97**,** 2626-31.

ONICHTCHOUK, D., CHEN, Y. G., DOSCH, R., GAWANTKA, V., DELIUS, H., MASSAGUE, J. & NIEHRS, C. 1999. Silencing of TGF-beta signalling by the pseudoreceptor BAMBI. *Nature,* 401**,** 480-5.

OZAWA, T., BRENNAN, C. W., WANG, L., SQUATRITO, M., SASAYAMA, T., NAKADA, M., HUSE, J. T., PEDRAZA, A., UTSUKI, S., YASUI, Y., TANDON, A., FOMCHENKO, E. I., OKA, H., LEVINE, R. L., FUJII, K., LADANYI, M. & HOLLAND, E. C. 2010. PDGFRA gene rearrangements are frequent genetic events in PDGFRA-amplified glioblastomas. *Genes Dev,* 24**,** 2205-18.

OZDAMAR, B., BOSE, R., BARRIOS-RODILES, M., WANG, H. R., ZHANG, Y. & WRANA, J. L. 2005. Regulation of the polarity protein Par6 by

TGFbeta receptors controls epithelial cell plasticity. *Science,* 307**,** 1603-9.

PADUA, D. & MASSAGUE, J. 2009. Roles of TGFbeta in metastasis. *Cell Res,* 19**,** 89-102.

PAN, D., ESTEVEZ-SALMERON, L. D., STROSCHEIN, S. L., ZHU, X., HE, J., ZHOU, S. & LUO, K. 2005. The integral inner nuclear membrane protein MAN1 physically interacts with the R-Smad proteins to repress signaling by the transforming growth factor-{beta} superfamily of cytokines. *J Biol Chem,* 280**,** 15992-6001.

PENG, S. B., YAN, L., XIA, X., WATKINS, S. A., BROOKS, H. B., BEIGHT, D., HERRON, D. K., JONES, M. L., LAMPE, J. W., MCMILLEN, W. T., MORT, N., SAWYER, J. S. & YINGLING, J. M. 2005. Kinetic characterization of novel pyrazole TGF-beta receptor I kinase inhibitors and their blockade of the epithelial-mesenchymal transition. *Biochemistry,* 44**,** 2293-304.

PETROSKI, M. D. & DESHAIES, R. J. 2005. Function and regulation of cullin-RING ubiquitin ligases. *Nat Rev Mol Cell Biol,* 6**,** 9-20.

PICCOLO, S., SASAI, Y., LU, B. & DE ROBERTIS, E. M. 1996. Dorsoventral patterning in Xenopus: inhibition of ventral signals by direct binding of chordin to BMP-4. *Cell,* 86**,** 589-98.

PINTARD, L., WILLEMS, A. & PETER, M. 2004. Cullin-based ubiquitin ligases: Cul3-BTB complexes join the family. *EMBO J,* 23**,** 1681-7.

PLATTEN, M., WICK, W., WILD-BODE, C., AULWURM, S., DICHGANS, J. & WELLER, M. 2000. Transforming growth factors beta(1) (TGF-beta(1)) and TGF-beta(2) promote glioma cell migration via Up-regulation of alpha(V)beta(3) integrin expression. *Biochem Biophys Res Commun,* 268**,** 607-11.

QIU, T., GRIZZLE, W. E., OELSCHLAGER, D. K., SHEN, X. & CAO, X. 2007. Control of prostate cell growth: BMP antagonizes androgen mitogenic activity with incorporation of MAPK signals in Smad1. *EMBO J,* 26**,** 346-57.

RADDEN, L. A., CHILD, K. M., ADKINS, E. B., SPACEK, D. V., FELICIANO, A. M. & KING, T. R. 2013. The wooly mutation (wly) on mouse chromosome 11 is associated with a genetic defect in Fam83g. *BMC Res Notes,* 6**,** 189.

RAFTERY, L. A., TWOMBLY, V., WHARTON, K. & GELBART, W. M. 1995. Genetic screens to identify elements of the decapentaplegic signaling pathway in Drosophila. *Genetics,* 139**,** 241-54.

RIGBOLT, K. T., PROKHOROVA, T. A., AKIMOV, V., HENNINGSEN, J., JOHANSEN, P. T., KRATCHMAROVA, I., KASSEM, M., MANN, M., OLSEN, J. V. & BLAGOEV, B. 2011. System-wide temporal

characterization of the proteome and phosphoproteome of human embryonic stem cell differentiation. *Sci Signal,* 4**,** rs3.

ROLLASON, R., KOROLCHUK, V., HAMILTON, C., JEPSON, M. & BANTING, G. 2009. A CD317/tetherin-RICH2 complex plays a critical role in the organization of the subapical actin cytoskeleton in polarized epithelial cells. *J Cell Biol,* 184**,** 721-36.

ROSS, S., CHEUNG, E., PETRAKIS, T. G., HOWELL, M., KRAUS, W. L. & HILL, C. S. 2006. Smads orchestrate specific histone modifications and chromatin remodeling to activate transcription. *EMBO J,* 25**,** 4490-502.

ROSS, S. & HILL, C. S. 2008. How the Smads regulate transcription. *Int J Biochem Cell Biol,* 40**,** 383-408.

ROWNING, B. A., WELLS, J., WU, M., GERHART, J. C., MOON, R. T. & LARABELL, C. A. 1997. Microtubule-mediated transport of organelles and localization of beta-catenin to the future dorsal side of Xenopus eggs. *Proc Natl Acad Sci U S A,* 94**,** 1224-9.

SAHA, A. & DESHAIES, R. J. 2008. Multimodal activation of the ubiquitin ligase SCF by Nedd8 conjugation. *Mol Cell,* 32**,** 21-31.

SANCHEZ, N. S. & BARNETT, J. V. 2012. TGFbeta and BMP-2 regulate epicardial cell invasion via TGFbetaR3 activation of the Par6/Smurf1/RhoA pathway. *Cell Signal,* 24**,** 539-48.

SANTAMARIA, A., NAGEL, S., SILLJE, H. H. & NIGG, E. A. 2008. The spindle protein CHICA mediates localization of the chromokinesin Kid to the mitotic spindle. *Curr Biol,* 18**,** 723-9.

SANVITALE, C. E., KERR, G., CHAIKUAD, A., RAMEL, M. C., MOHEDAS, A. H., REICHERT, S., WANG, Y., TRIFFITT, J. T., CUNY, G. D., YU, P. B., HILL, C. S. & BULLOCK, A. N. 2013. A new class of small molecule inhibitor of BMP signaling. *PLoS One,* 8**,** e62721.

SAPKOTA, G., ALARCON, C., SPAGNOLI, F. M., BRIVANLOU, A. H. & MASSAGUE, J. 2007. Balancing BMP signaling through integrated inputs into the Smad1 linker. *Mol Cell,* 25**,** 441-54.

SAPKOTA, G., KNOCKAERT, M., ALARCON, C., MONTALVO, E., BRIVANLOU, A. H. & MASSAGUE, J. 2006. Dephosphorylation of the linker regions of Smad1 and Smad2/3 by small C-terminal domain phosphatases has distinct outcomes for bone morphogenetic protein and transforming growth factor-beta pathways. *J Biol Chem,* 281**,** 40412-9.

SAPKOTA, G. P. 2013. The TGFbeta-induced phosphorylation and activation of p38 mitogen-activated protein kinase is mediated by MAP3K4 and MAP3K10 but not TAK1. *Open Biol,* 3**,** 130067.

SASAI, Y., LU, B., STEINBEISSER, H., GEISSERT, D., GONT, L. K. & DE ROBERTIS, E. M. 1994. Xenopus chordin: a novel dorsalizing factor activated by organizer-specific homeobox genes. *Cell,* 79**,** 779-90.

SAVAGE, C., DAS, P., FINELLI, A. L., TOWNSEND, S. R., SUN, C. Y., BAIRD, S. E. & PADGETT, R. W. 1996. Caenorhabditis elegans genes sma-2, sma-3, and sma-4 define a conserved family of transforming growth factor beta pathway components. *Proc Natl Acad Sci U S A,* 93**,** 790-4.

SAWYER, J. S., ANDERSON, B. D., BEIGHT, D. W., CAMPBELL, R. M., JONES, M. L., HERRON, D. K., LAMPE, J. W., MCCOWAN, J. R., MCMILLEN, W. T., MORT, N., PARSONS, S., SMITH, E. C., VIETH, M., WEIR, L. C., YAN, L., ZHANG, F. & YINGLING, J. M. 2003. Synthesis and activity of new aryl- and heteroaryl-substituted pyrazole inhibitors of the transforming growth factor-beta type I receptor kinase domain. *J Med Chem,* 46**,** 3953-6.

SAYED, M. G., AHMED, A. F., RINGOLD, J. R., ANDERSON, M. E., BAIR, J. L., MITROS, F. A., LYNCH, H. T., TINLEY, S. T., PETERSEN, G. M., GIARDIELLO, F. M., VOGELSTEIN, B. & HOWE, J. R. 2002. Germline SMAD4 or BMPR1A mutations and phenotype of juvenile polyposis. *Ann Surg Oncol,* 9**,** 901-6.

SCHEUFLER, C., SEBALD, W. & HULSMEYER, M. 1999. Crystal structure of human bone morphogenetic protein-2 at 2.7 A resolution. *J Mol Biol,* 287**,** 103-15.

SCHNEIDER, D., KLEEFF, J., BERBERAT, P. O., ZHU, Z., KORC, M., FRIESS, H. & BUCHLER, M. W. 2002. Induction and expression of betaig-h3 in pancreatic cancer cells. *Biochim Biophys Acta,* 1588**,** 1-6.

SCHNEIDER, S., STEINBEISSER, H., WARGA, R. M. & HAUSEN, P. 1996. Beta-catenin translocation into nuclei demarcates the dorsalizing centers in frog and fish embryos. *Mech Dev,* 57**,** 191-8.

SCHULTE, G. & BRYJA, V. 2007. The Frizzled family of unconventional G-protein-coupled receptors. *Trends Pharmacol Sci,* 28**,** 518-25.

SCHUTTE, M., HRUBAN, R. H., HEDRICK, L., CHO, K. R., NADASDY, G. M., WEINSTEIN, C. L., BOVA, G. S., ISAACS, W. B., CAIRNS, P., NAWROZ, H., SIDRANSKY, D., CASERO, R. A., JR., MELTZER, P. S., HAHN, S. A. & KERN, S. E. 1996. DPC4 gene in various tumor types. *Cancer Res,* 56**,** 2527-30.

SCIAN, M. J., STAGLIANO, K. E., DEB, D., ELLIS, M. A., CARCHMAN, E. H., DAS, A., VALERIE, K., DEB, S. P. & DEB, S. 2004. Tumor-derived p53 mutants induce oncogenesis by transactivating growth-promoting genes. *Oncogene,* 23**,** 4430-43.

SEKELSKY, J. J., NEWFELD, S. J., RAFTERY, L. A., CHARTOFF, E. H. & GELBART, W. M. 1995. Genetic characterization and cloning of

mothers against dpp, a gene required for decapentaplegic function in Drosophila melanogaster. *Genetics,* 139**,** 1347-58.

SEKI, A., COPPINGER, J. A., JANG, C. Y., YATES, J. R. & FANG, G. 2008. Bora and the kinase Aurora a cooperatively activate the kinase Plk1 and control mitotic entry. *Science,* 320**,** 1655-8.

SEO, S. R., LALLEMAND, F., FERRAND, N., PESSAH, M., L'HOSTE, S., CAMONIS, J. & ATFI, A. 2004. The novel E3 ubiquitin ligase Tiul1 associates with TGIF to target Smad2 for degradation. *EMBO J,* 23**,** 3780-92.

SEOANE, J. 2008. The TGFBeta pathway as a therapeutic target in cancer. *Clin Transl Oncol,* 10**,** 14-9.

SHI, Y. & MASSAGUE, J. 2003. Mechanisms of TGF-beta signaling from cell membrane to the nucleus. *Cell,* 113**,** 685-700.

SHIBUYA, H., IWATA, H., MASUYAMA, N., GOTOH, Y., YAMAGUCHI, K., IRIE, K., MATSUMOTO, K., NISHIDA, E. & UENO, N. 1998. Role of TAK1 and TAB1 in BMP signaling in early Xenopus development. *EMBO J,* 17**,** 1019-28.

SHIROMIZU, T., ADACHI, J., WATANABE, S., MURAKAMI, T., KUGA, T., MURAOKA, S. & TOMONAGA, T. 2013. Identification of Missing Proteins in the neXtProt Database and Unregistered Phosphopeptides in the PhosphoSitePlus Database As Part of the Chromosome-Centric Human Proteome Project. *J Proteome Res*.

SIEGEL, P. M. & MASSAGUE, J. 2003. Cytostatic and apoptotic actions of TGF-beta in homeostasis and cancer. *Nat Rev Cancer,* 3**,** 807-21.

SILVA, A. P., XAPELLI, S., GROUZMANN, E. & CAVADAS, C. 2005. The putative neuroprotective role of neuropeptide Y in the central nervous system. *Curr Drug Targets CNS Neurol Disord,* 4**,** 331-47.

SINGER, J. D., GURIAN-WEST, M., CLURMAN, B. & ROBERTS, J. M. 1999. Cullin-3 targets cyclin E for ubiquitination and controls S phase in mammalian cells. *Genes Dev,* 13**,** 2375-87.

SINGH, A. & MORRIS, R. J. 2010. The Yin and Yang of bone morphogenetic proteins in cancer. *Cytokine Growth Factor Rev,* 21**,** 299-313.

SIT, S. T. & MANSER, E. 2011. Rho GTPases and their role in organizing the actin cytoskeleton. *J Cell Sci,* 124**,** 679-83.

SOKOL, S., CHRISTIAN, J. L., MOON, R. T. & MELTON, D. A. 1991. Injected Wnt RNA induces a complete body axis in Xenopus embryos. *Cell,* 67**,** 741-52.

SOOND, S. M. & CHANTRY, A. 2011. Selective targeting of activating and inhibitory Smads by distinct WWP2 ubiquitin ligase isoforms

differentially modulates TGFbeta signalling and EMT. *Oncogene,* 30**,** 2451-62.

SORRENTINO, A., THAKUR, N., GRIMSBY, S., MARCUSSON, A., VON BULOW, V., SCHUSTER, N., ZHANG, S., HELDIN, C. H. & LANDSTROM, M. 2008. The type I TGF-beta receptor engages TRAF6 to activate TAK1 in a receptor kinase-independent manner. *Nat Cell Biol,* 10**,** 1199-207.

STAMOS, J. L. & WEIS, W. I. 2013. The beta-catenin destruction complex. *Cold Spring Harb Perspect Biol,* 5**,** a007898.

SUETSUGU, S., MIKI, H. & TAKENAWA, T. 1999. Identification of two human WAVE/SCAR homologues as general actin regulatory molecules which associate with the Arp2/3 complex. *Biochem Biophys Res Commun,* 260**,** 296-302.

SUGIMORI, K., MATSUI, K., MOTOMURA, H., TOKORO, T., WANG, J., HIGA, S., KIMURA, T. & KITAJIMA, I. 2005. BMP-2 prevents apoptosis of the N1511 chondrocytic cell line through PI3K/Akt-mediated NF-kappaB activation. *J Bone Miner Metab,* 23**,** 411-9.

SUMARA, I. & PETER, M. 2007. A Cul3-based E3 ligase regulates mitosis and is required to maintain the spindle assembly checkpoint in human cells. *Cell Cycle,* 6**,** 3004-10.

SUMARA, I., QUADRONI, M., FREI, C., OLMA, M. H., SUMARA, G., RICCI, R. & PETER, M. 2007. A Cul3-based E3 ligase removes Aurora B from mitotic chromosomes, regulating mitotic progression and completion of cytokinesis in human cells. *Dev Cell,* 12**,** 887-900.

SUN, J., LIU, Y. H., CHEN, H., NGUYEN, M. P., MISHINA, Y., UPPERMAN, J. S., FORD, H. R. & SHI, W. 2007. Deficient Alk3-mediated BMP signaling causes prenatal omphalocele-like defect. *Biochem Biophys Res Commun,* 360**,** 238-43.

SUN, P. D. & DAVIES, D. R. 1995. The cystine-knot growth-factor superfamily. *Annu Rev Biophys Biomol Struct,* 24**,** 269-91.

TAKAHASHI, S., YOKOTA, C., TAKANO, K., TANEGASHIMA, K., ONUMA, Y., GOTO, J. & ASASHIMA, M. 2000. Two novel nodal-related genes initiate early inductive events in Xenopus Nieuwkoop center. *Development,* 127**,** 5319-29.

TAKENAWA, T. & SUETSUGU, S. 2007. The WASP-WAVE protein network: connecting the membrane to the cytoskeleton. *Nat Rev Mol Cell Biol,* 8**,** 37-48.

TANG, L. Y., YAMASHITA, M., COUSSENS, N. P., TANG, Y., WANG, X., LI, C., DENG, C. X., CHENG, S. Y. & ZHANG, Y. E. 2011. Ablation of Smurf2 reveals an inhibition in TGF-beta signalling through multiple mono-ubiquitination of Smad3. *EMBO J,* 30**,** 4777-89.

TEN DIJKE, P. & HILL, C. S. 2004. New insights into TGF-beta-Smad signalling. *Trends Biochem Sci,* 29**,** 265-73.

THAPA, N., LEE, B. H. & KIM, I. S. 2007. TGFBIp/betaig-h3 protein: a versatile matrix molecule induced by TGF-beta. *Int J Biochem Cell Biol,* 39**,** 2183-94.

TOJO, M., HAMASHIMA, Y., HANYU, A., KAJIMOTO, T., SAITOH, M., MIYAZONO, K., NODE, M. & IMAMURA, T. 2005. The ALK-5 inhibitor A-83-01 inhibits Smad signaling and epithelial-to-mesenchymal transition by transforming growth factor-beta. *Cancer Sci,* 96**,** 791-800.

TOWNSEND, T. A., ROBINSON, J. Y., DEIG, C. R., HILL, C. R., MISFELDT, A., BLOBE, G. C. & BARNETT, J. V. 2011. BMP-2 and TGFbeta2 shared pathways regulate endocardial cell transformation. *Cells Tissues Organs,* 194**,** 1-12.

TREMBLAY, K. D., DUNN, N. R. & ROBERTSON, E. J. 2001. Mouse embryos lacking Smad1 signals display defects in extra-embryonic tissues and germ cell formation. *Development,* 128**,** 3609-21.

UHL, M., AULWURM, S., WISCHHUSEN, J., WEILER, M., MA, J. Y., ALMIREZ, R., MANGADU, R., LIU, Y. W., PLATTEN, M., HERRLINGER, U., MURPHY, A., WONG, D. H., WICK, W., HIGGINS, L. S. & WELLER, M. 2004. SD-208, a novel transforming growth factor beta receptor I kinase inhibitor, inhibits growth and invasiveness and enhances immunogenicity of murine and human glioma cells in vitro and in vivo. *Cancer Res,* 64**,** 7954-61.

VAN HOOF, D., MUNOZ, J., BRAAM, S. R., PINKSE, M. W., LINDING, R., HECK, A. J., MUMMERY, C. L. & KRIJGSVELD, J. 2009. Phosphorylation dynamics during early differentiation of human embryonic stem cells. *Cell Stem Cell,* 5**,** 214-26.

VAN SEVENTER, G. A., SALMEN, H. J., LAW, S. F., O'NEILL, G. M., MULLEN, M. M., FRANZ, A. M., KANNER, S. B., GOLEMIS, E. A. & VAN SEVENTER, J. M. 2001. Focal adhesion kinase regulates beta1 integrin-dependent T cell migration through an HEF1 effector pathway. *Eur J Immunol,* 31**,** 1417-27.

VARGA, A. C. & WRANA, J. L. 2005. The disparate role of BMP in stem cell biology. *Oncogene,* 24**,** 5713-21.

VERMEULEN, K., BERNEMAN, Z. N. & VAN BOCKSTAELE, D. R. 2003a. Cell cycle and apoptosis. *Cell Prolif,* 36**,** 165-75.

VERMEULEN, K., VAN BOCKSTAELE, D. R. & BERNEMAN, Z. N. 2003b. The cell cycle: a review of regulation, deregulation and therapeutic targets in cancer. *Cell Prolif,* 36**,** 131-49.

WAKEFIELD, L. M. & HILL, C. S. 2013. Beyond TGFbeta: roles of other TGFbeta superfamily members in cancer. *Nat Rev Cancer,* 13**,** 328-41.

WANG, G., LI, C., WANG, Y. & CHEN, G. 2013. Cooperative assembly of Co-Smad4 MH1 with R-Smad1/3 MH1 on DNA: a molecular dynamics simulation study. *PLoS One,* 8**,** e53841.

WESSELY, O., AGIUS, E., OELGESCHLAGER, M., PERA, E. M. & DE ROBERTIS, E. M. 2001. Neural induction in the absence of mesoderm: beta-catenin-dependent expression of secreted BMP antagonists at the blastula stage in Xenopus. *Dev Biol,* 234**,** 161-73.

WILEY, D. M., KIM, J. D., HAO, J., HONG, C. C., BAUTCH, V. L. & JIN, S. W. 2011. Distinct signalling pathways regulate sprouting angiogenesis from the dorsal aorta and the axial vein. *Nat Cell Biol,* 13**,** 686-92.

WILLIAMS, L. T. 1989. Signal transduction by the platelet-derived growth factor receptor. *Science,* 243**,** 1564-70.

WRANA, J. L., ATTISANO, L., WIESER, R., VENTURA, F. & MASSAGUE, J. 1994. Mechanism of activation of the TGF-beta receptor. *Nature,* 370**,** 341-7.

WRIGHT, J. T., FRAZIER-BOWERS, S., SIMMONS, D., ALEXANDER, K., CRAWFORD, P., HAN, S. T., HART, P. S. & HART, T. C. 2009. Phenotypic variation in FAM83H-associated amelogenesis imperfecta. *J Dent Res,* 88**,** 356-60.

WRIGHTON, K. H., LIN, X., YU, P. B. & FENG, X. H. 2009. Transforming Growth Factor {beta} Can Stimulate Smad1 Phosphorylation Independently of Bone Morphogenic Protein Receptors. *J Biol Chem,* 284**,** 9755-63.

WRIGHTON, K. H., WILLIS, D., LONG, J., LIU, F., LIN, X. & FENG, X. H. 2006. Small C-terminal domain phosphatases dephosphorylate the regulatory linker regions of Smad2 and Smad3 to enhance transforming growth factor-beta signaling. *J Biol Chem,* 281**,** 38365-75.

XAVIER, S., NIRANJAN, T., KRICK, S., ZHANG, T., JU, W., SHAW, A. S., SCHIFFER, M. & BOTTINGER, E. P. 2009. TbetaRI independently activates Smad- and CD2AP-dependent pathways in podocytes. *J Am Soc Nephrol,* 20**,** 2127-37.

XIE, Z., FANG, M., RIVAS, M. P., FAULKNER, A. J., STERNWEIS, P. C., ENGEBRECHT, J. A. & BANKAITIS, V. A. 1998. Phospholipase D activity is required for suppression of yeast phosphatidylinositol transfer protein defects. *Proc Natl Acad Sci U S A,* 95**,** 12346-51.

XU, J., LAMOUILLE, S. & DERYNCK, R. 2009. TGF-beta-induced epithelial to mesenchymal transition. *Cell Res,* 19**,** 156-72.

XU, P., LIU, J. & DERYNCK, R. 2012. Post-translational regulation of TGF-beta receptor and Smad signaling. *FEBS Lett,* 586**,** 1871-84.

XU, Y. & PASCHE, B. 2007. TGF-beta signaling alterations and susceptibility to colorectal cancer. *Hum Mol Genet,* 16 Spec No 1**,** R14-20.

YAMASHITA, M., FATYOL, K., JIN, C., WANG, X., LIU, Z. & ZHANG, Y. E. 2008. TRAF6 mediates Smad-independent activation of JNK and p38 by TGF-beta. *Mol Cell,* 31**,** 918-24.

YE, L., LEWIS-RUSSELL, J. M., KYANASTON, H. G. & JIANG, W. G. 2007. Bone morphogenetic proteins and their receptor signaling in prostate cancer. *Histol Histopathol,* 22**,** 1129-47.

YI, J. Y., SHIN, I. & ARTEAGA, C. L. 2005. Type I transforming growth factor beta receptor binds to and activates phosphatidylinositol 3-kinase. *J Biol Chem,* 280**,** 10870-6.

YU, P. B., DENG, D. Y., LAI, C. S., HONG, C. C., CUNY, G. D., BOUXSEIN, M. L., HONG, D. W., MCMANUS, P. M., KATAGIRI, T., SACHIDANANDAN, C., KAMIYA, N., FUKUDA, T., MISHINA, Y., PETERSON, R. T. & BLOCH, K. D. 2008a. BMP type I receptor inhibition reduces heterotopic [corrected] ossification. *Nat Med,* 14**,** 1363-9.

YU, P. B., HONG, C. C., SACHIDANANDAN, C., BABITT, J. L., DENG, D. Y., HOYNG, S. A., LIN, H. Y., BLOCH, K. D. & PETERSON, R. T. 2008b. Dorsomorphin inhibits BMP signals required for embryogenesis and iron metabolism. *Nat Chem Biol,* 4**,** 33-41.

YUE, J. & MULDER, K. M. 2000. Activation of the mitogen-activated protein kinase pathway by transforming growth factor-beta. *Methods Mol Biol,* 142**,** 125-31.

ZAWEL, L., DAI, J. L., BUCKHAULTS, P., ZHOU, S., KINZLER, K. W., VOGELSTEIN, B. & KERN, S. E. 1998. Human Smad3 and Smad4 are sequence-specific transcription activators. *Mol Cell,* 1**,** 611-7.

ZHANG, B., HALDER, S. K., KASHIKAR, N. D., CHO, Y. J., DATTA, A., GORDEN, D. L. & DATTA, P. K. 2010. Antimetastatic role of Smad4 signaling in colorectal cancer. *Gastroenterology,* 138**,** 969-80 e1-3.

ZHANG, L., HUANG, H., ZHOU, F., SCHIMMEL, J., PARDO, C. G., ZHANG, T., BARAKAT, T. S., SHEPPARD, K. A., MICKANIN, C., PORTER, J. A., VERTEGAAL, A. C., VAN DAM, H., GRIBNAU, J., LU, C. X. & TEN DIJKE, P. 2012. RNF12 controls embryonic stem cell fate and morphogenesis in zebrafish embryos by targeting Smad7 for degradation. *Mol Cell,* 46**,** 650-61.

ZHANG, Y., CHANG, C., GEHLING, D. J., HEMMATI-BRIVANLOU, A. & DERYNCK, R. 2001. Regulation of Smad degradation and activity by Smurf2, an E3 ubiquitin ligase. *Proc Natl Acad Sci U S A,* 98**,** 974-9.

ZHANG, Y. E. 2009. Non-Smad pathways in TGF-beta signaling. *Cell Res,* 19**,** 128-39.

ZHENG, M. & MCKEOWN-LONGO, P. J. 2002. Regulation of HEF1 expression and phosphorylation by TGF-beta 1 and cell adhesion. *J Biol Chem,* 277**,** 39599-608.

ZHONG, J., BAQUIRAN, J. B., BONAKDAR, N., LEES, J., CHING, Y. W., PUGACHEVA, E., FABRY, B. & O'NEILL, G. M. 2012. NEDD9 stabilizes focal adhesions, increases binding to the extra-cellular matrix and differentially effects 2D versus 3D cell migration. *PLoS One,* 7**,** e35058.

ZHOU, G., MYERS, R., LI, Y., CHEN, Y., SHEN, X., FENYK-MELODY, J., WU, M., VENTRE, J., DOEBBER, T., FUJII, N., MUSI, N., HIRSHMAN, M. F., GOODYEAR, L. J. & MOLLER, D. E. 2001. Role of AMP-activated protein kinase in mechanism of metformin action. *J Clin Invest,* 108**,** 1167-74.

ZHOU, Q., HEINKE, J., VARGAS, A., WINNIK, S., KRAUSS, T., BODE, C., PATTERSON, C. & MOSER, M. 2007. ERK signaling is a central regulator for BMP-4 dependent capillary sprouting. *Cardiovasc Res,* 76**,** 390-9.

ZHU, H., KAVSAK, P., ABDOLLAH, S., WRANA, J. L. & THOMSEN, G. H. 1999. A SMAD ubiquitin ligase targets the BMP pathway and affects embryonic pattern formation. *Nature,* 400**,** 687-93.